Investigating the Effect of Processing Parameters in the Electrospinning of Nanofibres

MOHAMMAD MAHFUZUR RAHMAN CHOWDHURY

A Thesis Submitted in Fulfilment of the Requirement for the Degree of Doctor of philosophy

Heriot -Watt University
The School of Textiles and Design

November 2010

ABSTRACT

Nylon 6, Nylon 6.6, PEO/water, PEO/water/Ethanol, PVA/$FeCl_3$ and PEO/wood pulp have been successfully electrospun into nanofibres in the range of 200 nm to 1500 nm. A comprehensive understanding of the effect of processing parameters on the morphological structure of these nanofibres has been established. Parameters such as concentration of polymer solution, applied voltage, electrospinning collection distance and flow rate have been found to affect fibre morphology. For Nylon 6 and Nylon 6.6 uniform nanofibres were produced using polymer solution concentrations, 20 wt.% and 25 wt.%, applied voltage of 15 kV, spinning distance of 8 cm and volume feed rate of 0.20 ml/hr. The produced nanofibres average diameter was 924 nm and 827 nm. For PEO/water, PEO/water/Ethanol and PEO/wood pulp optimum conditions of polymer solution concentration of 14 wt.% and 10 wt.%, an applied voltage of 15 kV, spinning collection distance of 11cm and volume feed rate of 0.20 ml/hr and 0.25 ml/hr, produced uniform nanofibres. The produced nanofibres average diameter was 452 nm, 544 nm and 494 nm. As for PVA/$FeCl_3$, optimum conditions of polymer solution concentration of 8 wt.%, an applied voltage 15 kV, spinning collection distance 11 cm and flow rate 0.25 ml/hr produced uniform magnetic nanofibres. The produced nanofibres average diameters were 789 nm. These parameters have consequently been optimized to obtain uniform quality at different ranges of nanofibres. In this context it was established that the processing parameters vary significantly from one polymer to another but in general, the concentration the most important role in obtaining uniform fibre diameter without thin and thick places and beads. Applied voltage also played a significant role in determining the diameter of nanofibres and little significant effect on the fibre morphology was observed with the variation of spinning collection distance and noticeable structural change with a change in the solution flow rate.

A selective range of microscopic techniques such as, Scanning Electron Microscopy, Atomic Force Microscopy and Transmission Electron Microscopy were used to characterise and evaluate the nanofibres produced during this study. DSC, X-ray diffraction and FTIR was used to identify the thermal properties of Nylon 6.6, PEO and PEO/wood pulp nanofibres produced.

Nanofibres produced in this study have a wide range of potential applications in different fields, including, biomedical, magnetic sensor, mats for composite protective clothing, filtration, aerospace and others.

DEDICATION

I would like to dedicate this work to my parents who are not alive and during their time they have supported me in many ways. I would also like to thank my wife who has given me the strength to finish this thesis and the rest of my family who has encouraged me to overcome many difficult challenges and hard times.

AKNOWLEDGMENTS

I would like to start by thanking my advisor, Sr.Prof.George. K. Stylios for taking me under his wing as a PhD student and not only sharing his knowledge with me throughout my time at Heriot-Watt, but by being a leader in the field of textile engineering to whom I aspire. Without your constant encouragement, advice, demands, and financially support, this work would not be possible.

I would like to thank Prof. Roger. H. Wardman, Prof. Robert Christie, Mrs Fiona S.Wildron, Dr. Lisa Macintyre, Dr. Alex Fotheringham. Dr. Roger Spark, Dr. Michael Wan, Dr. Daniel Abraham, Dr. Shah M Reduwan Billah, Dr Xiaoming Zhao, Mr Peter Sandison, Mr Liang Luo, Mr Andrew McCullough, Mr. Jim Mcvie, Mrs Margaret Robson, Mrs Ann, Mrs Eleanour Drummond for their insights support and encouragements.

I would also like to thank Dr Hudson from Strathclyde University, Professor Wilson and Mrs Marian Millar from the School of Engineering & Physical Sciences for their help to assist me doing the solutions physical properties.

On a more personal note, I want to thank my wife. Thank you for your patience, love and devotion; you are my inspiration. To my sons Taseen, thank you for bringing Daddy so much joy and happiness; I love you both so much. To my brothers and sisters, thank you for believing in me and for encouraging me all along.

I would like to thank my mom and dad. They were the ones that pushed me to be the best that I can be and they never settled for anything less. Without them, I would not be where I am today…literally

I would also like to thank the rest of the student body and faculty in the School of Textile and Design. The friendships that were made will extend well beyond the duration of our graduate careers. The faculty that are not on my committee have taught me well and I have learned something from all of you, whether that be in a class room, a discussion about my thesis topic or over a drink at the university parties. Thank you all so very much.

Last, but most importantly, I want to thank God for giving me wisdom and strength, without Him I could do nothing.

DECLARATION STATEMENT

TABLE OF CONTENT

Chapter 8: Process optimization of PVA Ferro gel nano fibre blends by the electro spinning process

Chapter 9: Effects of electrospinning process parameters on nanofibres obtained from PEO/Wood pulp blends

Chapter 11: Conclusion and future work

Appendices

LIST OF TABLES

LIST OF FIGURES

Chapter 1: Nanotechnology and nanofibres

1.1 Introduction

The term “nano” is historical. Nano comes from from the Greek word “nannas”. A nanometre is a billionth of a meter, or 80000 times thinner than human hair. So, nanometre domain covers sizes bigger than several atoms but smaller than the wavelength of visible light. Nanotechnology refers to the science and engineering concerning materials, structures and devices which at least one of the dimensions is 100nm or less [1]. Therefore nanotechnology can be defined as the science and engineering involved in the design, synthesis, characterization and application of materials and devices whose smallest functional organization in at least one dimension is on the nanometre scale or one billionth of a meter [2]. Classified by nanofiller dimensionality, there are a number of types of nanocomposites such as Zero-dimensional (nanoparticle), one-dimensional (nanofibre), two-dimensional (nanolayer), and three-dimensional (interpenetrating network) systems can all be imagined [3]. Also, lamellar nanocomposites can be divided into two distinct classes, intercalated and exfoliated. In intercalated nanocomposites, the polymer chains alternate with the inorganic layers in a fixed compositional ratio and have defined number(s) of polymer layers in the intralamellar space. In exfoliated nanocomposites, the number of polymer chains between the layers is almost continuously variable and the layers stand >100 Å apart. Determining and altering how materials and their interfaces are constructed at nano and atomic scales will provide the opportunity to develop new materials and products. Because of this ability, nanotechnology represents a major opportunity to improve all the materials performance and functionality develop new generations of products, and open new market segments in the coming decades [4]. Nano technology was first recognized after the talk by Richard Feynman. The talk title was “There’s plenty of room at the bottom” when in 1959 Feynman [5] gave a lecture about it where he observed that the principles of physics do not deny the possibility of manipulating things atom by atom. He suggested using small machines to make even tinier machines, and so on down to the atomic level itself. In his time, it was not possible for us to

manipulate single atoms or molecules because they were far too small for the tools existed at that time. Thus, his speech was completely theoretical and seemingly fictional. He described how the laws of physics do not limit our ability to manipulate single atoms and molecules. However he correctly predicted that the time would come in which atomically precise manipulation of matter would arrive. In fact, many of the concepts and techniques he envisioned at that time are indeed being used today in nanotechnology. Prof. Feynman described such atomic scale fabrication as a bottom-up approach, as opposed to the top-down approach that we are accustomed to. The current top down method for manufacturing involves the construction of parts through methods such as cutting, carving and moulding. In 1974 Nario Taniguchi [6] of Tokyo University defined nanotechnology, ‘‘Nano technology mainly consists of the processing of separation, consolidation and deformation’’ still stands as the basic statement today. In 1981 K.Eric Drexler focuses the nano technology and their consequences for the future. Drexler popularized the field of nanotechnology by publishing two of the earliest books on the field i) Engines of Creation, ii) The coming Era of nanotechnology and nanosystems and molecular machinery, manufacturing and computation. Nanoparticles are tiny particles on the order of one billionth of a meter scale. To put this size in perspective, the flu virus is roughly 2 microns, a sheet of paper is about 100,000 nanometres thick, and mycoplasma is 200 nm in size. Or, to look at it another way, approximately 1/70th the diameter of a red blood cell. The use of nanosized objects allows us to explore and interact at the cellular level in an unprecedented fashion [7]. Although the development of such molecular machines is still far beyond the current possibilities of nanotechnology, other developments in nanotechnology have been incredibly fast in recent years; so fast, that it is easy to forget that processes based on nanotechnology and materials containing nanostructures have already been used in materials science for more than a thousand years without knowing their exact length scale. Therefore an important breakthrough for nanotechnology was the development of imaging techniques with a resolution in the nanometre range, such as electron microscopes [8] and scanning probe microscopes [9-10]. These imaging tools have enabled researchers to measure the sizes of fabricated structures, thereby classifying them as nanostructures, and to visualize and understand processes and phenomena at the nanoscale. Research has been carried out on very small components, many of which depend on quantum effects and may involve movement of a very small number of electrons in their action. Such devices would act faster than larger components. Considerable interest has been shown in the production of structures on a

molecular level by suitable sequence of chemical reaction or lithographic techniques. It is also possible to manipulate individual atoms on surfaces using a variant of the atomic force microscope to make, for example, high density data storage devices.

1.2 The principles of nanotechnology, classification and application

Nanotechnology, the creation of functional materials, devices, and systems through control of matter at the 1-100 nm scale, has become one of the most interesting disciplines in science and technology. The intense interest in nanotechnology is driven by various fields and is leading to a new industrial revolution. A scientific and technical revolution has just begun based upon the ability to systematically organize and manipulate matter at nanoscale. This highly multidisciplinary field is strongly related to fundamental sciences such as physics, chemistry, and biology [11]. At the nanoscale, fundamental mechanical, electrical, optical, and other properties can significantly differ from their bulk material counterparts. Nanotechnology and nanoscience regard the study, control, manipulation, and assembly of nanoscale components into materials, systems and devices for human interest and needs [12]. Among the various nanostructures recently developed for practical applications, membranes made of nanofibres produced from synthetic and natural polymers have received increased attention due to their ease of fabrication and the ability to control their compositional, structural and functional properties [13]. With the emergence of nanotechnology, researchers become more interested in studying the unique properties of nanoscale materials.

Electrospinning, an electrostatic fibre fabrication technique has evinced more interest and attention in recent years due to its versatility and potential for applications in diverse fields. The notable applications include in tissue engineering, biosensors, filtration, wound dressings, drug delivery, and enzyme immobilization. The nanoscale fibres are generated by the application of strong electric field on polymer solution or melt. The non-wovens nanofibrous mats produced by this technique mimics extracellular matrix components much closely as compared to the conventional techniques [14]. Let us briefly introduce some common subfields of nanotechnology.

i) Nanostructured: Nanostructured materials are modulated over nanometre length scales in zero to three dimensions. They can be assembled with modulation dimensionalities of zero (atom clusters or filaments), one (multilayer's), two (ultrafine-grained over layers or coatings or buried layers), and three (nanophase materials), or

with intermediate dimensionalities. As far as "nanostructures" are concerned, one can view this as objects or structures whereby at least one of its dimensions is within nano-scale. The difference between a nanostructure and a nanodevice can be viewed upon as the analogy between a building and a machine (whether mechanical, electrical or both). It goes without saying that as far as nanoscale is concerned, one should not pigeon-hole these nano-elements for an element that is considered a structure can at times be used as a significant part of a device [1]. Nanostructured materials can also be built in such a way that they will be biocompatible for implants. Nanostructured materials and sensors, that are currently used or will be used in the future in automotive industry, is almost certain that will find application in aerospace industry as well, where the demand for safety is also great. Concentrating on space applications, it can be pointed out that the trend towards miniaturization is greater. The demand of small satellites orbiting the earth has increased over the past few years, due to special demands in communications. The Internet, mobile phones, TV stations and other domestic applications require satellites. Companies are trying to make them smaller, because it is easier to be put on orbit, maintained them there and cause little pollution, when they are put out of order [15].

ii) ***Nanoparticle***: A "nanoparticle" can be considered as a zero-dimensional nanoelement, which is the simplest form of nanostructure. Fine powders of size smaller than 10 nm are, for example, applied in cosmetic or pharmaceutical industries, for ceramic coatings, for water based paints or fine emulsions production, or as toner in reproducing systems. Nanoparticles are also applied in production of semi-conductor devices, or for thin solid film deposition [16]. Monosized solid particles or liquid droplets are also used for scientific or measuring instruments calibration, or in fundamental aerosol dynamics studies [17].

iii) ***Nanorod or nanotube***: Nanorods or nanotubes are one-dimensional nano-element from with a slightly more complex nanostructure can be constructed of. Nanorods have wide application; Prominent among them is in the use in display technologies. By changing the orientation of the nanorods with respect to an applied electric field, the reflectivity of the rods can be altered, resulting in superior displays. Picture quality can be improved radically. Each picture element, known as pixel, is composed of a sharp-tipped device of the scale of a few nanometres. Such TVs, known as field emission TVs, are brighter as the pixels can glow better in every colour they take up as they pass through a small potential gap at high currents, emitting electrons at the same

time. Nanorod-based flexible, thin-film computers can revolutionise the retail industry, enabling customers to checkout easily without the hassles of having to pay cash [18]. Nanotube can be used as a single molecule circuit, or as part of a miniaturized electronic component, thereby appearing as a nanodevice. Hence the function, along with the structure, is essential in classifying which nanotechnology sub-area it belongs to [1].

iv) ***Nanoplatelet or a nanodisk***: Nanoplatelet or nanodisks are two-dimensional elements which, along with its one-dimensional counterpart, are useful in the construction of nanodevices [1].

v) ***Nanomaterials***: Nonomaterial refers to a nano-sized material while in other instances a nanomaterial is a bulk material with nano-scaled structure [1]. New applications for nano materials can be created with novel or significantly enhanced properties. Such properties include transparency, hydrophobicity, photoluminescence, toughness and hardness, chemical sensing and bioavailability. Products produced from these materials exhibit unique properties and have a wide range of high value commercial applications in rapidly expanding markets. The key characteristics demanded of nanoparticles to capture high value markets include: small particle size, narrow size distribution, low levels of agglomeration and high dispersibility [19].

vi) ***Nanocrystals***: Nanocrystals appear to be a misnomer. It is understood that a crystal is highly structured and that the repetitive unit is indeed small enough. Hence a nanocrystal refers to the size of the entire crystal itself being nano-sized, but not of the repetitive unit [1].

vii) ***Nanophotonics***: Nanophotonics refers to the study, research, development and/or applications of nano-scale object that emit light and its corresponding light. These objects are normally quantum dots. Whilst the emission of photon is largest for bulk (3dimensional), followed by quantum well (2- dimensional) and finally quantum dot (0-dimensional), the ranking is reversed in terms of efficiency [6].

viii) ***Nanomagnetics***: The term of term nonmagnetic is self explanatory; we actually view it in terms of highly miniaturized magnetic data storage materials with very high memory. This can be attained by taking advantage of the electron spin for memory storage hence the term "spin-electronics", which has since been more popularly and more conveniently known as "spintronics" [9].

ix) ***Nanobioengineering***: In nanobioengineering, the novel properties at nano-scale are taken advantage of for bioengineering applications. The many naturally occurring nanofibrous and nanoporous structure in the human body further adds to the impetus for research and development in this sub-area. Closely related to this is molecular fictionalization whereby the surface of an object is modified by attaching certain molecules to enable desired functions to be carried out - such as for sensing and/or filtering chemicals based on molecular affinity [9].

x) ***Nano medicine***: Nanomedicine is an important area of research and development in the field of nanotechnology [20]. Nanomedicine, which involves the use of nanotechnology in drug development, offers ever more exciting promises of new diagnoses and cures. It has been defined as the monitoring, repair, construction and control of human biological systems at the molecular level, using engineered nanodevices [21] and nanostructures. Nanomedicine is a science that uses nanotechnology to maintain and improve human health at the molecular scale. Nanomedicine is the medical application of nanotechnology. Examples of applications that are currently under investigation include the development of drug delivery systems [22] and targeting nanoparticles for imaging, and fabrication of implants or scaffolds for tissue engineering. Polymers are good candidates for application in all these areas, since there are many biocompatible and biodegradable polymers available, and the mechanical, chemical and surface properties of polymers can easily be modified, as well as their size [23-24]. Current and potential applications of nanotechnology in medicine range from research involving diagnostic devices, drug delivery vehicles to enhanced gene therapy and tissue engineering procedures [20]. Its advantage over conventional medicine lies on its size. Particle size has effect on serum lifetime and pattern of deposition. This allows drugs of nanosize be used in lower concentration and has an earlier onset of therapeutic action. It also provides materials for controlled drug delivery by directing carriers to a specific location. Major efforts are underway; however, very little attention is devoted to assessment of health risks to human or to the ecosystem. Inhaled nanoparticles have already been related to lung injury. It is recognized that physico-chemical properties in conjunction with environmental factors and stability of the nanomaterial all contribute to the overall toxicological responses [18].

xi) ***Nanomechanics***: Nanomechanics are a branch of nanoscience studying fundamental mechanical (elastic, thermal and kinetic) properties of physical systems at the nanometre scale. Nanomechanics has emerged on the cross-road of classical mechanics, solid-state physics, statistical mechanics, materials science, and quantum

chemistry. As an area of nanoscience, nanomechanics provide a scientific foundation of nanotechnology. Nanomechanics is that branch of nanoscience, which deals with the study and application of fundamental mechanical properties of physical systems at the nanoscale, like elastic, thermal, kinetic [25].

xii) ***Nanofibres***: nanofibres would geometrically fall into the category of 1- dimensional nano-scale elements that includes nanotubes and nanorods. However, the flexible nature of nanofibres would align it along with other highly flexible nano-elements such as globular molecules (assumed as 0-dimensional soft matter), as well as solid and liquid films of nanothickness (2-dimensional). A nanofibre is a nanomaterial in view of its diameter, and can be considered a nanostructured material if filled with nanoparticles to form composite nanofibres [13].

1.3 Nano fibre and electrospinning

Nanofibres are typically the fibre lengths are many orders of magnitude greater than the fibre diameters. The primary external length scales are therefore the fibre diameter and the fibre length. Although there are a variety of nanofibres available, the vast majority of nanofibres of interest in nanotechnology are made from polymer precursors, typically by processes such as electrospinning. When the diameters of polymer fibre materials are shrunk from micrometers (e.g. 10–100 mm) to submicron's or nanometers (e.g. $10x10^{-3}$–$100x10^{-3}$ mm), there appear several amazing characteristics such as very large surface area to volume ratio (this ratio for a nanofibre can be as large as 103 times of that of a microfibre), flexibility in surface functionalities, and superior mechanical performance (e.g. stiffness and tensile strength) compared with any other known form of the material. These outstanding properties make the polymer nanofibres to be optimal candidates for many important applications. A number of processing techniques such as drawing [26], template synthesis [27-28], phase separation [29], self-assembly [30-31], electrospinning [32-33], etc. have been used to prepare polymer nanofibres in recent years. Drawing is a process similar to dry spinning in fibre industry, which can make one-by-one very long single nanofibres. However, only a viscoelastic material that can undergo strong deformations while being cohesive enough to support the stresses developed during pulling can be made into nanofibres through drawing. The template synthesis, as the name suggests, uses a nanoporous membrane as a template to make nanofibres of solid (a fibril) or hollow (a tubule) shape. The most important feature of this method may lie in that nanometer tubules and fibrils of various raw materials such as electronically conducting polymers, metals, semiconductors, and carbons can be

fabricated. On the other hand, the method cannot make one-by-one continuous nanofibres.

Nanofibres can also be made as foam by phase separation. The phase separation consists of dissolution, gelation, and extraction using a different solvent, freezing, and drying resulting in nanoscale porous foam. The process takes relatively long period of time to transfer the solid polymer into the nano-porous foam. Self-assembly is a process in which individual, pre-existing components organize themselves into desired patterns and functions. However, similarly as in the case of phase separation the self-assembly is time-consuming in processing continuous polymer nanofibres.

Thus, the electrospinning process seems to be a method which can be further developed for mass production of one-by-one continuous nanofibres from various polymers [34]. Electrospinning is a novel and efficient fabrication process that can be utilized to assemble fibrous polymer mats composed of fibre diameters ranging from several microns down to fibres with diameter lower than 100 nm [35]. The process of electrospinning has been known for almost 70 years and the first patent was issued to Formhals in 1934 [36], Polymeric nanofibres produced by electrospinning have become a field of great interest for the past few years, with more polymers being nano processed with more end uses.

1.4 Chapter organisation, aims and objectives

The main aim of this thesis is to successfully produce Nylon 6, Nylon 6.6, PEO, PVA and Wood pulp to investigate processing parameters effect during nano fibre production by the electrospinning method. The morphology of the produced nanofibres and analyses of the thermal properties of the produced nano fibre has been carried out. The main focus of this study is to investigate the impact of the processing parameters for the formulation of polymer solution for nanofibre production using electrospinning techniques. In this context, a range of polymers was carefully selected which have a greater potential for a variety of uses, including biomedical application, and protective clothing. The selected polymers were, Nylon 6, Nylon 6.6, PEO, PVA and Wood pulp. These polymers are widely available, soluble and compatible for medical and industrial application requirements and most importantly researchers have not fully discovered the effect of the parameter during processing.

The research objectives are fulfilled in eight chapters, the arrangements which are described below:

Chapter 3: *Experimental electrospinning technique set up and materials*: This chapter describes the electrospinning process, the experimental set up and the polymer have used in this project.

Chapter 4: *Experimental methods, morphology and characterization technique*: This chapter focuses on the nano fibre characterization techniques. Solution properties and fibre morphology characterisation technique analysed in this chapter. The SEM, AFM, TEM, DSC, X-ray diffraction, and FTIR used to characterize the produced nano fibre morphology. Their experimental principles are briefly described in this chapter.

Chapter 5: *Effect of experimental parameters on the morphology of electrospun Nylon 6 fibres*: The physical properties of the polymer solution and the electrospinning process parameters are investigated in order to establish their effect on Nylon 6 nanofibre morphology, average diameter and uniformity. The polymer solution concentration, applied voltage and electrospinning distance, solution flow rate are optimized to enable uniform nanofibre diameter distribution.

Chapter 6: *Processing parameter study of Nylon 6.6 electrospun fibres*: The physical properties of the polymer solution and the electrospinning process parameters are investigated in order to establish their effect on Nylon 6.6 nanofibre morphology, average diameter and uniformity. The polymer solution concentration, applied voltage and electrospinning distance, solution flow rate are optimized to enable uniform nanofibre diameter distribution. Uniform diameter nanofibres can be produced for alignment. This chapter also analyses the Nylon 6.6/MWCNT composite fibre morphology and the thermal properties of the Nylon 6.6 granule and Nylon 6.6 nano mat.

Chapter 7: *The effect of experimental parameters on the morphology of electrospun PEO nanofibres and analyses their thermal properties:* The physical properties of the polymer solution and the electrospinning process parameters are investigated in order to establish their effect on PEO nanofibre morphology, average diameter and uniformity. The polymer solution concentration, applied voltage and electrospinning distance, solution flow rate are optimized to enable uniform nanofibre diameter distribution. To improve the electrospinning process viscosity, Ethanol was added to the PEO/Water solution. PEO powder and nano fibre thermal properties are also analysed in this chapter.

Chapter 8: *Process optimization of PVA Ferro gel nano fibre blends by the electro spinning process*: This chapter reports to use of biodegradable polymer PVA and mix with $FeCl_3$ to produced blend or composite fibre. Composite fibres were prepared by using Ferro gel processing and electrospinning. Effects of instrument parameters including solution concentration, electric voltage, tip–target distance, flow rate on the morphology of electrospun PVA fibres were evaluated. The produced fibre share magnetic properties.

Chapter 9: *Effects of electrospinning process parameters on nanofibres obtained from PEO/wood pulp blends*: This chapter investigates the effect of processing parameters on cellulose fibre. PEO is used with Wood pulp and produced composite fibre.Wood pulp presence at the PEO/wood pulp nano fibre measured by TEM. Their thermal properties have also been investigated.

Chapter 10: *Potential end uses of produced electrospun nanofibre:* This chapter describes and discusses the application of the produced nano fibres and it analyses potential industrial and medical applications.

Chapter 11: *Conclusion and future work*:

This chapter has been discussing the research conclusion and the scope for future work.

1.5 References

[1.1] S. Ramakrishna, K. Fujihara and W.Teo*, An Introduction to electrospinning and nanofibres,* World Scientific Publishing Co Pte Ltd, **ISBN 10:** 9812564543 (2005)

[1.2] A. S. Gabriel*, Introduction to nanotechnology and its applications to medicine,* Surgical Neurology, **61**, 216–220 (2004)

[1.3] D. Schmidt, D. Shah, E. P. Giannelis*, New advances in polymer/ layered silicate nanocomposites.* CurrentOpinion in Solid State and Materials Science, **6**, 205– 212 (2002)

[1.4] T. H.Wegner, J. E. Winandy, M. A. Ritter, *Nanotechnology opportunities in residential and non-residentialconstrucxtion,* 2nd International Symposium on Nanotechnology in Construction, Bilbao, Spain (2005)

[1.5] R. Feynman, *There's plenty of room at the bottom, an invitation to enter a new field of physics*, Engineering and Science **23**, pp. 22–36 (1960)

[1.6] N. Taniguchi, *On the basic concept of 'nano-technology*', Proceedings of the International Conference of Production Engineering, Society of Precision Engineering, Tokyo, Japan (1974)

[1.7] K. E. Drexler, *Molecular engineering*: *An approach to the development of general capabilities for molecular manipulation,* Proceedings of the National academies of Science USA, **78**, 5275-5278 (1981)

[1.8] E. Ruska, Rev. Mod. Phys**, 59** (3), 627-638 (1987)

[1.9] G. Binnig, C.F. Quate and C. Gerber, Phys. Rev. Lett.**, 56** (9), 930-933 (1986)

[1.10] G. Binnig and H. Rohrer, Helv. Phys. Acta **55** (6), 726-735 (1982)

[1.11] A. Merkoçi, *Nanobiomaterials in electroanalysis,* Electroanalysis **19**: 739-741 (2007)

[1.12] J. Weiss, P. Takhistov, D. J. McClements, *Functional materials in food nanotechnology*, J. Food Sci., **71**: R107-R116 (2006)

[1.13] C. Burger, B.S. Hsiao, B. Chu, *Nanofibrous materials and their applications,* Annu. Rev. Mater. Res.*,* **36**: 333-368 (2006)

[1.14] N. Bhardwaj, S.C.Kundu, *Electrospinning: a fascinating fibre fabrication technique*, Biotechnology advances, JBA-06289; No of Pages 23 (2010).

[1.15] A.G.Mamalis, *Recent advances in nanotechnology*, Journal of Materials Processing Technology, Volume **181**, Issues 1-3, and Pages 52-58 (2007)

[1.16] A. Jaworek, *Electrospray droplet sources for thin film deposition*, A review, J. Materials Sci. **42** (1) 266–297 (2007).

[1.17] A. Jaworek, *Micro- and nanoparticle production by electrospraying*, Powder Technology, Volume **176**, Issue 1, Pages 18-35 (2007)

[1.18] W.V. Prescott and A.I.Schwartz, *Nanorods, nanotubes and nanomaterials research progress*, Nova Science Publishers, USA (2008)

[1.19] M.G. Lines, *Nanomaterials for practical functional uses*, Journal of Alloys and Compounds, Volume **449**, Issues 1-2, Pages 242-245 (2008)

[1.20] T. Flynn and C.Wei, *The pathway to commercialization for nanomedicine*, Nanomedicine: Nanotechnology, Biology and Medicine, Volume **1**, Issue 1, Pages 47-51 (2005)

[1.21] J.Miller, *The Columbia Science and technology law review 2003: Beyond biotechnology: FDA regulation of nanomedicine*, **4** Colum. Sci. & Tech. L. Rev. 2 (2003)

[1.22] M. Goldberg, R. Langer and X.Q. Jia, J. Biomater. Sci., Polym, Ed.**, 18** (3), 241-268 (2007)

[1.23] P.Y.W. Dankers and E.W.M. Bull, Chem. Soc. Jpn. **80** (11), 2047-2073 (2007)

[1.24] P.Y.W. Dankers, M.C. Harmsen, L.A. Brouwer, M.J.A. van Luyn and E.W. Meijer Nat. Mater.**, 4** (7), 568-574 (2005)

[1.25] http://en.wikipedia.org/wiki/Nanomechanics(access on 21/04/2010)

[1.26] T. Ondarcuhu, C. Joachim, *Drawing a single nanofibre over hundreds of microns*, Europhys Lett; **42** (2):215–20 (1998)

[1.27] L. Feng, S. Li, H. Li, J. Zhai, Y. Song, L. Jiang, D. Zhu, *Super-hydrophobic surface of aligned polyacrylonitrile nanofibres,* Angew Chem Int Ed;**41** (7):1221–3 (2002)

[1.28] C.R. Martin, *Membrane-based synthesis of nanomaterials*, Chem Mater; **8**:1739–46 (1996)

[1.29] P.X.Ma, R. Zhang, *Synthetic nano-scale fibrous extracellular matrix*, J Biomed Mat Res; **46**:60–72 (1999)

[1.30] G. Liu, J. Ding, L. Qiao, A. Guo, B.P. Dymov, J.T. Gleeson, T. Hashimoto and K. Saijo, *Polystyrene-block-poly(2-cinnamoylethyl methacrylate) nanofibres-Preparation, characterization, and liquid crystalline properties*, Chem-A European J; **5**:2740–9 (1999)

[1.31] G.M.Whitesides and B.Grzybowski, *Self-assembly at all scales*, Science; **295:**2418–21 (2002)

[1.32] J. M. Deitzel, J.D. Kleinmeyer, J.K. Hirvonen, N.C.B.Tan, *Controlled deposition of electrospun poly (ethylene oxide) fibres*, Polymer; **42**:8163–70 (2001)

[1.33] H. Fong, D.H. Reneker, *Electrospinning and formation of nanofibres*, In: Salem DR, editor. Structure formation in polymeric fibres. Munich: Hanser, p. 225–46 (2001)

[1.34] Z. M. Huang, Y. Z. Zhang, M. Kotaki, S. Ramakrishna, *A review on polymer nanofibres by electrospinning and their applications in nanocomposite*s, Composites Science and Technology, Volume **63**, Issue 15, Pages 2223-2253 (2003)

[1.35] A. Frenot and L. S. Chronakis, *Polymer nanofibres assembled by electrospinning*, Current Opinion in Colloid and Interface Science **8**, 64–75 (2003)

[1.36] A. Formhals, US Patent, 1-975-504 (1934).

Chapter 2: Literature survey and background study

2.1. Short history of the polymer spinning

The demand for synthetic fibres has increased drastically over the last 50 years. Rayon (1910), Acetate (1924) the grand quests to out do the silkworm lead to Rayon. These earliest synthetic fibres were still based on cotton or tree pulp cellulose ("biopolymers"). The pulp was deconstructed into fluffy white cellulose, and then turned into a viscose resin which was squeezed through spinnerets that resembled a shower head, and hardened as a "manufactured fibre from natural plants." Because of the Great War and other more profitable uses such as dope for airplane wings and celluloid for motion pictures, it took until 1924 for "artificial silk" to grab significant market share of hosiery, blouses, and linings. These "cellulosic fibres" have passed their peak as cheap petro-based fibres (nylon and polyester) and have displaced regenerated pulp fibres [1].

The first synthetic fibre Nylon 6.6 was developed by Wallace H.Carothers in the laboratories of DuPont in the year 1937. Paul Shlack of IG Farbenindustrie then invented Nylon 6 fibre processing technique in 1938. DuPont and Calico printers association in UK, developed acrylic and polyester fibres, respectively. In 1954, Natta and Zielger patented a process for industrial production of polypropylene fibres. The Poly (vinylalchol) fibre was developed in Germany during the Second World War [2].

These polymer fibres are traditionally produced by spinning from solution, melt, liquid crystalline state, or gel state are now also used in wide range of applications from textiles to composite reinforcement [3]. Low tenacity, high surface area to volume ratio, superior mechanical, chemical and biological properties were the ideal requirements of the produced fibres. The diameter of fibres produced by this conventional process typically varied from 10 to 500 μm [4]. A constant attempt has been made to produce fibres with diameter of sub micron size for various kinds of applications. Unlike conventional fibre spinning techniques, electrostatic spinning or electrospinning is a process that is capable of producing polymer fibres in the nanometre diameter range. Electrospinning is not a new technology for polymer fibre production. It has been known since the 1930's: however, it did not gain significant industrial importance due to the low output of the process, inconsistent and low molecular orientation, poor mechanical properties and high diameter distribution of the electrospun fibres [5]. Now

in our days these electrospinning processes uses a high voltage electric field to produce fibres of nano scale diameter from a polymer melt or solution. The ease with which the deposition of polymer fibres on a target substrate can be controlled enables formation of complex three-dimensional shapes. The electrospinning of two different polymers together is also possible to achieve intermediate properties of the two polymers. A wide range of properties can be achieved by varying the type of polymer spun. Small insoluble particles, soluble drugs, and anti-bacterial agents can also be incorporated into the fibre to achieve the desired end properties [6].

Though the technology of producing polymer fibres from an electro statically driven jet of polymer solution or melt has been known for more than 100 years, it was first patented in the year 1934 [7]. Conventional fibre spinning e.g., melt spinning, dry spinning or wet spinning, rely on mechanical forces to produce fibres by extruding polymer melt or solution through spinnerets and subsequently drawing the resulting filaments as they solidify or coagulate. Electrospinning offers a fundamentally different approach to fibre production by introducing electrostatic forces to modify the fibre formation process. Since then many detailed studies have been carried out to study the electrospinning process from both solution and melt [8].

In 1981, Larrondo and Manley [9] were able to produce nano sized fibres by electrospinning rapidly crystallizing polyethylene and polypropylene from the melt.

Reneker and Chun [10] revived the interest in electrospinning process in the early 1990's by studying more than 20 polymers in their laboratory; demonstrating the ability to produce nano sized fibres from many polymers. Most of the fibres made by Reneker were spun from solution, though a few polymers were spun from melt using vacuum and air. Subsequently, wide range of polymers used in conventional fibre spinning process was using the electrospinning process. These include Nylon (6, 66, 64), Poly(ethylene terepthalate), Poly(ethylene oxide), Polystyrene, Polycarbonate, Kevlar, polyacrylonitrile, poly(vinylalchol), Poly(benzimidazole), Polyaniline and biopolymers like proteins, DNA, polypeptides produced from solution. The Poly(ethylene terepthalate), polyethylene and polypropylene have also been spun from melt. The electro spinning process is also used to spin electrically conducting and photonic polymers [6, 9- 10].

The important properties of these nano size fibres make them commercially for filtration, catalysis and adsorption. Large length to diameter ratio and small mass to

volume ratio of these nano-sizes fibres widens the areas of their application further. These properties of nano fibres are exploited by current researchers to determine appropriate conditions for electrospinning various polymers and biopolymers for many applications, including multifunctional membranes, biomedical structural elements (scaffolding used in tissue engineering, wound dressing, drug delivery, artificial organs and vascular grafts), protective shields in specialty fabrics, filter media for submicron particles in separation industry, composite reinforcement and structures for nano-electronic machines [6].

Another interesting application of the electrospinning process is the possibility of spinning two mutually insoluble polymers by spinning them from a common solvent. When polymer blends are spun from a common solvent using this method, there is a possibility of phase separation like in any other method used to produce polymer fibres. However the rapid evaporation of the solvent may prevent phase separation, making this method suitable to produce a homogenous phase for almost any polymer pair that is melt immiscible but soluble in a common solvent.

2.2 Literature review

2.2.1 Introduction

In the second half of the 20th century, the use of polymers in our daily life has grown tremendously. Polymers are used in different forms and for a wide range of applications. Noticeable among these are the synthetic and regenerated polymers that have found applications in not only the textile and apparel sector but also in numerous industrial usages like tire cords, reinforcing and structural agents, barrier films, food and packaging industry, automotive parts, etc. The process of making fibres from polymers generally involves spinning, wherein the polymer is extruded through a spinneret to form fibres under suitable shear rates and temperatures. This conventional fibre formation process is generally followed by drawing that involves the plastic stretching of the as-spun material to increase its strength and modulus. Depending on whether the polymer is in the molten state or in solution, the process is likewise termed as molten state or in solution; the process is likewise termed as melt-spinning or solution spinning respectively. Typical diameters obtained by these conventional spinning methods are about 10 µm and higher [11].

Over the last ten years, a novel technique has been re-explored to generate polymeric fibres in the submicron range. This technique, termed as electrospinning, produce filaments that are in a diameter range one or two orders of magnitude smaller than those obtained from the conventional melt-spinning and solution process because it can generate submicron polymeric fibres. A number of processing technique such as drawing, template synthesis, phase separation, self assembly, electrospinning, etc have been used to prepare polymer nano fibres in recent years [12]. Let us consider them further.

2.2.2 Drawing

Nanofibres have been fabricated with citrate molecules through the process of drawing. A micropipette with a diameter of a few micrometers was dipped into the droplet near the contact line using a micromanipulator (figure 2. 1).

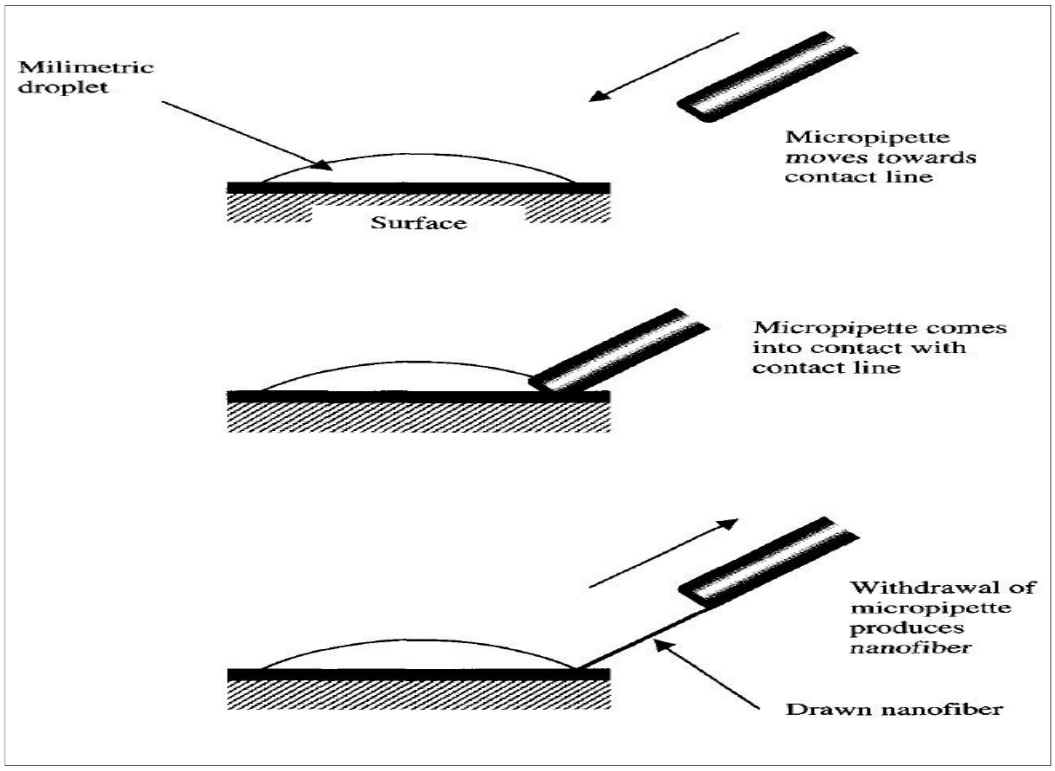

Figure 2.1, Nano fibres by the drawing process [13].

Micropipette was then withdrawn from the liquid and moved at a speed of approximately $1x10^{-4}$ ms^{-1} resulting in a nanofibre being pulled. The pulled fibre was deposited on the surface by touching it with the end of the micropipette. The drawing nano fibre was repeated several times on every droplet. The viscosity of the material at

the edge of the droplet increased with evaporation. At the beginning of evaporation corresponding to part X of the curve, in figure 2.2 the drawn fibre breaks due to Rayleigh instability. During the second stage of evaporation corresponding to part Y of the curve nano fibres is successfully drawn. In the final stage of evaporation of the droplet as corresponding to part Z in the curve. The solution was concentrated at the edge of the droplet and broke in a cohesive manner. Thus, drawing a fibre requires a viscoelastic material that can undergo strong deformation while being cohesive enough to support the stresses developed during pulling. This process can be considered a dry spinning at a molecular level [13].

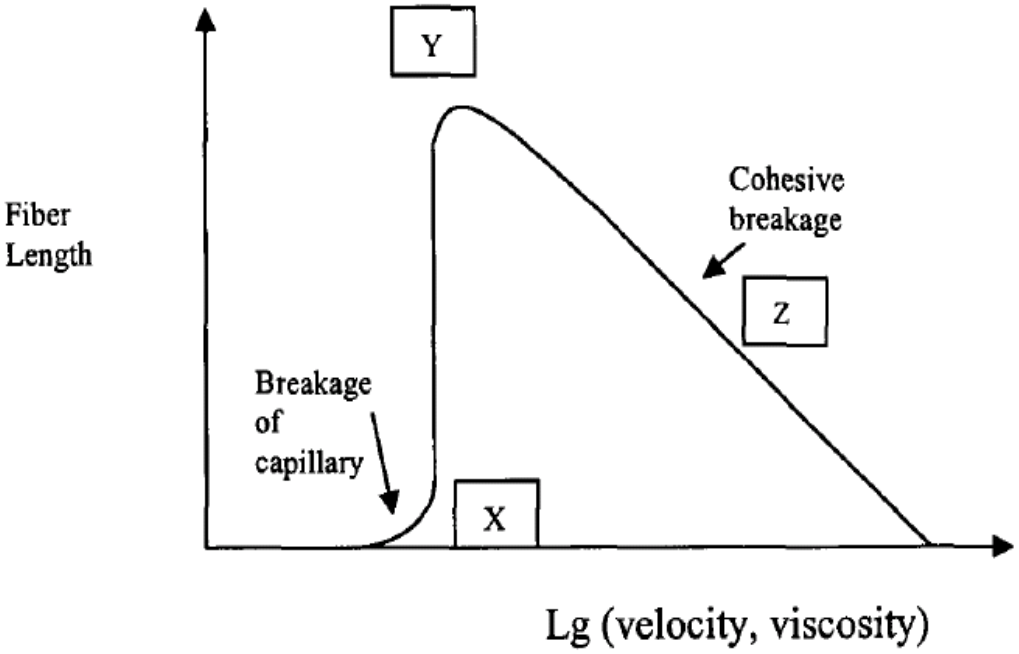

Figure 2.2, Schematic representation of the length of the drawn nano fibre as a function of the drawing velocity and viscosity of the material [13].

***2.2.3 Template synthesis*:**

Template synthesis of nanostructures has been developed independently [14]. Che et. al [15] used template method for chemical vapor deposition when they synthesised carbon nanofibres. Template synthesis implies the use of a template or mold to obtain desire materials or structures [figure 2.3].

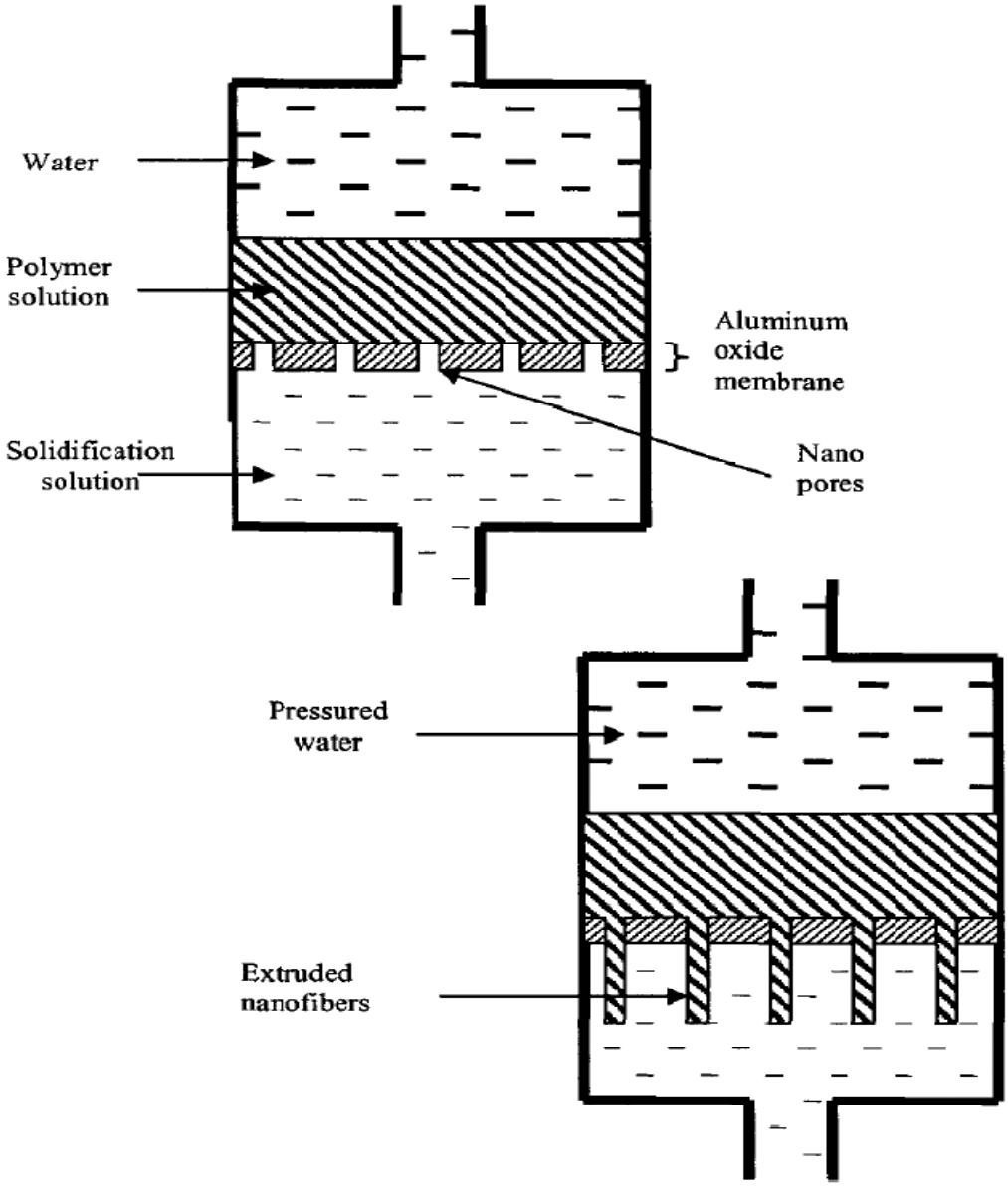

Figure 2.3, Schematic diagram of template synthesis [15].

Hence the casting method and DNA replication can be considered as template-based synthesis for the case of nano fibre creation [16]. The template refers to a metal oxide membrane through thickness pores of nano scale diameter. Under the application of water pressure on the side and restrain from the porous membrane cause extrusion of the polymer which, upon coming into contact with a solidifying solution, gives rise to nanofibre whose diameters are determined by the pores. The template synthesis, as the name suggests, uses a nonporous membrane as a template to make nanofibres of solid (a fibril) or hollow (a tubule) shape. The most important feature of this method may lie in

that nanometer tubules and fibrils of various raw materials such as electronically conducting polymers, metals, semiconductors, and carbons can be fabricated. On the other hand, the method cannot make one-by-one continuous nanofibres.

2.2.4 Phase separation

Phase separation consists of dissolution, gelation, and extraction using a different solvent, freezing, and drying resulting in a nanoscale porous foam. The process takes relatively long period of time to transfer the solid polymer into the nano-porous foam. In phase separation, a polymeric is firstly mixed with a solvent before undergoing gelation. The main mechanism in the process is as the name suggests the separation of phase due to physical incompatibility. One of the phases which are that of the solvent is then extracted, leaving behind the other remaining phase. A detailed procedure for producing nano fibres (PLLA) has been described by Ma and Zhang [17], Zhang and Ma 2002 [18]. They refer to five 5 major steps,

i) Dissolution of polymer. ii) Liquid–liquid phase separation process. iii) Polymer gelation (controls the porosity of nanoscale scaffolds at low temperature). iv) Extraction of solvent from the gel with water. v) Freezing and freeze-drying under vacuum.

The processes they used are as follows;

1) Tetrahydrofuran (THF) was added to PLLA for making solution with the required concentration (1% to 15%). The solution was stirred at 60˚ C for two hours to produce homogenous solution.
2) Two milliliters' of the solution at 50^0C was poured into Teflon vial and then refrigerator set gelation temperature (-18^0C to 45^0C) which was chosen based on the PLLA concentration. Upon formation of the gel it was kept at the gelation temperature for two hours.
3) The vial that contains the gel was immersed in distilled water to allow solvent exchange and the water was changed three times a day for two days.
4) The gel was the removed from water blotted with filter paper and then transferred to freezer at -18^0C and kept for two hours.
5) Finally the frozen gel was transferred into freeze-drying vessel and freeze-dried at -55^0C under a vacuum of 0.5 mm of Hg for a week.

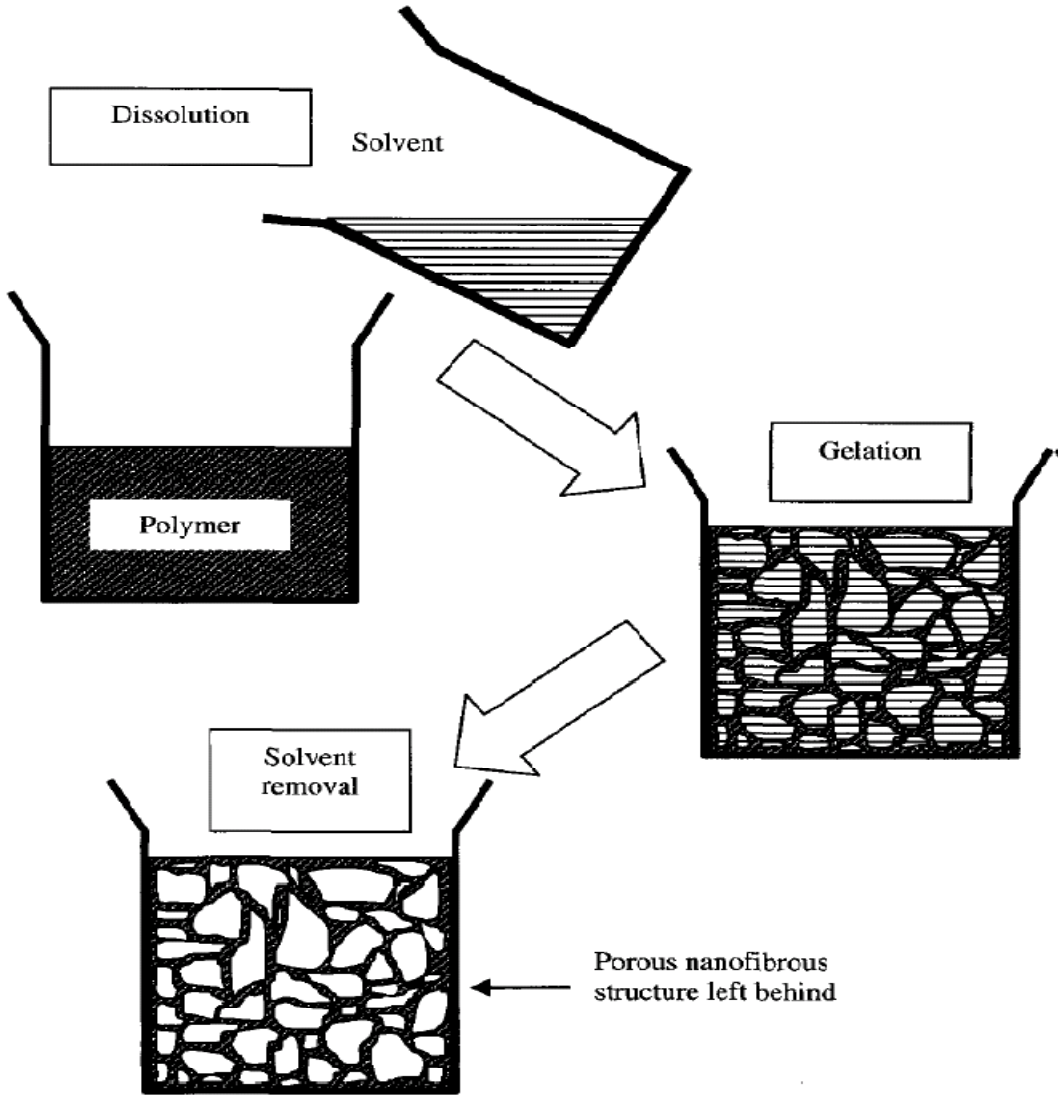

Figure 2.4, Generic Schematic of Phase separations for obtaining nanofibrous structure [17-18].

Tan et.al used this process to get mechanical tensile properties for single nanofibre and composite fibres [19]. Gelation was found to be the most critical step that controlled the porous morphology of the nanofibrous foams. The duration of gelation varied with polymer concentration and temperature. Low gelation temperature led to the formation of the nanoscale fibre networks, whereas high gelation temperature led to the formation of a platelet-like structure due to the nucleation of crystals and their growth. This limitation of platelet-like structure formation was overcome by increased cooling rates that produced uniform nanofibres. However, the average diameter of fibres was not significantly affected by gelation condition or polymer concentration [20].

The advantage of the phase separation process is that it is a relatively simple procedure and the requirements are very minimal in terms of equipment compared with techniques, such as electrospinning, and self-assembly. It is possible to directly fabricate a medical scaffold for a desired anatomical shape of a body part with a mold. Another advantage is the simultaneous presence of nano and macro architecture that can be beneficial in terms of cell response at the nanofibre level, and in terms of cell distribution and tissue architecture at the macro porosity level [21].

2.2.5 Self assembly

The self-assembly is a process in which individual, pre-existing components organize themselves into desired patterns and functions. However, similarly to the phase separation the self-assembly is time-consuming in processing continuous polymer nanofibres. In general self-assembly of nano fibres refer to the buildup of nano scale fibres using smaller molecules as basic building blocks. Various techniques have been reported by Yu et. al [22], Fields et. al [23] and Hartgerink et. al [24, 25]. Figure 2. 5 based on the process used by Hartgerink et. al [25]. Here a small molecule (figure 2.5 – top) arranged in a concentric manner such that bonds can form among the concentrically arranged small molecules (figure 2.5- middle) which, upon extension it normal gives the longitudinal axis of a nano fibre (figure 2.5-bottom).

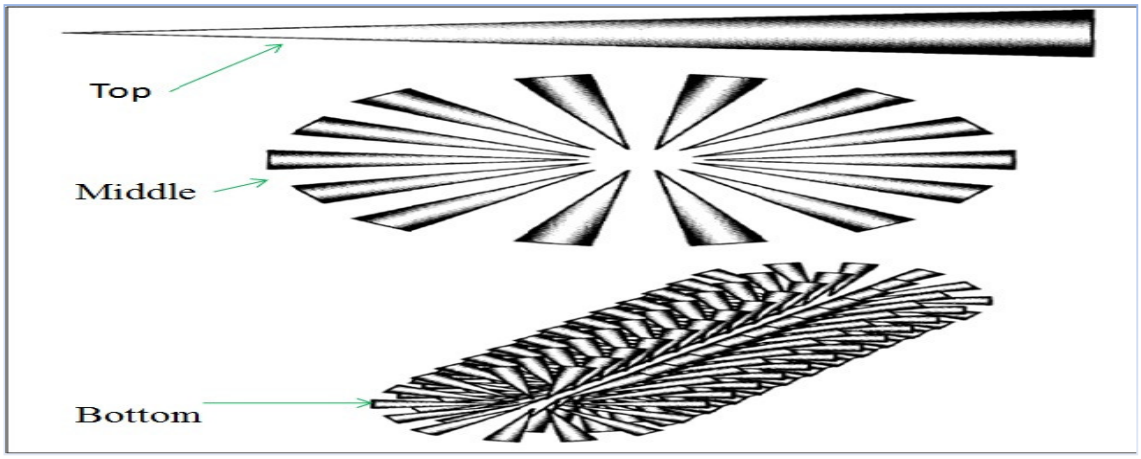

Figure 2.5, Schematic diagram for self assembly. Shape of the macromolecular nano fibre [24, 25].

The main mechanism for a generic self-assembly is the intermolecular forces that bring the smaller units together and the shape of the smaller units of molecules which

determination the over shape of the macromolecular nanofibre. In another study, Hartgerink et. al [26] investigated the effect of variations in the molecular structure of the PAs on the self-assembled nanofibres. It was observed that modifications in the alkyl chain length of the PA alter the pH sensitivity of nanofibres, which affects self-assembly. Modification of the C- terminal region (i.e., the region that is expressed on the surface of the nanofibres after self-assembly) led to changes in length and stiffness of the nanofibres. Replacement of cystine residues by alkaline did not affect the self-assembly of the PAs into nanofibres. These results suggested that the self-assembled nanofibres show potential for development as novel biomaterials [26, 27]. This study also introduced three different methods of forming self-assembled PAs, including pH-controlled self-assembly, drying on surface-induced self-assembly, and divalent-ion-induced self-assembly. The study demonstrated that PAs can be self-assembled reversibly into nanofibres that result in the formation of gels through pH changes. These PA nanofibres can also be reversibly polymerized to improve their stability. The reversibility of these two procedures makes the self-assembly technique attractive as it enables the fabrication of remarkably versatile materials. In addition, this technique produces a good yield of nanofibres with low polydispersity. Therefore, the self-assembly technique, by virtue of the modifications possible in the structure of the PA, enables a variety of self-assemblies including layered and lamellar structures, and by virtue of the aforementioned reversibility's lends flexibility to the system. Thus, the self-assembly technique shows good potential for further exploration with the goal of designing novel scaffolds for tissue engineering applications

2.2.6 Electrospinning

Electrospinning represents an attractive technique for the processing of polymeric materials into nanofibres. This technique also offers the opportunity for control over thickness and composition of the nanofibres along with porosity of the nanofibre meshes using a relatively simple experimental setup [10].

This technique incorporates the generation of a strong electric field between the polymeric melt within the extruder and metallic collecting devices [28-29]. Expected improvements in the technique of electrospinning from liquid crystal or other disentangled systems may produce even thinner fibres [10].

Another technique of produce polymeric nanofibres has recently been introduced by Nanofibre Technology Inc. of Aberdeen, NC. In this method nanofibres are created by

melt blowing fibre with a modular die. The fibres produced are a mixture of both micron and submicron sizes. Another technique that is used to produce nanofibre is spinning bio-component fibres that split or dissolve. There are several approaches to using this technology to make nanofibres such as island-in-the-sea. The production of live islands-in-the-sea (INS) fibres using a standard spin/draw process [30].

2.2.6.1 Review of the electrospinning process

There is a lot of talk about the electrospinning process and their application in the patent and academic literature. The electrospinning of fibres dates back to 1934 when Formhals [31] invented the electrostatic apparatus. As shown in figure, 2.6. The spinning solution was discharged using a high electric field from an electrode of positive polarity. The fine filaments were attracted towards the movable electrode of negative polarity. A stripping device facilitated the removal of fibres in the form of fibrous sliver. A major drawback of such a setup was the difficulty to remove the fine fibres that adhered to the moving parts of the collecting belts, drums, wheels etc. Formhals formed fibres from a solution of cellulose acetate in ethylene glycol at a potential difference of 5-7 kV.

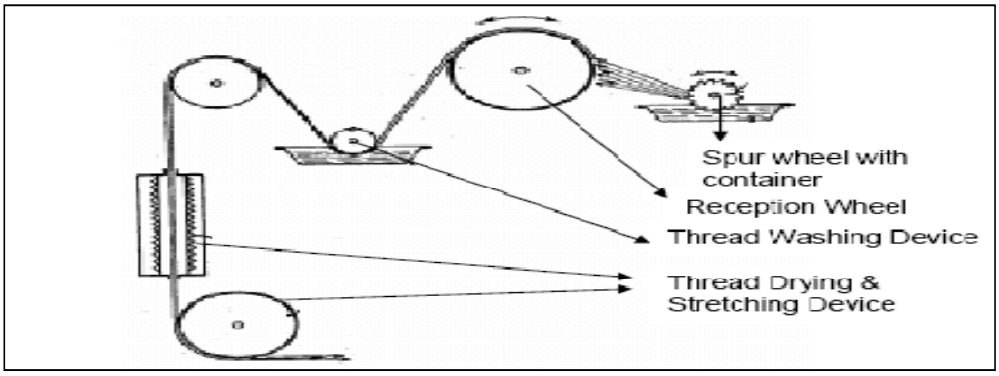

Figure 2.6, Apparatus for electrostatic spinning used by Formhals [31].

Taylor showed that instability of an elongated drop would not occur unless a pressure differential exists. His paper demonstrated that a conical interface between two fluids could exist in equilibrium in an electric field [32]. At the onset of instability, the droplet elongates and its end develops a conical shape called the "Taylor Cone", which theoretically had a semi angle close to 49.3˚ at the vertex. This was even shown and proved through unstable and charged drops of liquid emitted to give a space-charge zone in front of the cone. As the electric field approaches the breakdown field at the

apex the radius of curvature of the apex of the cone changes accordingly to sustain the field. The electric pressure due to the maximum charge that can reside on the cone surface is balanced by the surface tension of the liquid.

In 1969 Taylor published theoretical and experimental work on the disintegration of pure as well as mixture of liquids drops and electrified jets [33]. Taylor correlated his experimental observations with a theoretical model and in this process he obtained an expression for critical potential at which the droplets become unstable. He showed that Zelany's mechanism of droplet disintegration was based on a false assumption that instability happens when the internal pressure is the same as that outside the droplet. In his experimental set up (figure 2.7), he explains the voltage required for the fluid to be drawn from the tube. The polymer was stored in reservoir C and when the voltage was increased, the surface of the meniscus of the fluid, D, emerging out from the metal tube A, became convex till the critical voltage, after which it no longer can be stable. The potential difference was maintained by two parallel plates B and E. At this point it emits a jet towards the target plate B.

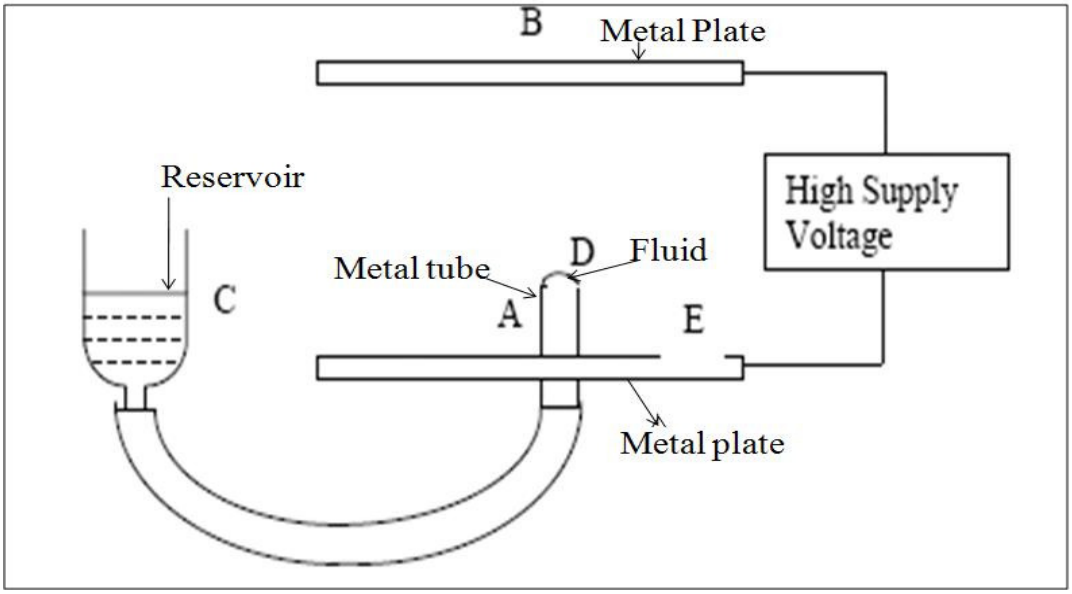

Figure 2.7, Schematic drawing of the apparatus used by Taylor (A-metal tube, B &E-metal plates, C-reservoir, D-hemispherical droplet) [33].

In 1966, Simons [34] invented a process to produce a patterned non-woven fabric by electrospinning that was collected on a segmented receiver. The segmented receiver had two sets of segments such that one of the sets was at a different potential then the other causing the preferential deposition of fibres leading to patterned fabric that had regions

of low and high fibre density. Filaments were electrospun from a solution of polyurethane in methylethyleketon having a viscosity in the range of 100 to 3000 centipoises. In a different process Isakoff [35] devised a process to prepare fibrous sheets of organic synthetic polymers in which filamentary web of fibres were electrostatically charged before being collected on a grounded movable surface. Fibres were electrically charged after they were formed by conventional solution spinning to facilitate their passage in a controlled trajectory.

Utilizing a different geometry of the electrospinning apparatus, Fine et. al [36] electrospun a thermoplastic elastomer where a cup-like apparatus contained the charged polymer solution that rotated about its vertical axis. The centrifugal forces pushed the polymer solution to the edge of the cup and into the ambient air. The presence of an electrical field caused the formation of the jet was attracted to a grounded movable aluminum screen that was driven slowly around the rollers in the form of a belt. The combined action of electrostatic and centrifugal forces led to the formation of high strength fibrous sheets. Instead of placing the polymer solution in a cup, Guignard [37-38] utilized another movable belt that carried the charged molten polymer. Here, two movable belts were used, as shown in figure 2.8. As one of the belts, which carried the charged molten polymer, approached the grounded belt, formation of several jets from the surface of the exposed melt took place. These jets travelled towards the grounded collector belt and got deposited in the form of short filaments on the grounded belt.

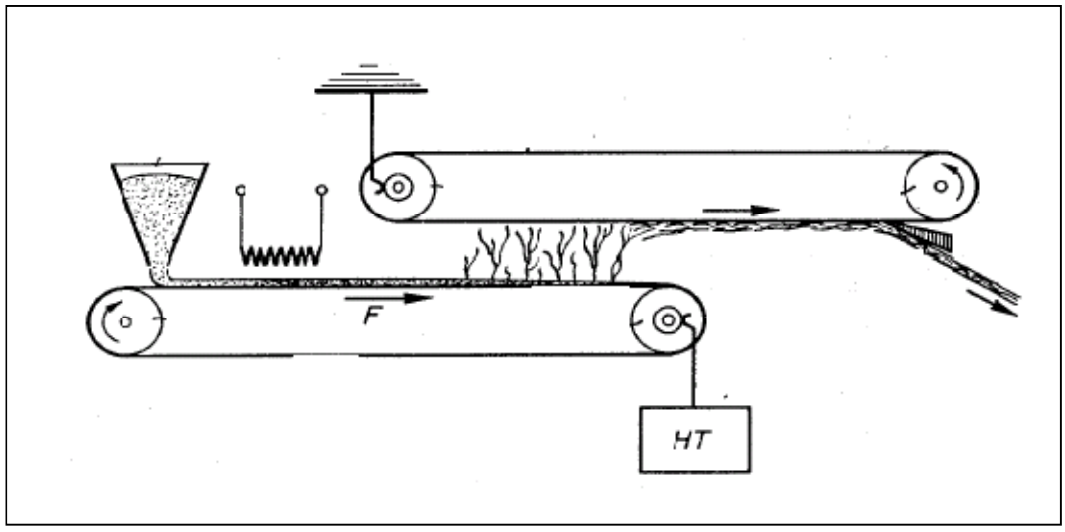

Figure 2.8, Schematic of Guignard's electrospinning set up [37].

Baumgarten in 1971 [39] carried out experiments involving electrostatic spinning to produce acrylic micro fibres. The acrylic resin used was a commercial copolymer of 93.6% acrylonitrile, 6% methyl acrylate and 0.4% sodium styrene sulfonate and the solution was prepared in dimethyl formamide. The experimental apparatus (figure 2.9) consisted of stainless steel capillary tube through which the polymer drop was suspended and to maintain constant drop, infusion pump was incorporated. Potential difference was maintained between capillary tube and a ground metal screen. A camera was attached in line with the spinning fibre for photographic study. The analysis showed that viscosity of the solution increased, the spinning drop changed its shape to conical from hemisphere and the length of the jet increased. It was also observed that the fibre diameter increased with increased viscosity and was approximately proportional to jet length. Electron photomicrographs obtained showed that the fibre had the appearance of smooth, straight cylinders. As the solution flow rate increased, the jet length almost doubled but there was not much change in the diameter of the fibres.

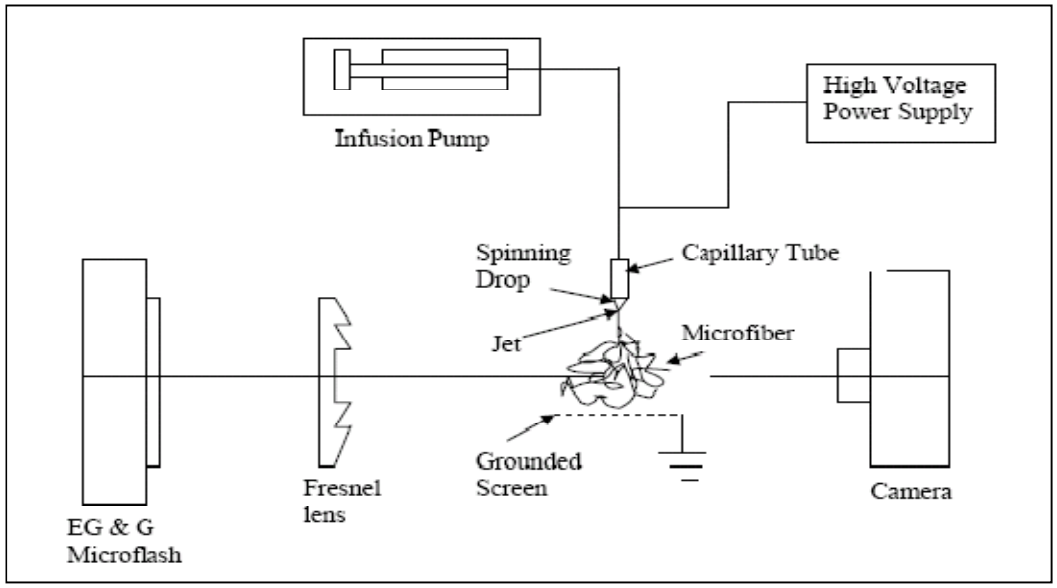

Figure 2.9, Electrospinning apparatus with photographic setup used by Baumgarten [39].

In other study, in 1977 Martin et. al [40-41] extended the concepts of a single component electrospinning to electrospin a mat of organic fibres from liquid containing components from a single nozzle/syringe. They were also able to electrospin polymeric solution having different compositions (blend) simultaneously from multiple nozzle/syringes. Collectors were either a stationary metal screen or movable belt. The

patent claimed the mat to be composed of fibres of a high molecular weight thermoplastic polymer based either on a fluorinated hydrocarbon, silicon or a urea/formaldehyde. The resulting mats were flexible, non absorbent, porous and hydrophobic. The spinning material is fed into an electrostatic field from a syringe rervoir to the tip of an earthed syringe needle shown at figure 2.10 (5). An electrostatically charged surface was placed at an appropriate distance. Fibre is formed between the tip of the syringe needle and the charged surface. Potential maintained was around 20 kV at a distance of 5-35 cm between syringe needle and collecting surface. Mats collected on a rotating non conducting belt had a few microns to few centimetres thick, highly porous, low diameter and high surface area. These fibre mats were supposedly made for medical purpose specially wound dressing.

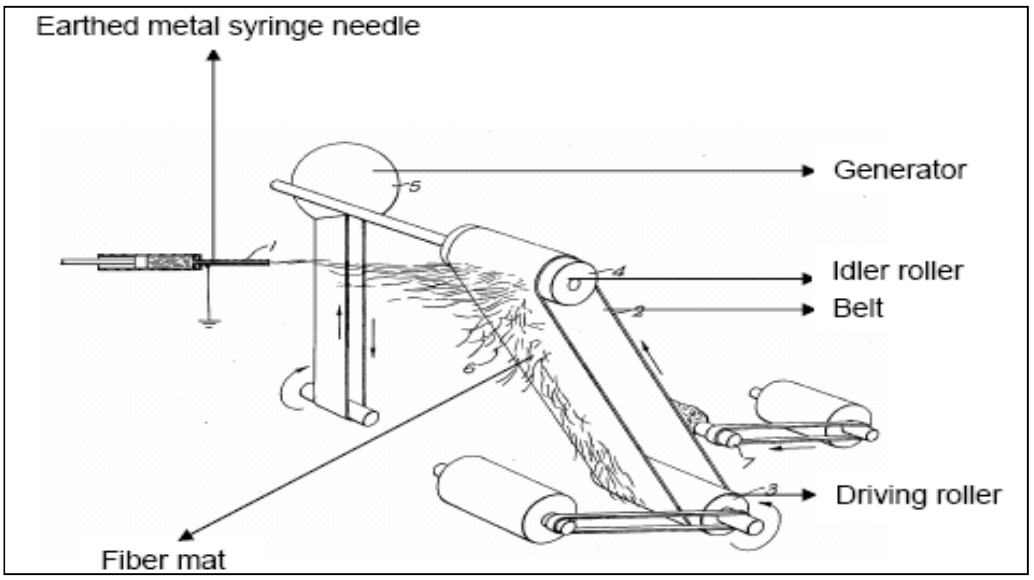

Figure 2.10, Schematic diagrams used by Martin et. al to produce continuous fibres [40].

Simm et.al [42] in 1978 described a process of producing filters made of electrostatically spun fibres from polystyrene. The spraying of the spinning solution placed in storage tank was from a rotating annular electrode, overcoming the problem of blockage of spray edge by the drying up of liquid (figure 2.11). Spinning takes place in the spray chamber and movable electrodes like conveyor belts carry the collected fibres. Apart from the air temperature and relative humidity for producing thin, dry filaments, it was observed that electrical conductivity of the spinning solution affects the thickness of the fibres formed.

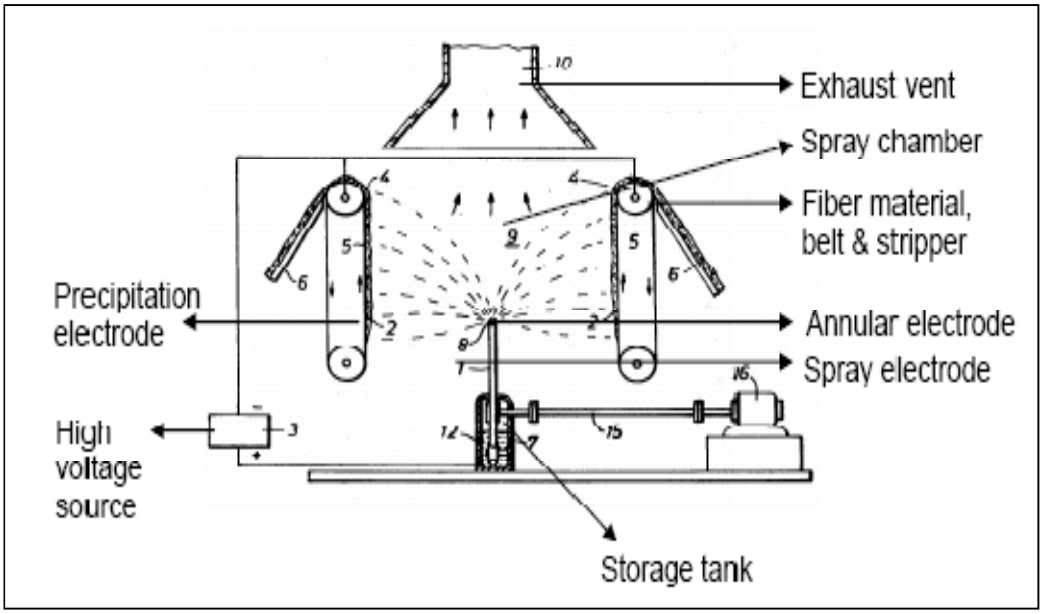

Figure 2.11, Apparatus for the production of fibre used by Simm et. al [42].

In 1982, Bornatt [43] conducted simultaneous electrospinning by using several nozzles/syringes to form fibres. As shown in figure 2.12, the syringe was filled with the polymer solution and placed a certain distance from the collector that was in the form o a long metallic cylinder. The syringe was kept at a ground potential whereas an electrical potential of 50 kV was applied to the collector. The electrostatic forces caused the formation of jets that were attracted towards the rotating collector. Solidified polymer filaments of poly (tetrafluoroethelene) and poly (ethylene oxide) were wound on the rotating collector in this fashion to form a tubular product. The tubular products were suggested to find application as synthetic blood vessels and urinary ducts. Utilizing a slightly different approach, Simm et. al [42] were able to fabricate a composite filter based on electrospun fibres. They invented a process for the production of fibre filters in which a solution of polystyrene in methylene chloride was electrospun from annular electrode onto two equidistant collector electrodes in the form of movable belts. The collector electrodes were already covered with a layer of cellulose fibres produced by conventional spinning method. Thus a composite filter that had electrospun polystyrene fibres on top of a layer of cellulose fleece was fabricated.

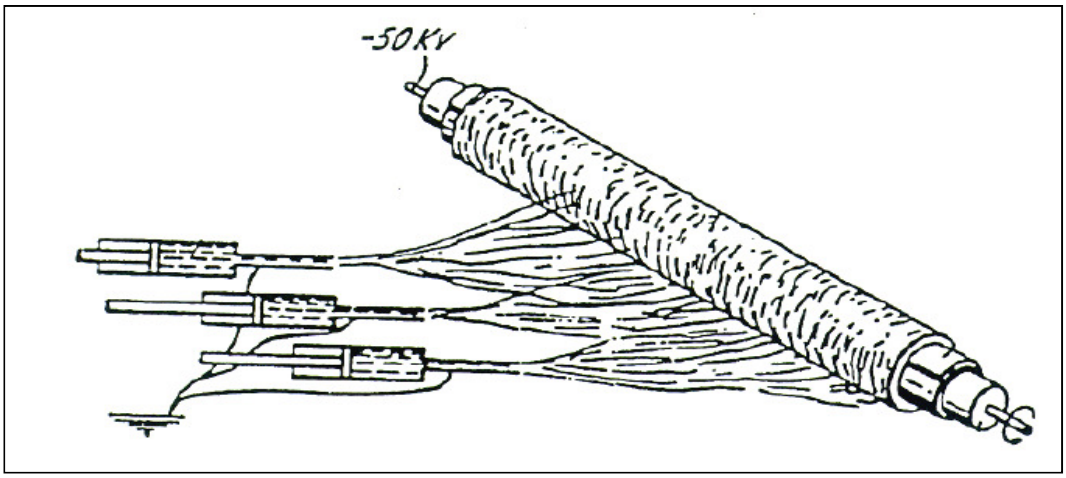

Figure: 2.12, Schematic of Bornat's electrospinning set up [43].

How [44] described a process for the production of synthetic vascular grafts from polyurethane. The polymer solution was ejected through a stainless steel nozzle from a syringe, where in the nozzle is earthed (figure 2.13). Flow of the polymer solution through the nozzle is maintained by the syringe piston, which is subjected to a constant hydraulic force. Fluid from the nozzle is fed to an electrostatic field surrounding a charged mandrel which is charged to around 12 kV. Because of high electric potential, filaments are drawn and collected here. The invention essentially relies on the controlling the speed of rotation of the mandrel (rpm between 2000 to 20000) such that a desired degree of anisotropy is present in the graft. This is because; the purpose for which these grafts are produced is that the natural arteries are generally anisotropic.

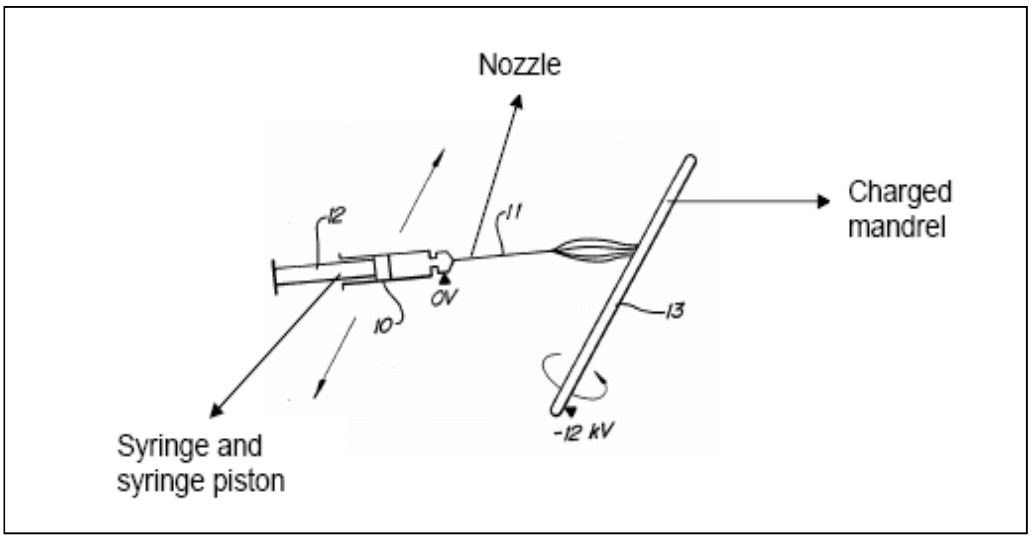

Figure 2.13, Diagrammatic illustration of electrospinning system used by How [44].

Berry [45] invented a method for producing electrostatically tubular fibrous spun products using polyurethanes. The spinning solution is fed into the electrostatic field through capillary needle. The emerging droplets were attracted towards on electrostatically charged mandrel kept at a distance. The mandrel consisted of two charged grids, and a potential of 6 to 12 kV is maintained. Because of the two charged grids the tubular fibrous structure produced had fibres of different diameters and varying fibre orientations along their length, as the needle traversed. These low diameter fibres were oriented circumferentially around the tube. Offered little resistance to bending and assumed a very tight loop without kinking. The produce assembly had greater axial compliance and when compressed along its axis, it shorted with a minimal tendency to buckle.

In 1999, Pike [46] produced that a web containing superfine micro fibres. The web contains a blend of a first group of split micro fibres which contained a first polymer component and a second group of split micro fibres which contained a second polymer component, wherein at least one of the polymer components is hydrophilic. His invention additionally provides a melt blown fibre web having at least two groups of fibres, wherein each group of the fibres has a distinct cross-sectional configuration.

In 2000, Scardino et. al [47] have patented a process to make a hybrid/composite yarn. The electrospun fibres having diameters ranging from 0.4 nm to 1 nm were suctioned into an air vortex and then combined with carrier filaments (obtained from conventional spinning technique) to form non woven or linear (yarns) assemblies. The yarns were later utilized for weaving, braiding or knitting fabrics. The electrospinning principles utilized were very similar to those mentioned above with some differences in the engineering details of the apparatus.

In 2001, Frank. K. Ko et. al [48] stated that the electrospinning process can produce ultrafine conductive polymer fibres. To make conductive polymer fibres they used polyethylene oxide and polyaniline blend. They used the process to make conductive polymer fibres by electrospinning from a polymer dissolved in an organic solvent. A high voltage electric field is generated between opposite charged polymer fluids in a glass syringe (4) in which the capillary tip (5) a metallic collection screen (2) and cause a polymer jet (3) to flow the screen (2) as the solvent evaporates and collecting fibres on the screen as seen figure 2.14.

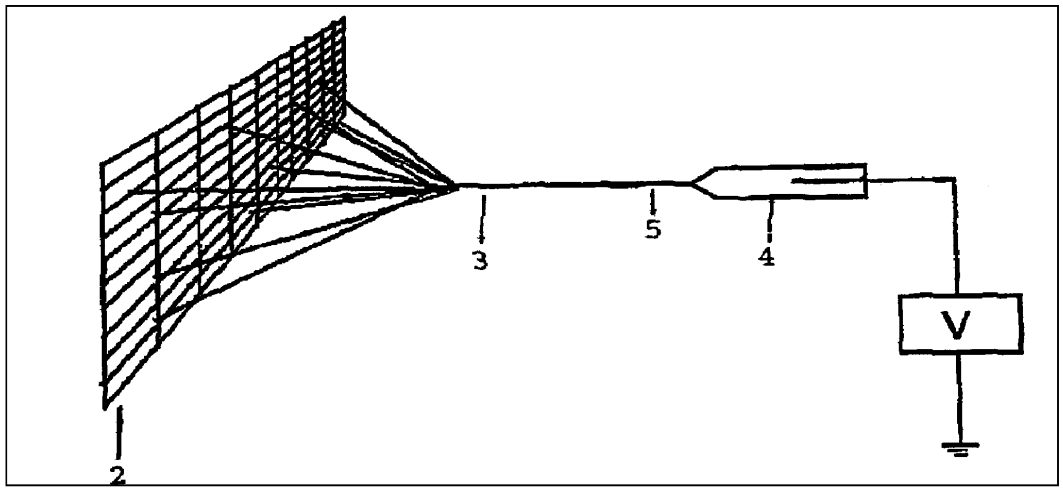

Figure 2.14, Schematic diagram of electrospinning by Frank. KO et. al [48].

In 2002, Balkus et. al [49] describes a system to produce nano composites fibre. They used a nitrogen source, whose pressure can be controlled by a foot-pedal, as was attached to the other ends of the plastic barrels. A glass "T'' is used to split the source of the nitrogen outlet. A low nitrogen pressure is applied to the gel to ensure a steady flow of the viscose gel. The two syringe barrels are placed one above the other in such a way that the needles are in close proximity to each other. A single negative electrode is attached to the target. A distance of 20-25cm was maintained between the tip of the syringe barrels with needles, and the targets which get exposed to high voltage, and are placed in a plexi-glass box for safety.

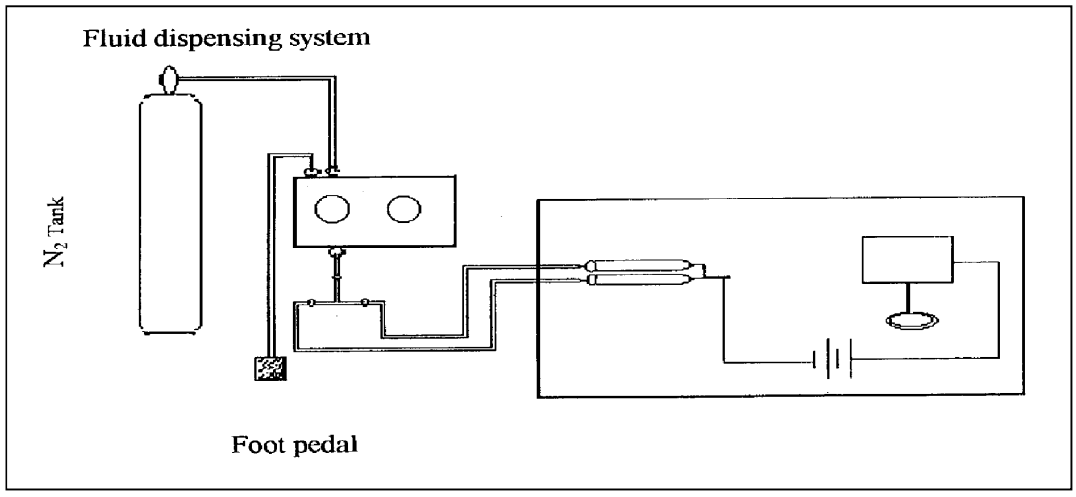

Figure 2.15, Schematic diagram of electrospinning process by Balkus [49].

In 2005, Hag-Yong Kim [50] devised a method for preparing a non-woven fabric coated with nano fibres comprising the steps of: spinning the nano fibres on one surface or both

surfaces of a fabric by one or more electrospinning apparatuses including a spinning dope drop device, and bonding the nanofibres.

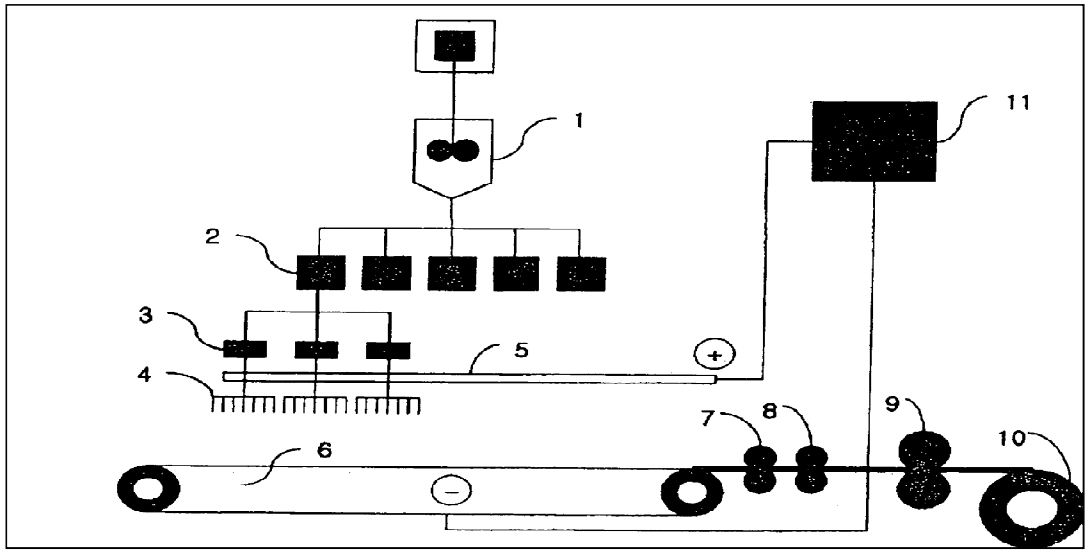

Figure 2.16, Schematic diagram of electrospinning process by Kim [50].

The electrospinning apparatus includes a spinning dope main tank 1 for storing a spinning dope: a metering pump 2 for quantitatively supplying the spinning dope: a nozzle block 4 having block-type nozzles composed of a polarity of pins and discharging the spinning dope in a fibre shape: a collector 6 positioned at the lower end of the nozzle block 4, for collecting spun single fibres: a voltage generator 11 for generating a high voltage; a voltage transmission rod 5 for transmitting the voltage generated in the voltage generator 11 to the upper end of the nozzle block 4; and spinning dope drop device 3 positioned between the metering pump 2 and the nozzle block 4. They used Nylon 6 polymer and produced coated electrospun fibres.

In 2006, Andrady et. al [51] use rotable spray head to produce electrospinning fibre. Electrospray/electrospinning techniques are used to form particles and fibres as small as one nanometer in a principal direction. The phenomenon of electrospray involves the formation of a droplet of polymer melt at one end of a needle, the electric charging of that droplet, and an expulsion of parts of the droplet because of the repulsive electric force due to the electric charges. In electrospraying, a solvent present in the parts of the droplet evaporates and small particles are formed but not fibres. The electrospinning

technique is similar to the electrospray technique. However, in electrospinning and during the expulsion, fibres are formed from the liquid as the parts are expelled.

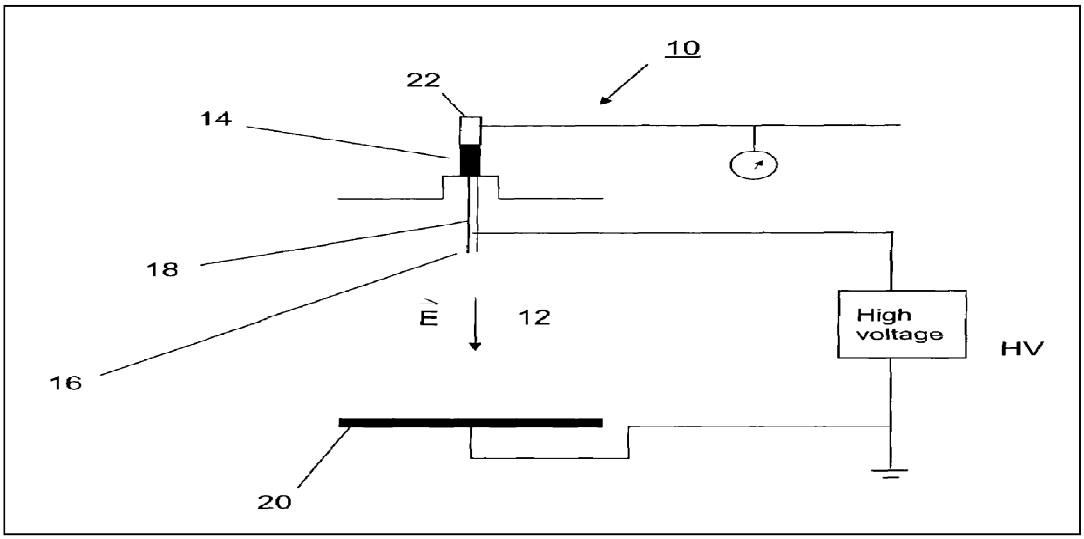

Figure 2.17, Schematic diagram of electrospinning process by Andrady [51].

For the production of nanofibres, a basic electrospinning apparatus by Andrady et. al [51] is shown in figure 2.17. The apparatus 10, produces an electric field 12, that guides a polymer melt or solution 14, extruded from a tip 16, of a needle 18, to an electrode 20, an enclosure/ syringe 22, store the polymer solution 14. Conventionally, one end of a voltage source HV is electrically connected directly to the needle 18, and the other end of the voltage source HV is electrically connected to the electrode 20. The electric field 12 created between the tip 16 and the electrode 20 causes the polymer solution 14 to overcome cohesive forces that hold the polymer solution together. A jet of the polymer 14 is drawn from the tip 16 toward the electrode 20 by the electric field 12 (i.e. electric field extracted), and dries during flight from the needle 18 to the electrode 20 to form polymeric fibres. The fibres are typically collected downstream on the electrode 20.

In 2006, Dubson et. al [52] patented the method for manufacturing polymer shells via electrospinning. They used polycarbonate as a polymer because of their good fibre forming abilities and chloroform as a solvent. The fibre shells later use as vascular grafts.

In 2007, Laurencin et. al [53] developed Polymeric nanofibres which are useful in a variety of medical and other applications, such as filtration devices, medical prosthesis, scaffolds for tissue engineering, wound dressings, controlled drug delivery systems,

cosmetic skin masks, and protective clothing. These can be formed of any of a variety of different polymers, either non-degradable or degradable. In a preferred embodiment demonstrated in the following examples, nanofibres are formed of biodegradable and non biodegradable polyphosphazenes, their blends with other polyphosphazenes or with organic/inorganic metallic polymers as well as composite nanofibres of polyphosphazenes with nano-sized particles such as hydroxyapatites.

In 2008, Yong Lak Joo et. al [54] discovered an apparatus and process avoiding the disadvantages of conventional electrospinning apparatus can be avoided and providing useful melt electrospinning production of polymer and nanocomposite fibres/non-woven's. This solution electrospinning apparatus is suitable for polymers which are not dissolvable in acceptable solvents at room temperature, and can be provided by this on unique heating apparatus/ process. This system is providing a temperature for the polymer or nanocomposite and solution there of being subjected to electrically induce bending instabilities/whipping motions and fibre elongation to provide against premature solidification and to provide against induction of relaxation of molecular orientation and potentiate flashing off of solvent, without affecting the electrically induced bending instabilities. The collected fibres got impart stability and molecular orientation.

2.2.6.2 Electrospinning technique

Since 1934, there have been significant advancements in the field of electrospinning, yet many new ideas to fully quantify the process wait to be discovered. For the most part, researchers have focused on electrospinning from solution with limited efforts to produce fibres from a melt. Electrospinning from solution has been extensively studied because it offers quicker success in the race to develop fibres with diameters less than 100 nm as a result of the small viscosities that need to be overcome to produce a continuous jet [55-56].

The operational principle of electrospinning is quite simple. In this non mechanical, electrostatic technique, a high electric field is generated between a polymer fluid contained in a spinning dope reservoir with a capillary tip or a spinneret, and a metallic fibre collection grounded surface. When the voltage reaches a critical value, the charge overcomes the surface tension of the deformed drop of the suspended polymer solution formed on the tip of the spinneret and a jet is produced. The electrically charged jet

undergoes a series of electrically induced bending instabilities during its passage to the collection surface that results in the hyper-stretching of the jet. This stretching process is accompanied by the rapid evaporation of the solvent molecules that reduce the diameter of the jet, in a cone shaped volume called the "envelope cone" or ''Taylor cone''. Bending instability may be attributed to the extremely high viscosity associated with melt as has been demonstrated by Taylor [33] or the small distance that the jet traverses before contacting the collection device. The dry fibres are accumulated on the surface of the collection plate resulting in a non-woven mesh of nano to micron diameter fibres. The process can be adjusted to control the fibre diameter by varying the electric field strength and polymer solution concentration; whereas the duration of electrospinning controls the thickness of fibre deposition [7], as it will be seen later.

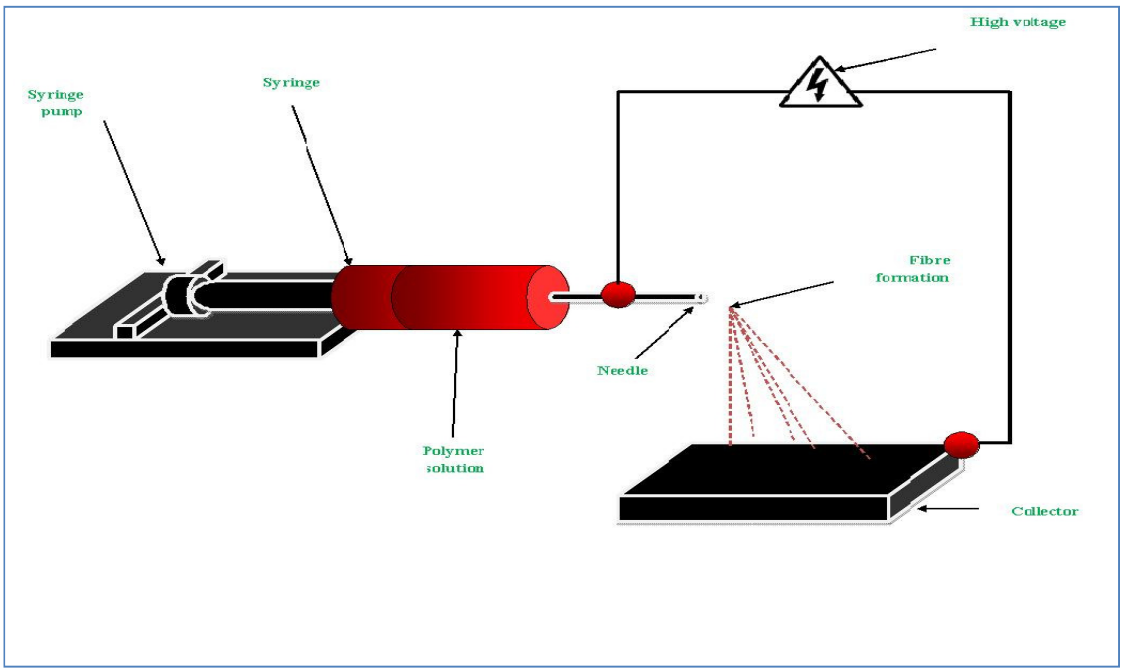

Figure 2.18, Shows a schematic design of an electrospinning system.

Various researchers have used different types of method for producing nano sized fibres by electrospinning. Reneker and Koombhongse [57] mounted the capillary in the vertical direction using gravity to produce a droplet on the tip of the capillary for displacement. In other cases the capillary is mounted at an angle to control the flow of the droplet. Many used a setup with a horizontal capillary with a displacement pump to generate a droplet at its tip; a high voltage is applied at the capillary by connecting an electrode at the tip of the capillary. A metal sheet is generally used as a target for collection of fibres spun. However, researchers have also used a grounded water bath

[58] and a rotating aluminium cylinder [59] to collect the fibres as non-woven fabric. Zussman [60] and other researchers [61-62] used the electrospinning process to align the individual nano fibres on a tapered and grounded wheel like -bobbin. The bobbin was able to wind continuously at its tip like edge.

2.3 Electrospinning theory and process

There are three steps to produce fibres by electrospinning.

2.3.1 Process of fibre formation

The electrospinning technique may be considered as a variant of the electrostatic spraying (or electrospray) process. Both of these techniques involve the use of a high voltage to induce the formation of liquid jets. In electrospray, small droplets or particles are formed as a result of the break-up of the electrified jet that is often present in a solution of low viscosity. In electrospinning, a continous fibre is generated as the electrified jet (composed of highly viscous polymer solution) is continuously stretched. To understand the fundamental principle underlying the process of electrospinning, consider a spherically charged droplet of a low molecular weight conducting liquid that is held in vacuum. As shown in figure 2.19, the droplet is under the influence of two forces, the disintegrative electrostatic repulsive force and the surface tension that strives to hold the droplet within a spherical shape.

Figure 2.19, The phenomenon of Electrospraying: when the electrostatic repulsive forces overcome the surface tension of the liquid, the droplet disintegrates into smaller droplets [57].

At equilibrium, the two forces completely balance each other, and this is expressed by the following equation, $\frac{1}{8\pi\varepsilon_0}\frac{Q^2}{R^2} = 8\pi R\sigma_s$

Where Q is the electrostatic charge on the surface of the droplet, R is the radius of the droplet, ε_0 is the dielectric permeability of vacuum and σ_0 is the surface tension coefficient. With increasing electric field strength, the charge on the surface of the

droplet increases until it reaches a critical point where the electrostatic repulsive force overcomes the surface tension. When this happens the droplet disintegrates leading to the formation of smaller droplets (figure, 2.19). This process is termed as electrospraying and has been utilized extensively for automotive spray painting. If this concept is extended to a high molecular weight polymer solution that has sufficient chain entanglements, then instead of the formation of the droplets, a steady jet is formed that later solidifies in a polymer filament. Thus, the fundamental principle underlying fibre formation by electrospinning can be stated as follows: a high electric potential is applied to a polymer solution (or melt) suspended from the end of a spinneret providing an electrostatic charge to the polymer solution. At low electric potentials, the disintegrative electrostatic repulsive forces that primarily reside on the liquid surface are balanced by the surface tension. At high electric potentials, the electrostatic repulsive force at the surface of the fluid overcomes the surface tension and this result in the ejection of a charged jet. The jet extends along a straight line for a certain distance, and then bends and follows a looping and spiralling path. The electrostatic repulsion forces can elongate the jet to several thousand times leading to the formation of a very thin jet (Jet Initiation). When the solvent evaporates, solidified polymer filaments are collected on a grounded target in the form of a non-woven fabric (Bending Instability). The small diameter provides a large surface to volume ratio that makes these electrospun fabrics interesting candidates for a number of applications.

Electrospinning includes three stages. In the first stage, a polymer jet issues from the nozzle. In the second stage, this jet will be accelerated and stretched smoothly by electrostatic forces. In the third stage, a (bending instability) happens further downstream when the jet gets sufficiently thin, and the fibre spirals violently [63]. These three stages will be described after discussing the fundamental aspect.

2.3.2 Electrical charges theory

In an uncharged ionic solution, there are the same numbers of positive and negative ions in each volume element of the solution and no external field is created [64]. In the 1960s [65] Taylor discovered that it is impossible to account that the fluid is either a perfect dielectric or perfect conductor. The reason is that any perfect dielectric still contains a non-zero free charge density [66]. This charge will typically live on the interface between fluids. If there is also a nonzero electric field tangent to the interface then there will be a nonzero tangential stress on the interface. The only possible force

that can balance a tangential stress is viscosity; hence under these conditions the fluids will necessarily be in motion. This has become known as the (leaky dielectric model) for electrically driven fluids. When an external electric field is applied to the solution, the voltage will polarize the ions [67]. Typically, negative ions are forced toward the positive electrode and positive ions are forced toward the negative electrode. The difference in the number of positive and negative ions in a particular region is often called the excess charge or simply the charge [64]. The excess charge establishes an electrical field that extends for large distances. Adding a soluble salt will increase the electrical conductivity of the solution by increasing the number of ions per unit volume, but cannot increase the excess charge [67]. The higher conductivity may, however, shorten the time required for the excess charge, in the form of ions, to move to a particular region in response to changes in the electrical field, or in the shape of a segment of the jet.

2.3.3 Initiation of the jet

The initiation and formation of the jet is a complex and interesting process with many variations. In electrospinning, initiation is less important than the maintenance of a stable jet, but is an essential step which deserves separate attention. Jet initiation is one of the direct consequences of exposing a fluid drop in contact with a conductor to a strong electric field. As a result much of the work on jet initiation has been done in tandem with theoretical treatments of electrospraying. Much of the literature on electrically driven jets has concentrated on the initiation processes that transform a liquid surface into a jet. The behavior of electrically driven jets, the shape of the jet originating surface, and the jet instability are some of the critical areas in the electrospinning process that require further research. Rayleigh [68] and Zeleny [69] gave initial insight into the study of the behaviour of liquid jets, later followed by Taylor. Yarin et.al [70] studied the formation of a conical meniscus (already referred to as the Taylor Cone) and the phenomenon of jetting from liquid droplets in electrospinning of nanofibres. It was concluded that the critical half angle of the conical meniscus of the charged fluid does not depend on the fluid properties for Newtonian fluids, since an increase in surface tension was always accompanied by an increase in the critical electric field. It was shown both theoretically and experimentally, that as a liquid surface develops a critical shape; its configuration approached the shape of a cone with a half angle of 33.5˚ rather than a Taylor Cone of 49.3˚. In elastic or unrelaxed viscoelastic fluids, the geometrical sharpness of the critical hyperboloid was found to

depend on both elastic and surface tension forces. Observations of many single jets show that the surface of the liquid near the base may start as a nearly flat surface across the open tip of the pipette. The base region stabilizes at a size and shape that is determined by these flow processes and by the rate which is supplied to the tip. The shape of the base region adjusts to carry charge and mass away from the tip of the pipette at an equilibrium rate. Flow patterns in the base and parameters such as elongational flow and time dependent elasticity of the liquid affect the diameter and shape of the base [10].

2.3.4 The stability of the electrospinning jet

A stable electrospinning jet has four distinct regions (figure 2.20). The jet emerges from the charged surface at the base region and travels through the jet region, divides into many fibres in the splaying region and stops in the collecting region. The base is the region where the jet emerges from the liquid polymer. The geometry of the jet, near the base, is a tapered cone in which velocity of the liquid increases as the polymer is accelerated along the axis of the jet. The base may have circular cross sections, or it may have some other shape if surface tension of the liquid anchors the jet to the lip of a hole or some other stationary object. A jet of liquid can be ejected from a surface that was essentially flat before the field was applied because electric field is strong enough. The electrical charging of the jet occurs in the vicinity of the base. The electrical conductivity of typical molten polymers is large enough to supply the small currents that are required for electrospinning, if the electrode in the melt is close to the base of the jet. Solutions have higher conductivity and form jets readily. It is useful to assume that the charge density in the jet is equal to the charge that flows onto a conducting sphere with a diameter of the jet, divided by the volume of the sphere. The low mobility of the carrier charge prevents them from flowing a significant distance through the liquid polymer while the jet carries the volume element under consideration to the collector. A nearly equivalent estimate is that the charge per unit area on the surface of a cylindrical element, with length equal to the diameter of the jet, adjacent to the base of the jet is the same as the charge per unit area on a flat surface at the base [68-70].

The jet is the region beyond the base where the electrical forces continue to accelerate the polymer liquid and stretch the jet. In this region, the diameter of the jet decreases and the length increases in way that keeps constant the amount of mass per unit time passing any point on the axis. A stable electrospinning jet travels from a polymer

solution or melt to a collector, for example, a metal screen. The jet is driven by a high electrical potential applied between the solution or melt and the collector. Electrical charges, usually in the form of ions, tend to move in response to the electrical field that is associated with the potential. The charges, which have drift velocities through the liquid polymer that are smaller than the velocity of the jet along its axis, transfer the forces from the electric field to the polymer mass. The electrical forces which stretch to the fibre are resisted by the elongational viscosity of the jet [69].

The acceleration of the polymer in the jet is mediated by the transfer of the forces through the viscoelastic jet, in which the viscoelastic parameters are changing at the same time as the solvent evaporates from the jet and the temperature of the jet changes [70]. The charges in the jet carry the liquid polymer in which the charge is embedded in the direction of the electric field. This is the mechanism which moves charge from the reservoir of liquid polymer to the collector, and thereby completes an electrical circuit which provides the energy needed to accelerate the polymer, to increase its surface area, and drive the flow and deformation which change the shape of the liquid into a jet. If the polymer is in the form of a solution in which the solvent has a high vapour pressure, evaporation of the solvent from the jet may reduce the mass flow velocity. The taper of the jet is also affected by solvent evaporation, since loss of the solvent can have a large effect on the viscoelasticity of the liquid polymer. The best estimates of the jet velocity come from measurement of the mass of the fibres that are collected in a known time interval, the diameter of the jet and the concentration of the solution. These observations are limited to jets large enough to measure with a relatively low power optical microscope with a working distance that keeps it far enough from the jet (are not changed by the presence of the microscope). Splaying occurs in a region in which the radial forces from the electrical charges carried by the jet become larger than the cohesive forces within the jet, and the single jet divides into many charged jets with approximately equal diameters and charge per unit length. As the jet progresses from the base toward the collector, the forces from the external electric field accelerate and stretch the jet. Stretching and evaporation of the solvent molecules cause the jet diameter to become smaller. The charge on the fibre tends to expand the jet in the radial directions and stretch in the axial direction. As the radius of the jet becomes smaller, the radial forces from the charge become large enough to overcome the cohesive forces of the fibre and cause it to split into two or more fibres that are to splay. This jet division process occurs several more times in rapid succession and produces a large number of

small electrically charged fibres moving toward the collector. The divided jets repel each other, thereby acquiring lateral velocities and chaotic trajectories, which gives a bush-like appearance in the region beyond the point at which the first jet splays. Splaying converts a single jet into many much thinner jets. Thin fibres can also be created by elongating a single jet if splaying does not occur. Splaying and elongation appear to occur simultaneously in many cases [70-72].

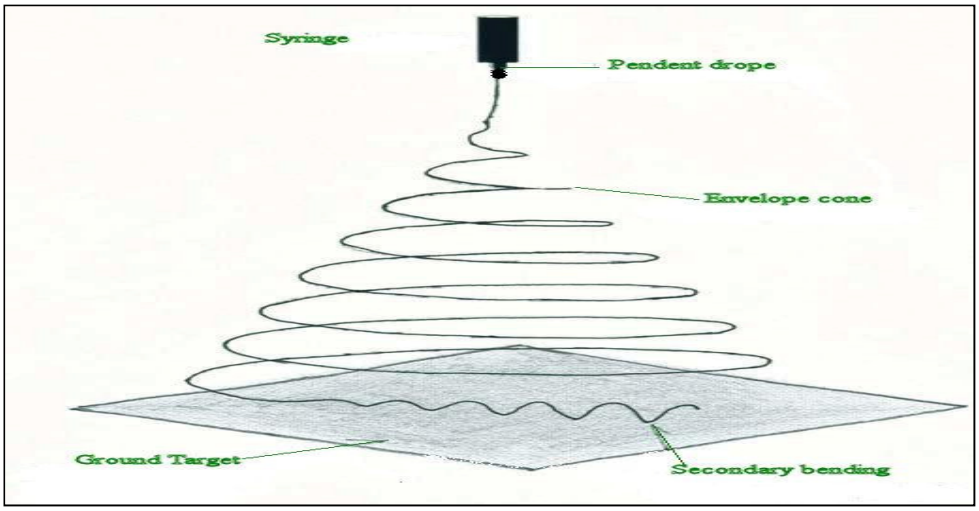

Figure 2.20, Electrospinning jet showing different orders of bending instabilities [64].

Measurements of the longitudinal fracture behaviour of polymers and elastomers indicate that the surface tension of the jet is a minor component of the fracture surface energy which must be supplied for a fibre split. Fracture surface energy is a term used to describe the total energy utilized to create a unit area of new surface [64, 68-70].

2.3.5 Stops in the collection region

The collection region is where the jet is stopped. The polymer fibre that remains after the solvent evaporates may be collected on a metal screen. For polymers dissolved in non-volatile solvents, water or other appropriate liquids can be used to collect the jet, then remove the solvents, and coagulate the polymer fibre. Mechanical reels or aerodynamic currents can also be used for collection. If the jet arrives with a high velocity at a stationary collector, the jet tends to coil or fold. Since the jet is charged, a fibre lying on the collector tends to repel fibres that arrive later. The amount of charge on the fibres can be changed by ions created in corona discharge and carried to the collection region by air currents. The charge may be also be removed by charge migration through the fibre to the conducting substrate, although for dry fibres with low

electrical conductivity, this charge migration may be quite slow [10]. In order to obtain ordered and aligned nanofibres, special collector patters are necessary to be designed. Rotating rollers and aerodynamic currents have been used for collecting aligned nanofibres. In addition, conductive, nonsolvent liquids, water or other appropriate liquids have been also utilized to remove the solvent and coagulate the polymer fibres resulting in a wet electrospinning 'electro wet spinning [58, 73].

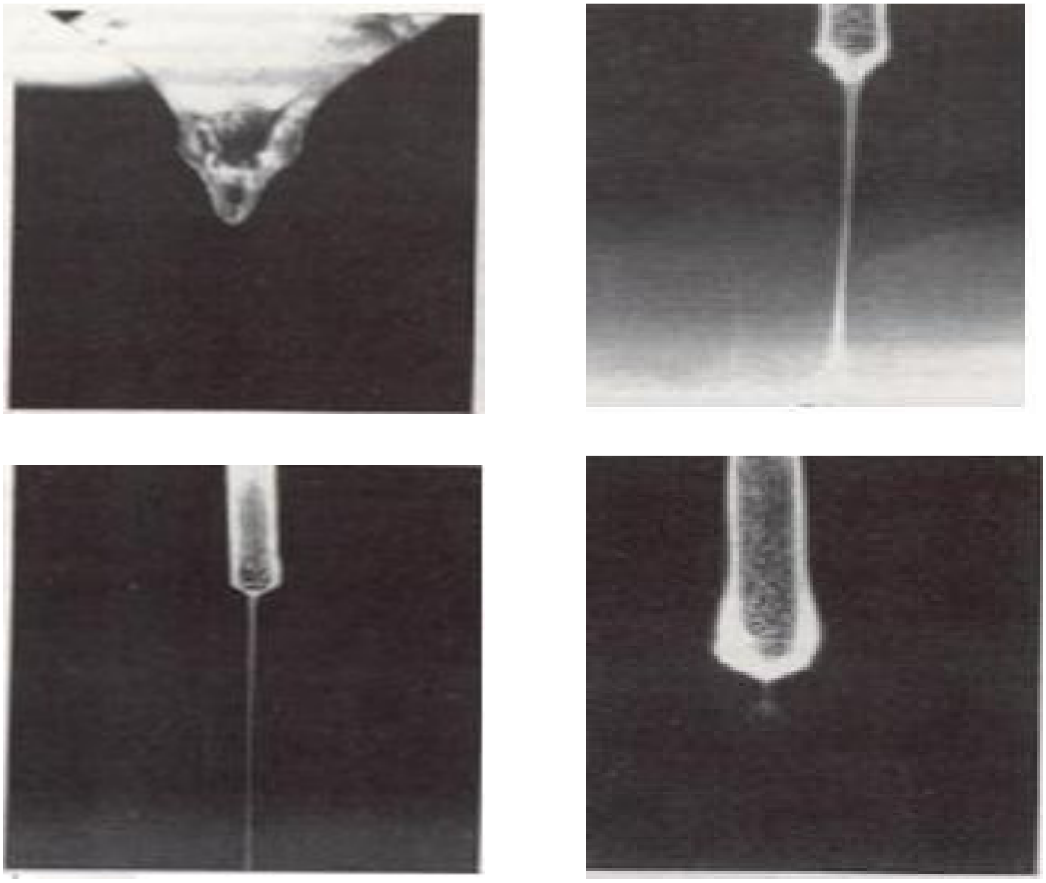

Figure 2.21, Jet ejection process during the electrospinning [64].

The electrospinning process is a convenient, inexpensive, and effective method of preparing polymer nanofibres whose diameter is in submicron scales. Figure 2.21 shows a second part of electrospinning process where we can see how the jet ejected. An electric field is used to create a charged jet of polymer solution. As this jet travels in air, the solvent evaporates leaving behind a charged fibre that can be electrically (splitted) and collected on a metal screen.

2.4 Structure – property process relationship

Most of the research work done on electrospinning has explored the types of polymer solution solvent systems used for nano fibre spinning. Before nano fibres are produced by applying electrospinning their parameters need to be considered. Many parameters can influence the transformation of polymer solutions into nanofibres through electrospinning. These parameters include (a) the solution properties such as viscosity, elasticity, conductivity and surface tension, (b) governing variables such as hydrostatic pressure in the capillary tube, electric potential at the capillary tip and the gap (distance between the tip and the collecting screen), and (c) ambient parameters such as solution temperature, humidity and air velocity in the electrospinning chamber [12]. These parameters play very important roles in the formation of the fibres and it is the aim of this study.

2.4.1 Solution processing parameters

Continuous and uniform fibres can be electrospun from polymer solution where there is a strong electric field and it adequate chain entanglement [74-76]. Concentration of the polymer solution often determines if it will electrospin at all and generally has a dominant effect on the fibre diameter as well as fibre morphology [77-78]. Nanofibres are produced from evaporation or solidification of the polymer liquid jet, the nanofibres morphology depends primarily on the polymer contents in the jet and its physical and chemical properties [79]. Two of the important factors that affect the viscosity of the spinning solution are the molecular weight and the concentration of the organic or inorganic polymer solution used to spin fibres [62, 80-81]. Here the molecular weight reflects the length of individual molecular chains. As the molecular weight of the solution increases, the chain entanglement increases and hence, the viscosity increases [82-83]. When the spinning solution leaves the nozzle tip during electrospinning, the solution is stretched as it travels towards the grounded metal plate. During the stretching, the large molecular chains present inside the solution entangle among each other and prevent the spinning solution from breaking up into droplets. The increase in the concentration of the molecules present in the spinning solution also causes greater extent of chain entanglement and, causes increase in viscosity of the solution. As a result, low viscosity or monomeric solutions do not form fibres during electrospinning.

Polymer solution concentration plays the most important role in determining the nanofibres morphology. As the polymer solution concentration increases, the viscosity increases and higher electrical forces are required to overcome both the surface tension and the viscoelastic forces for stretching the jet into nanofibres. Hence, the spinnability of polymer solution is relevant to its viscoelastic properties [79, 84]. Solution viscosity is generally identified as the dominant variable that determines fibre diameter [85]. The type of polymer used in the preparation of the solution affects the viscosity of solution and in turn the fibre structure formed. The solution viscosity has been found to influence fibre diameter. The droplet shape and the jet trajectory [74]. Solution with lower viscosity may result in formation of droplets instead of fibres. It was known that the viscosity of the polymer plays a major role in the production of the fibres and their size and is one of the most studied parameters when electrospinning. Larrondo and Manley [9] showed that viscosity was important when they electrospun fibres from the melt. The critical viscosities and applied electrical fields required for melt-electrospinning were much higher than those required when spinning from solution. It was seen that as the viscosity of the solution or melt increased, the fibre diameter increased exponentially. Nanofibres spun from such solutions can have an uneven appearance and tend to be deposited over relatively smaller area on the collector plate.

Surface tension is another factor that affects the morphology of the electrospun fibres. Surface tension has the effect of decreasing the surface area per unit mass of a fluid. Here during electrospinning, the solvent present in the spinning solution has a tendency to congregate together, and induce the formation of spherical beads in the fibres. As the viscosity of the solution is increased, the solvent molecules tend to interact with the polymer molecules rather than among each other, hence, reducing the tendency to form beads, thus producing more uniform and smooth fibres [86]. The surface tension of the polymer solutions change with concentration and also with the chemical nature of the polymer [87]. It also likely changes in time, the jet becoming progressively more or less concentrated during its passage from the tip to the collector plate. Surface tension is temperature dependant and is affected by the presence of an electric field; making it one more elusive factor to quantify in an electrospinning model. Surface tension of the polymer can be controlled by careful selection of the solvent. In general, increasing polymer concentration will increase the surface tension of the solution. The influence of surface tension of solvents in electrospinning is well discussed in the literature [86].

The conductivity of the spinning solution also plays a role in the morphology of the fibres. Polymers are mostly conductive, with a few exceptions of dielectric materials, and the charged ions in the polymer solution are highly influential in jet formation. The ions increase the charge-carrying capacity of the jet, thereby subjecting it to higher tension with the applied electric field. Baumgarten showed that the jet radius varied inversely as the cube root of the electrical conductivity of the solution [39]. The conductivity is increased by addition of small amount of salts or polyelectrolytes into the spinning solution. As the charge of the spinning solution is increased, the repulsion of the charges on the surface of the fibres causes the fibres to extend and hence, causes a decrease in diameter of the collected fibres. The dielectric constant of the solvents used in the spinning solution also plays an important role in fibre diameter. As the dielectric constant of the solvent increases, the diameter of the fibres is found to decrease [88]. Finally, the electrical conductivity of the polymer solution is a key factor in determining the electrospinning current, net charges density and fibres morphology [89].

2.4.2 External processing parameters

Other parameters that affect the electrospinning process and the morphology of the fibres are the external properties that include the applied voltage, the distance between the tip and collector and flow rate. The electrospinning process produces fibres only if the applied voltage is above the given limiting value required to overcome the surface tension of the solution. In electrospinning experiments, the electric current associated with the process can typically be measured with a microammeter. The droplets or fibres transport charge across the gap between the charged needle and the electrically grounded target, closing the circuit [74]. The applied voltage is one of the crucial properties that affect the size of the fibres. The high voltage induces the required charges in the spinning solution along with the external electric field, which causes an increase in the electrostatic force that overcomes the surface tension of the solution and forms fibres. Research has shown that an approximate voltage of 6 kV is enough to distort the drop of the spinning solution at the tip of the pipette to form a Taylor Cone during jet initiation. Further increase in voltage causes faster jet formation. If the voltage is increased to 30 kV, the Taylor Cone at the tip of the syringe recedes, due to the increase in speed of fibre formations. The rate at which the solution reaches the tip of the syringe is termed the flow-rate. For a given voltage, there is a corresponding flow rate required for a steady Taylor Cone to be maintained [32, 90]. Deitzel et. al, have inferred that the change in the spinning current is related to the change in the instability mode [74]. Under a higher electric field multiple jets are generated from the droplet at

the spinneret tip which will provide smaller diameter of electrospun fibres, but non uniform fibre diameters distribution. It has been also noted that with too high level of electric field, the resulting nanofibres became beaded and rougher [79].

The structure and morphology of electrospun fibres is easily affected by the nozzle to collector distance because of their dependence on the deposition time, evaporation rate, and whipping or instability interval [90].

The other factor which affects the electrospinning process is the collection process. The most popular form of collected nanofibre is as a nonwoven mat. As described above, in most instances, the process enters an instability region and the fibres are distributed in a random formation [12]. Megelski et. al, were able to notice the formation of a beaded morphology for electrospun polystyrene fibres upon shortening of the distance between the capillary tip and the collector, which can be attributed to inadequate drying of the polymer fibre prior to reaching the collector [91]. Thick and flat fibres are obtained when the distance of the tip of the nozzle is too close to that of the collector. This is because the solvents present in the fibre jet do not have enough time to evaporate, and hence, the fibres are still wet when deposited on the collector, which causes the fibres to blend or stick together. As the spinning distance is increased, the flight time of the jet also increases and the fibre diameter decrease [92].

The flow rate of the polymer from the syringe is an important process parameter as it influences the jet velocity and the material transfer rate. Electrospinning under high volume feed rate does not render a sufficient viscous stretching for the fibres by the electric forces. On the other hand, with too low volume feed rate, the pendant droplet may be disappeared and the jet is generated from the sidewall of the spinneret tip. This is possibly due to the insufficient polymer solution delivered to the cone volume after the jet has formed at the apex of the spinneret. It has been also found that the lower the polymer solution volume feed rate is, the smaller the fibres are formed [93- 96]. The feed rate need to be matches to the speed of fibre formation, instability in the fibre formation otherwise it will causes bead formation. An ideal situation is such that the speed of jet formation matches the feed rate in such a way that the Taylor Cone at the tip of the nozzle is not disturbed during the entire electrospinning process [74, 97]

Environmental conditions around the spinneret, like the surrounding air, its relative humidity (RH), vacuum conditions, surrounding gas, etc., influence the fibre structure and morphology of electrospun fibre. Baumgarten observed that acrylic fibres spun in

an atmosphere of more than 60% relative humidity do not dry properly and get entangled on the surface of the collector. The breakdown voltage of the atmospheric gases is said to influence the charge retaining capacity of the fibres [39]. Srinivasarao et al. proposed a new mechanism for pore formation by evaporative cooling called "breathe figures". Breathe figures occur on the fibre surfaces due to the imprints of condensed moisture droplets caused by the evaporative cooling of moisture in the air surrounding the spinneret. Megelski et al. investigated the pore geometry of PS fibres at varied RH and emphasized the importance of phase separation mechanisms in explaining the pore formation of electrospun fibres [91].

2.5 Electrospun polymer nano fibre

Hundreds of polymers have been electrospun to produce nanofibres for various applications. Bazbouz and G.Stylios used Nylon 6 polymer to produce nano yarn which can be use as reinforcement fibre [79]. Koombhongse et .al [98] spun different fibres and reported flat ribbon like structures and branched fibres. Norris et. al [99] during electrospinning of polyaniline/PEO blends from chloroform solvent produced conductive fine fibre. During polyetherurethane electrospinning from Dimethyl Acetamide solvent observed the dependence of fibre diameter distribution and the occurrence of beaded structures on the flow rate and applied electric potential. Bognitzki et. al [100] electrospun of poly-L-lactide (PLLA), polycarbonate (PC), polyvinylcarbazole from dichloromethane solvent, obtained the relationship between the volatility of solvents used and the pore structure of fibres. Kim and Reneker [101] electrospun of polybenzimidazole (PBI) from N,N-dimethyl acetamide (DMAc) solvent produced birefringent fibres. Fong et. al [102] electrospun, Nylon 6 and Nylon 6 montmorillonite (NLS) from 1,1,1,3,3,3-hexa fluoro-2-Propanol (HFIP) and DMF solvent, observed cylindrical fibres along with some ribbon shaped fibres (~10μ) with 100–200 nm thickness. They also electrospun Polyethylene oxide, Polycarbonate (PC), Polyurethane (PU) from Isopropyl alcohol (IPA), DMF/THF, DMF solvents respectively developed nonwoven fibres by different fibre charging methods like electrostatic spinning and corona charging. Tsai et .al [103] electrospun random copolymer PMMA-r-TAN fibre and obtained nanofibres with specific surface chemistry, tribocharging, and concluded that electrospun fibres have higher filtration efficiency than other nonwoven mat. Lee et. al [104] during the electrospinning of Polyvinyl chloride from THF, DMF solvent studied the effect of volume ratio of mixed solvents on the structure and morphology of electrospun fibres. Demir et .al [105]

observed during electrospinning of polyurethane urea copolymer solution in DMF, that the average fibre diameter increases with the solution concentration. Reneker et. al [106] examined during electrospinning of Styrene-Butadiene- Styrene (SBS) triblock copolymer from 75% THF and 25% DMF that the morphology of fibres with respect to micro-phase separation and experimented with annealing process for accelerating the ordering process and stress relaxation. Reneker et. al [107] made carbon nanofibres, from precursor polymers and from mesosphere pitch, by pyrolysis. The resulting carbon nanofibres had diameters from 50 to 500nm. The morphology ranged from highly oriented, crystalline, nano fibres to very porous ones with high values of surface area per unit mass. Zeng Jun et. al [108] electrospun PLA fibres and observed cylindrical morphology. Deitzel et.al [109] investigated the feasibility of damping the bending instability and controlling the deposition of electrospun PEO fibres deposited on a substrate through the use of an electrostatic lens element. The PEO electrospun fibre mats and yarn were analyzed using wide angle X-ray diffraction (WAXD), optical microscopy and Environmental SEM (ESEM) Kenawy et. al [110] studied the release of tetracycline hydrochloride from electrospun fibres as a potential for drug delivery. Srinivasan and Reneker [111] studied the crystal structure and morphology of electrospun Kevlar fibres from sulphuric acid. Kim and Lee [111] examined the melt spinning and reported the thermal properties of electrospun PET and PEN fibres. Yannas [112] electrospun natural polymers as biomaterials are collagen, hyaluronic acid, gelatin, chitosan, elastin, silk, and wheat protein. Natural polymers offer the advantage of being very similar, often identical, to macromolecular substances present in the human body. Therefore, the biological environment is prepared to recognize and interact with natural polymers favorably. Yang et. al [113] produced biomaterials form synthetic polymer PLA by electrospinning process. Price et. al [114] explored the possibility of using carbon nanofibres for bone tissue engineering. They compared osteoblast adhesion on carbon nanofibres with that of conventional carbon fibres and showed greater osteoblast adhesion on carbon nanofibres. Ramay et. al [115] used HA with β-tricalcium phosphate (β-TCP) to develop biodegradable nano-composite porous scaffolds. Silk fibroin is another potential natural biomaterial for nanofibrous scaffolds. Min et. al [116] has reported the in vitro cytocompatibility of silk nanofibres with keratinocytes and fibroblasts. The compatibility, fibre diameter, and high porosity make it a suitable candidate material for scaffolding technology. Conventional electrospinning produces randomly oriented nanofibres; however, Mo et. al [117] developed an aligned biodegradable PLLA-CL (75:25) nanofibrous scaffold using a rotating collector disc for collection of aligned

electrospun nanofibres. These aligned nanofibres were explored to fabricate tubular scaffolds that could be used for engineering blood vessels. Their results demonstrated that the nano-sized fibres mimic the dimensions of natural ECM, provide mechanical properties comparable to human coronary artery, and form a well defined architecture for smooth muscle cell adhesion and proliferation [118-120]. A wide variety of polymeric materials have been used as delivery matrices, and the choice of the delivery vehicle polymer is determined by the requirements of the specific application. Polymeric nanofibres have recently been explored for their ability to encapsulate and deliver bioactive molecules for therapeutic applications [121]. Hui Lee et. al [122] developed a method which combining electrospinning and salt leaching/gas foaming processes by incorporating MMT nano platelets. The scaffolds they produced had dual porous structure containing the nano-sized pores formed by electrospinning and the micro-sized pores formed by salt leaching/gas forming. This developed MMT/PLLA nanocomposites gave a robust structural integrity of scaffolds and tiny pinholes on the surface of scaffold walls during biodegradation. Jin, Wen-Ji et. al [123] prepared polymer nanofibres containing Ag nanoparticles. The polymer they used Poly (N-vinylpyrrolidone) (PVP). T. Jarusuwannapoom et.al [124] used polystyrene polymer solution to reveal the morphological characterization. Kim et.al [125] investigated the effects of alcoholic solvents on the charge transport properties of tosylate-doped poly (3, 4-ethylenedioxythiophene) (PEDOT-OTs). The use of different alcoholic solvents in the oxidative chemical polymerization of 3, 4-ethylenedioxythiophene (EDOT) with iron (III)-*p*-tosylate led to a change in the electrical conductivity of PEDOT-O. Yoon et. al [126] electrospun PAN scaffold with chitosan coating which later used for water filtration. Youliang Hong et. al [127] developed of TiO_2 surface-residing electrospun nanofibres with controllable density of TiO_2 on the support fibre surface by means of an electrospinning technique and a sol–gel process. Lee et.al [128] electrospun TiO_2 nanofibres by mixing of TiO_2/polyvinylpyrrolidone. They used titanium tetraisopropoxide (Ti (OCH (CH3)2)4 and PVP to make the fibre. Zhang et. al [129] fabricated PPV nanofibres where they used the solvent of Ethanol/water. These kinds of fluorescent fibres have potential applications for photo electronic devices such as LEDs and flat panel displays. Lee et. al [130] produced submicron scale composite fibres of SiO_2/TiO_2. A sol-gel precursor of tetraethyl orthosilicate (TEOS) and titanium (IV) isopropoxide (TiP), followed by calcinations has been used to produce that fibre. Xin et. al [131] electrospun of poly (p-phenylene vinylene) (PPV) polyelectrolyte precursor/poly (vinyl pyrrolidone) (PVP) blends with different composition ratios. They

used Ethanol as a solvent. PPV/PVP nanofibre can be conveniently transferred onto various surfaces for many applications, including the fabrication of nanodevices and the characterization of nanofibre properties. Maretschek et. al [132] electrospun of emulsions composed of an organic poly(L-lactide) solution and an aqueous protein solution yielded protein containing nanofibre nonwovens (NNs) having a mean fibre diameter of approximately 350 nm. They can be useful for controlled release of proteins. Zhao et. al [133] successfully prepared PLA/LDHs composite fibres by the method of electrospinning. This polymer/LDHs composite material may have prospective application as the basis of environmental friendly systems. Uyar et.al [134] successfully produced Cyclodextrin functionalized PMMA nanofibres (PMMA/CD) by electrospinning technique with the goal to develop functional nanowebs. Bead-free uniform electrospun PMMA/CD nanofibres obtained from a homogeneous solution of CDs and PMMA in dimethylformamide (DMF) using three different types of CDs, α-CD, β-CD and γ-CD. These CD functionalized nanowebs may have the potential to be used as molecular filters and/or nanofilters for waste treatment purposes. Sutthiphong et. al [135], fabricated Ultrafine 1, 6-diisocyanatohexane-extended poly (1, 4-butylene succinate) (PBSu-DCH) fibres by electrospinning. Potential has been reported for use of the electrospun PBSu-DCH fibre mats as bone scaffolds. It has been proved that composite a nanofibre was successfully fabricated with incorporation of nanoparticles by electrospinning with intent to transform nanoparticle properties into fibrous structure. Previous work of carbon nanotubes (CNT) nanocomposite fabrication by F.KO et. al has proved that co-electrospinning of CNTs with polymer provides an excellent method for translation of mechanical and electrical properties of CNT in polymer fibril matrix with 1 to 5 % by weight CNT in a polyacrylonitrile (PAN) matrix. A 4 to 5 fold increase of mechanical properties was found with introduction of less than 1.5% by weight of CNT to the PAN matrix [136]. Magnetic particles embedded nanofibres produced by same technique also has shown the improvement in magnetic as well as electrical property comparing to pure polymer fibres which can be used in various fields including biomedical and electrical applications [137-138].

Brief introductions to the underlying principles of electrospinning were provided. In addition, a literature review that discussed the review of the electrospinning, the process of fibre formation and the applications of these electrospun submicron fibres were discussed in some detail. The ability to produce high specific surface fibres by electrospinning has generated significant interest in the scientific community in the last fifteen years. From a through literature review it has been observed that there is still a

strong need for a comprehensive study on the impact of processing parameters on polymer based nanofibres production. Consequently this study concentrates on a rigorous study on the impact of processing parameters for nanofibres production based on selected polymers such as Nylon 6, Nylon 6.6, PEO, PVA and Wood pulp.

Nylon 6: Nylon 6 is one of the most widely used engineering thermoplastics. It is semi crystalline polyamide which offers an excellent combination of mechanical performance and cost but has poor dimensional stability due to water absorption. It also has high-lubricity and moderate strength. Fong [139] used Nylon 6 polymer with HFIP solution and electrospun, and collected as the nonwoven fabric. Bazbouz and Stylios [140] used Nylon 6 with MWCNT and produced nano yarn. Cai et. al [141] used Nylon 6 with *organic-modified Fe-montmorillonite* (Fe-OMT) and produced composite fibre.

Nylon 6.6: Nylon 6.6 is the premium Nylon fibre. It is the fibre that is most often specified by professional architects and designers. Nylon 6.6 is the most resilient and performs well in commercial settings like offices, airports, and other places that get a lot of wear and tear. Nylon 6.6 has additional molecules that give extra strength and the resilience compared to Nylon 6. Nylon 6.6 is the most widely used because of its overall balance of properties [142].

PEO: Polyethylene Oxide (PEO) is a synthetic polymer that is readily available in a range of molecular weights. It's a water soluble, easy and reliable polymer to use. Because of good biocompatibility PEO fibres are very much interesting for biomedical applications [143].

PVA: PVA is produced commercially from polyvinyl acetate, usually by a continuous process. The physical characteristics and its specific uses depend on the degree of polymerization and the degree of hydrolysis. Poly-vinyl alcohol has various applications in the biomedical industries [144].

Wood pulp: Wood Pulp has been widely used as the raw material for papermaking. Depending on the process that transforms natural woods into fibrous mass. Regenerated cellulose fibres have been used for various industrial applications, including textiles and precursors for carbon fibres. Lyocell and rayon are two examples of commercially available regenerated cellulose fibre [145].

2.6 References

[2.1] P. Walsall, *Inventory of synthetic fibre*, Whole earth summer (1997)

[2.2] A. A. Vaidya, *Production of synthetic fibres*, **11**, 7-16, New Delhi, India (1988)

[2.3] J. M. Deitzel, J. Kleinmeyer, D. Harris, N.C.B.Tan, *The effect of processing variables on the morphology of electrospun nano fibres and textiles*, Polymer, **42**, 261-272 (2001)

[2.4] A. Ziabicki, *Fundamentals of fibre formation: the science of fibre spinning and drawing*, **ISBN-10:** 0471982202, John Wiley & Sons Ltd (1976)

[2.5] P. Gibson, H. S. Gibson, D. Rivin, *Transport properties of porous membranes based on electrospun nano fibres, Colloids and surfaces A: physicochemical and engineering aspects*, **187-188**,469-481 (2001)

[2.6] A. Frenot, I. S. Chronakis, *Polymer nanofibres assembled by electrospinning, Current opinion in colloid and interface science,* Volume **8**, Number 1, pp. 64-75 (12) (2003)

[2.7] A. Formhals, US patent 1, 975-504 (1934)

[2.8] Y. M. Shin, M. M. Hohman, M. P. Brenner, G. C. Rutledge, *Experimental characterization of electrospinning : the electrically forced jet and instabilities*, Polymer, **42**, 9955-9967 (2001)

[2.9] L. Larrondo, R. S. J. Manley, *Electrostatic fibre spinning from polymer melts. 1. experimental observations on fibre formation and properties*, Journal of polymer science: Part B: Polymer physics, **19**, 909-920 (1981)

[2.10] D.H. Reneker and I. Chun, *Nanometer diameter fibres of polymer, produced by electrospinning*, Nanotechnology, **7**, 216-223 (1996)

[2.11] A, Formhals, US, 2,123,992 (1934)

[2.12] Z. M. Hung,Y. Z. Zhang, M. Kotaki and S. Ramakrishna, *A review on polymer nanofibres by electrospinning and their application in nano composites,* Composite science and technology, **63**, 2223-2253 (2003)

[2.13] T. Ondarçuhu, C. Joachim, *Drawing a single nanofibre over hundreds of microns*, Europhys. Lett**. 42**, 215-220 (1998)

[2.14] C. R. Martin, *Nanomaterials: A Membrane-Based Synthetic Approach*, Science, Vol. **266**. no. 5193, pp. 1961 – 1966 (1994)

[2.15] G. Che, B. B. Lakshmi, C. R. Martin, E. R. Fisher and S. Ruoff, *Chemical vapour based synthesis of carbon nanotubes and nanofibres using a template method. Chem Mater,* **10,** 260–7 (1998)

[2.16] J. J. Feng, *Stretching of a straight electrically charged viscoelastic jet*, J.Non-Newtonian Fluid Mech.**116**, 55-70 (2003)

[2.17] P. X. Ma, R. J. Zhang, *Synthetic nano-scale fibrous extracellular matrix*, J: Biomed, Mater Res; **46**, 60–72 (1999)

[2.18] R. J. Zhang and P. X. Ma, *Processing of polymer scaffolds: phase separation*, In: Atala A, Lanza RP, editors. *Methods of tissue engineering.* San Diego: Academic Pr; pp. 715–24 (2002)

[2.19] E. P. S. Tan and C. T. Lim, *Nanomechanical testing for polymeric nanofibres*, International conference on experimental mechanics &Third conference of the Asian Committee on Experimental Mechanics : (Singapore, 29 November - 1 December0, (2004)

[2.20] R.Vasita and D. S. Katti, *Nanofibres and their applications in tissue engineering*, Int J Nanomedicine. March; **1**(1): 15–30 (2006)

[2.21] P. X. Ma, J. W. Choi, *Biodegradable polymer scaffolds with well-defined interconnected spherical pore network*, *Tissue Eng,***7**, 23–33 (2001)

[2.22] Y. C. Yu, P. Berndt, M. Tirrell and G. B. Fields, *Self-assembling amphiphiles for construction of protein molecular architecture,* J. Am. Chem Soc*,* **118**, 12515–20 (1996)

[2.23] Y. C. Yu, V. Roontga, V. A. Daragan, K. H. Mayo, M. Tirrell, G. B. Fields, *Structure and dynamics of peptide-amphiphiles incorporating triple-helical protein-like molecular architecture,* Biochemistry*,* **38**:1659–68 (1999)

[2.24] G. B. Fields, J. L. Lauer, Y. Dori, P. Forns, Y. C.Yu, M. Tirrel, *Protein-like molecular architecture: biomaterial applications for inducing cellular receptor binding and signal transduction*, *Biopolymers,* **47**,143–51 (1998)

[2.25] J. D. Hartgerink, E. Beniash, S. I. Stupp, *Self-assembly and mineralization of peptide-amphiphile nanofibres*. *Science*; **294**, 1684–8(*2001)*

[2.26] J. D. Hartgerink, E. Beniash, S.I. Stupp, *Peptide-amphiphile nanofibres: a versatile scaffold for the preparation of self assembling materials*, Proceedings of the National Acad, Sci. U. S. A*;* **99**:5133–8 (2002)

[2.27] J. J. Hwang, D. A. Harrington, H. A. Klok, S.I. Stupp, A. Atala, R.P. Lanza, *Cell-synthetic surface interaction: self-assembling biomaterials,* In: Atala A, Lanza RP, editors*. Methods of tissue engineering,* San Diego: Academic Pr; pp. 741–50 (2002)

[2.28] S. Lee, S. K. Obendorf, *Use of electrospun nanofibre web for protective textile materials as barriers to liquid penetration*, Textile Research Journal, Vol. **77** no. **9** 696-702 (2007)

[2.29] K. Baumgarten, *Electrostatic spinning of acrylic microfibres,* J Colloid Interface Science, **36** (no.1); 71-9 (1971)

[2.30] www.hillsinc.net/polymeric.shtml access by 05/03/2009

[2.31] A. Formhals, US, 2,123,992 (1934)

[2.32] G. I. Taylor, *Disintegration of water drops in electric field*, jets proceedings of the royal society of London series a mathematical and physical sciences, Vol. **280**, 383, (1964)

[2.33] G. I. Taylor, *Electrically driven jets,* proceedings of the royal society of London series a mathematical and physical sciences, Vol. **313**, 453-475 (1969)

[2.34] H. L. Simons, US Pat, 3, 280, 229 (1966)

[2.35] L. Isakoff, US Pat, 3, 593, 074 (1971)

[2.36] J. Fine, N. J. Passaic, A. T. Sigismondo, US Pat, 4, 223,101 (1980)

[2.37] C. Guignard, US Pat, 4, 230, 650 (1980)

[2.38] C. Guignard, US Pat, 4, 287, 139 (1981)

[2.39] P. K. Baumgarten , *Electrostatic spinning of acrylic Microfibres*, Journal of colloid and interface Science,Vol **36**,No 1,71-79 (1971)

[2.40] G.H. Martin, I. Derek, US Pat 4, 043, 331 (1977)

[2.41] G.H. Martin, I. Derek, .US Pat, 4, 044, 404 (1977)

[2.42] W.L. Simm, G.O. Claus, R.B. Bonart, V.F.G. Bela, US Pat, 4, 069,026 (1978)

[2.43] A. Bornat, US Pat, 4, 323, 525 (1982)

[2.44] How, US Pat, 4552, 707 (1985)

[2.45] J.P. Berry, US Pat 5, 024, 789 (1991)

[2.46] Pike, US Pat 5,935, 883 (1999)

[2. 47] F.L. Scardino, R.J. Balonis, US Pat, 6, 106, 913 (2000)

[2.48] F. KO et. al, US Pat. 7264762 (2001)

[2.49] Balkus et. al, US Patent 0168756 A1 (2003)

[2.50] H.Y. Kim, US Pat. 11263991 (2005)

[2.51] Andrady et al.US Patent 7134857, Nov 14 (2006)

[2.52] Dubson et al, Patent no US 7, 112, 293B2 (2006)

[2.53] Laurencin et. al**,** US Pat (7, 235, 295, June 26 (2007)

[2.54] Y. L. Joo et al US Pat 12007409 (2008)

[2.55] M. J. Lyons, PhD Thesis, Unviersity of Drexel (2004)

[2.56] S. B. Warner, A. Buer, M. Grimler, S.C. Ugbolue, G. C. Rutledge, M. Y. Shin, NTC Annual Report, Project M98-D01 (1999)

[2.57] D. H. Reneker, S. Koombhongse, W. Liu, *Flat polymer ribbons and other shapes by electrospinning*, Journal of polymer science: part B: Polymer physics, **39**, 2598-2606 (2001)

[2.58] D. H. Reneker and G. Srinivasan, *Structure and morphology of small diameter electrospun aramid fibres*, Polymer international, **30**, No 2, 195-201 (1995)

[2.59] J. S. Kim and D. H. Reneker, *Polybenzimidazole nanofibre produced by electrospinning,* Polymer engineering and science, Vol .**39**, 849-854 (1999)

[2.60] E. Zussman, A. Theron, A. L.Yarin, *Electrostatic field assisted alignment of electrospun nano fibres*, Nanotechnology, Vol. **12,**384-390 (2001)

[2.61] R. Jaeger, M. M. Bergshoef, C.M. I. BatlleI, H. Schönherr, G. J. Vancso, *Electrospinning of ultra thin polymer fibres*, Macromolecular symposia, **127**, 141-150 (1998)

[2.62] J. Doshi and D.H. Reneker, *Electrospinning process and applications of electrospun fibres*, Journal of electrostatics **35**, 151-160 (1995)

[2.63] J. J. Feng, *The stretching of an electrified non-Newtonian jet: a model for Electrospinning*, Phys. Fluids, **14,** 3912-3926 (2002)

[2.64] D. H. Reneker, A. L. Yarin, H. Fong and S. Koombhongse, *Bending instability of electrically charged liquid jets of polymer solutions in Electrospinning*, J. Appl. Phys, **87**, 4531-4547 (2000)

[2.65] J. R. Melcher and G. I. Taylor, *Electro hydrodynamics*: *a review of the role of interfacial shear stresses*, Annul. Rev. Fluid Mech, **1**, 111-122 (1969)

[2.66] M. M. Hohman, M.Y. Shin, G. C. Rutledge and M. Brenner, *Electrospinning and electrically forced jets. I. stability theory*, Phys Fluids, **13**, 2201-2220 (2001)

[2.67] J. S. Kim, D. S. Lee, *Thermal properties of electrospun polyesters*, Polymer journal, Vol. **32**, No. 7 pp616-618 (2000)

[2.68] X.L. Raleigh, Philosophical Magazine, **44**, 184 (1884)

[2.69] J. Zeleny, *Instability of Electrified Liquid Surfaces*, Phys. Rev. **10**, 1 - 6 (1917)

[2.70] A. L. Yarin, S. Koombhongse, D. H. Reneker, *Bending instability in electrospinning of nanofibres*, J. Appl. Phys. **89**, 3018 (2001)

[2.71] J. M. Deitzel, D. Kleimeyer, J. K. Hurvanen, N. C. B. Tan, *Controlled deposition of electrospun poly(ethylene oxide) fibres*, Polymers, **42**, 8163-8170 (2001)

[2.72] T. A. Kowalewski, A. L. Yarin, S. Blonski, *Experiments and modelling electrospinning process*, The 5th Euromech Fluid Mechanics Conference, 24-28, Toulose, France (2003)

[2.73] M. S. Khil, S. R. Bhattarai, H. Y. Kim, S. Z. Kim, K. H. Lee, *Novel fabricated matrix via electrospinning for tissue engineering*, Journal of Biomedical Materials Research part B: Applied Biomaterials, **72**, 117-124 (2005)

[2.74] J. M. Deitzel, J. Kleinmeyer, D. Harris and N. C. B. Tan, *The effect of processing variables on the morphology of electrospun nanofibres and textiles*, Polymer, **42** (1):261-272 (2001)

[2.75] V. Pornsopone, P. Supaphol, R. Rangkupan and S.Tantayanon, *Electrospinning of methacrylate-based copolymers: effects of solution concentration and applied electrical potential on morphological appearance of as –spun fibres*, Polymer engineering and Science, **45** (8):1073-1080 (2005)

[2.76] T. Subbiah, G. S.Bhat, R.W.Tock, S.Parameswaran and S. S. Ramkumar, *Electrospinning of nanofibres*, Journal of Applied Polymer Science **96** (2):557-569 (2005)

[2.77] M. M. Demir, I. Yilgor, E. Yilgor and B. Erman, *Electrospinning of poly-urethane fibres.* Polymer, **43** (11):3303-3309 (2002)

[2.78] X. Zong, H. K. Kim, D. Fang, S. F. Ran, B. S. Hsiao and B. Chu, *Structure and process relationship of electrospun bioabsorbale nanofibre membranes,* Polymer **43** (16):4403-4412 (2002)

[2.79] M. Bazbouz, *An investigation of yarn spinning from electrospun nanofibres*, PhD thesis, Heriot-Watt University, UK (2009)

[2.80] J. Zeng, H. Hou, J. H. Wendorff, A. Greiner, *Processing parameters for electrospun poly(vinyl alcohol) (PVA) nanofibres and photo-mediated crosslinking of*

modified PVA nanofibres, Polymer Preprints (American Chemical Society, Division of Polymer Chemistry), **44** (2), 174-175 (2003)

[2.81] V. Nyame, H. Dong, W. E. Jones, *Systematic study of the physiochemical properties of polymer nanofibre,* Abstracts of Papers, 226th American Chemical Society National Meeting, New York, NY, United States, CHED-208 (2003)

[2.82] M. G. McKee, M. T. Hunley, J. M. Layman, T. E. Long, *Solution rheological behavior and electrospinning of cationic polyelectrolytes,* Macromolecules, **39** (2), 575-583 (2006)

[2.83] S. L.Shenoy, W.D. Bates, H. L. Frisch, G. E. Wnek, G. E. *Role of chain entanglements on fibre formation during electrospinning of polymer solutions:good solvent, non-specific polymer-polymer interaction limit*, Polymer, **46** (10), 3372-3384 (2005)

[2.84] T. Jarusuwannapoom, W. Hongrojjanawiwat, S. Jitjaicham, L. Wannatong, M. Nithitanakul, C. Pattamaprom, *Effect of solvents on electrospinnability of polystyrene solutions and morphological appearance of resulting electrospun polystyrene fibres*, European Polymer Journal, **41**, 409-421 (2005)

[2.85] Z. Jun, H. Q Hou, A. Schaper, J. H. Wendorff and A. Greiner, *Poly-L-Lactide nanofibres by electrospinning influence of solution viscosity and electrical conductivity on fibre diameter and fibre morphology,* E-Polymers **009**: 1-9 (2003)

[2.86] H. Fong, I. Chun, D. H. Reneker, *Beaded nanofibres formed during electrospinning*. Polymer, **40** (16), 4585-4592 (1999)

[2.87] K. H. Lee, H. Y. Kim, M. S. Khil, Y. M. Ra, and D. R. Lee, *Characterization of nano-structured poly (ε-caprolactone) nonwoven mats via electrospinning,* Polymer **44** (4):1287-1294 (2003)

[2.88] W. K. Son, J. H. Youk, T. S. Lee, W. H. Park, *The effects of solution properties and polyelectrolyte on electrospinning of ultrafine poly(ethylene oxide) fibres,* Polymer, **45** (9), 2959-2966 (2004)

[2.89] S. Theron, E. Zussman, A. L. Yarin, *Experimental investigation of the governing parameters in the electrospinning of polymer solutions*, Polymer, **45**, 2017-2030 (2004)

[2.90] Alpa. C. Patel, Bioapplicable, *Nanostructured and nanocomposite materials for catalytic and biosensor applications*, PhD thesis, Drexel University ,USA (2006)

[2.91] S. Megelski, J. S. Stephens, D. B. Chase and J. F. Rabolt*, Micro and nanostructured surface morphology on electrospun polymer fibres*, Macromolecules **35** (22), pp. 8456–8466 (2002)

[2.92] C. J. Buchko, L. C. Chen, Y. Shen, D. C. Martin, *Processing and microstructural characterization of porous biocompatible protein polymer thin films,* Polymer, **40** (26), 7397-7407 (1999)

[2.93] T. Jarusuwannapoom, W. Hongrojjanawiwat, S. Jitjaicham, L. Wannatong, M. Nithitanakul, C. Pattamaprom, *Effect of solvents on electrospinnability of polystyrene solutions and morphological appearance of resulting electrospun polystyrene fibres*, European Polymer Journal, **41**, 409-421 (2005)

[2.94] J. H. Yu, S. V. Fridrikh, G. C. Rutledge, *The role of elasticity in the formation of electrospun fibres*, Polymer, **47**, 4789-4797 (2006)

[2.95] P. Supaphol, C. Mit-Uppatham, M. Nithitanakul, *Ultrafine electrospun polyamide-6 fibres: effect of emitting electrode polarity on morphology and average fibre diameter*, Journal of Polymer Science Part B: Polymer Physics, **43**, 3699-3712 (2005)

[2.96] A.L Yarin, S. Koombhongse, D. H. Reneker, *Taylor cone and jetting fromliquid droplets in electrospinning of nanofibres,* Journal of Applied Physics, **90** (9), 4836-4846 (2001)

[2.97] D.W. Hutmacher, T. Schantz, I. Zein, K. W. Ng , S. H. Teoh , K. C.Tan, *Mechanical properties and cell cultural response of polycaprolactone scaffolds designed and fabricated via fused deposition modelling,* J Biomed Mater Res, **55** (2), 203-16 (2001)

[2.98] S. Koombhongse, W. Liu, D. H. Reneker, J. Polym Sci: Part B: Polymer Physics, **39**, 2598 (2001)

[2.99] I. D. Norris, M. M. Shaker, F. K. Ko, A. G. Mac Diarmid, Synthetic Metals, **114**,109 (2000)

[2.100] M. Bognitzki, W. Czado, T. Frese, A. Schaper, M. Hellwig, M. Steinhart et.al, Adv. Mater. , **13**, 70 (2001)

[2.101] Y.Kim, D.H. Reneker, Polymer Engineering and Science, **39**,849 (1999)

[2.102] H. Fong, W. Liu, C. Wang, R.A. Vaia, Polymer, **43**, 775 (2002)

[2.103] P.P. Tsai, H. Gibson, P. Gibson, J. Electrostatics, **54**, 333 (2002)

[2.104] K. H. Lee, H. Y. Kim, Y. M. La, D. R. Lee, N. H. Sung, J. Polym Sci: Part B: Polymer Physics, **40**, 2259 (2002)

[2.105] M. M. Demir, I .Yilgor, E. Yilgor, B. Erman, Polymer, **43**, 3303 (2002)

[2.106] D. H. Reneker, W. Kataphinan, A. Theron, E. Zussman, A.L. Yarin, Polymer, **43**, 6785 (2002)

[2.107] H. Fong, D. H. Reneker, J.Polymer Sci: Part B: Polymer Physics, **37,** 3488 (1999)

[2.108] Z. Jun, H.Hou, A. Schaper, J. H. Wendorff, A. Greiner, e-polymers, **9** (2003)

[2.109] J. M. Deitzel, W. E. Kosik, S. H. McKnight, N. C. B. Tan, J. M. DeSimone, S. Crette, ARL Technical Report, ARLTR-2512 (2001)

[2.110] E. R. Kenawy et. al, J.Controlled Release, **81**, 57 (2002)

[2.111] G. Srinivasa, D.H. Reneker, Polymer International, **36**, 195 (1995)

[2.112] Yannas, IV. Natural materials. In: Ratner BD, Hoffman AS, Schoen FJ, et al., editors. *Biomaterial science: an introduction to materials in medicine*. 2. San Diego: Elsevier Academic Pr, pp. 127–36 (2004)

[2.113] F. Yang, C.Y. Xu, M. Kotaki, S. Wang and S. Ramakrishna, *Characterization of neural stem cells on electrospun poly (L-lactic acid) nanofibrous scaffold*, J Biomat Sci Polym Ed. **15**:1483–97 (2004)

[2.114] R. L. Price, K. Ellison, K. M. Haberstroh, T. J. Webster, *Nanometer surface roughness increases select osteoblast adhesion on carbon nanofibre compacts,* J Biomed Mater Res, **70A**:129–38 (2004)

[2.115] H. R. R. Ramay and M. Zhang, *Biphasic calcium phosphate nanocomposite porous scaffolds for load-bearing bone tissue engineering*, Biomaterials, **25**:5171–80 (2004)

[2.116] B. M. Min, G. Lee, S. H. Kim, Y.S. Nam, T. S. Lee and W. H. Park, *Electrospinning of silk fibroin nanofibres and its effect on the adhesion and spreading of normal human keratinocytes and fibroblasts in vitro,* Biomaterials, **25**:1289–97 (2004)

[2.117] X. Mo, Z. Chen, H. J. Weber, *Electrospun nanofibres of collagen-chitosan and P(LLA-CL) for tissue engineering*, Frontiers of Materials Science in China ,Volume **1**, Number **1**, 20-23 (2007)

[2.118] X. Mo, H. J. Weber, *Electrospinning P(LLA-CL) nanofibre: a tubular scaffold fabrication with circumferential alignment*, Macromol Symp*,* **217:417**–20 (2004)

[2. 119] Y. K. Luu, K. Kim, *B. S.* Hsiao, B. Chu, M. Hadjiargyrou, Journal of Controlled Release, **89** (2), 341-353 (2003)

[2.120] C.Y. Xu, R. Inai, M. Kotaki et al*. Electrospun nanofibre fabrication as synthetic extracellular matrix and its potential for vascular tissue engineering,* Tissue Eng. *b;* **10**:1160–8 (2004)

[2.121] J. Heller and A.S. Hoffman, *Drug delivery systems*, In: B.D. Ratner, A.S. Hoffman, F.J. Schoen and J.E. Lemons, Editors, Biomaterials science, Elsevier, San Diego, pp. 628–629 (2004)

[2.122] Y. H. Lee, J. H. Lee, I. G. An, C. Kim, D. S. Lee, Y. K. Lee and J. D. Nam*, Electrospun dual-porosity structure and biodegradation morphology of Montmorillonite reinforced PLLA nanocomposite scaffolds*, Biomaterials, V. **26**, n 16, June, , p 3165-3172 (2005)

[2.123] W. Jin, H. K. Lee, R. H. Jeong et al, *Preparation of polymer nanofibres containing silver nanoparticles by using Poly(N-vinylpyrrolidone*, Macromolecular Rapid Communications, V. **26**, n 24, Dec 22, p 1903-1907 (2005)

[2.124] T. Jarusuwannapoom et al, *Effect of solvents on electro-spinnability of polystyrene solutions and morphological appearance of resulting electrospun*

polystyrene fibres, European Polymer Journal,Volume **41**, Issue 3, Pages 409-421 (2005)

[2.125] T. Y. Kim and J. E. Kim, *Effects of alcoholic solvents on the conductivity of tosylate-doped poly(3,4-ethylenedioxythiophene) (PEDOT-OTs)*, Polymer International, Vol. **55,** n 1, p 80-86 (2006)

[2.126] K. Yoon, K. Kim, X. Wang, D. Fang, B. S. Hsiao and B. Chu**,** *High flux ultra filtration membranes based on electrospun nanofibrous PAN scaffolds and chitosan coating*, Polymer, Vol. **47**, n 7, Single Chain Polymers, p 2434-2441 (2006)

[2.127] Y. Hong, D. Li, J. Zheng, G. Zou, *Sol-gel growth of titania from electrospun polyacrylonitrile nanofibres*, Nanotechnology, Vol. **17**, n 8, p 1986-1993 (2006)

[2.128] S. J. Lee, N. I. Cho, D.Y. Lee, *Effect of collector grounding on directionality of electrospun titania fibres*, Journal of the European Ceramic Society **27**, 3651–3654 (2007)

[2.129] W. Zhang, Z. Huang, E. Yan, C. Wang, Y. Xin, Q. Zhao, Y.Tong, *Preparation of poly(phenylene vinylene) nanofibres by electrospinnin*g, Materials Science and Engineering: A, Volume **443**, Issues 1-2,pp. 292-295 (2007)

[2.130] S.W. Lee, Y.U. Kim, S. S. Choi, T.Y. Park, Y. L. Joo, S. G. Lee, *Preparation of SiO_2/TiO_2 composite fibres by sol–gel reaction and electrospinning,* Materials Letters, Volume **61**, Issue 3, Pages 889-893 (2007)

[2.131] Y. Xin, Z. Huang, J. Chen, C. Wang, Y. Tong and S. Liu**,** *Fabrication of well-aligned PPV/PVP nanofibres by electrospinning*, Materials Letters, Volume **62**, Issues 6-7, Pages 991-993 (2008)

[2.132] S. Maretschek, A.Greiner, T. Kissel, *Electrospun biodegradable nanofibre nonwovens for controlled release of proteins*, Journal of Controlled Release, Volume **127**, Issue 2, Pages 180-187 (2008)

[2.133] N. Zhao, S. Shi, G. Lu and M. Wei , *Polylactide (PLA)/layered double hydroxides composite fibres by electrospinning method*, Journal of Physics and Chemistry of Solids, Volume **69**, Issues 5-6, Pages 1564-1568 (2008)

[2.134] T. Uyar, Y.Nur, J. Hacaloglu, F.Besenbacher, *Electrospinning of cyclodextrin functionalized poly(methyl methacrylate) (PMMA) nanofibres*, Polymer, Volume **50,** Issue 2, , Pages 475-480 (2009)

[2.135] S. Sutthiphong, P. Pavasant, P. Supaphol, *Electrospun 1,6-diisocyanatohexane-extended poly(1,4-butylene succinate) fibre mats and their potential for use as bone scaffolds*, Polymer, Volume **50**, Issue 6, Pages 1548-1558 (2009)

[2.136] F. KO. FK, Y. Gogotsi, A. Ali, N. Naguib, H. Ye, GL.Yang, C. Li and P.Willis, *Electrospinning of continuous carbon nanotube-filled nanofibre yarns*, Advanced Material*s*; **15** (14):1161-1165 (2003)

[2.137] M. Wang, H. Singh, T.A. Hatton and G. C Rutledge, *Field-responsive Superparamagnetic composite nanofibres by electrospinning,* Polymer **45** (16):5505-5514 (2004)

[2.138] H. Yang, L. Loh, T. Han and F. KO, *Nanomagnetic particle filled piezoelectric Polymer nanocomposite wires by co-elctrospinning,* American Chemical Society. N.Y (2003)

[2.139] H. Fong, *Electrospun nylon 6 nanofibre reinforced BIS-GMA/ TEGDMA dental restorative composite resins,* Polymer, **45** (7):2427—2432 (2004)

[2.140] M. B. Bazbouz, G. K. Stylios, *Novel mechanism for spinning continuous twisted composite nanofibre yarns*, European Polymer Journal, Vol. **44** (1), 1-12 (2008)

[2.141] Y. Cai, Y. Wu, Q. Wei, K. Zhang, Z. Xu, W. Gao, L. Song, Y. Hu, *Structure, surface morphology, thermal and flammability characterizations of polyamide6/organic-modified Fe-montmorillonite nanocomposite fibres functionalized by sputter coating of silicon*, Surface and Coatings Technology, Volume **203**, Issues 3-4, 25, Pages 264-270 (2008)

[2.142] L. Lingaiah, K. N. Shivakumar, R. Sadler, *Electrospinning of Nylon 66 polymer nanofabrics*, American Institute of Aeronautics and Astronautics (2008)

[2.143] N. B. Graham, *Poly (ethylene oxide) and related Hydrogels and Hydrogels in medicine and pharmacy*, Vol. II (Ed.: N. A. Peppas), CRC, Boca Raton, pp. 96-97 (1986)

[2.144] B. Bolto, T. Tran, M. Hoang, Z. Xie , *Crosslinked poly(vinyl alcohol) membranes,* Progress in Polymer Science, **34** , 969–981 (2009)

[2.145] M. J. John, S. Thomas, *Biofibres and biocomposites*, Carbohydrate Polymers, **71**, 343–364 (2008)

Chapter 3: Experimental electrospinning technique set up and materials

3.1 Electrospinning set up

The basic requirements for electrospinning include a suitable solvent to dissolve the polymer, an appropriate solution viscosity and surface tension, an adequate voltage power supply and an appropriate electrode collection distance between the dispensing needle and ground plate. While all of these parameters are interdependent, the construction of an electrospinning apparatus was the first priority in this project. Once an integrated apparatus was built, it allowed for the easy manipulation of all of the necessary electrospinning parameters. The design included a semi-isolated system where the polymer solution, syringe pump, syringe, dispensing needle, ground plate were enclosed in a safety box. External components included a high voltage power supply connected to the dispensing needle and ground plate via electrodes, an AC to DC transformer. As displayed in figure 3.1.

A Glassman MK35P2.0-22 (New Jersey, USA) high voltage DC power supply is used to generate potential differences between 12 kV to 18 kV. One electrode of a high voltage is applied to a vertically (25-gauge) blunt-ended metal needle. The polymer solution is fed from a syringe to a needle via Teflon® tubing and the flow rate is controlled using a digitally controlled, positive displacement syringe pump (Harvard Apparatus M22 PHD 2000), the flow rate is 0.20 ml/hr-0.30 ml/hr. Fibres were obtained using an earthed collection system, which consist of a copper collector plate measuring 15 cm × 15 cm.

The general experimental set up for the study of the effect of processing on electrospun fibre morphology is as follows. A 10 ml quantity of a polymer solution is prepared and placed in a 10 ml syringe. The syringe is then clamped to a ring stand that was 5, 8, 11 and 14 cm above a grounded metal screen. The pump pressure is set between 0.20-0.30 ml/hr, at voltages of 12, 15, 18 kV applied to the needle to initiate the jet and splitting into nanofibres. The process runs 2-5 minutes to ensure adequate sample collection. After collection the nanofibre mats were held under vacuum at ambient temperature for days in order to ensure complete drying of the samples. Some nano mats doesn't need to put in vacuum because after the electrospinning collect dried fibres. A weight is applied

to the syringe plunger so that it can held constant when varying the distance between the needle and the collector. Studies have carried out to understand the relationship between the electrospinning process, the structure of fibre formed and their properties and application.

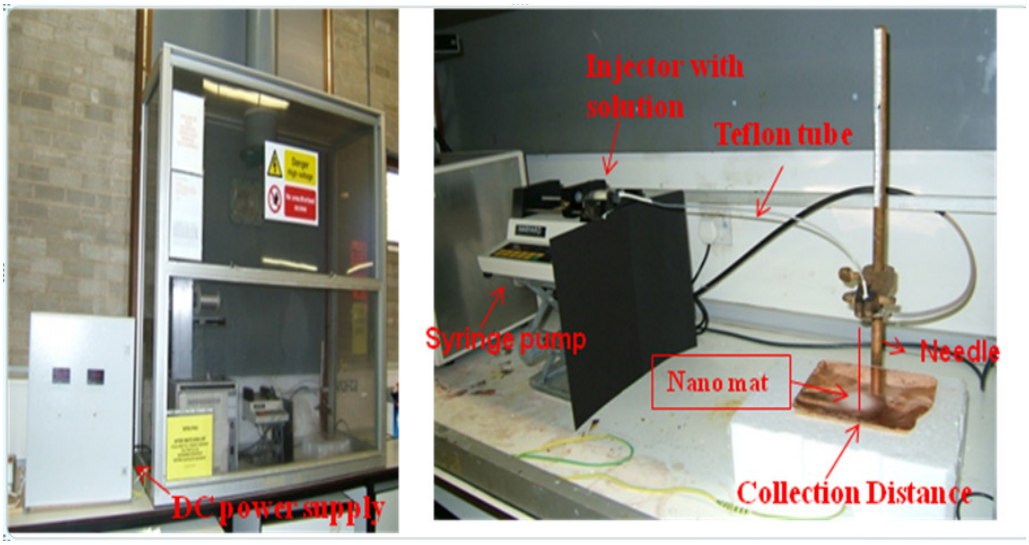

Figure 3. 1, Electrospinning process set up**.**

Figure 3.2, Electrospinning power meter.

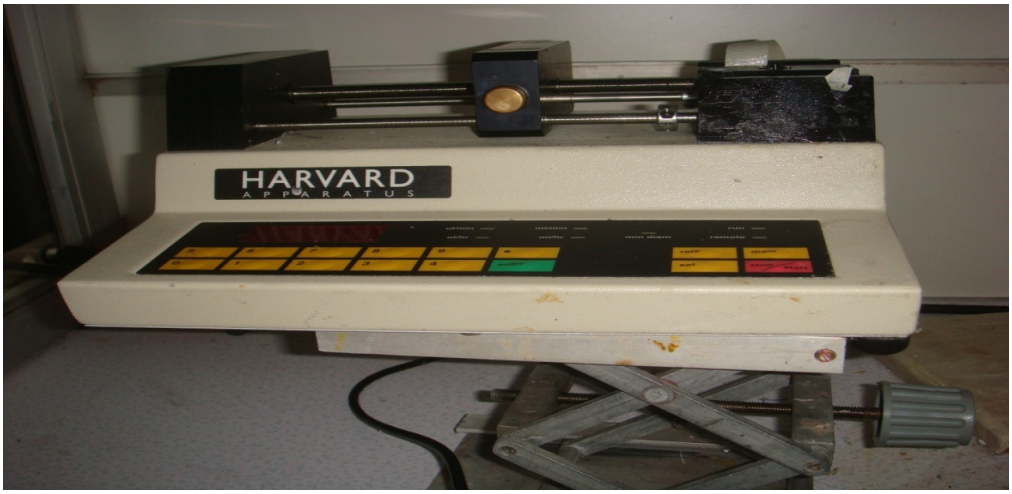

Figure 3.3, Metering pump.

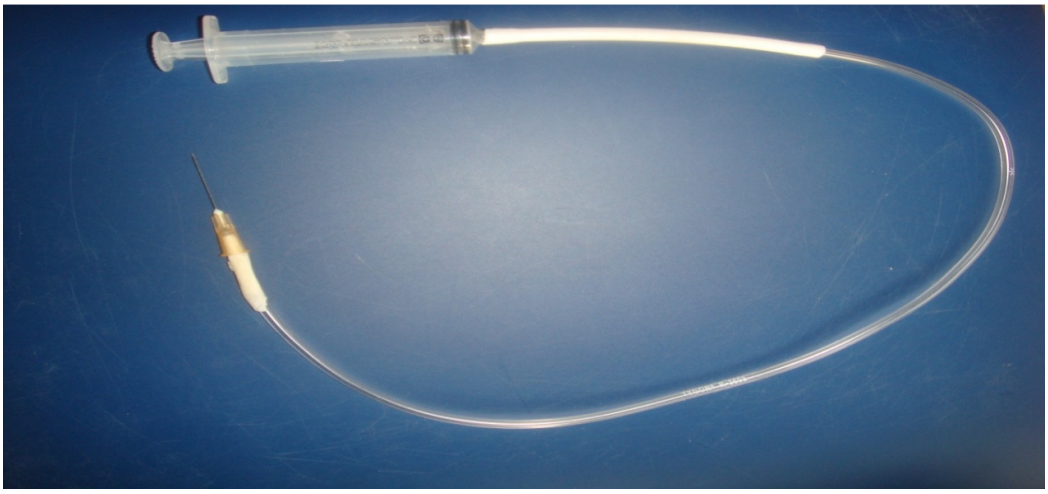

Figure 3.4, Syringe and needle with connecting tube.

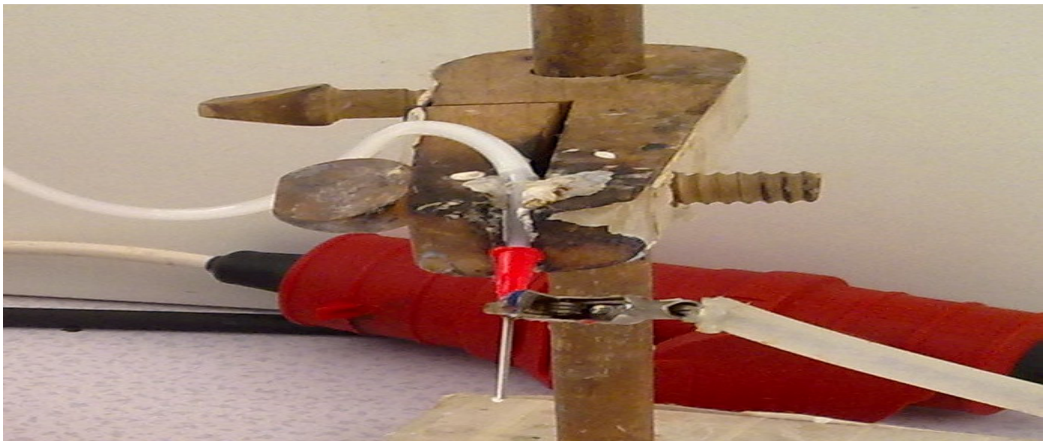

Figure 3. 5, Insulating arm and needle.

3.2 Electrospinning types

There are two types of electro spinning systems. The type of electrospinning process can greatly influence the resulting product in addition to adjusting polymer solution or processing parameters. This can include choices in nozzle configuration (single, single with emulsion, side-by-side, or coaxial nozzles), or solution vs. melt spinning [1]. Depending on the application a number of nozzle configurations have been employed. Perhaps the simplest and most common configuration is the single nozzle technique. A charged polymer solution flows through a single capillary in this configuration. (figure 3.6)

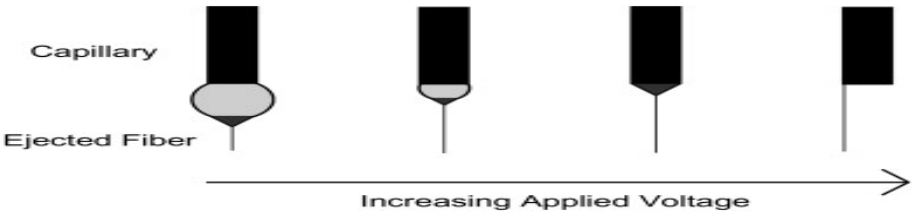

1)

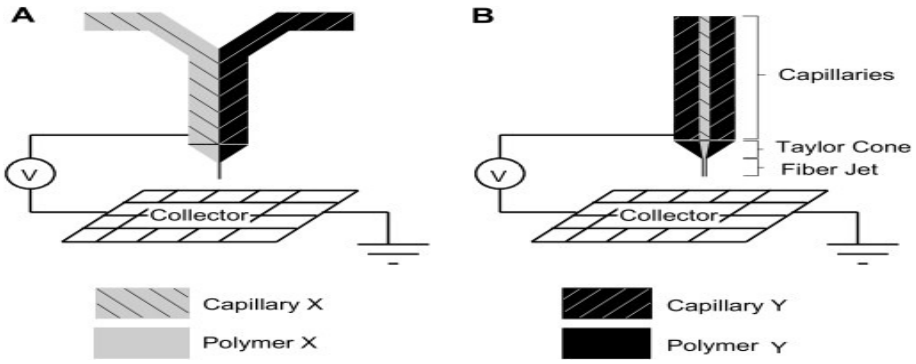

2)

Figure 3.6, Jetting configuration [2].

This configuration is very versatile and has been used to electrospin single polymer solutions [2] as well as polymer blends out of polymers soluble in a common solvent [3]. As an example, Qi et al. used a single nozzle configuration with an emulsion to electrospin composite fibres containing bovine serum albumin (BSA) loaded Ca-alginate microspheres microencapsulated in poly(l-lactic acid) (PLLA) fibres [4]. While electrospinning polymer blends is often desirable in order to achieve the desired combination of properties, it may not be possible using a single needle configuration if the polymers of interest are not soluble in a common solvent. Thus, it may be necessary

to use a side-by-side configuration. In this configuration two separate polymer solutions flow through two different capillaries, which are set side-by-side [figure 3.6]. Gupta and Wilkes used a side-by-side configuration to electrospin bicomponent systems out of poly (vinyl chloride)/segmented polyurethane and poly (vinyl chlorine)/poly (vinylidiene fluoride) [5]. On the other hand when electrospinning a polymer, typically one of two methods can be used. The polymer can be dissolved in a suitable solvent and electrospun or the polymer can be directly electrospun from a melt. In general, solution electrospinning results in a greater range of fibre sizes, while melt spun fibres are typically limited to micron size or larger [6] and [7], however, there are specific advantages and disadvantages to each method. In this research we used single nozzle technique to electrospun all polymers.

3.3 Polymer materials

The following materials have been chosen for this research;

1) The first solution was prepared using Ultramid resin grade B35F natural (Nylon 6) purchased from BASF, UK, with melting temperature 220ºC. The polymer was dissolved in Formic acid (96.7% from Sigma Aldrich, UK). The polymer concentration was 15 wt.% to 25 wt.%.
2) Nylon 6.6 from BASF, UK. The polymer concentration was 15 wt.% - 25 wt.%. The solvent used Formic acid (96.7%).
3) PEO from Fisher Scientific, UK with molecular weight 300,000 g/mol. The polymer concentration was 10 wt.% - 14 wt.%. The solvent used was HPLC grade water.
4) PEO from Fisher Scientific, UK with molecular weight 300,000 g/mol. The polymer concentration was 10 wt.% - 14 wt.%. The solvent used is HPLC grade water and Ethanol. The mixture was 60/40.
5) PVA from Across organic, UK and $FeCl_3$ from Sigma Aldrich, UK. The solution was 6 wt.% - 10 wt.%.
6) PEO with wood pulp from Domtar Group, Canada. The solution was 10 wt.% to 14 wt.%.

3.4 References

[3.1] S. J. Travis and H. A. V. Recum, *Electrospinning*: *applications in drug delivery and tissue engineering,* Biomaterials Vol. **29**, Issue 13, p.1989-2006 (2008)

[3.2] E. P. Tan, S.Y. Ng and C.T. Lim, *Tensile testing of a single ultrafine polymeric fibre*, Biomaterials **26** (13), pp. 1453–1456 (2005)

[3.3] J. Stitzel, J. Liu, S. J. Lee, M. Komura, J. Berry and S. Soker *et. al*, *Controlled fabrication of a biological vascular substitute*, Biomaterials **27** (7), pp. 1088–1094. (2006)

[3.4] H. Qi, P. Hu, J. Xu and A. Wang, *Encapsulation of drug reservoirs in fibres by emulsion electrospinning: morphology characterization and preliminary release assessment*, Biomacromolecules **7** (8), pp. 2327–2330 (2006)

[3.5] P. Gupta and G. L. Wilkes, *Some investigations on the fibre formation by utilizing a side-by-side bicomponent electrospinning approach*, Polymer **44** (20), pp. 6353–6359 (2003)

[3.6] L. Larrondo and R. S. J. Manley, *Electrostatic fibre spinning from polymer melts. 1. experimental-observations on fibre formation and properties*, J Polym Sci B Polym Phys **19** (6), pp. 909–920 (1981)

[3.7] L. Larrondo and R. S. J. Manley, *Electrostatic fibre spinning from polymer melts. 2. examination of the flow field in an electrically driven jet*, J Polym Sci B Polym Phys **19** (6), pp. 921–932 (1981).

Chapter 4: Experimental Methods, Morphology and characterization technique

4.1 Characterization technique

Structural parameters of nanofibre mats (such as fibre diameter and distribution, fibre orientation and pore size and distribution and material properties (such as melting temperature, glass transition temperature and setting temperature) determine the physical and mechanical properties of the fibre mat. Processing parameters were identified. The influence of these processing parameters on the structural parameters and material properties of the produced fibre mats need to be revealed in order to produce webs of predetermined properties for certain end use. For electrospinning we can say that the characterization techniques can be divided into two categories; the first one is related to the characterization of the polymer solution and the second will be related to the electro-spun fibres and fibre composites. The following sections describe the methods implemented to measure the structural parameters and material properties of the nano fibre mats produced for this study.

4.2 Polymer solution characterisation

The main parameter that affects the fibre diameter formation in the electro-spinning process is the polymer solution viscosity [1]. Although there is other important parameters like surface tension and solution electrical conductivity, the most important one is however viscosity because it is affected by the types of solvent and the polymer molecular weight meaning that this parameter is inter-related with others.

4.2.1 Viscosity

The viscosities of polymer solutions were measured with an AR-1000 rheometer, (TA Instruments Inc, UK, figure 4.1). The measurement is done in the continuous ramp mode at room temperature (25˚C) using cone and plate geometry. Samples are placed between the fixed peltier plate and rotating cone (diameter: 4cm, vertex angle: 2˚) attached to the driving motor spindle. The change in viscosity and shear stress with change in shear rate is measured. A computer interfaced to the machine recorded the resulting shear stress vs. shear rate data. The viscosity of the polymer solution was reported in Pa.s.

Figure 4.1, Viscosity measuring instrument.

4.2.2 Surface tension

Surface tension is the primary force opposing Coulomb repulsion and its role in determining electrospinnability cannot be overstated. In the instability region of the jet that obtains fibre extension, electrostatic forces are countered primarily by surface tension forces. Bead formation in electrospinning can be induced by changing the surface tension of the solution [2]. Surface tension and viscosity of the solution that determine the window within which a specific polymer/solvent combination can be electrospun [3]. The surface tension of the polymer solution changes with concentration and as well as with the chemical nature of the polymer [4]. It also changes with time, as the jet becomes progressively concentrated during its passage from the tip to the collector plate. Surface tension is temperature dependent and is affected by the presence of an electric field, making it one of the more elusive factors to quantify in an electrospinning model. The surface tension of polymer solutions can be conveniently measured using the simple Du Nouy ring technique [5], where a wire

loop of known circumference is dipped in the solution and the maximum force needed to slowly raise it out of the solution is measured. The Wilhelmy plate method [6] essentially substitutes a platinum plate for the ring. With small samples of solution available for the measurement, however, a platinum rod might be substituted for the plate. In practice it is important to minimize the evaporation of solvent during the measurement. In our experiment Model 'OS' Balance/Tensiometer, UK used and a 4 cm circumference platinum ring to measure the surface tension of the polymer solution (figure 4.2). The surface tension was reported in unit mN/m.

Figure 4.2, Surface tension measurement: Torsion balance.

4.2.3 Electrical conductivity

The electrospinning process fundamentally requires the transfer of electric charge from the electrode to the spinning droplet at the terminus of the tip. Minimal electrical conductivity in the solution is therefore essential for electrospinning; solutions of zero conductivity cannot be electrospun. Solvents commonly used in electrospinning have conductivities that are much lower than that of even distilled water, dichloromethane as a value of only 0.03 mS/m. On dissolving a polymer in the solvent, however, the solution conductivity generally increases due to the availability of conducting ionic species (mostly from impurities or additives) from the polymer. With increasing polymer concentration in solution, however, its electrical conductivity may decrease [7]. On the other hand the polymer itself has ionic functionalities as with polyelectrolyte, however, the solution conductivity will be much higher (relative to those of uncharged polymers) and markedly concentration dependent [8]. The most common way of

measuring the resistivity of a semiconductor material or solution is by using a four-point co-linear probe. This technique involves bringing four equally spaced probes in contact with the material of unknown resistance. The two outer probes are used for sourcing current and the inner two probes are used for measuring the resulting voltage drop across the sample. Each probe has a resistance *R*p, a probe contact resistance *R*cp and a spreading resistance *R*sp associated with it. However, these resistances can be neglected for the two voltage probes because the voltage is measured with a high impedance voltmeter, which draws very little current. Thus the voltage drops across these resistances are insignificantly small and the voltage reading from the voltmeter is approximately equal to the voltage drop across the semiconductor sheet resistance. A schematic of the process is shown in figure 4.3 and apparatus figure 4.4. By using the four-point probe method, the semiconductor sheet resistance can be calculated as

$$Rs = KV/I$$

Where *V* is the voltage reading from the voltmeter, I is the current carried by the two current carrying probes, and K is a correction factor. Electric conductivity was measured by using four point probe method. The following formulas were used to measure the solution conductivity, Rs= *KV/I.* Each experiment was performed at 20º C. The charge induction and charge retention characteristics vary according to the polymer type, so when identical voltage is applied to the polymer, electrical responses are different.

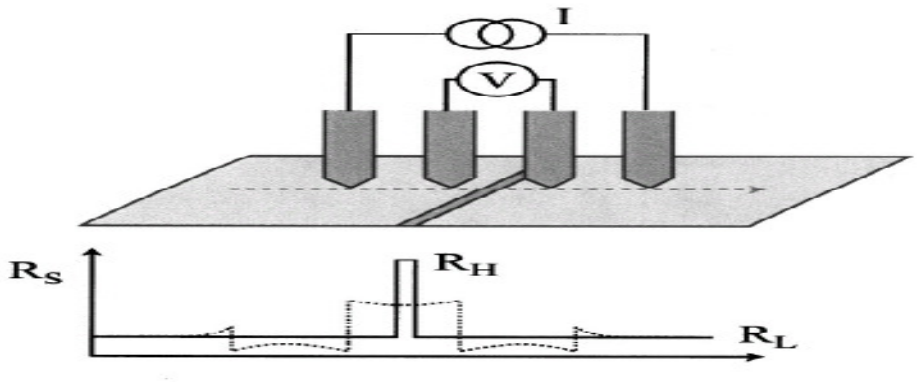

Figure 4.3, Schematic diagram of four- point prove method.

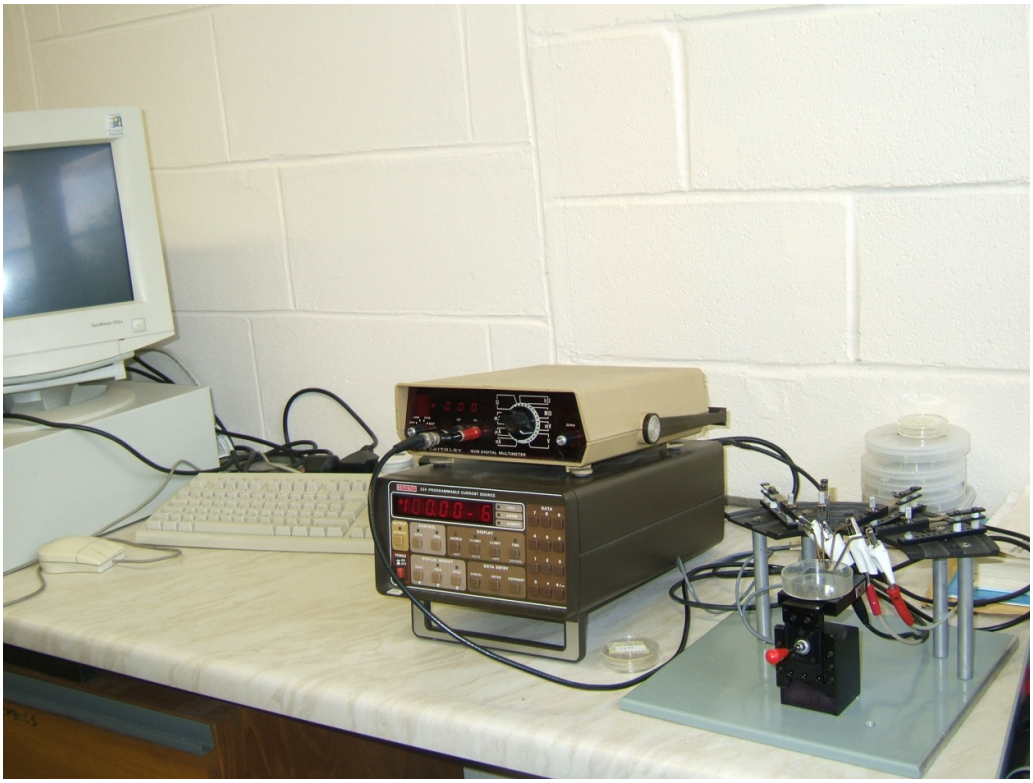

Figure 4.4, Four point probe method apparatus.

4.3 Characterization technique for the Produced nano fibres

4.3.1 Scanning Electron Microscopy (SEM)

Scanning Electron Microscopy (Hitachi S-530, Scanning Electron Microscope, UK, figure 4.5) was used to provide magnified images of the surface topography of the electrospun fibres. The morphologies of electrospun fibres obtained from polymer solutions were characterized by this type of microscopy. The SEM is an important tool capable of producing higher resolution images of a sample surface. Electrospinning process produces very fine fibres down to a few nanometres. SEM has many advantages over traditional microscopes. The SEM has a large depth of field, which allows more of a specimen to be in focus at one time. The SEM also has much higher resolution so closely spaced specimens can be magnified at much higher levels. Because the SEM uses electromagnets rather than lenses, the researcher has much more control in the degree of magnification. All of these advantages, as well as the actual strikingly clear images, make the Scanning Electron Microscope of the most useful instruments in characterizing the nanofibre mats produced by electrospinning. One advantages of using

the SEM to observe surface morphology is that simple preparation in generally much simpler than for Transmission electron microscopy [9- 10].

Figure 4.5, Laboratory Scanning Electron Microscopy.

4.3.2 Sample preparation for SEM

Electrospun Nylon 6, Nylon 6.6, Nylon 6.6/MWCNT, PEO with water, water/Ethanol, PVA/$FeCl_3$, PEO with Wood pulp nonwoven mats were sputter coated with gold-palladium for 45 seconds at 18 mA (Polaron Sc7620,Quorum technologies Ltd, UK) as shown in figure 4.6.

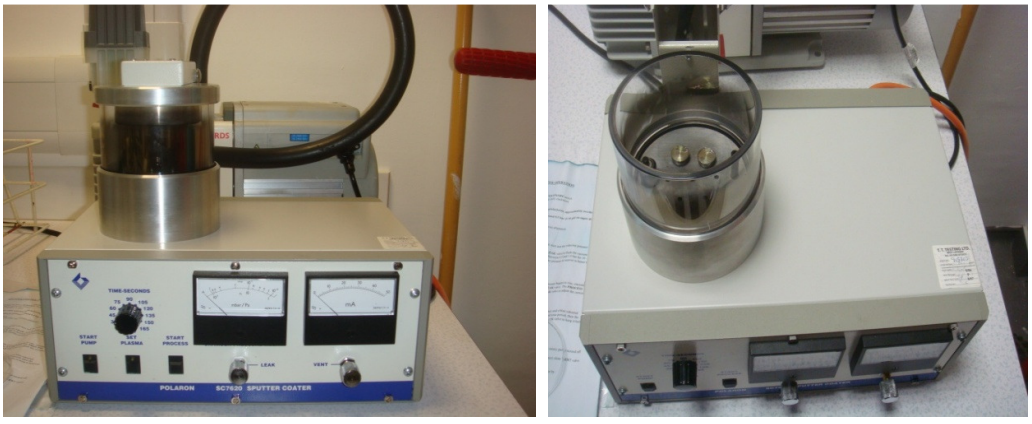

Figure 4.6, Sample preparation technique for SEM.

Fibres images were produced using a Hitachi S-530 Scanning Electron Microscope UK. Micrographs were taken of 3 random areas of each sample at 10 kV between 1000 and 20,000 times magnification. Photographs was processed using (Corel paint shop pro

X version 10.00) software. The fibres were analyzed by using software Image J, USA. Measuring the average diameter of the fibres viewed on photograph, a transect line was drawn from bottom right to the top left of the SEM image and fibre diameter were measured at the point the line transacted, perpendicular to the fibre length. These result used for fibre distribution profiles.

4.3.3 Atomic Force Microscopy

Optical microscopes and Scanning microscopes produce photographic (light) images. The atomic force microscope produces images rather in an analogous way to a blind man reading Braille. The action of the scanning produces a reaction, in the case of this microscope, a deflection of the scanning tip, which is translated into a measurable medium. The tip deflection is registered on a photo detector, as a change in placing of a laser beam on the detector surface and from there, is translated as a change in voltage. The computer and software gather the changes in voltage and are designed to re-draw these changes as a topographic image. Depending on the parameters set by operator, the images can consist of millions of data points, which by application of the data handling package can be retranslated to highlight different aspects of a sample; surface. Binnig and his co-workers invented AFM which can image the nonconducting surfaces [11].

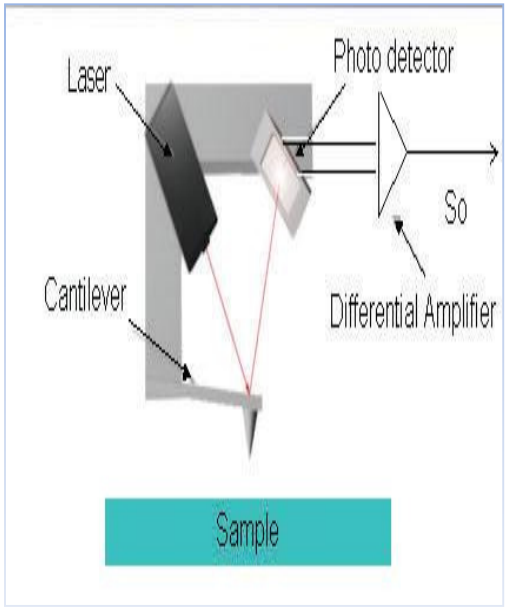

a) b)

Figure 4.7, a) Schematic of AFM, b) Laboratory Atomic Force Microscopy,

4.3.4 Sample preparation for AFM

An Atomic force microscopy (Model 5400, AFM, UK, figure 4.7) was used to characterize the morphology of the electrospun fibres**.** A flat, smooth surface is required for the sample to attach with and a firm attachment of the fibres on the substrate is required in order to get the images. Mica was used as the substrate as they are able to hold the fibres strong enough to withstand the vibration of the tip on the sample during imaging. Mica was cut into small pieces (5 mm X 5mm) and the top layer was removed using an adhesive tape to obtain a fresh surface. The mica was passed through the electrospinning jet to get a sparse distribution of the fibres.

4.3.5 Transmission Electron Microscopy (TEM)

Transmission Electron Microscopy (TEM) images were taken to see the molecular structure of the MWCNTS and other composite particle at a high magnification, and their position in the polymer fibres, that is not possible to observe with Electron microscope, Scanning Electron Microscope or Atomic Force Microscope. The other purpose of using this method was to compare the amorphous polymer fibre with the composite containing nanofibres at a higher magnification and also to see the presence of particle at the fibres in a lower magnification. TEM (JEOL JEM-2010, figure 4.8) was performed on the electrospun nanofibres. Observations were carried out at an accelerating voltage of 200 kV for most samples to avoid damaging the fibres. Other details about TEM can be found elsewhere [12].

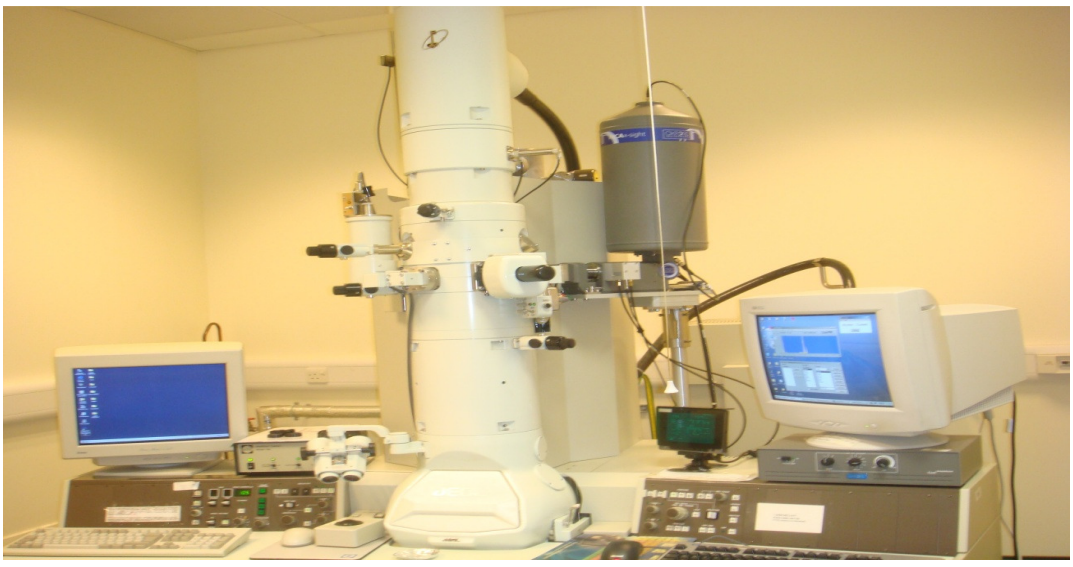

Figure 4.8, Laboratory Transmission Electron Microscopy.

4.3.6 TEM sample preparation

Lacey Carbon–coated Copper TEM grids (figure 4.9) with a diameter of 3 mm were used to collect the fibres directly from the electrospinning jet during the spinning process. The grid containing the fibres sample was allowed to dry at room temperature overnight. The samples were placed inside the sample holder then the sample holder was placed inside the objective apparatus of the microscope. High Vacuum was created. The voltage was set at 200 kV. The airlock was opened to allow the electron beam pass on the sample. Beam current was adjusted and time was allowed for the filament to heat up. When the Image started to show up in the screen, they were focused and images of the area of interest were saved.

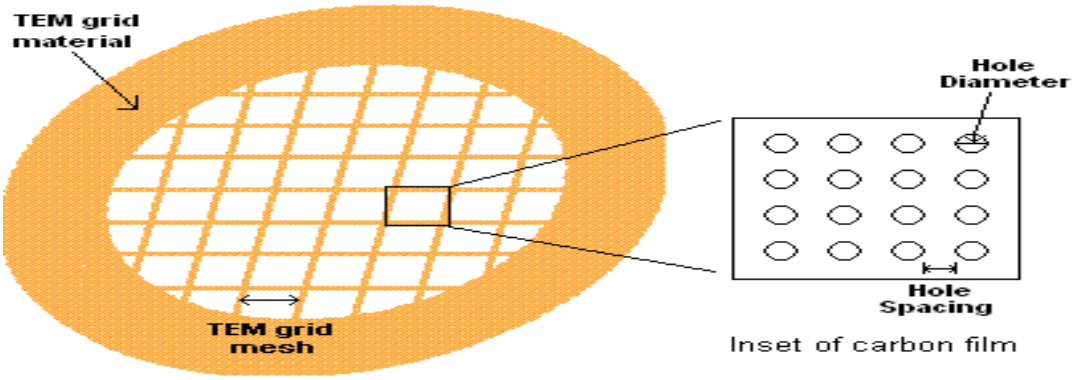

Figure 4.9, TEM grids [13].

4.4 Differential Scanning Calorometry (DSC)

Differential scanning calorimetry is a technique used to study the thermal transitions of a polymer. This is a thermo analytical technique in which the difference in the amount of heat required to increase the temperature of a sample and reference are measured as a function of temperature. Both the sample and reference are maintained at very nearly the same temperature throughout the experiment. Generally, the temperature program for a DSC analysis is designed such that the sample holder temperature increases linearly as a function of time. The reference sample should have a well-defined heat capacity over the range of temperatures to be scanned. The basic principle underlying this technique is that, when the sample undergoes a physical transformation such as phase transitions, more (or less) heat will need to flow to it than the reference to maintain both at the same temperature [14]. Whether more or less heat must flow to the sample depends on whether the process is exothermic or endothermic. Glass transition temperature of polymer and composite nanofibres (Nylon 6.6, PEO and PEO/wood

pulp) were investigated using a Metler DSC 30 (USA) figure 4.10, attached with a cooling system under a nitrogen atmosphere. DSC instrument were run from 40 °C to 400 °C with a heating rate of 10 °C /min. The sample weight was about 5 mg. The specimens were sealed in an aluminium pans by pressing and the prepared samples were placed in the furnace of DSC with an empty reference pan. The heat flow rate as function of temperature was recorded automatically. Glass transition temperature of specimens was identified from the DSC curves.

Figure: 4.10, Differential Scanning Calorimetry machines.

4.5 X -ray diffraction

X-ray diffraction (XRD) is one of the most important non-destructive tools used to analyze all kinds of matter ranging from fluids, to powders and crystals. From research to production and engineering, XRD is an indispensable method for materials characterization and quality control. X-ray crystallography, the study of crystal structures through X-ray diffraction techniques, generally leads to an understanding of the material and molecular structure of a substance. When an X-ray beam bombards a crystalline lattice in a given orientation, the beam is scattered in a definite manner characterized by the atomic structure of the lattice. This phenomenon, known as X-ray diffraction, occurs when the wavelength of X-rays and the inter-atomic distances in the lattice have the same order of magnitude. Other details about Xray-diffraction can be found elsewhere [15].

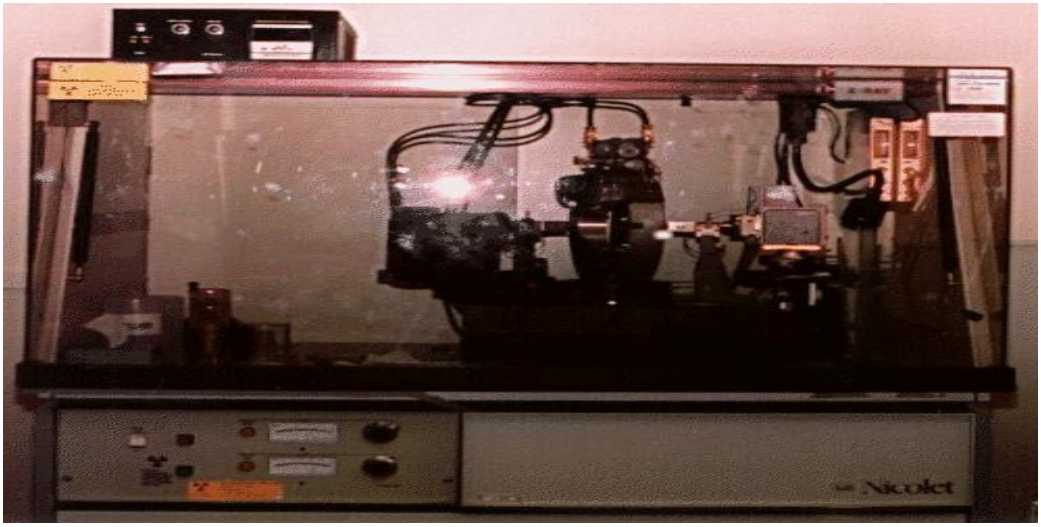

Figure 4.11, X-ray diffraction machines.

In this study, The X-ray diffraction spectra (XRD) of polymer powder and nanofibre were obtained with an X'Pert-MPD Philips diffractometer (UK), figure 4.11, using the Cu-Kα radiation wavelength(λ=1.54Å). The scanning range was set from 5˚ to 90˚, the step size was 0.04˚ with a scanning rate of 1 step/s. The operating conditions were 45 kV and 40 mA employing a 0.15 mm slit in front of the detector.

X-ray diffraction spectra were used in this project to determine the crystallinity of the produced nanofibres, the type and structure of the crystals in the nanofibres and degree of orientation of the crystals/crystallites. In this thesis Nylon 6.6, PEO and PEO/Wood pulps X-ray diffraction analysed.

4.6 Fourier transforms infrared spectroscopy

FTIR spectroscopy is a characterization technique widely used in physics, chemistry and biology. It has the advantages of high spectral resolution, good signal-to-noise ratios, and the ability to measure a broad region of the spectrum in a short amount of time. The infrared spectrum is formed because of the absorption of electromagnetic radiation at frequencies that correlate to the vibration of specific sets of chemical bonds from within a molecule. The vibrational spectrum of a molecule is considered to be a unique physical property and is characteristic of the molecule. Figure 4.12 shows a photograph of the Excalibur Series Perkin Elmer, UK, and this FTIR spectrometer used in the study. Each spectrum was acquired in reflectance mode with accumulations of 200-400 scans, resolution of 4 cm^{-1} and a spectral range of 400- 4000 cm^{-1}.

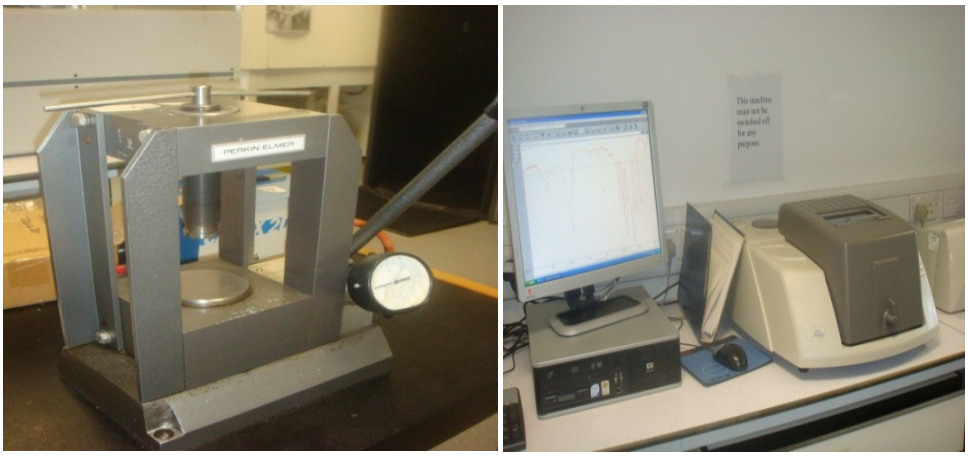

a) b)

Figure 4.12, FTIR, a) Sample preparation, b) Machine

FTIR is used to investigate the performance of the polymer and its blend because the IR spectrum represents typical absorption bands sensitive to the molecular conformation of polymers. In this thesis PEO/Wood pulp composite fibres molecular interaction analysed by FTIR.

4.7 References

[4.1] J. Doshi and D. H. Reneker, *Electrospinning process and applications of electrospun fibres*, Journal of electrostatics, **35**, 151-160 (1995)

[4.2] H. Fong, D. H. Reneker, *Elastomeric nanofibres of styrene-butadiene-styrene triblock copolymers,* Journal of Polymer Science, Part B: Polymer Physics. **37** (24) (1999)

[4.3] J. M. Deitzel, J. D. K. Meyer, J. K. Hirvonen and N. C. B. Tan, *Controlled deposition of electrospun poly (ethylene oxide) fibres,* Polymer engineering and Science, Vol. **42** issue19, P. 8163-8170 (2001)

[4.4] K. H. Lee, H.Y.Kim, M. S. Khil, Y. M. Ra, and D. R. Lee, *Characterization of nano-structured poly (ε-caprolactone) nonwoven mats via electrospinning.* Polymer **44** (4):1287-1294 (2003)

[4.5] S. H.Teng, P. Wang and H. E. Kim, *Blend fibres of chitosan–agarose by electrospinning*, Materials Letters, **63**, 2510–2512 (2009)

[4.6] X. Wang, H. Niu, T. Lin, X. Wang, Polymer Engineering and Science, **49**, 1582 (2009)

[4.7] Z. Jun, H. Q. Hou, A. Schaper, J. H.Wendorff and A. Greiner, *2 Poly-L-lactide nanofibres by electrospinning influence of solution viscosity and electrical conductivity on fibre diameter and fibre morphology*, E-Polymers, **009**:1-9 (2003)

[4.8] M. G. McKee, M. T. Hunley, J. M. Layman, and T. E. Long, *Solution rheological behavior and electrospinning of cationic polyelectrolytes*, Macromolecules **39** (2):575 (2006)

[4.9] P.J. Goodhew, F. J. Humphreys and R. Beanland, *Electron microscopy and analysis*, Wykeham publication Ltd, London and Winchester springer-verlag, New York, **9** (1975)

[4.10] L.C. Sawyer and D.T. Grubb, G.F. Meyers, *Polymer microscopy*, 3rd ed XIV, 540 p. 301 illus., ISBN: 978-0-387-72627- 4 (2008)

[4.11] G. Binnig, C.F. Quate, C.H. Gerber and E. Weibel, *Atomic Force Microscope*, Phys Rev.Ltd, **56.** 930-933 (1986)

[4.12] D. B. Williams and C. B. Carter, Transmission Electron Microscopy, Plenum Press, New York (1996)

[4.13] http://www.emsdiasum.com/microscopy access by 12/02/2010

[4.14] P. Erno, *A practical guide to instrumental analysis,* Boca Raton, Florida. pp. l8l-191 (1995)

[4.15] B. E. Warren, X-ray Diffraction, General Publishing Company, **ISBN:** 9780486663173, New York (1969)

Chapter 5: Effect of Experimental parameters on the morphology of electrospun Nylon 6 fibres

5.1 Introduction

Electrospinning is capable of producing continuous nano fibres from polymer solutions or melts in high electric fields [1-7]. Although more than 100 different types' polymers have been successfully produced by electrospinning, a systematic study of electrospinning parameters for optimizing Nylon 6 is yet to be achieved. The important properties of these nano size fibres, which make them commercially important are small diameter, large surface area to volume ratio, and small pore size; the ideal requirements for filtration, catalysis and adsorption. These properties of nano fibres are exploited by current researchers to determine appropriate conditions for electrospinning various polymers and biopolymers for eventual applications including multifunctional membranes, biomedical structural elements (scaffolding used in tissue engineering [8], wound dressing [9], drug delivery, artificial organs and vascular grafts [10], filter media or filtration [11]. Design of the polymeric nanofibres to meet specific needs for useful applications requires a thorough knowledge of the electrospinning parameters and their effect on nanofibre diameters and morphologies.

In these chapters the effects of the solution properties and processing parameters on the morphology of electrospun Nylon 6 nanofibres have been systematically studied to produce a wide range of fibre diameters with uniform fibre diameter distribution.

5.2 Experimental work

5.2.1 Preparation of polymer solution

Nylon 6 was purchased from BASF, UK. The polymer was dissolved in Formic acid (96.7% from Sigma Aldrich, UK) at a temperature of 20˚ C and stored it at the same temperature. It has a good resistance to many commercial solvents and can be only dissolved in a few solvents such as formic acid [12]. Various concentrations ranging from 15 to 25 wt.% were prepared and used for the experiments. All electrospinning experiments were carried out at room temperature in air.

5.2.2 Electrospinning set up and process

High voltage DC power supply was used to generate potential differences of between 12 kV to 18 kV. One electrode of a high voltage was applied to a vertically blunt-ended metal needle (25-gauge). The Polymer solution was fed from a syringe to a needle via Teflon® tubing and the flow rate was controlled using a digitally controlled, positive displacement syringe pump (Harvard Apparatus M22 PHD 2000), the flow rates was 0.200µl/hr to 0.300µl/hr. Fibres were obtained using an earthed collection system, which consisted of a copper collector plate measuring 15cm × 15cm.

The experimental set up for the study of the effect of concentration on electrospun fibres morphology was as follows. A 10 ml quantity of a Nylon 6 /formic acid solution was prepared. The solution placed in a 10 ml syringe. The syringe then clamped to a ring stand that was 5, 8 and 11 cm above a ground metal screen. The pump pressure was set at 0.200 ml/hr to 0.300 ml/hr and voltage of 12 to 18 kV was applied to the needle to initiate the jet. The process runs for 2-5 minutes to ensure adequate sample to collect. After collection of the nanofibre mats, they were held under vacuum at ambient temperature for 24 hours to ensure complete drying the samples. The physical effect of voltage on nano fibre morphology was the same at the various concentrations. The weight applied to the syringe plunger was held constant when varying the needle to collector distance.

5.2.3 Measurements and characterization (solution properties)

Surface tension for each solution was determined by the torsion balance for surface and interfacial tension measurement method. The instrument uses a 4 cm circumference platinum ring (Model 'OS' Balance/Tensiometer, UK). The surface tension was reported by unit mN/m. Solution viscosities were measured with an AR-1000 Rheometer, TA instruments, UK The measurement was done in the continuous ramp mode at room temperature (25º C) using cone and plate geometry. The sample was placed between the fix Peltier plate and a rotating cone (diameter: 4 cm, vertex angle: 2º) attached to the driving motor spindle. The changes in viscosity and shear stress with change in shear rate were measured. A computer interfaced to the machine recorded the resulting shear stress vs. shear rate data. The viscosities of the polymer solution were reported in unit Pa.s. Electric conductivity was measured by using four probe methods. Each experiment was performed at 20˚C. The charge induction and charge retention characteristics varied

according to the polymer type, so when identical voltage was applied to the polymer, electrical responses were different. It was reported by unit S/cm.

Table 5.1: Physical properties of Nylon 6/formic acid at different concentration.

Nylon6 conc. (wt.%)	Viscosity (Pa.s)	Surface Tension (mN/m)	Electric conductivity (S/cm)	Fibre diameter (nm)
15	2.842	44.8	0.0044	200-750
20	3.358	48.5	0.00294	700-1250
25	4.856	53	0.00116	700-1550
Formic acid	0.000 2	28	0.09	

5.2.4 Morphological characterization

i) Scanning Electron Microscopy: A Scanning Electron Microscope (Hitachi S-530, UK) was used to characterize the morphology of the electrospun nanofibres. The samples were sputter coated with carbon and examined at an accelerating voltage of 10 kV.

ii) Diameter of the fibre: To measure the diameters of the electrospun Nylon 6 nano fibres, an image analyzer (Image J, US) was used.

5.3 Result and discussion

5.3.1 Effect of solution concentration on fibre morphology

Solution concentration and viscosity are two closely correlated factors, increase in solution concentration always results in increase in solution viscosity, and decrease in solution concentration always results in decrease in solution viscosity. Therefore, these two factors were investigated. Increase the concentration, viscosity and surface tension favours the uniform fibres. The viscosity and the surface tension of the solution have an important role in fibre formation in the electrospinning process. Larrondo and Manley [13] showed that viscosity was important when they electrospun fibres from the melt.

The critical viscosities and applied electrical fields required for melt-electrospinning were much higher than those required when spinning from solution. It was seen that as the viscosity of the solution or melt increased, the fibre diameter increased exponentially. For electrospun 15 wt.% Nylon 6 solutions in formic acid, mostly droplets and some short fibres with beads were also observed. At 15 wt.% Nylon 6 concentration (figure 5.1 & table 5.2), 200-750 nm fibres with a lot of beads were observed. These beads disappear as the fibre diameter is increased with increasing polymer concentration. At 20 wt.% Nylon 6 concentrations (figure 5.1 & table 5.2), the number of beads and the bead size decreased. The diameter of the fibre increased to 700-1250 nm. At 25 wt.% Nylon 6 concentration (figure 5.1 & table 5.2) cylindrical electrospun fibres were observed with the diameters of 700-1500 nm. The average fibre diameter becomes gradually large with increasing concentration, which is consistent with the result obtained by Ryu et.al [14] and Reneker et.al [15]. The average diameter of the fibre has increased from 553 to 1071 nm for 15-25 wt.% Nylon 6 solutions (figure 5.2). As the concentration (and consequently the viscosity) was increased, beads were observed to form. The fibre diameter became larger and the shape of the beads changed from spherical to spindle like. At concentration 20 wt.%, uniform electrospun fibres were observed. As we seen from the figure 5.1, SEM result that high concentration provides highly uniform fibres of the Nylon 6 polymer solutions. When the concentration increases to 25 wt.% or more, ribbon like nanofibres are observed. The formation of ribbon like nanofibre is due to rapid solvent vaporization from the surface of the jet. To get a further insight into crucial parameters, the detailed characterization of the polymer solutions used for electrospinning was done in terms of viscosity, electrical conductivity, and surface tension. As expected, solution viscosity increased significantly with increasing Nylon 6 solution concentration, whereas electric conductivity also decreased with surface tension not showing very significantly differences.

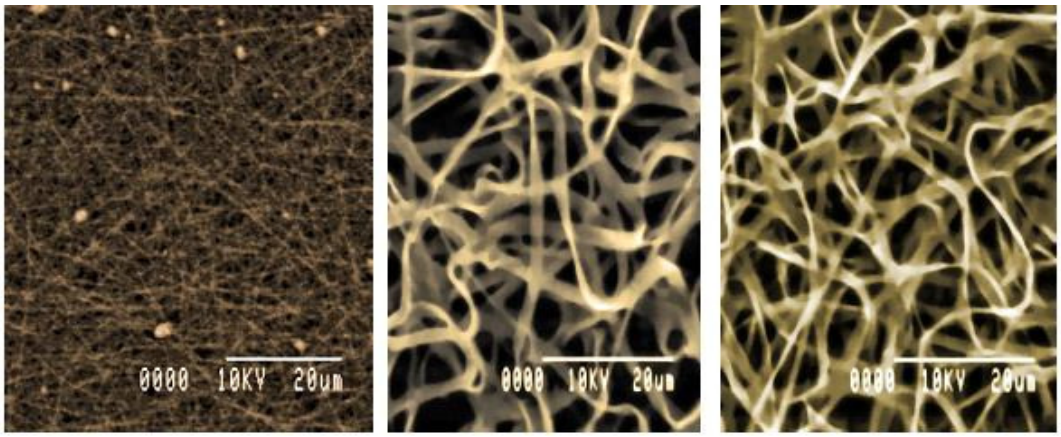

a) b) c)

Figure 5.1, SEM micrographs of Nylon 6 electrospun fibre at a voltage of 15 kV, collector distance 8 cm for different polymer concentration (a) 15 wt.%, (b) 20 wt.% and (c) 25 wt.%.

Table 5.2, Fibre diameter in different polymer concentration (15 wt.%, 20 wt.% and 25 wt.%) at constant electric fields (15 kV) and a constant spinning distance of 8 cm.

Solution concentration (wt.%)	15	20	25
Fibre diameter (nm)	350	720	736
	367	760	875
	470	790	922
	530	795	970
	550	870	1030
	568	920	1085
	600	950	1160
	625	1070	1195
	720	1136	1363
	750	1230	1377
Average fibre diameter (nm)	553	924	1071
STDEV (nm)	132	172	207

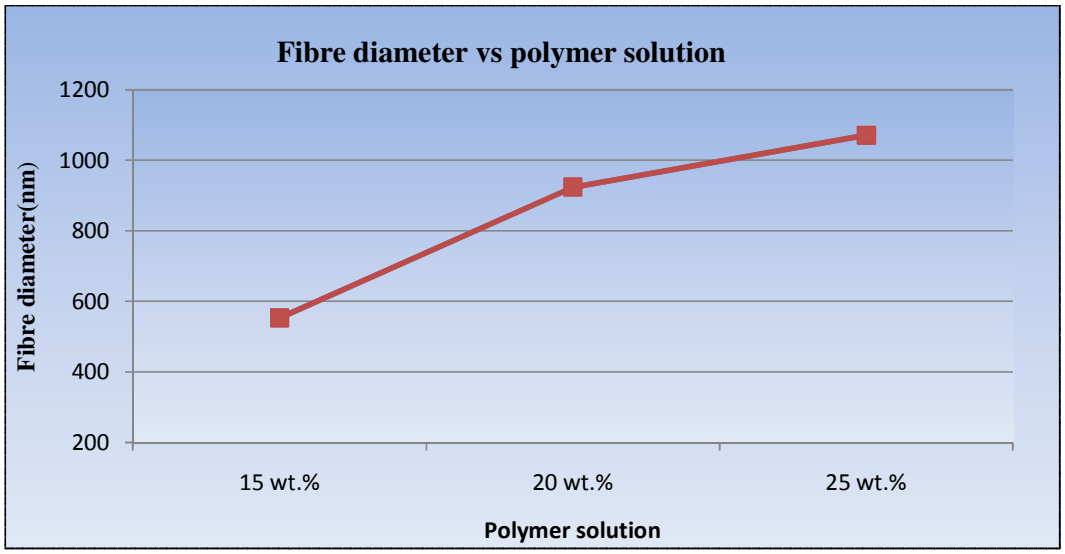

Figure 5.2, Relationship between the average fibre diameter and different polymer concentration (15 wt.%, 20 wt.% and 25 wt.%) at constant electric fields (15 kV) and a constant spinning distance of 8 cm.

As the result shown in figure 5.2 the diameter of the electrospun fibres dramatically decrease with decreasing polymer concentration when the spinning distance is small and the polymer solution has a lower concentration (like 15 wt.%), the solution reaches the collection plate before full evaporation of the solvent. This explains the formation of droplets and beads at the low polymer concentration and short spinning distance. Higher concentration produced nano fibres with fewer beads and lower concentration produce nano fibre with higher beads. Changing the fibre morphology can be attributed to a competition between the surface tension and viscosity. When the polymer concentration is 15 wt.% fibres with average diameter of 553 nm are produced, 20 wt.% fibres with average of diameter 924 nm, when the solution increases by 25 wt.% then fibre diameter is also increases to 1071 nm.

It has also been observed that as the wet nanofibres are no longer stressed by the electric field when they are laid on the collector, they undergo a solidification process as a result of the surface tension and the relaxation process controlled by the viscoelastic property of the wet nanofibres. Beaded fibres are typically observed in electrospinning when using solutions of low concentration and viscosity. Finally, the morphology of electrospun Nylon 6 nanofibres mats changes from curled at high concentration and containing beads at low concentration.

5.3.2 Effect of applied electric field on fibre morphology

The electrospinning process produces fibres only if the applied voltage is above a given limiting value required to overcome the surface tension of the solution. The electrical field is defined as the applied voltage divided by the distance between the tip and collector. Higher electric field values are obtained either through decreasing the distance between the tip and collector or by applying higher voltages. There exists controversy in the literature as to the effect of increasing the voltage on the final diameter of the electrospun nanofibre. In electrospinning experiments, the electric current associated with the process can typically be measured in a microampere. The droplets or fibres transport charge across the gap between the charged needle and the electrically grounded target, i.e. closing of the circuit. [16]. High voltages and high electric field strengths are also associated with higher productivity [6, 17-22], which is mainly considered to be due to increase in electrical current and electrostatic stresses, which in turn draw more material out of nozzle [23]. Experimental voltage effect analysis was performed for the Nylon 6 electrospinning solution using an output voltage range between 12 kV and 18 kV. Tip to target distance was held 8 cm and the polymer solution was 20 wt.%. There was a slight decrease of fibre diameter when the applied electric field is increased. Increasing the applied voltage, i.e., increasing the electric field strength will increase the electrostatic repulsive force on the fluid jet which favours fibre formation, shown in figure 5.3.

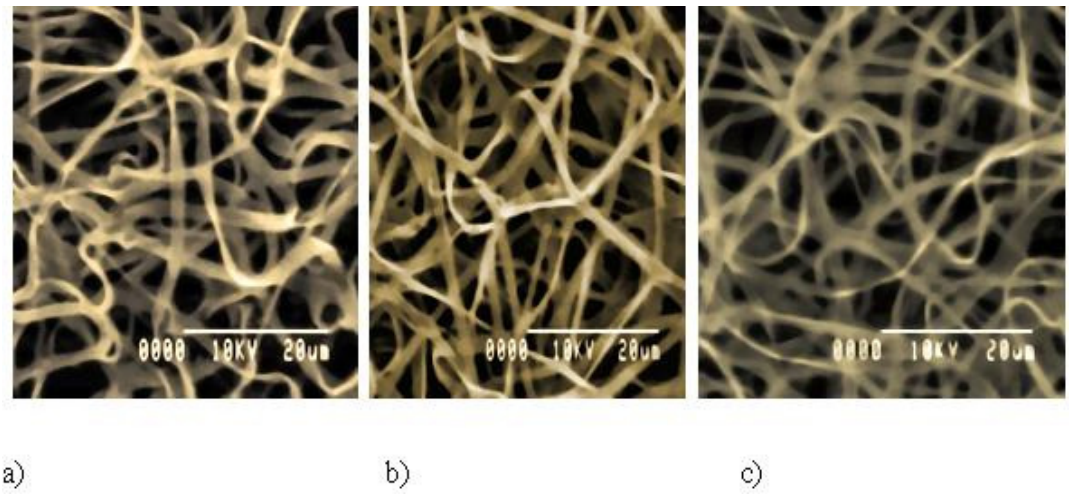

Figure 5.3, Effect of voltage on morphology with 20 wt.% Nylon 6 polymer solution, tip to target distance 8 cm and different applied voltage ; a) 12 kV, b) 15 kV and c) 18 kV.

Table 5.3, Fibre diameter in different applied electric voltage (12 kV, 15 kV and 18 kV) at the constant polymer solution (20 wt.%) and collection distance (8 cm).

Applied voltage (kV)	12	15	18
Fibre diameter (nm)	949	841	830
	1016	987	968
	1091	1050	1040
	1177	1076	1062
	1241	1182	1171
	1354	1208	1193
	1395	1289	1271
	1458	1392	1372
	1897	1592	1571
	1956	1695	1636
Average fibre diameter (nm)	1353	1231	1211
STDEV (nm)	343	268	258

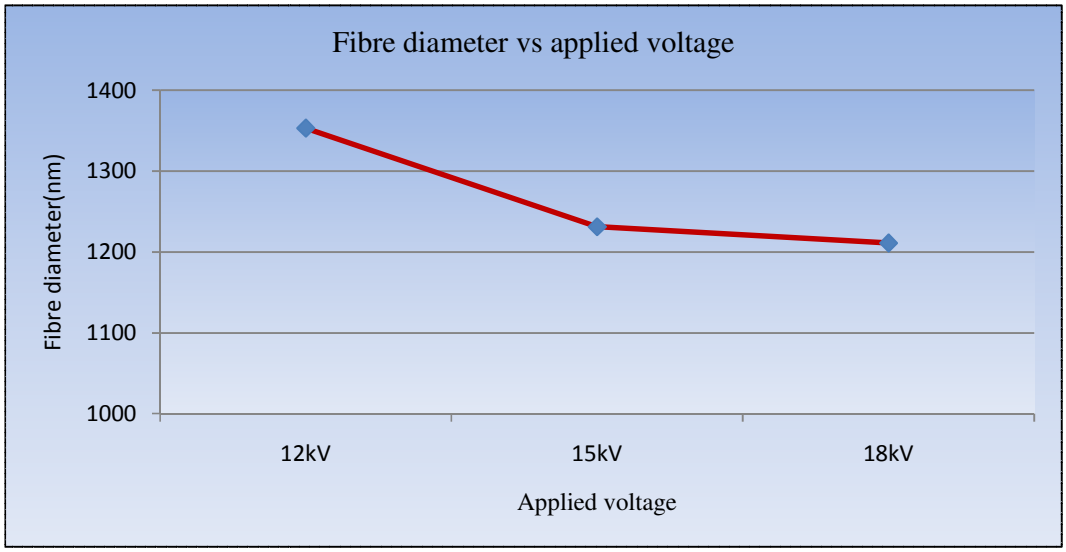

Figure 5.4, Relationship between the average fibre diameter and different applied electric voltage (12 kV, 15 kV and 18 kV) at the constant polymer solution (20 wt.%) and collection distance (8 cm).

At 20 wt.% Nylon 6 concentration, an increase in the applied voltage from 12, 15 kV to 18 kV, decreases the average fibre diameter from 1353 nm, 1231 nm and 1211 nm, shown in table 5.3 and figure 5.4. Increasing the applied voltage does increase the electrical force and creates smaller fibre diameters. Decreasing fibre diameter is due to the higher voltage or field because the higher voltage induces higher electrostatic forces on the jet and the higher repulsive forces favour the formation of the thinner fibres. Increasing the applied voltage to a certain level changes the shape of the pendant droplet from which the jet originates, so stable fibre shape can not be achieved.

5.3.3 Effect of distance from tip to collector on fibre morphology

The type of material chosen for the grounded collector determines the degree of surface charge build up during the electrospinning process. It has been demonstrated that polymer fibre deposition during electrospinning is inversely proportional to surface charge accumulation on the collector [24]. Therefore, a more highly conducting collecting plate is chosen to increase the density of the deposited electrospun nanofibres. Tip-collector distance has a direct influence on jet flight time and electric field strength. A decrease in this distance shortens flight times and solvent evaporation time, and increases the electric field strength, which results in increase of bead formation. The effect of decreasing tip-collector distance is almost the same as increasing of voltage [25-27].

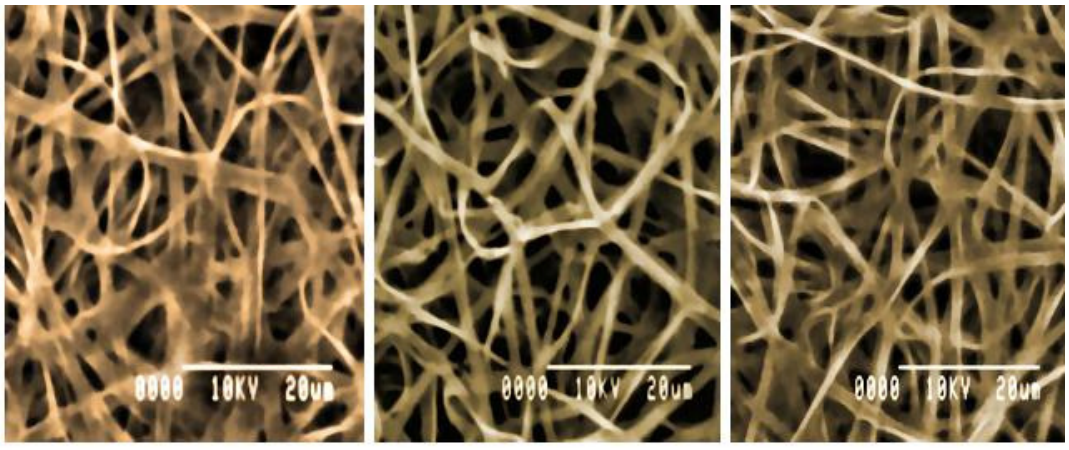

Figure 5.5, Scanning electron microscopy (SEM) images of electrospun 20 wt.% Nylon 6 fibres obtained from formic acid solution at different collecting gap distance (a) 5 cm, (b) 8 cm and (c) 11 cm and electric power 15 kV constantly.

Small gap between the tip to collector (like 5 cm), the electrospun fibres with average 1212 nm in diameter were produced. At greater distances from the tip to the collector, about 8 cm and 11 cm, electrospun fibres of average 1002 nm and 936 nm in diameter were produced. The wider gap allowed more time for the fluid jet to stretch fully and for the solvent to evaporate completely. When the gap is increased more, the collected fibres are dried and fully stretched, and the fibre diameter is reduced. At distances from tip to collector of 5, 8 and 11cm, electrospun fibre with average diameter 1212 nm, 1002 nm and 936 nm were observed respectively, as shown in figures 5.5 and table 5.4.

Table 5.4, Fibre diameter in different collection distance (5 cm, 8 cm, 11 cm) when the polymer solution (20 wt.%) and electric field constant (15 kV).

Collection distance (cm)	5	8	11
Fibre diameter (nm)	684	631	596
	853	741	671
	874	840	677
	991	919	858
	1035	955	860
	1225	1072	1035
	1471	1090	1016
	1569	1161	1125
	1664	1282	1224
	1751	1327	1302
Average fibre diameter (nm)	1212	1002	936
STDEV (nm)	379	227	243

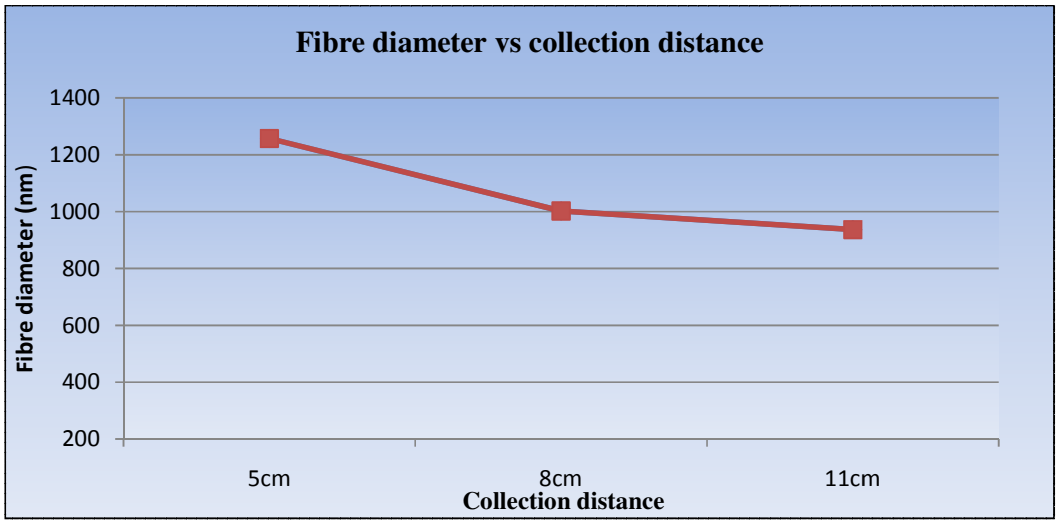

Figure 5.6, Relationship between the average fibre diameter and collection distance (5 cm, 8 cm and 11 cm) when the polymer solution (20 wt.%) and electric field constant (15 kV).

Comparing the fibres diameter at 5, 8 and 11 cm spinning distance with keeping the applied voltage and polymer concentration constant (figure 5.6) shows that the fibre diameter obtained at 11 cm and 8 cm spinning distance, is lower than those obtained at 5 cm spinning distance in the concentration range 20 wt.%. It is due to the longer spinning distance, which enables the solvent to evaporate more efficiently even at the same electric field, and produced smaller diameter fibres comparing with the fibre diameter obtained at 5 cm spinning distance.

5.3.4 Effect of flow rate on fibre morphology

Solution flow rate must also be accounted for in the characterization of electrospun fibre morphology. Essentially, solution flow rate adjustments are made in order to maintain a stabilized Taylor cone during electrospinning [26]. To a certain extent, increasing the flow rate while maintaining the Taylor cone produces larger fibre diameters [27]. Increasing the flow rate too much causes fibres to be collected without sufficient solvent evaporation leading to flattened web-like appearance [28]. Optimally, a lower solution flow rate, while maintaining the Taylor cone is more ideal since it permits time for solvent evaporation and produces better fibres. However, a solution flow rate below the threshold for a given voltage causes evaporation at the needle tip, thus preventing electrospinning. At the low flow rate (about 0.20-0.25 ml/hr) the electrospun fibre is cylindrical and uniform. At higher flow rates (about 0.26- 0.30 ml/hr) the fibre surface

is rougher. If the flow rate is much above 0.30 ml/hr, the fluid jet bents from the outset and breaks before it progresses any further. No straight segment is observed. This causes non uniform, rough surface and non cylindrical fibres and merging of fibres at crossing points. Nylon 6 fibres with average diameter 1000 nm, 1126 nm, 1388 nm and 1599 nm were electrospun at 0.20 ml/hr, 0.25 ml/hr, 0.26 ml/hr and 0.30 ml/hr applied flow rate respectively, as shown in figure 5.7, table 5. 5 and figure 5.8.

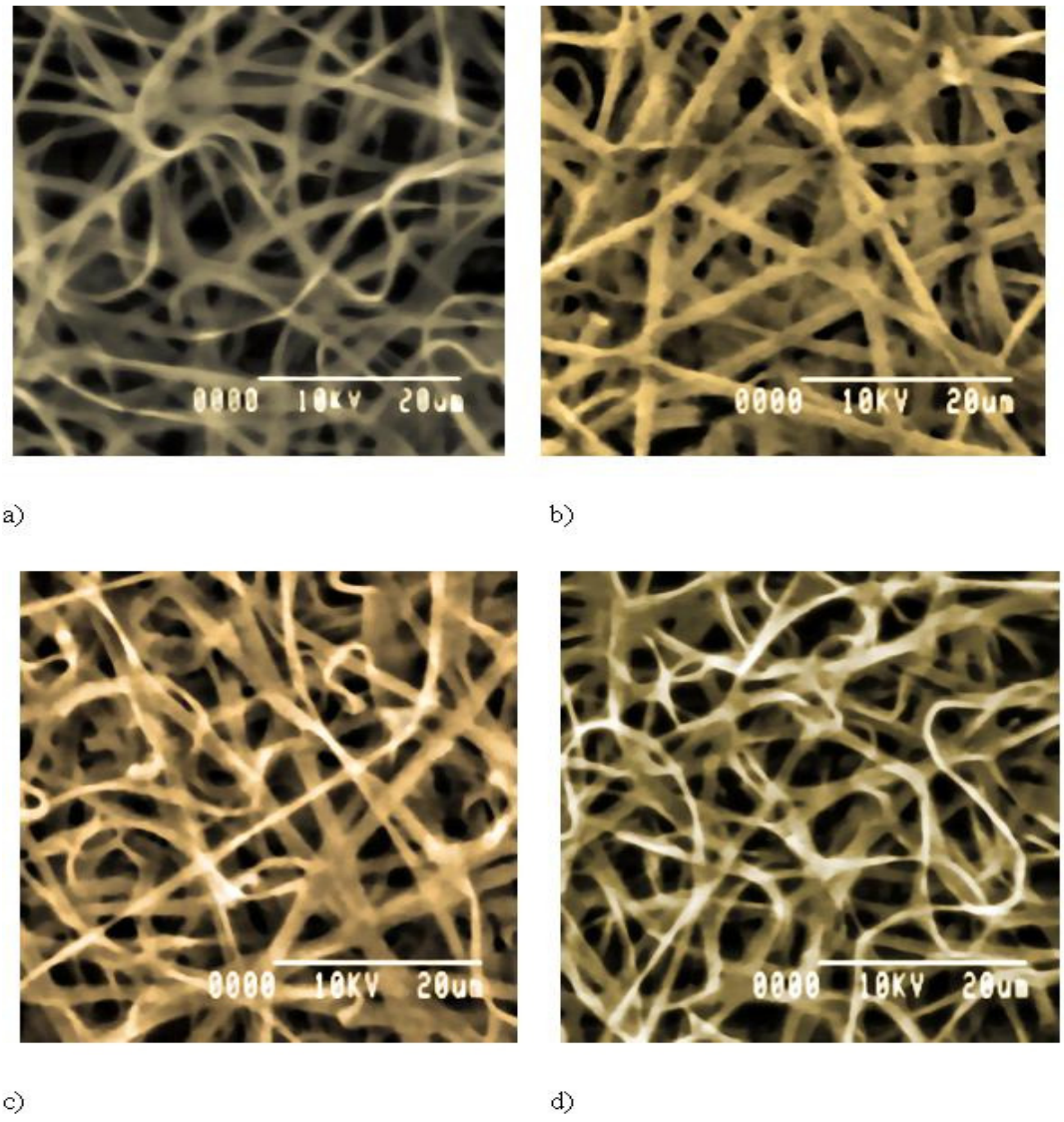

Figure 5.7, SEM images of electrospun fibres (Nylon 6 solution from formic acid), a) 0.20 ml/hr, b) 0.25 ml/hr, c) 0.26 ml/hr, d) 0.30 ml/hr and the solution was 20 wt.% and electric field was 15 kV and tip to collector distance was 8 cm.

Table 5.5, Fibre diameter in different solution flow rate (0.20 ml/hr, 0.25 ml/hr, 0.26 ml/hr and 0.30 ml/hr) when the polymer solution (20 wt.%) and electric voltage (15 kV) and collection distance (8 cm) constant.

Flow rate (ml/hr)	0.20	0.25	0.26	0.30
Fibre diameter (nm)	624	694	1054	1213
	695	792	1077	1332
	704	910	1299	1597
	804	954	1332	1599
	924	1074	1407	1625
	1077	1189	1421	1656
	1248	1269	1467	1685
	1274	1373	1522	1710
	1300	1440	1623	1749
	1354	1565	1682	1825
Average fibre diameter (nm)	1000	1126	1388	1599
STDEV (nm)	284	289	207	188

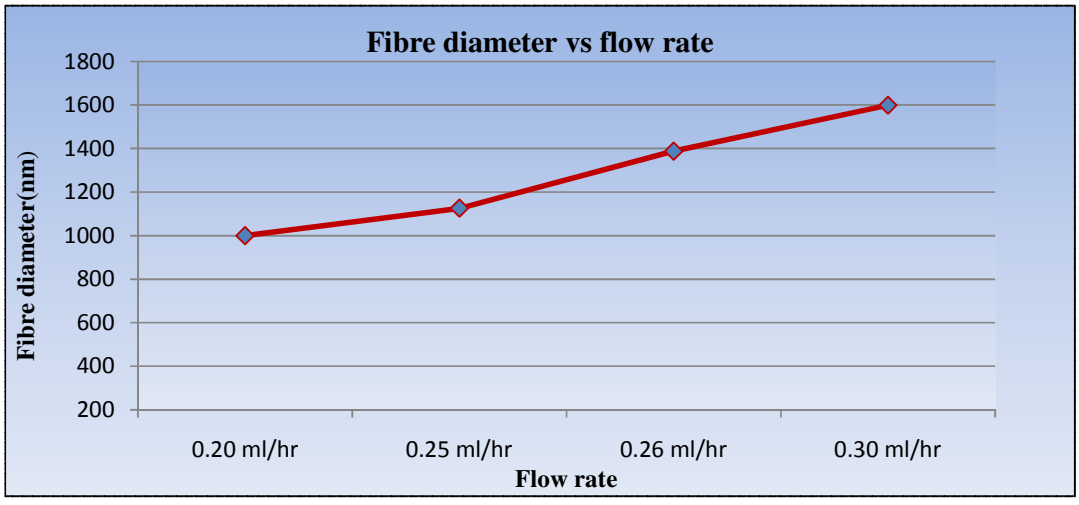

Figure 5.8, Relationship between the average fibre diameter and solution flow rate(0.20 ml/hr, 0.25 ml/hr, 0.26 ml/hr and 0.30 ml/hr) when the polymer solution (20 wt.%) and electric voltage (15 kV) and collection distance (8 cm) constant.

Finally we can say that at low feed rates 0.20 ml/hr- 0.25 ml/hr, solvent have sufficient amount of time to evaporate until the fibres are collected on the plate and thinner and uniform fibres are produced. At high feed rate 0.26 ml/hr - 0.30 ml/hr which seems above the quasi-stable point, solution is not completely carried away to the collector, which resulted in unstable jet and larger fibres.

5.4 Conclusion

Ultramide Nylon 6 nanofibres have been successfully produced. Nylon 6 nonwoven mats have been created from solution at different concentrations. It has been established that the diameter of the electrospun fibre is affected by viscosity, surface tension and electrical conductivity of the polymer solution, applied electric field and collection distance. Electrospun Nylon 6 nanofibres with a smaller diameter can be produce with a lower polymer solution concentration (15 wt.%) but nonuniform/beaded fibres are found, as the solution concentration increases (20 wt.% - 25 wt.%), then viscosity beyond a critical value resulted in the formation of smooth fibres with larger diameters (924 nm to 1071 nm). The applied voltage (12 kV to 18 kV) reflects on the force to pull a solution out from the spinneret, so higher applied voltage (18 kV) affects the charge density and thus the electrical force, which influence the elongation of the jet during electrospinning and produce thinner fibres (1211 nm). Tip to collection distance and flow rate also made impact to produce uniform fibres. Larger distance (11 cm) may enhance the evaporation of solvent, leading to thinner fibres (936 nm) and with the short distance (5 cm) wet fibres with flatten cross-section have been obtained. Higher flow rate (0.30 ml/hr) produced large diameter nanofibres. As we seen in figure 5.1, the optimal condition for uniform fibre diameter of Nylon 6 nanofibres are; polymer solution concentration of 20 wt.% and applied voltage of 15 kV, volume feed rate 0.20 ml/hr and a spinning distance of 8 cm. These optimum parameters can produce uniform Nylon 6 nanofibres of diameter 924 nm.

5.5 References.

[5.1] A. Formhals, *Method and apparatus for spinning*, US Patent, 2160962 (1939)

[5.2] A. Formhals, *Artificial thread and method of producing same field*, US Patent, 2187306 (1940)

[5.3] A. Formhals, *Producing of artificial fibres from fibre forming liquids*, US patent, 2323025 (1943)

[5.4] A. Formhals, *Method and apparatus for spinning*, US Patent, 2349950 (1944)

[5.5] A. Formhals, *Process and apparatus for preparing artificial threads*, US patent, 1975504 (1934)

[5.6] P. K. Baumgarten, *Electrostatic spinning of acrylic microfibres*, Journal of Colloid and Interface Science, **36**, 71-79 (1971)

[5.7] D. H. Reneker, I. Chun, *Nanometer diameter fibres of polymer produced by electrospinning*, Nanotechnology, **7**, 216-223 (1996)

[5.8] A. Fertala, W. B. Han, F. K. Ko, *Mapping critical sites in Collagen II for relational design of gene-engineered proteins for cell-supporting materials*, Journal of Biomedical Research, **57**,48-58 (2001)

[5.9] H. J. Jin, S. Fridrikh, G. C. Rutledge, D. Kaplan, *Electrospinning Bombyx Mori silk with Poly (Ethylene oxide)*, Abstracts of Papers, American chemical Society, **224**, 408-420 (2002)

[5.10] Y.C. Ahn, S. K. Park, G. T. Kim, Y. J. Hwang, C. G. Lee, H. S. Shin , J. K. Lee, *Development of high efficiency nanofilters made of nanofibres*, Current Applied Physics, **6**, 1030-1035 (2006)

[5.11] J. Zeng, X. Xu, X. Chen, Q. Liang, X. Bian, L.Yang and X. Jing, *Biodegradable electrospun fibres for drug delivery*, Journal of Controlled Release, Volume **92**, Issue 3, Pages 227-231 (2003)

[5.12] C. Mit-uppatham, M. Nithitanakul, P.Supapol, *Ultrafine electrospun polyamide-6 fibres: effect of solution conditions on morphology and average fibre diameter*, Macromolecular Chemistry and Physics, **205**, 2327-23338 (2004)

[5.13] L. Larrondo, R. S. J. Manley, *Electrostatic fibre spinning from polymer melts; electrostatic deformation of pendent drop of polymer melt*, Journal of Polymer Science, **19**:p.933 (1981)

[5.14] Y. J. Ryu, H. Y. Kim, K. H. Lee, H. C.Park and D. R. Lee, *Transportproperties of electrospun Nylon 6 nonwoven mats*, European Polymer Journal, **39**, 1883-1889 (2003)

[5.15] S. Koombhongse, W. Liu, D. H. Reneker, *Flat polymer ribbons and other shapes by electrospinning*, Journal of Polymer Science Part B: Polymer Physics, **9,** 2598-2606 (2001)

[5.16] J. M. Deitzel, J. D. K. Meyer, J. K. Hirvonen and N. C. B.Tan, *The effect of processing variables on the morphology of electrospun nano fibres and textiles*, Journal of polymer science, Vol **1**, p. 261-272 (2001)

[5.17] C. J. Buchko, L. C. Chen, Y. Shen and D. C. Martin, *Processing and microstructural characterization of porous biocompatible protein polymer thin films*, Polymer, 40, 7397–7407 (1999)

[5.18] X. M. Mo, C.Y. Xu, M. Kotaki, S. Ramakrishna, *Electrospun P(LLA-CL) nanofibre: a biomimetic extracellular matrix for smooth muscle cell and endothelial cell proliferation*, Biomaterials, Volume **25**, Issue 10, , Pages 1883-1890 (2004)

[5.19] S. Kidoaki, I. K. Kwon, T. Matsuda, Biomaterials, **26,** p.37–46 (2005)

[5.20] C. Mit-uppatham, M. Nithitanakul, P.Supapol, *Ultrafine electrospun polyamide-6 fibres: effect of solution conditions on morphology and average fibre diameter*, Macromolecular Chemistry and Physics, **205**, 2327-23338 (2004)

[5.21] K. Morota, H. Matsumoto, T. Mizukoshi, Y. Konosu, M. Minagawa, A.Tanioka, Y. Yamagata and K.Inoue, *Poly (ethylene oxide) thin films produced by electrospray deposition: morphology control and additive effects of alcohols on nanostructure*, J Colloid Interface Sci, **279** (2):484–92 (2004)

[5.22] P. Heikkila, A. Harlin, *Parameter study of electrospinning of polyamide 6*, European Polymer Journal, **44,** 3067–3079 (2008)

[5.23] S. A.Theron, E. Zussman, A. L.Yarin, *Experimental investigation of the governing parameters in the electrospinning of polymer solutions*, Polymer, **5** (6):2017–30 (2004

[5.24] R. Kessick, J. F, G.Tepper*, The use of AC potentials in electrospraying and electrospinning process,* Polymer, **45**:2981-2984 (2004)

[5.25] A. Frenot, and I. S. Chronakis, *polymer nanofibres assembled by electrospinning*, Current Opinion in Colloid and Interface Science, **8**, 64–75 (2003)

[5.26] S. Ramakrishna, K. Fujihara and W. Teo*, An Introduction to electrospinning and nanofibres,* World Scientific Publishing Co Pte Ltd, **ISBN 10:** 9812564543 (2005)

[5.27] H. Homayoni, S. A. H. Ravandi and M. Valizadeh, *Electrospinning of chitosan nanofibres: Processing optimization,* Carbohydrate Polymers **77**, 656–661 (2009)

[5.28] G. C. Rutledge, Y. L, S. V.Fridrikh, S. B. Warner, V. E. Kalayci, P. Patra, *Electrostatic Spinning and Properties of Ultrafine fibres*, National Textile centre (2001)

Chapter 6: Processing parameter study of Nylon 6.6 electrospun fibres

6.1 Introduction

Nylon 6.6 is often used to produce fibres with the diameter in the order of 20-30 μm by conventional melt spinning. However, the fibres with much smaller diameters are preferred for many industrial applications. For example, the Nylon 6.6 fibre-reinforced composites will have good transparent property if the fibre diameter is lower than that of light wavelength. So the novel spinning methods with the advantages in producing smaller fibre should be developed to fulfil these industrial requirements, and electrospinning is proved to be such a powerful method. Although many researchers have studied Nylon 6.6 none of these have analyzed systematically the influence of the processing parameters on the electrospinning process, and fibre alignment and the making of composite fibre with multi wall carbon nano tube (MWCNT). It has found that morphology such as fibre diameter and uniformity of the electrospun polymer fibres are dependent on many processing parameters. Under certain condition, not only uniform fibres but also beads free fibres can be produced by electrospinning. Therefore, these parameters should be carefully optimized while controlling fibre diameter and its alignment. On the other hand, when initial instability of the jet, fibres are often collected as randomly oriented structures in the form of nonwoven mats, which are acceptable only for some applications such as filters, wound dressings and tissue scaffolds. Meanwhile, obtaining continuous aligned nanofibres and high-volume production is very important for many areas such as fibre reinforcement and device manufacture [1-2].

Several techniques have been developed to align electrospun nanofibres and some breakthroughs have been obtained. The results are promising, but these methods need to be further improved for practical applications. In the technique of using a rotating drum as the collector [3- 4] only partial fibre alignments have been achieved. Some newer techniques can produce well-aligned fibres, but only of limited length [5- 6], scan disk fabrication [7-8] which can cause thicker jet formation, Coagulation bath collector [9-10] which produced partial aligned fibres and thickness [11- 12]. In recent years researchers have developed several collection mechanisms to control the deposition of the electrospun nanofibres and to obtain continuous fibre alignment by manipulating the dynamic motion of the collector or the electric field strength and geometrical shape or

both [13]. Nylon 6.6 found to have excellent strength as a polymer material which possesses high mechanical properties. Comparing other synthetic fibres, great advantages of Nylon 6.6 fibres are; resistance to abrasion and flexing, and the supply of tactile feeling. Nylon 6.6 fibres can be produced in a variety of cross-section shape and fineness. Composite fibres can also be produced by combining Nylon 6.6 with other types of fibres. Heat storage or warmth retention fibres consisting of extremely fine filament yarns in which carbonaceous materials are converting light to heat can also be inserted. Anti-static Nylon 6.6 fibres inhibiting electro-static charge, transparent Nylon 6.6 fibres can exhibit transparent and beautiful colors, making Nylon 6.6 fibres available with varied performance. Nylon 6.6 has a tighter molecular structure than Nylon 6 due to a higher level of hydrogen bonding and maximum alignment between molecular chains, creating a tighter structure that better resists crushing, matting and stain penetration. In this chapter, the effects of various preparatory parameters, such as solution properties, applied voltage and distance from needle to collector, flow rate and diameter of the electrospun nano fibre, align nanofibres, Nylon 6.6/MWCNT composite fibres and their morphology will be presented and discussed.

6.2 Experimental

6.2.1 Preparation of polymer solution

Nylon 6.6 is purchased from BASF, UK with 255º C - 265º C melting temperature. The polymer was dissolved in formic acid (96.7% from Sigma Aldrich, Gillingham, UK) at a temperature of 20º C and stored at the same temperature. Various concentrations ranging from 15 to 25 wt.% were prepared and used for the experiments. All electrospinning experiments were carried out at room temperature in air. The polymer solution was fed from 10 ml capacity syringe (Fisher Co., UK) to a vertically oriented (25 gauge) blunt-ended metal needle spinneret via Teflon tubing. The feed rate was digitally controlled by syringe pump and power supply used to connect the needle directly.

6.2.2 Measurements and characterization (solution properties)

Solution viscosities were measured with an AR-1000 Rheometer, TA instruments, UK. The viscosities of the polymer solution were reported in unit Pa.s. Surface tension for each solution was determined by the torsion balance (Model 'OS' Balance/Tensiometer, UK) for surface and interfacial tension measurement method.

The surface tension was reported by unit mN/m. Electric conductivity was measured by using four probe methods and reported with unit S/cm.

6.2.3 Morphological characterizations

The SEM and AFM were used as a primary tool to provide a more detailed analysis of Nylon 6.6 fibre morphologies. Atomic force microscopy (Model 5400, AFM, UK) was used to characterize the morphology of the electrospun fibres specially their diameter range and their structures. Since SEM and AFM analysis could not be provided in real-time, only a few selected samples were examined using this method. JEOL JEM TEM 2010, UK used to find the CNT particle inside the composite fibre. The glass transition temperature (Tg), the melting temperature (T_m), the amount of residual solvent ($X_{r.s}$) and the apparent amount of crystallinity of the nanofibres were measured by Metler DSC 30 (USA). The nanofibres were heated between 40º C and 400° C at 10° C/min. The amount of crystallinity was calculated as the ratio between the melting enthalpy of the sample and the melting enthalpy of a theoretical 100% crystalline sample ($\Delta Hf^{o}_{m)}$. X'Pert-MPD Philips diffractometer (UK) used for X-ray diffraction. To measure the diameters of the electrospun Nylon 6.6 nano fibres, an image analyzer (Image J, USA) was used.

6.2.4 Effect of Polymer solution properties: Solution concentration, viscosity and surface tension on fibre morphology

Polymer solutions are essentially non-Newtonian fluid; elongation flow resists the breakup of the viscoelastic jet, leading to the formation of long threads of mini jets. As a result, the morphology of the nanofibres would depend on polymer concentration that will affect viscosity [14]. The solution viscosity has been found to influence fibre diameter. It is known that the viscosity of the polymer plays a major role in the production of the fibre and their size and is one of the most studied parameters in electrospinning [15]. Deitzel et. al explain that solution surface tension and viscosity play important roles when produce nano fibre by electrospinning process [16]. Low concentration solution forms droplets due to the influence of surface tension, while higher concentration prohibits fibre formation due to higher viscosity. Table 1 showed that as expected, solution viscosity decreased significantly with decreasing concentration also surface tension decrease, as a result, the beaded fibres instead of continuous ultra fine fibres were obtained.

Table 6.1, Influence of Nylon 6.6 concentrations on viscosity, electric conductivity, and surface tension and fibre diameters.

Nylon6.6 conc. (wt .%)	Viscosity(Pa.s)	Surface Tension (mN/m)	Electric conductivity (S/cm)	Fibre diameter(nm)
15	0.5614	44.7	0.0046	250-600
20	2.22	46.5	0.0044	400-900
25	6.062	49	0.0041	600-1300
Formic acid	0.002	28	0.09	

The voltage (15 kV) and collection distance (8 cm) remained constant whilst used different concentrations (15 wt.%, 20 wt.% and 25 wt.%) non woven mats of fibres were electrospun. Three samples were prepared for each solution. The average data collected is shown in table (6.1). It shows that the average fibre diameter is increased with increasing polymer solution. When the surface tension increases and electrical conductivity of the solution decreases the fibre diameter has also increased. When the polymer solution is 15 wt.% the average fibre diameter becomes 380 nm, and by gradually increasing the solution from 20 wt.% to 25 wt.% the fibre diameters increases respectively from 596 nm to 827 nm (shown in table 6.2 and figure 6.2).

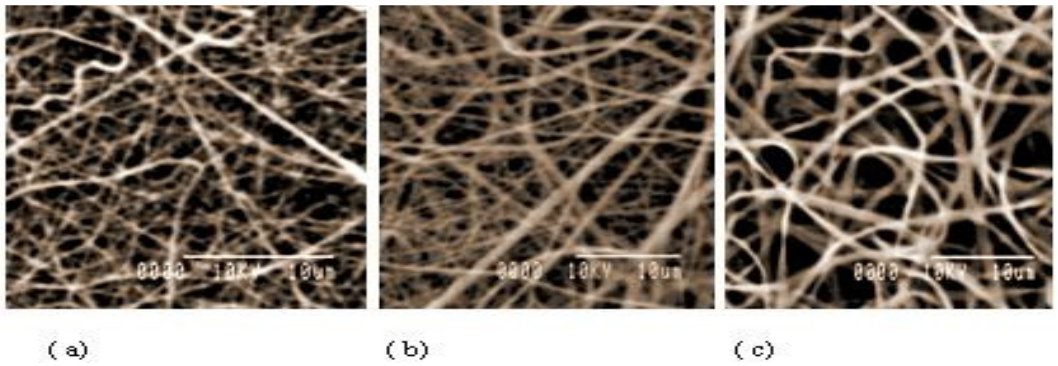

Figure 6.1, SEM micrographs of Nylon 6.6 electrospun fibre at a voltage of 15 kV, collector distance 8 cm for different polymer concentration (a) 15 wt.% (b) 20 wt.% (c) 25 wt.%.

Table 6.2, Nylon 6.6 electrospun fibre at a voltage of 15 kV, collector distance 8 cm for different polymer concentration (a) 15 wt.% (b) 20 wt.% (c) 25 wt.%.

Solution concentration (wt.%)	15	20	25
Fibre diameter (nm)	250	456	605
	279	478	606
	298	488	658
	339	510	722
	349	534	780
	363	554	871
	400	562	945
	454	755	995
	484	773	1003
	583	850	1085
Average fibre diameter (nm)	380	596	827
STDEV (nm)	103	142	177

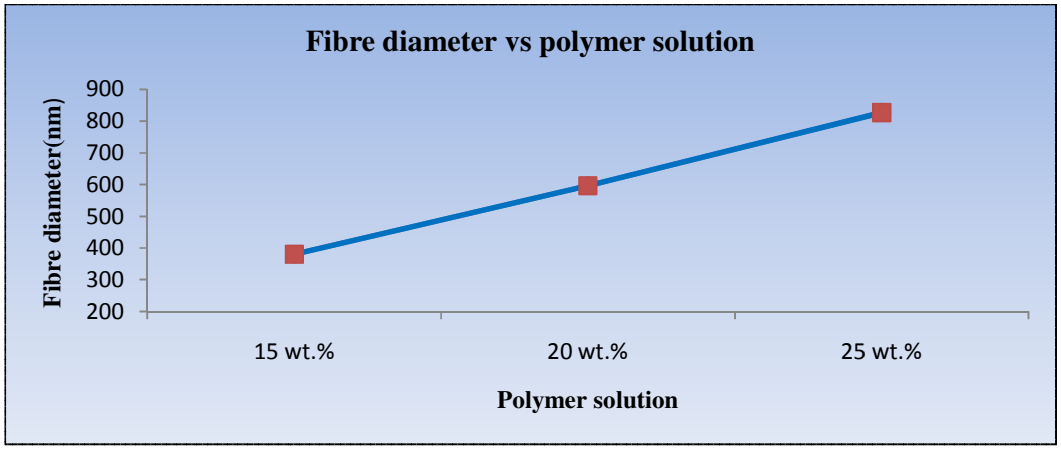

Figure 6.2, Relationship between the average fibre diameter and polymer solution where electric field (15 kV) and collection distance (8 cm) constant.

As we see that the figure 6.1 as the concentration (and consequently the viscosity) was increased, beads were formed. The fibre diameter became larger and the shape of the

beads changed from spherical to spindle like. At concentrations higher than 20 wt.%, uniform fibres were observed shown in figure 6.1 (c), under the following conditions, i.e. applied voltage being 15 kV and distance from spinneret to collector being 8 cm. As it is observed from the figure 6.1, high concentration gives better uniform fibres of the Nylon 6.6. To get a further insight into crucial parameters, the detailed characterization of the polymer solutions used for electrospinning was done in terms of viscosity, electrical conductivity, and surface tension. With further increases of solution concentration, fibres were formed from beads to bead-on-string to continuous cylindrical fibres were produced. Increasing the solution concentration increased the solution viscosity, which improved the spinnability of continuous fibres (table 6.1). Uniform fibres are obtained at higher concentration and lower concentration produced fibres with beads. If the concentration decreases, bigger beads were obtained with the formation of spots.

6.2.5 Effect of the applied electric voltage on fibre morphology

The voltage applied between the capillary and the metal target can be used to control the amount of polymer reaching the target. The number of droplets or fibres reaching the target is a function of the current flowing across the system. Hence the amount of fibre spun can be easily controlled by varying the voltage. At low voltage, a droplet of solution remains suspended at the end of the syringe needle, and the fibre jet originates from the cone at the bottom of the droplet. The size of the droplet formed at the end of capillary is large as the voltage is not high enough to transfer all the solution to the target. The nano fibres produced under this condition will typically have cylindrical morphology with few bead defects. Fong et al [17] also described that beads fibre caused due to instability of the jet of polymer solution. Baumgarten [18] showed that the diameter of the jet initially decreases as the field strength increases and then begins to increase as the field strength continues to increase. This effect means an increase in volumetric flow rate as the applied voltage increases beyond a certain level. The phenomenon is related to the fact that increasing the field increases the electrostatic stresses, which is turn; draw more material out of the syringe. When typical value voltage is increased, the cone will have receded and jet originates from the liquid surface within the syringe tip. The fibre morphology still remains cylindrical but with more bead effects [19]. In this study we investigate the effect of the spinning voltage on the fibre diameter keeping other parameters constant. The concentration of the solution and distance were fixed (25 wt.% and 8 cm). The voltage was changed from 12 kV to

15 kV and 18 kV, in order to explore the effect on the electrospun Nylon 6.6. These samples were observed in the SEM. The average fibre diameter was evaluated by randomly selecting up to 10 different portions of the fibrous mat and averaging the diameter over the number of portions selected in each portion.

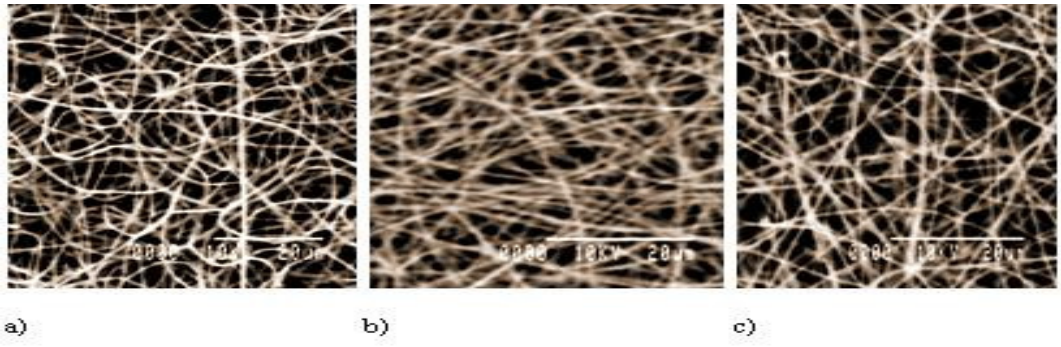

Figure 6.3, SEM micrograph of Nylon 6.6 electrospun fibre at a solution 25 wt.% and the collection distance was 8 cm. for different electric voltage (a) 12 kV (b) 15 kV (c) 18 kV.

Table 6.3, Nylon 6.6 electrospun fibre at a solution 25 wt.% and the collection distance was 8 cm. for different electric voltage (a) 12 kV (b) 15 kV (c) 18 kV.

Applied voltage (kV)	12	15	18
Fibre diameter (nm)	502	459	337
	504	469	427
	617	548	525
	629	593	581
	659	644	598
	745	724	627
	784	744	628
	833	820	674
	850	845	754
	1001	966	804
Average fibre diameter (nm)	712	681	595
STDEV (nm)	160	168	140

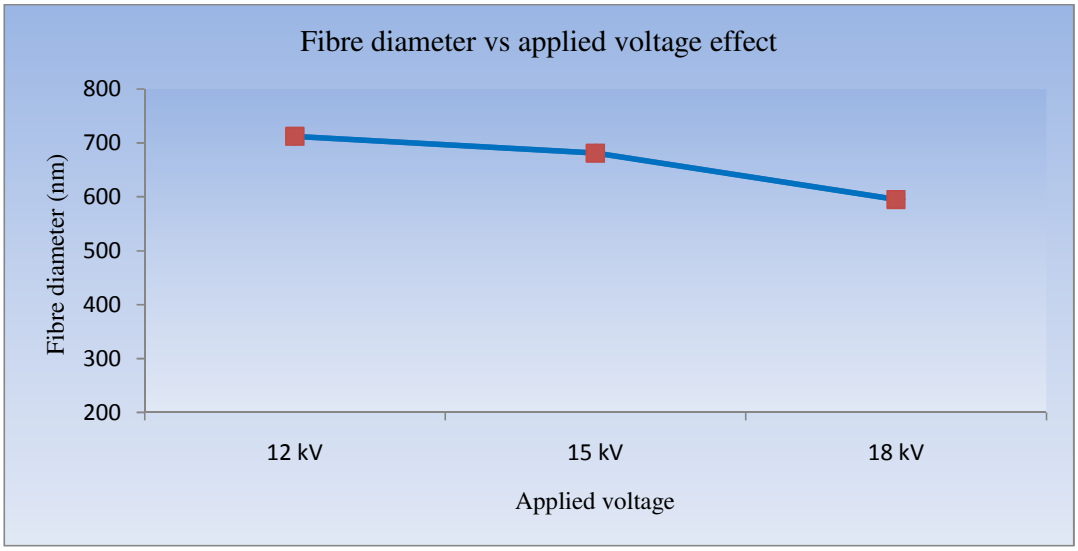

Figure: 6.4, The relationship between the average fibre diameter and the applied voltage with concentration of 25 wt.% and spinning distance 8 cm constant.

The collected fibres are shown in figure 6.3. The average diameter decreases from 712 nm to 595 nm as the voltage is increased from 12 kV to 18 kV and produces a 681 nm fibre at 15 kV as shown in table 6.3. When the nozzle to collector distance is constant, an increase in the applied voltage increases the intensity of the electric field across the solution and the collector. This further accelerates the whipping motion of the jet resulting in the thinning of the fibres, can be shown at figure 6.4. Table 6.3 and figure 6.4 shows that voltage played a part to produce uniform fibre and its fibre diameter. It was observed that the diameter of the electrospun fibres was dramatically changed with varied applied voltage. As the electric field strength was increased, the electrostically driven instability increased in magnitude and caused the jet to undergo higher amounts of whipping and plastic stretching that resulted in a decrease of the fibre diameter. That exceedingly uniform fibre is obtained by lower voltage and the fibre diameter was 600 nm to 850 nm. Higher voltage produces more fibres but they are not uniform, observing variation of the diameter of the ultra fine fibres and its asymmetry distribution. In general, increasing the applied voltage to a certain level would change the shape of the pendant drop from which the jet originated so that a stable shape could not be achieved. Generally we can say that the effect of voltage is got significant little effect in controlling fibre morphology.

6.2.6 Nozzle tip to collection process effect on fibre morphology

The distance between the nozzle and the collector plays an equally important role in determining the ultimate diameter of the fibres during the electrospinning process. As part of understanding the electrospinning process the effect of nozzle to collector distance was carefully investigated in this work. The final step in the electrospinning process is the collection process. In order to investigate the effect of the distance between the needle and the collector on the properties of resulting ultra fine fibres, the following spinning condition were fixed. The voltage was fixed at 15 kV and the solution concentration at 25 wt.% whilst the distances of 5 cm, 8 cm, and 11 cm were obtained.

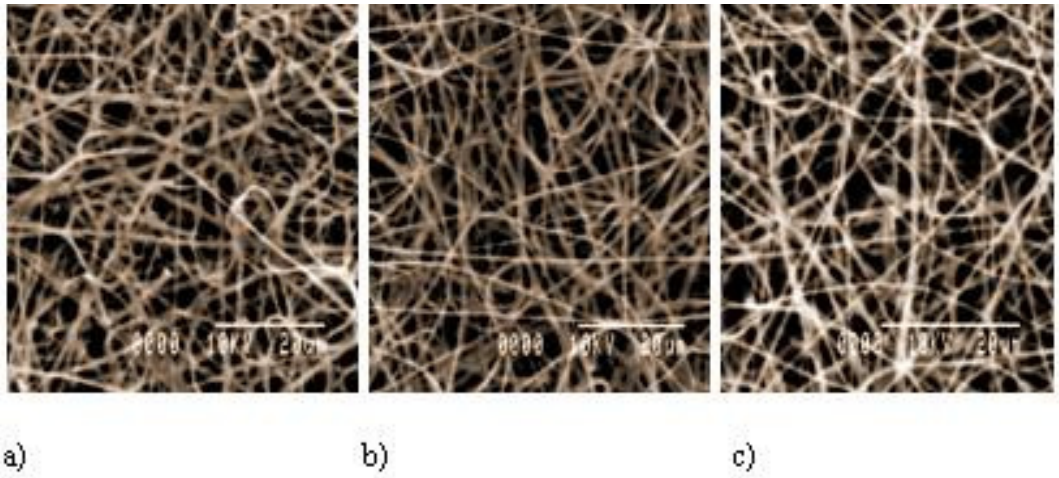

Figure 6.5, SEM micrographs of nylon 6.6 electrospun nano fibre at constant electric voltage of 15 kV and polymer concentrations 25 wt.% with different collection distance of 5 cm, 8 cm and 11 cm.

At low separation distance between the capillary end and the target, wet fibres are collected, primarily due to the presence of significant amount of residual solvent in the fibres. As the collection distance is increased, the time for the solvent to evaporate increases and as a result, dry solid fibres are collected in the target (figure 6.5). With increasing the distance between the capillary end and the target, the jet underwent a larger amount of electrically driven bending or whipping instability. Consequently, the amount of stretching or elongation of the jet increased, resulting in the fibre diameter to decrease.

Table 6.4, The fibre diameter and collection distance (5 cm, 8 cm, 11 cm) when the polymer solution (25 wt.%) and electric field constant (15 kV).

Collection distance (cm)	5	8	11
Fibre diameter (nm)	490	421	282
	621	502	392
	635	551	520
	640	578	564
	724	596	577
	786	744	677
	870	754	697
	1002	767	757
	1024	892	808
	1145	897	836
Average fibre diameter (nm)	794	670	611
STDEV (nm)	211	164	180

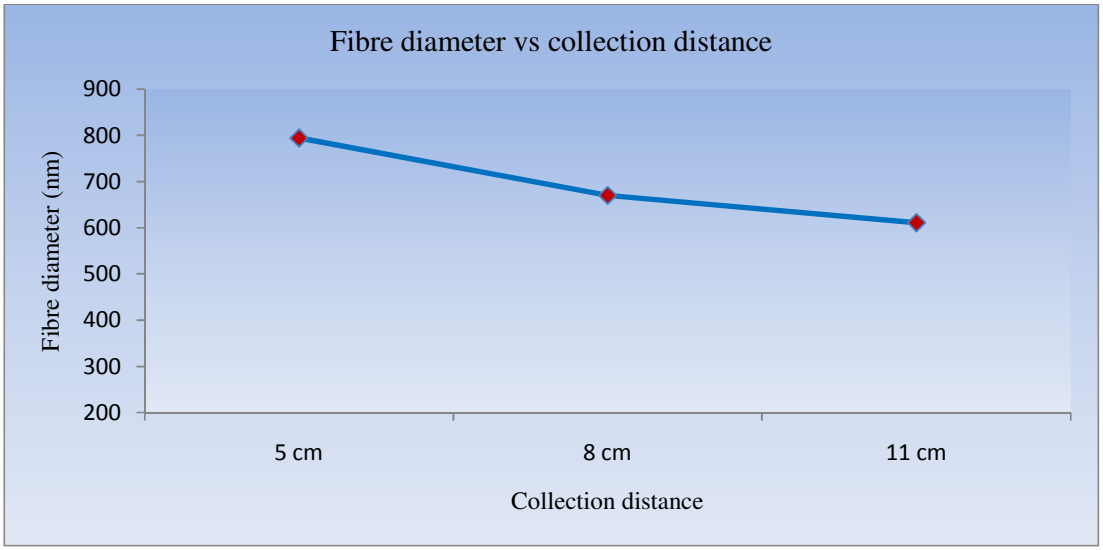

Figure 6.6, The relationship between the average fibre diameter and collection distance where solution concentration (25 wt.%) and applied voltage (15 kV) constant.

If we consider table 6.4 and 6.6 then we can see that when the fibre collection distance is 5 cm, collected fibre diameter between 490 nm to 1145 nm, is achieved with the average fibre diameter being 794 nm. Increasing the collection distance from 5 cm to 8 cm and 11 cm respectively the fibre diameter also decrease between 421 nm to 897 nm and 282 nm to 836 nm respectively. The average diameters are also lower than shorter distance 8 cm 670 nm and 11 cm 611 nm. Finally we understand that the fibres with smaller diameters are obtained by allowing the jet to cover more distance in the electric field. This also allows more time for the evaporation of solvent from the fibres that can result in decrease in the diameter. In this study, the tip-to-collector distance of 8 cm provides a result in uniform electrospun fibres.

6.2.7 Effect of flow rate on fibre morphology

Once the feed rate is sufficient for forming fibres, higher feed rate only provides more polymer solution than needed, since it was observed that the amount of excess polymer solution formed at the needle tip increased with increasing feed rate. When the flow rate exceeded a critical value (0.26 ml/hr), the delivery rate of the solution jet to the capillary tip exceeded the rate at which the solution was removed from the tip by the electric forces. This shift in the mass-balance resulted in a sustained but unstable jet and fibres with a broad distribution for the fibre diameter were formed. As shown in figure 6.7 (c & d).

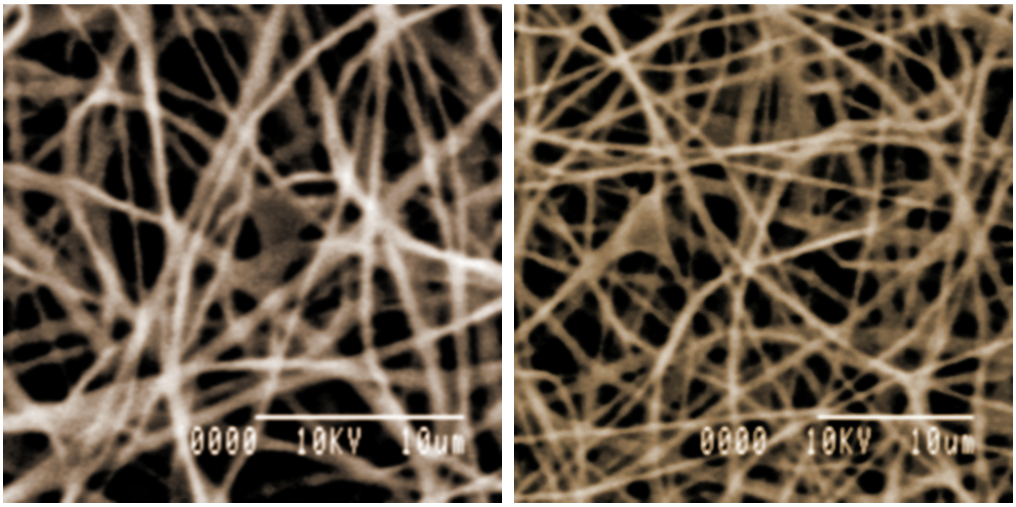

a) b)

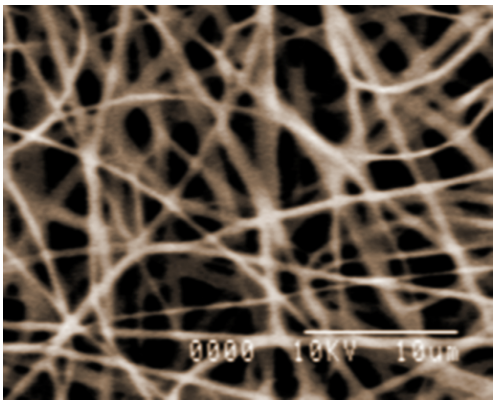

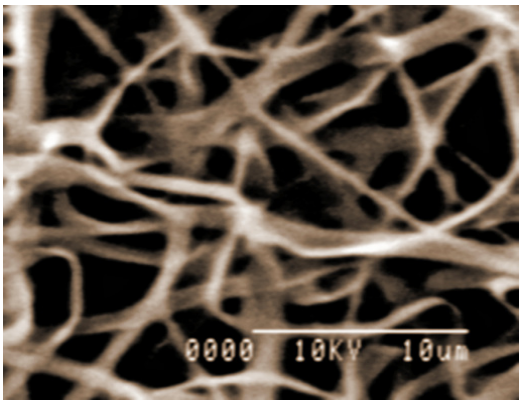

c) d)

Figure 6.7, SEM images of electrospun fibres (Nylon 6 solution from formic acid) with different flow rate a) 0.20 ml/hr, b) 0.25 ml/hr, c) 0.26 ml/hr and d) 0.30 ml/hr. Where the solution was 25 wt.% and electric field was 15 kV and tip to collector distance 8 cm constant.

Table 6.5, Fibre diameter in different solution flow rate (0.20 ml/hr, 0.25 ml/hr, 0.26 ml/hr and 0.30 ml/hr) when the polymer solution (25 wt.%) and electric voltage (15 kV) and collection distance (8 cm) constant.

Flow rate (ml/hr)	0.20	0.25	0.26	0.30
Fibre diameter (nm)	279	280	503	565
	367	364	507	567
	369	380	508	677
	392	437	513	802
	410	442	648	810
	413	504	680	862
	461	515	755	1096
	505	566	810	1492
	507	616	1024	1538
	575	643	1077	1549
Average fibre diameter (nm)	428	472	702	996
STDEV (nm)	86	116	214	397

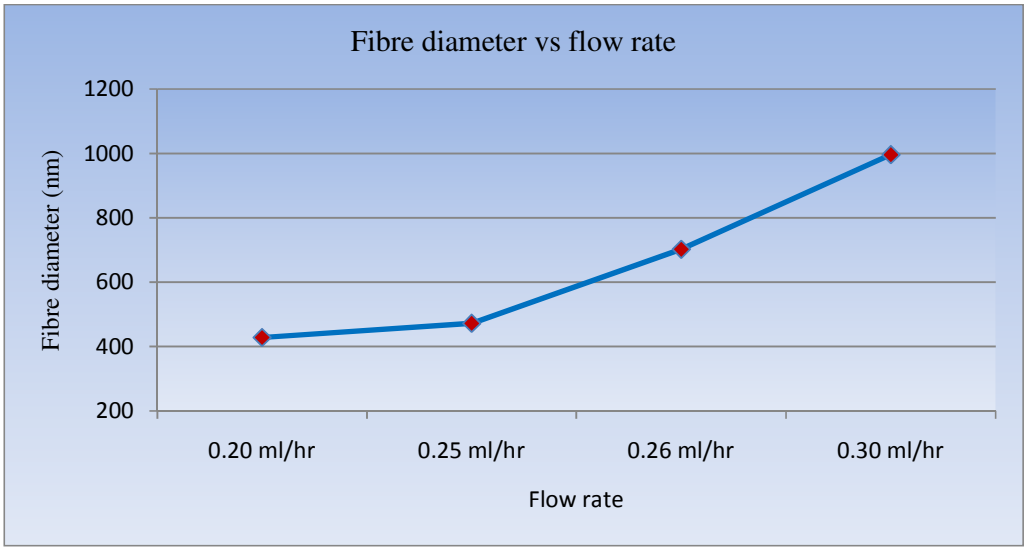

Figure 6.8, Relationship between the average fibre diameter and solution flow rate (0.20 ml/hr, 0.25 ml/hr, 0.26 ml/hr and 0.30 ml/hr) when the polymer solution (25 wt.%) and electric voltage (15 kV) and collection distance (8 cm) constant.

The feed rates of 0.20, 0.25, 0.26 and 0.30 ml/hr were adjusted by the syringe pump to determine the effect of mass throughput on fibre morphology. Polymer concentration, voltage and distance were kept constant at 25 wt.%, 15 kV and 8 cm respectively. Optimally, the goal of the electrospinning process is to allow the formation of an electrospun polymer jet, while replacing the drawn solution at the same rate. Essentially, the needle tip dispenser should constantly provide a bead of solution at the needle tip without clogging or dripping out. Below 0.25 ml/hr, needle tip solution beads do not form and the electrospinning solution is drawn off quicker than it was replaced. This resulted in inconsistent electrospinning and needle clogging, and rates below 0.20 ml/hr did not produce any electrospun product at all. Flow rates higher than 0.25 ml/hr caused the solution to begin to drip from the needle tip, which caused a globular sample deposition with larger diameter fibres as seen at figure 6.7. The average fibre diameters were in 428 nm for 0.20 ml/hr, 472 nm for 0.25 ml/hr, 702 nm for 0.26 ml/hr and 996 nm for 0.30 ml/ hr of feed rate (table 6.5 and figure. 6.8). At low feed rates (0.20 ml/hr), the solvent would have sufficient amount of time to evaporate until the fibres are collected on the plate, and hence thinner and uniform fibres are produced. At high feed rate (above 0.26 ml/hr), which seems above the quasi-stable point, the solution was not completely carried away to the collector, which resulted in unstable jet and larger fibres that can be seen at the figure 6.7.

6.2.8 Morphological analysis of Nylon 6.6 nano fibre

Processing parameters must be optimized when electrospun Nylon 6.6 nano fibres to get the desired morphology. Electrospun nano fibres with a small diameter can be found when the polymer solution concentration are lower (15 wt.%), but nonuniform or beaded fibres are found if these parameters were either too high or low.

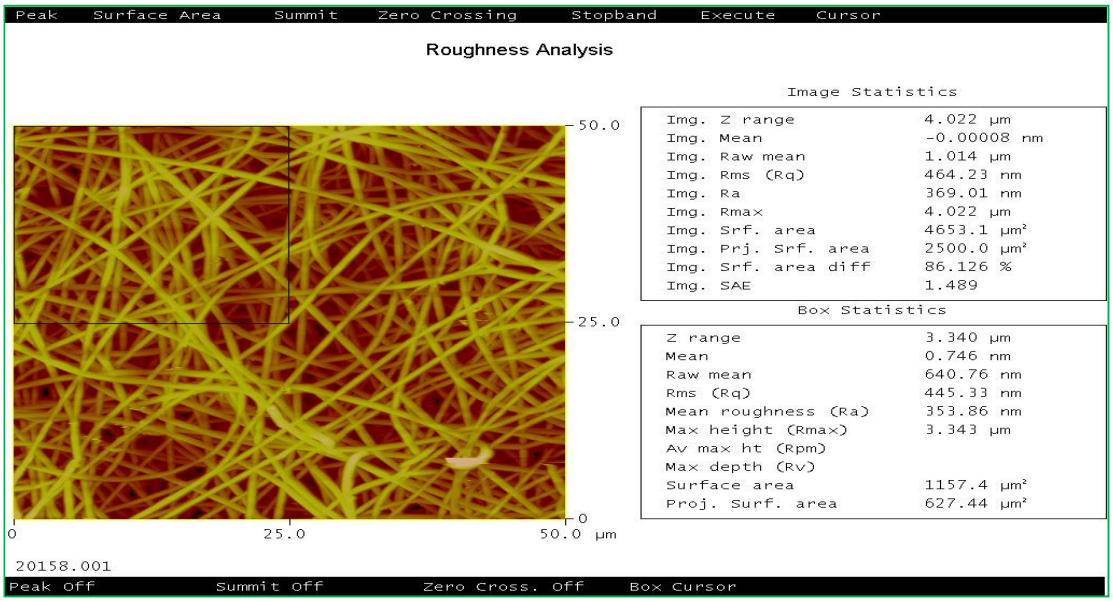

a)

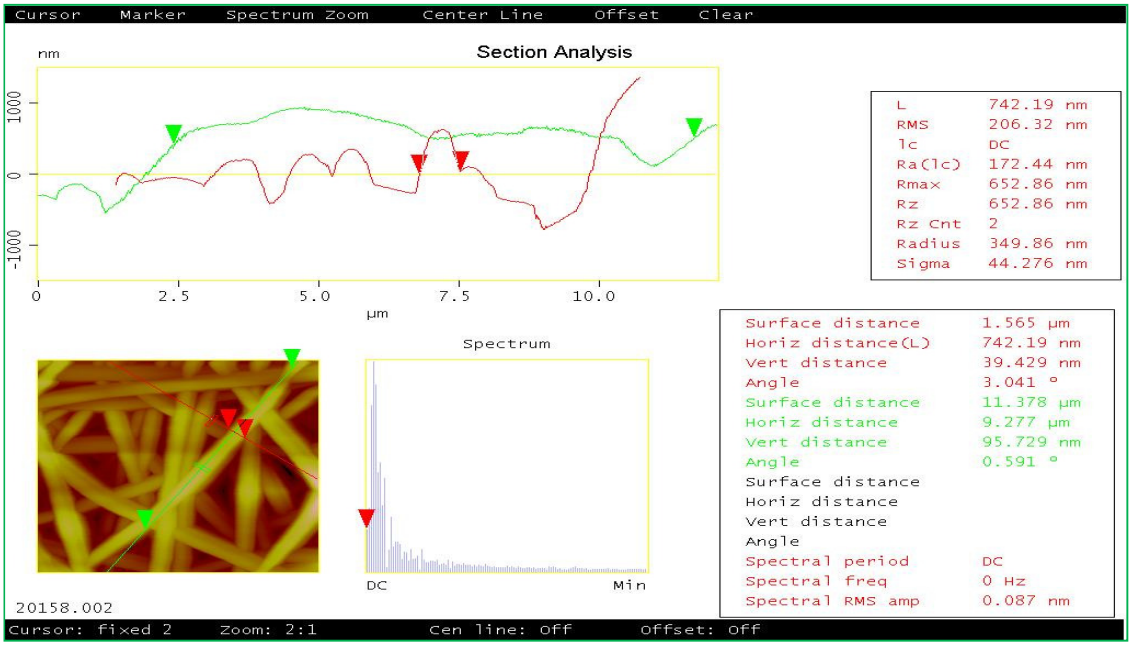

b)

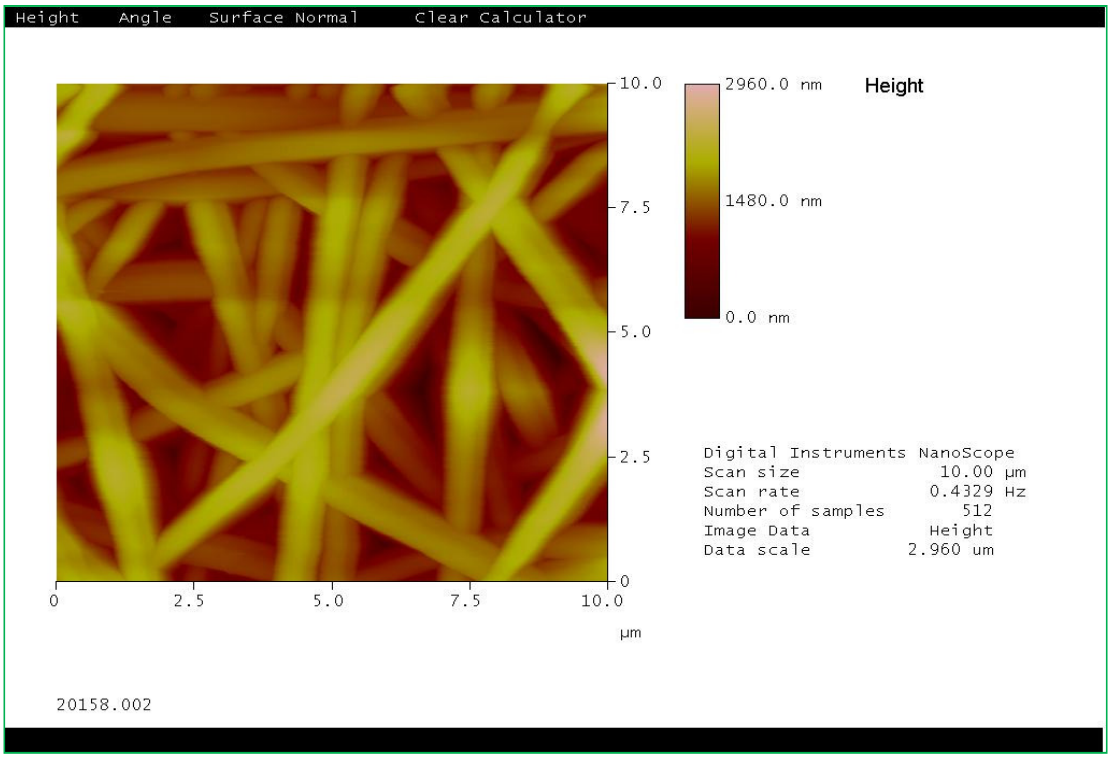

c)

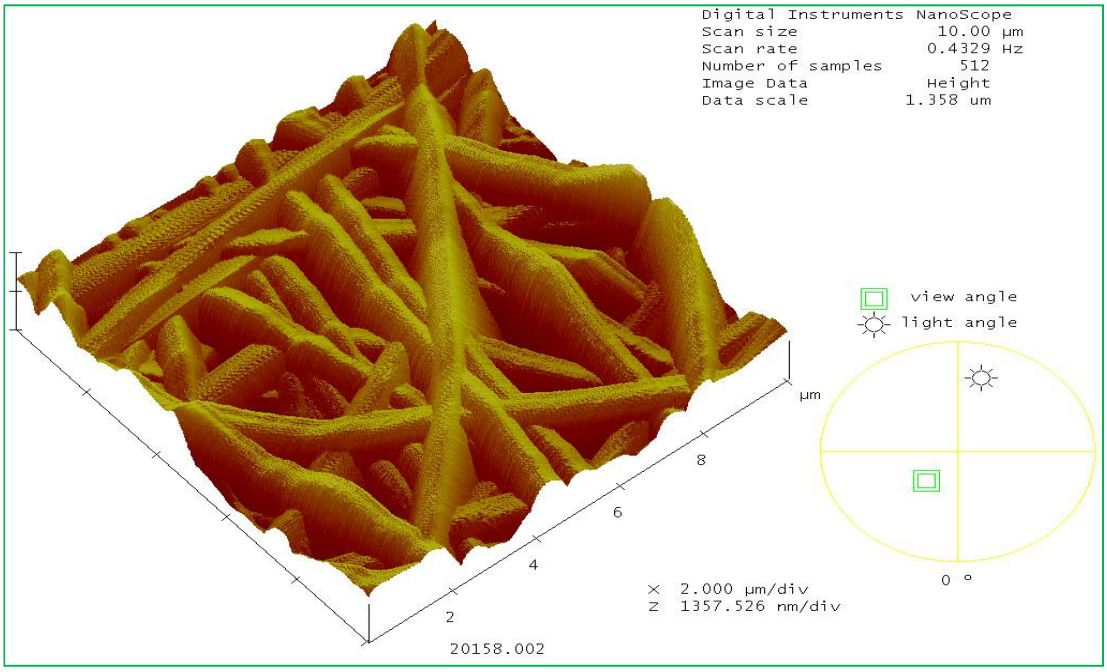

d)

Figure 6.9, AFM images for Nylon 6.6 where the polymer solution 25 wt.%, applied voltage 15 kV and collection distance 8 cm, a) roughness analysis, b) section analysis , c) Flatten, d) 3D of the Nylon 6.6 nano fibres where the fibre diameter 300 nm to 700 nm.

Lower voltage, such as less then 12 kV, is not strong enough to overcome the surface tension and viscoelastic forces of the polymer solution, but at higher voltages at this distance, an electrical discharge occurs. Increasing the applied voltage, the field strength will increase, increasing the electrostatic repulsion force on the fluid jet, which favors a thinner fibre formation. Fibre diameter will be lower at higher voltage producing more fibre but with low uniform. On the other hand when nozzle to collection distance is less then 5 cm, wet and nonuniform fibres with beads are produced. By increasing the distance between nozzle and collection, fibre uniformity increases with beads free fibres. Flow rate also influences uniform fibre formation. The analyzed AFM images shown in figure 6.9 show polymer solutions at 25 wt.% and the electric voltage at 15 kV and nozzle to collection distance at 8 cm produced uniform fibre diameters (827 nm). These optimum processing parameters were ideal for producing uniform Nylon 6.6 nano fibres.

6.3 Nylon 6.6 nano fibre alignment

During the electrospinning process, the fibres are attracted to the grounded target. Because of the difference in the electric field strength and parallel target geometry, parts of fibres got deposited on two separate grounds simultaneously. Several techniques have been developed to align electrospun nanofibres and some breakthroughs have been obtained. The results are promising, but these methods need to be further improved for practical applications. The nature of continuous fibre generation in the electrospinning enables continuous fibres between two targets with certain degree of orientation. The aligned fibre mats can be collected and processed into yarns for further application. The nanofibre nonwovens are acceptable only for some applications such as filters, wound dressings, tissue scaffolds and sensors etc [4, 20-23]. Meanwhile, obtaining continuously aligned nanofibres and high-volume production is very important for many areas such as fibre reinforcement and device manufacture. Several techniques have been developed to align electrospun nanofibres and some breakthroughs have been made. The primary principles to electrospin uniaxial align nanofibre bundles are changing the shape of a collector, appending an assistant electric field [24-25]. Consequently, a bigger mechanical force or electric force is loaded on fibres [12, 26]. So far, a lot of methods have been achieved to obtain uniaxial fibre bundles, for example, a pair of spaced electrically charged conductive plates [5-6, 22-24, 27], rotating wheel [1, 4, 28-29], rotating disk collector [30-32], rotating drum collector[3-

4], a tip collector [11, 25], an assistant electric field [23, 33], near-field electrospinning [34], grounded collector electrode water bath [35-37] and disk collector [38].

6.3.1 Materials and set up

A 25 wt.% solution concentration uses to produce Nylon 6.6 align fibre. The polymer solution was pumped to the 25-gauge, flat tipped, stainless steel spinneret at a rate of 0.20 ml/hr, through Teflon tubing. Two stainless steel spacers (28 mm OD, 25 mm ID, 2 mm thick) were used as the collection rings and were positioned using shielded, grounded, alligator clips with the top of the rings being 150 mm from the spinneret. Unless specifically mentioned, the two rings were 80 mm apart horizontally. A voltage of 15 kV was applied to the polymer solution with a power supply. Figure 6.10(a) schematic diagram of producing align fibres shown the set up.

6.3.2 Novel mechanism for producing align Nylon 6.6 nano fibres

When the polymer solution concentration are 25 wt.%, a applied voltage of 15 kV, a volume feed rate of 0.20 ml/hr and electrospinning collection distance of 8 cm this optimum conditions produced uniform Nylon 6.6 nanofibres. Here we present a novel mechanism that is based on a three dimensional alignment principle which is followed by the work done by Bazbouz and Stylios [38].

The nanofibre alignment mechanism involves collecting the electrically charged nanofibres between two faced electrically grounded collector disks. Two copper circular disks (28 mm OD, 2 mm thick) were used for collection. They were positioned by grounded alligator clips, with the top of the disks being 8 cm away from the spinneret. In this process, when placing the two grounded disks under the collection distance the vertical electric field lines are split into two parts and hence the geometrical shape of the electric field is changed rendering alignment of the fibres between the two disks.

To produce Nylon 6.6 aligned nano fibres we use polymer concentration of 25 wt.%, an applied voltage of 15 kV, volume feed rate of 0.20 ml/hr and the collection distance of 8 cm. This procedure reduced the diameter of the fibres from micrometer to the submicron range and their diameter was further adjusted by controlling the stretching ratio. No drying procedure to remove residual solvents was employed in this study.

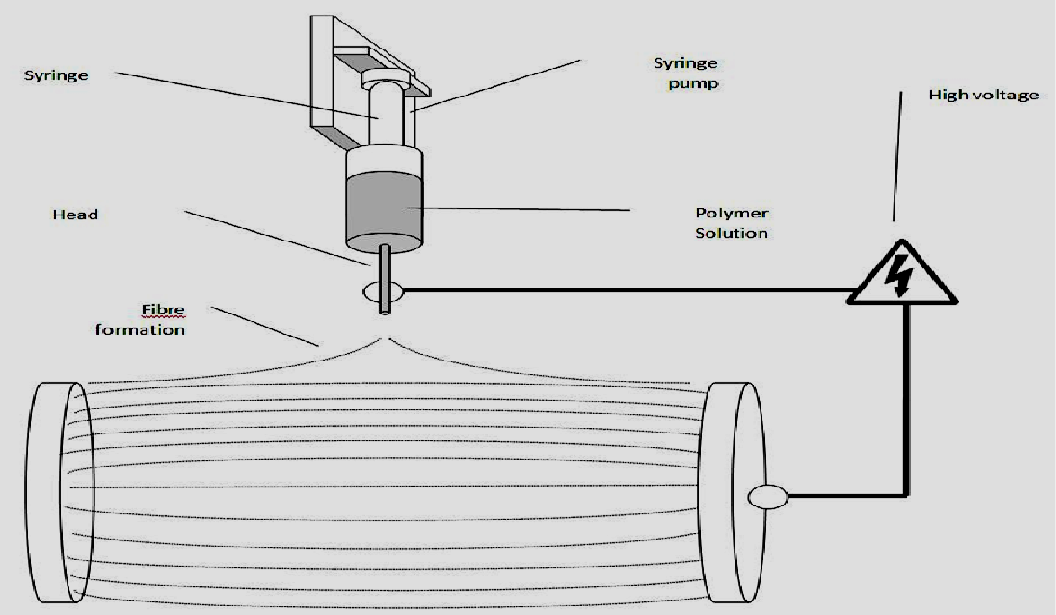

a)

b) c)

Figure 6.10, Schematic diagram of align nano fibre (a), experimental setup for produce align nano fibres (b & c) [38].

6.3.3 Align fibre charactezation technique

The electrospun fibres were collected on an aluminium stub with parallel strips of carbon tape applied to the surface to promote fibre adhesion to the stub. After

manufacture of the fibres, the stubs were passed through the suspended fibres between the collection rings. For SEM examination the formed fibre was collected and placed upon the specimen stub with tweezers. A SEM (Hitachi S-530, UK) was used to characterize the morphology of the electrospun nanofibres. The samples were sputter coated gold and examined at an accelerating voltage of 10 kV.

6.3.4 Alignment of electrospun nanofibres

With a view to some potential applications of the nanofibrous materials, there is a demand for methods of alignment of the nanofibres in one or few directions. As shown in figure 6.10 (c) that electrospun fibre directly deposited onto a grounded collector as a random mesh and in a second two copper disks were covered by long fibres bundles parallel between the two disks. The figure shown in 6.10 (c) that aligned nanofibres are at the right angles to the axis of the collection disks and have a uniform diameter distribution. Electrostatic interactions between the positive electrode on the spinneret and the ground disk made the fibres aligned and stretched. As a result the polymer fibres travel toward the disk collector, one end of the fibre is attached to one of the disks the other end of the fibre is gathered toward the other disks. The bending shape of the flying nanofibres is transformed into a linear shape between the grounded circular disks. When the charged fibres moved into the gap between the disks, the fibres will induce opposite charges on the surface of the disks. This opposite charges will attract the fibres to the grounded disks, leading to the alignment of the fibres in the gap between the grounded circular disks. The nanofibres suspended across the gap remain highly charged after deposition, thus the electrostatic repulsion between the deposited and upcoming fibres can further improve the alignment mechanism.

6.3.5 Results and discussion

A series of fibres deposited between the two collections disks (figure 6.11). Formation of these fibres was easily achievable, reproducible and was not subject to relatively small changes in spinneret-ground distance or applied voltage. The processing condition of fabricating aligned nanofibrous Nylon 6.6 was optimized and it was found that their properties were strongly influenced by the collection time and gap of disk width of electrospinning.

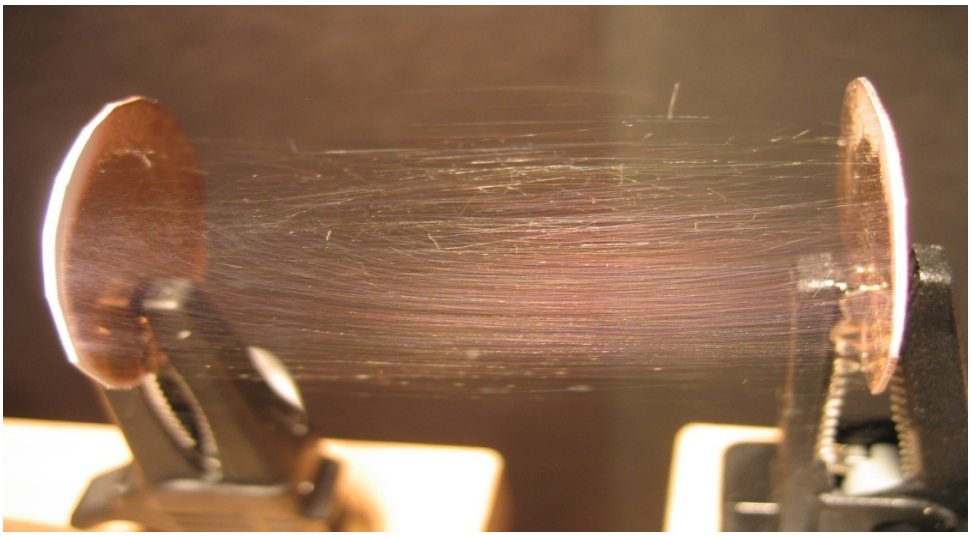

Figure 6.11, Aligned Nylon 6.6 fibre with two collection disks.

The morphological structure of aligned electrospun Nylon 6.6 fibres obtained from the 25 wt.% polymer solution is shown in figure 6.12. The SEM images in figure 6.12 show that well-aligned nanofibres have been formed. The average aligned fibre diameters are 724 nm and 519 nm. It was also noticed that the average diameter of aligned fibres was smaller than that of the random fibres obtained from the same processing conditions. The aligned fibres collected have lower average fibre diameters because their reduction and expansion values are lower than in the case of random collection, leading to a decrease in the fibre diameter. It is also confirmed that nanofibres were physically stretched and thinned by the electric fields associated with the parallel grounded disks.

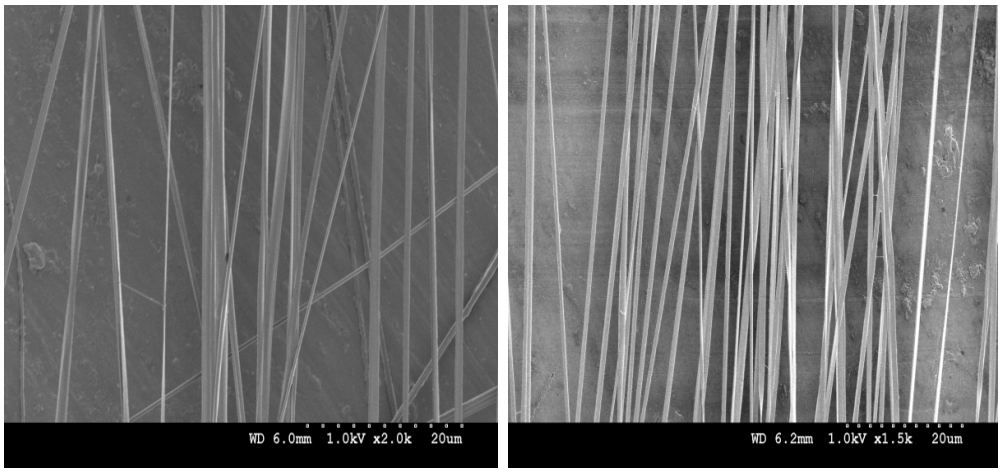

a) b)

Figure 6.12, SEM images of Nylon 6.6 nano fibres where the collection time 60 sec and disk gap 4 cm and 5 cm respectively.

The experiment carried out shows that the number of nanofibres distributed in the bundle depends on parameters such as the collection time and the gap width. However the applied voltage, spinning distance and flow rate are the main parameters effecting on the mass of the deposited fibres and the number of branches generated from the electrospinning jet. When the applied voltage increases, the nano fibre branching also increases and it makes the Nylon 6.6 nano fibre alignment difficult. It also increases the alignment across the gap because the voltage will increase the drawing forces. The images in figure 6.13 shows that as the deposition time increased and the width of the gap decreased, the number of Nylon 6.6 fibres increase and this make the bundle closer. This also in agreement with Morshed et.al [22].

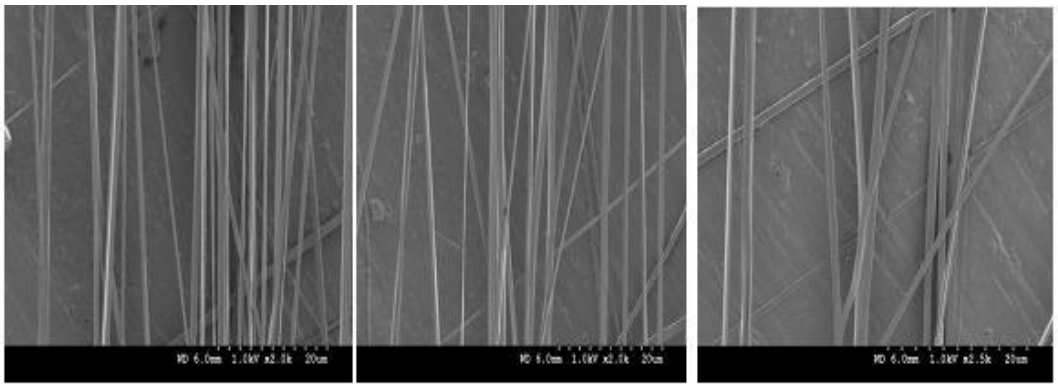

a) b) c)

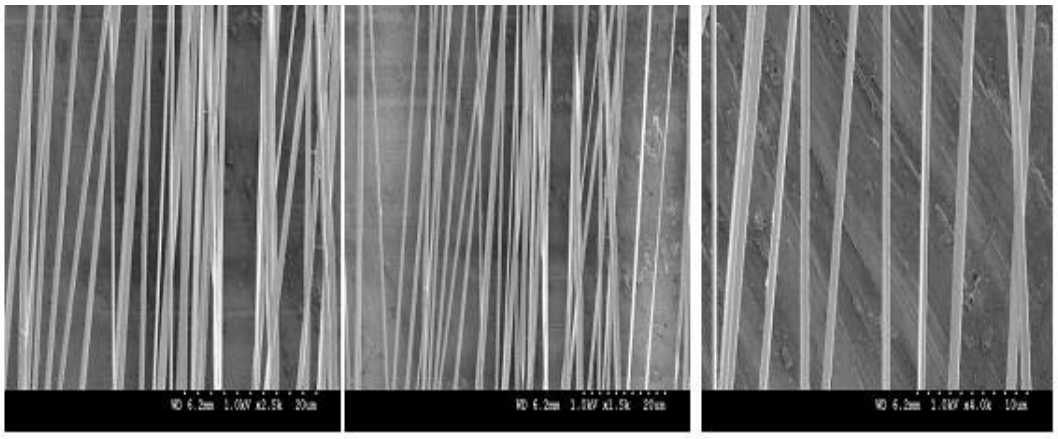

d) e) f)

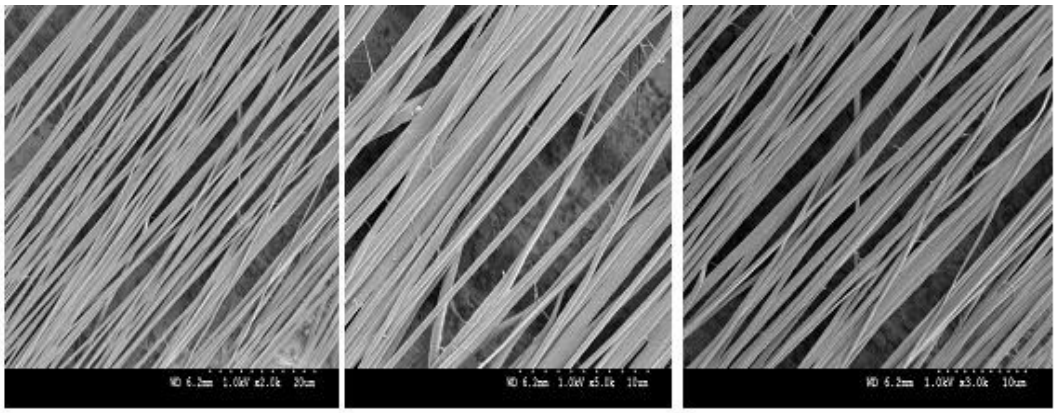

g) h) i)

Figure 6.13, SEM images of aligned Nylon 6.6 with a constant applied electric voltage and collection distance and solution concentration where the collection time 45, 60 and 120 sec and gap width 3,4 and 5 cm. a) 3 cm 45 sec, b) 4 cm 45 sec, c) 5 cm 45 sec, d) 3 cm 60 sec, e) 4 cm 60 sec, f) 5 cm 60sec, g) 3 cm 120 sec, h) 4 cm 120 sec, i) 5 cm 120 sec.

In this mechanism, a higher portion of aligned nanofibre mass has been obtained because of the large effective face surface of the disks, which stretch and span the fibre across the gap of the disks. When the gap distance increase more than 6 cm, there are fewer fibres obtained. With increasing the gap more than 6 cm it is very difficult to get align fibres because of the electrospinning jet has difficult deposition of fibres. This is also in agreement with Bazbouz and Stylios's work [38].

6.4 Thermal and X-ray diffraction (XRD) analysis

From the viewpoint of the commercial applications of these materials, the crystalline properties of the electrospun fibres may be one of the most important properties. DSC and X-ray diffraction experiments were performed on two samples. One was Nylon 6.6 granules and other was Nylon 6.6 electrospun mat which was made from 25 wt.% Nylon 6.6 concentration. All the graphs were plotted for temperature °C (X-axis) against the heat flow, mW (Y-axis), except for the Crystallinity curve where it is plotted for time against the heat flow.

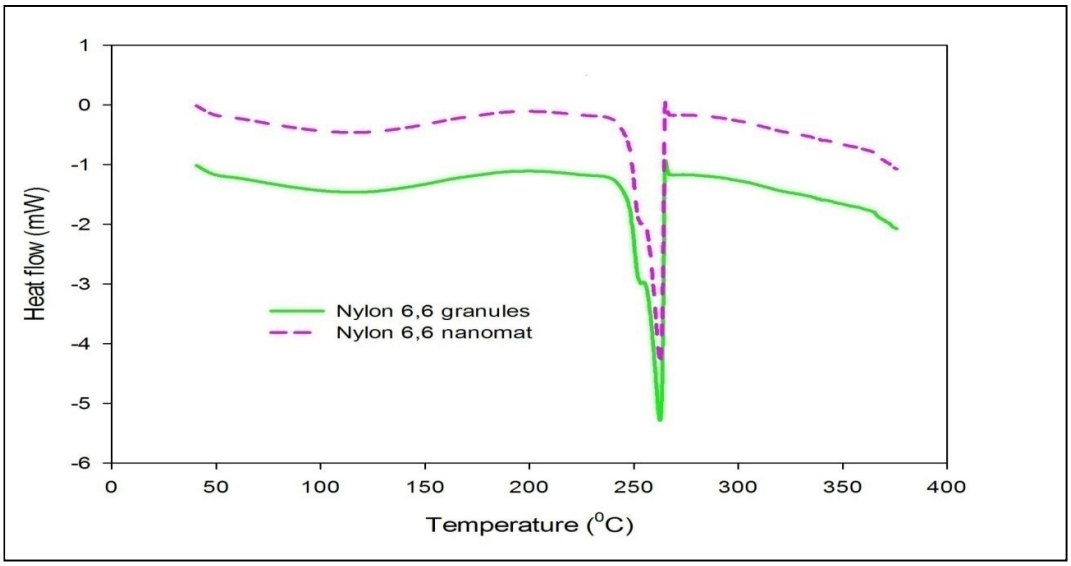

Figure 6.14, Differential scanning calorimeter (DSC) thermograms of Nylon 6.6 granules and Nylon 6.6 nanomat (applied voltage = 15 kV, TCD = 15 cm, polymer concentration=25 wt.%).

Figure 6.14, shows the DSC thermograms of Nylon 6.6 granules and Nylon 6.6 nanomats. It is well known that Nylon 6.6 is a semi-crystalline polymer. The Nylon 6.6 nano fibres sample shows a higher glass transition temperature than the Nylon 6.6 granules sample. The DSC result describe that Nylon 6.6 nanofibres glass transition temperature is higher than the one of Nylon 6.6 polymer (Tg = 50˚C). The T_m respectively for Nylon 6.6 granules and nano mat are 261.9˚C and 263.2˚C. Nanofibres have low amount of crystallinity compared to a textile fibre. Nylon 6.6 has around 40% crystallinity. The results are consistent with the results of Guerrini et. al, Lee et. al [40] and Reneker et. al [41]. The melting enthalpy of electrospun Nylon 6.6 is calculated as 117 J/g compared to 99 J/g for the unspun sample, suggesting an increase in the degree of crystallinity. The electrospinning probably enhances the polymer crystallization due to the chain orientation within the fibre. This can be understood as the solidification process of stretches chains under high elongational rate during the later stages of electrospinning may align the chain within the fibre and develop secondary bonding forces, which needs higher temperature to be broken. And finally, the overall effect of the electric field is a downward force on the charged jet, which draws it into a continuous fibre with better chain alignments. Similar result is also showed by Jia et.al [42] and Natthan et.al [43], Zong [44] and Yan Li et.al [45] also observed the low crystallinity of the electrospun poly (L-lactic acid) (PLLA) and Nylon 6, 66, 1010 fibres compared with those of the corresponding casting films.

X-ray is a powerful technique for determining the three dimensional structure of molecules, including complex biological macromolecules such as proteins and nucleic acids, that form crystals or regular fibres. It can be used to determine not only the crystallinity but also the type and structure of the crystals in the nanofibres and degree of orientation of the crystals/crystallites.

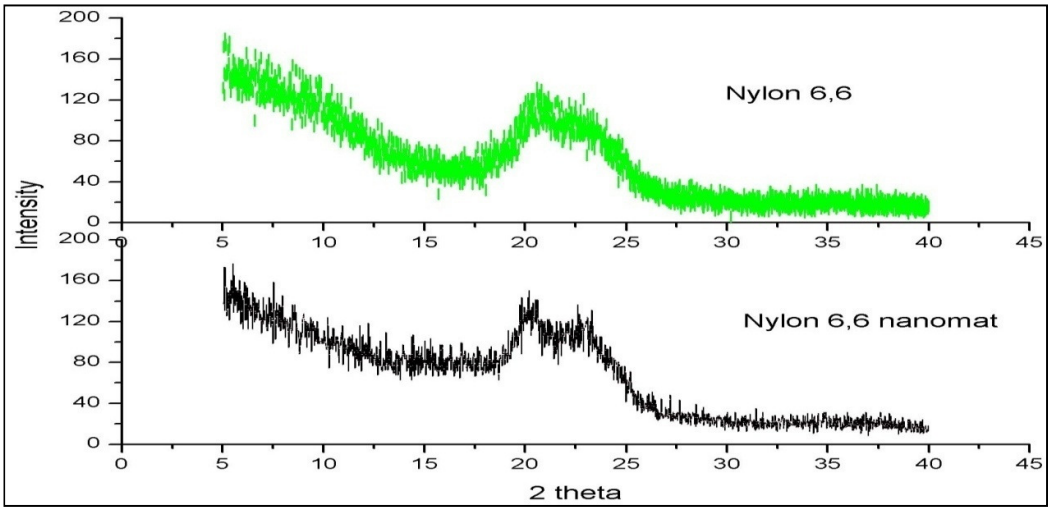

Figure 6.15, XRD patterns of a Nylon 6.6 granules and Nylon 6.6 nanomat.

Figure 6.15, shows the X-ray patterns of Nylon 6.6 granules and Nylon 6.6 electrospun fibres. The similarities between the patterns of the two systems strongly suggest structural similarity between the Nylon 6.6 granules and Nylon 6.6 electrospun fibres. The XRD pattern of electrospun fibres show broader peaks compared to raw Nylon 6.6, indicating that there is less crystalline region in the electrospun fibres. The decrease in crystallinity of the electrospun Nylon 6.6 nanofibre mats compared with that of the granules also can be confirmed by X-ray examination. Li et.al, described that two diffraction peaks at about 2θ = 20˚C and 2θ = 23˚C were the (100) and (010,110) of α phase crystals of typical triclinic form of Nylons [46]. However, the diffraction peaks associated with the electrospun Nylon 6.6 nano mat were relatively lower and broader compared with the higher and sharp peaks of the corresponding Nylon 6.6 granules. This indicates the easy packing of the crystal in the granules compared with those of the electrospun nano mat. In the electrospinning process, the structure of the fibre is formed under the influence of two simultaneous processes namely the evaporation of the solvent and the elongation of the fibres while crystallization from solution takes place under quiescent conditions. Thus, crystallization from solution results in more ordered α form whereas crystallization takes place under mechanical deformation during

electrospinning. This result is also similar to the result produced by Stephan et.al [46] and Dhanalakshmi et.al with the polymer of Nylon 6 and Nylon 11 [47]. They have attributed the formation of α, γ phase during the electrospinning process to the high stress experienced by Nylon 6 and Nylon 11 during fibre formation.

6.5 Nylon 6.6 nanofibres filled with carbon nanotubes

Nylon 6.6 has good chemical resistance and stability. Nylon 6.6 has been widely used as one of the most important thermoplastics because of its good thermal stability, fire resistance and mechanical properties.With adding MWCNT make Nylon 6.6 nanofibre more resistance, stable and strong. This study presents a new route for producing Nylon 6.6/MWCNT composites, which simultaneously optimizes the morphology of Nylon 6.6/MWCNT nano fibre mat.

6.5.1 Materials

MWCNT were obtained from Thomas Swan & co Ltd, UK. They were ready to use and dispersed in a solution. Formic acid obtained from Sigma Aldrich, UK, was used as a solvent for the Nylon 6.6 solution and it also used to disperse the MWCNTs. The dispersed nanotubes and the Nylon 6.6 solution were mixed together thoroughly in order to obtain a homogeneous distribution of the nanotubes in the polymer solution. Then the mixture was ready to spin. Electrospinning was used to spin composite nanofibres from the solution.

6.5.2 Preparation for Nylon 6.6/MWCNT solution

Nylon 6.6 solution of 25 wt.% concentration was prepared by dissolving the polymer in 98 % formic acid. MWCNTs (Thomas Swan &co Ltd) with a diameter of 20 ± 10 nm and length of 1-10 μm of 96 % purity were dispersed to disrupt possible agglomerates using an ultrasonic homogenizer (model 300 V/T, Biologics INC, UK) with a room temperature and operating at 25 Hz. Different ratio MWCNT were added 20 ml of formic acid and sonicated for 3 hours. The amount of formic acid used for dispersion was calculated as the same amounts of formic acid that suppose to be present in the final solution. The Nylon 6.6 solution was then mixed with MWCNT/FA dispersion. The mixture was sonicated for 3 to 4 hours for a homogenous suspension of the MWCNT in the solution. Three separate suspensions were prepared that should contain 2% to 4% MWCNT in the final composite polymer fibre mat.

6.5.3 Electrospinning for producing Nylon 6.6/MWCNT composite fibre

The Nylon 6.6/ MWCNTs solution was fed through a 5 ml capacity syringe to a vertically orientated blunt-ended metal needle (25-gauge) via Teflon® tubing and the flow rate was controlled using a digitally controlled, positive displacement syringe pump. The needle was held by one electrode connected to a high voltage DC power supply. Typical operating regimes at volume feed rate of 0.20 ml/hr, applied voltages of 15 kV and a working electrospinning distance of 8 cm were employed. A TEM was utilized to qualitatively determine the size distribution and structure of carbon nanotubes in the composite nanofibre on 100 square mesh Cu grids for samples of randomly collected nanofibres, and 100 parallel mesh Cu grids for samples of aligned nano fibre. Various polymer nanofibres were collected on a copper plate measuring 15cm × 15cm**.**

6.5.4 General discussion about CNT

It is always essential to have a good dispersion, uniform distribution and alignment of the CNTs in the polymer solution in order to optimize the mechanical, electrical and thermal properties of the final composite. Several strategies have been employed to disperse the CNTs which include chemical modification of CNTs through attaching functional groups to the surface of the CNTs, non-chemical functionalization of CNTs through wrapping the CNTs with a surfactant and optimum physical blending 'high speed shearing' of CNTs and polymer solution to obtain a stable and uniform suspension of CNTs in the polymer solution [48]. CNTs are either single walled nanotubes (SWNT) or multi walled nanotubes (MWNT), where SWNT is a tube with only one wall, and MWNT have many concentric tubes where the walls of the tubes are held together by weak van der Walls forces [49]. SWNTs are single cylindrical layers of this carbon atom network, as shown in figure 6.16 (a), whereas MWNTs consist of several layers in the form of concentric cylinders bounded by weak Van der Waals forces, as shown in figure 6.16 (b),

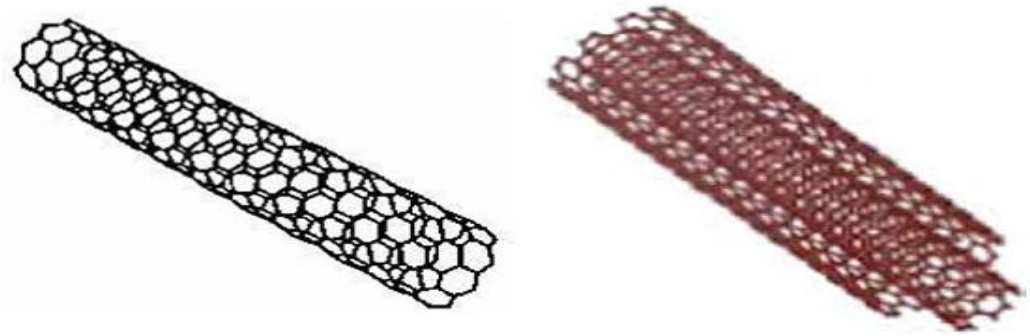

a) b)

Figure 6.16, Schematic illustration of (a) a single-walled nanotube (SWNT), and (b) a multi-walled nanotube (MWNT) [50].

6.5.5 Morphological analysis and diameter distributions of Nylon6.6/MWCNT electrospun fibres

SEM analysis:

The MWCNT were successfully co-electrospun with the Nylon 6.6 fibres at concentrations of 2, 3, and 4 %.wt (MWCNT weight concentration in the fibre form) of MWCNT with 25 wt.% of Nylon 6.6. It is assume that the higher the CNT concentration the higher is the viscosity of the prepared polymer, so for higher CNT concentrations, the content of Nylon 6.6 is decreased. Figure 6.17, demonstrates the SEM images of 2, 3 and 4 wt.% MWCNTs reinforced with Nylon 6.6. For low MWCNTs content, the fibres had regular morphology with small variations in diameter (250-600) nm. For high CNT content Nylon 6.6 fibres, the fibre morphologies and diameter were different form the low content and changed with increasing the content of CNTs. Firstly, good fibres alignment, less junctions and bundles of fibres were observed in the sample containing CNTs of (2-3 wt.%) compared to higher CNTs content. Secondly, the morphologies of fibres became more irregular, and numerous beads appeared when the CN content increased to 4 wt.%, figure 6.17(c). All these results indicate that adding of MWCNTs to Nylon 6.6 fibres it influences the solution viscosity, surface tension, and concentration. Figure 6.17(a and b) shows fibre diameter average of 225 to 230 nm and also images of smooth fine fibres of the Nylon 6.6/ MWCNT fibres. Also the alignment of fibres within the surface of the yarn is still maintained. The magnified images in figure 6.17 (d), shows that the aligned nanofibres are perpendicular

to the axis of the collection disks and have uniform fibre diameters distribution of 500 nm to 1050 nm. These images also indicate that the enhanced stretching applied by the alignment mechanism could lead to a high polymer chain orientation and a better arrangement of the MWCNTs inside the fibre itself. The presence of MWCNTs within the fibres was not clear with the SEM; hence TEM was employed to examine the CNTs behaviour in the fibres.

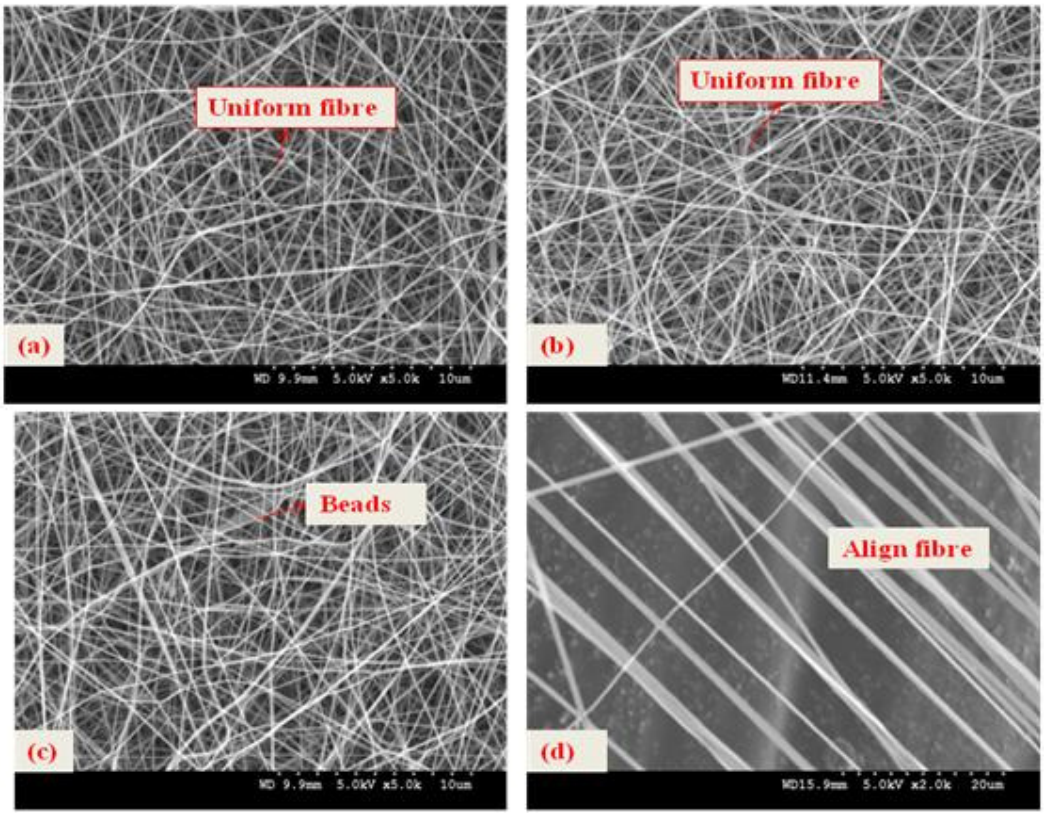

Figure 6.17, (a-c) are SEM images of randomly collected Nylon 6.6 nanofibres containing various concentrations of MWCNTs from 2 to 4 wt.% respectively in 25 wt.% Nylon 6.6/ formic acid solution, at 0.20 ml/h volume feed rate, 18 kV applied voltage and 8 cm electrospinning distance and (d) SEM images of the Nylon 6.6 align nano fibre where the solution 3 wt.% MWCNT.

TEM analysis

Transmission Electron Micrographs were obtained to characterize the nanofibres and give an evidence of the presence of the CNT within the fibres. Figure 6.18, shows TEM images of random and aligned Nylon 6.6 nanofibres containing various concentrations of MWCNTs from 2 to 4 wt.% in 25 wt.% Nylon 6.6 solutions.

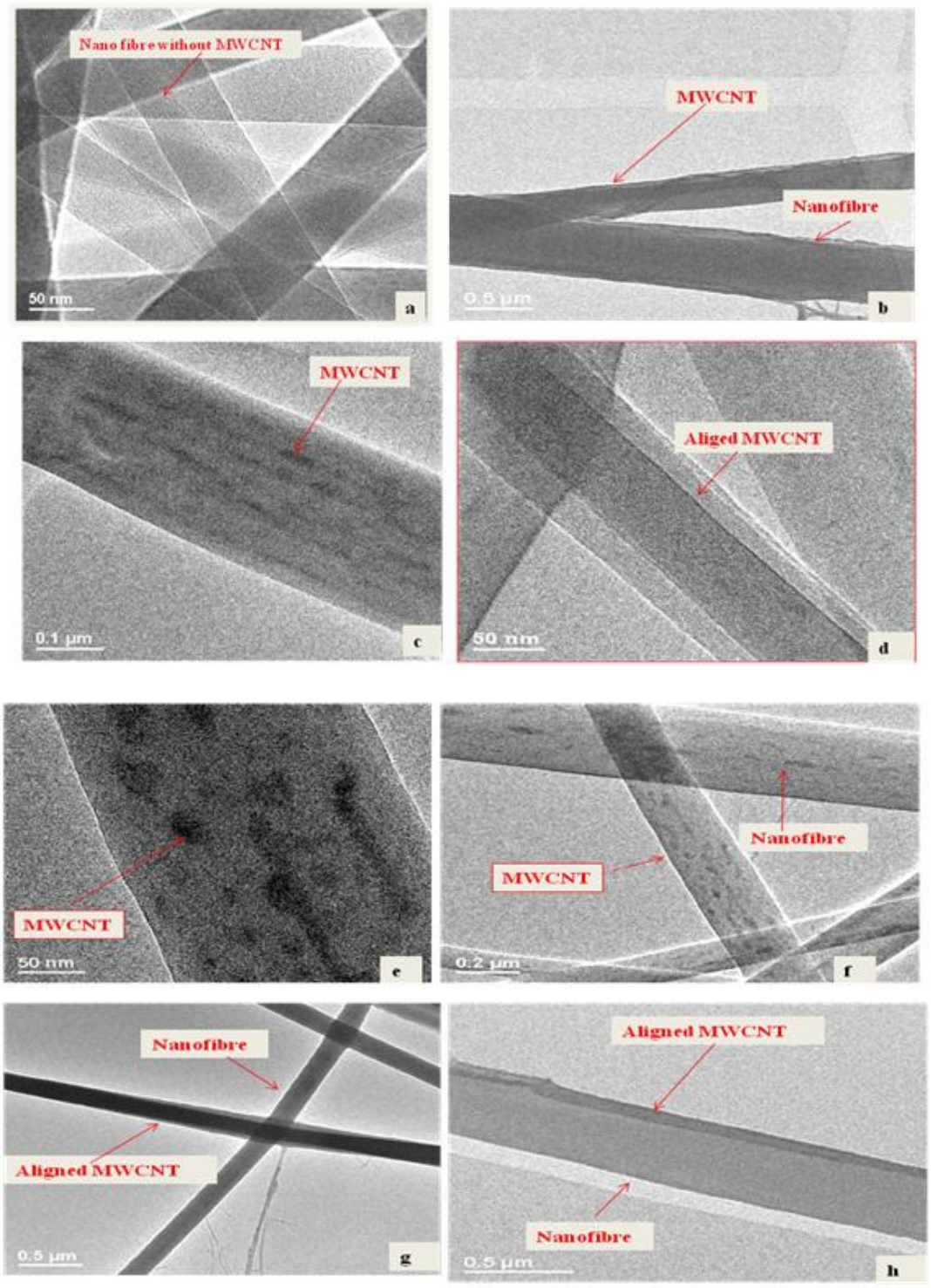

Figure 6.18, TEM images of random and aligned Nylon 6.6 nanofibres containing various concentrations of MWCNTs; 2 to 4 wt.% in 25 wt.% Nylon 6.6 solutions. (a, and b) show random nanofibres respectively with without MWCNT and 2 wt.% of MWCNTs in Nylon 6.6 nanofibres, (c, d and e) shows random and align nanofibres

with 3 wt.% of MWCNTs, (f and g) shows random and align nanofibres with 4 wt.% of MWCNTs, (h) show aligned nanofibres with 3 wt.% of MWCNTs.

The arrows indicate that MWCNTs are straight in the direction parallel to the fibre axis being subjected to aligned collection. Figure 6.18(a) shows that nano fibre without carbon nano tube. Figure 6.18 (b, c and d) reveals that the electrospun fibres contain MWCNTs and illustrate the good arrangements of the CNTs along the fibre and they can be aligned/self-organized into straight lines or bundle-like crystallites. Figure 6.18 (e and f) gives a good evidence of the presence of the CNT within the cross-section of the fibres and not only resting on the surface. The actual diameter of the MWCNT measured is around 22 nm. We can also observe from the figure 6.18 (g and h) that MWCNTs are aligned and straight along the direction of the fibre axis in the aligned nanofibres samples. However good insertion and uniform longitudinal distribution will improve the thermal conductivity, electrical conductivity and mechanical property of the MWCNTs/ polymer composite. The MWCNTs are found to be dispersed well and are aligned along the fibre axis. Zussman et.al and Bazbouz and Stylios [51-52] reported similar results. This alignment can be understood to be due to the sink flow field effects of CNTs inside the polymer solution during the electrospinning process. Initially the CNT rods are randomly oriented, but due to the sink-like flow in the capillary of the needle they get gradually oriented mainly along the stream lines, so that straight CNTs are almost oriented upon entering the region of the electrospun jet.

6.6 Conclusion

In conclusion we can say, solution and processing parameters such as viscosity, surface tension, solution electrical conductivity, applied voltage, tip to collector and flow rate significantly affect Nylon 6.6 nanofibre morphology. Increasing viscosity, expectedly, increased fibre diameter. Viscosity is the main parameters affecting fibre diameter. In experiments, the smallest fibre diameters were observed at the higher strength of the electric field. Flow rate also changed the fibre diameter, as higher flow rate gives larger diameter nanofibre and lower flow rate gives smaller diameter nanofibre. With 25 wt.% solution concentration, applied voltage at 15 kV, collection distance at 8 cm and flow rate 0.20 ml/hr produced uniform, beads free Nylon 6.6 nanofibres. About alignment we can say that the optimum disk distance for spinning Nylon 6.6 nanofibres is 4-5 cm. This provides the basis for twisting the nanofibre bundle for the formation of uniform nano yarn. DSC and X-Ray diffraction analysis demonstrated structural similarities

between granules and nano mats. The crystalline microstructure of electrospun fibres did not develop well due to the rapid solidified of the fibres during electrospinning. Nylon 6.6/ MWCNTs composite nanofibres have successfully been spun and we can say that MWCNTs cannot be completely embedded into the nanofibre when the loading concentration is increased above 3 wt.%. Produced nanofibrous mats have the potential to be use as fibre reinforcement, in cars, aeroplanes etc.

6.7 References

[6.1] J. Doshi and D. H. Reneker, *Electrospinning process and applications of electrospun fibres*, J electrostatics, **35**:2-3, pp 151-160 (1995)

[6.2] H. Pan, L. Li, L. Hu, X. Cui, *Continuous aligned polymer fibres produced by a modified electrospinning method*, Polymer **47**, 4901–4904(2006)

[6.3] J. A. Matthews, E. D. Boland, G. E. Wnek, D. G. S impson, G. L. Bowlin, *Electrospinning of collagen type II: a feasibility study*, Bio macromolecules, **3**:232–8 (2002)

[6.4] S. F. Fennessey and R. J. Farris, *Fabrication of aligned and molecularly oriented electrospun polyacrylonitrile nanofibres and the mechanical behaviour of their twisted yarns*, Polymer, Vol. **45**, no. 12, pp. 4217–4225 (2004)

[6.5] D. Li, Y. Wang, Y. Xia, *Electrospinning nanofibres as uniaxially aligned arrays and layer-by-layer stacked films*, Advanced Materials Volume **16**, Issue 4, Pages 361 – 366(2004)

[6.6] P. D. Dalton, D. Klee and M. Moller, *Electrospinning with dual collection rings*. Polymer, **46**, (3), 611-614 (2005)

[6.7] J. Kameoka, D. Czaplewski, H. Liu, H. G. Craighead, *Polymeric nano wire architecture,* Journal of Materials Chemistry, **14**, 1503-1505 (2004)

[6.8] J. Kameoka, R. Orth, Y. Yang, D. Czaplewski, R. Mathers, G. W. Coates, H. G. Craighead, *A scanning tip electrospinning source for deposition of oriented nano fibres*, Nanotechnology, **14,** 1124-1129 (2003)

[6.9] G. Srinivasan, D. H. Reneker, *Structure and morphology of small diameter electrospun aramid fibres*, Polymer International, **36**, 195-201 (1995)

[6.10] M. Gorantla, S. E. Bone, M. El-Ashry, D. Younga, *Continuous polymer nanofibres by extrusion into viscous medium: a modified wet spinning technique*, Applied Physics Letters, **88**, 0731151-0731151 (2006)

[6.11] B. Sundaray, V. Subramanian, T. S. Natarajan, R.Z. Xiang, C. C. Chang and W. S. Fann, *Electrospinning of continuous aligned polymer fibres*, Applied physics letters, Vol.**84,** pp.1222-1224 (2004)

[6.12] P. Katta, M. Alessandro, R. D. Ramsier, G. G. Chase, *Continuous electrospinning of aligned polymer nanofibres onto a wire drum collector*, Nano Letters, ***4*** (11), pp 2215–2218 **(2004)**

[6.13] W. E. Teo, S. Ramakrishna, *Review on design and nanofibre assemblies*, Nanotechnology, **17**, R89-R106 (2006)

[6.14] S. Zhang, W. S. Shim, J. Kim, *Design of ultra-fine nonwovens via electrospinning of Nylon 6: Spinning parameters and filtration efficiency*, Materials & Design Volume **30**, Issue 9, Pages 3659-3666 (2009)

[6.15] A. Formhals, US patent 1, 975-504 (1934)

[6.16] J. M. Deitzel, J. Kleinmeyer, D. Harris and N. C. B. Tan, *The effect of processing variables on the morphology of electrospun nanofibres and textiles*, Polymer, **42**(1):261-272 (2000)

[6.17] H. Fong, I. Chun and D. H. Reneker, *Beaded nano fibres formed during electrospinning*, Polymer, **40**:4585-4592 (1999)

[6.18] P. K. Baumgarten, *Electrostatic spinning of acrylic micro fibres*, J Colloid Interface Science, **36** (no.1); 71-9 (1971)

[6.19] M. M. Chowdhury, G. K. Stylios, *Effect of processing parameters on Nylon 6.6 nanofibres and their morphology*, Green Chemistry and Engineering International Conference on Process Intensification and Nanotechnology, p 161- 172, Albany, NY, USA (2008)

[6.20] H. Lee, H.Y. Kim, H. J. Bang, Y. H. Jung and S. G. Lee, *The change of bead morphology formed on electrospun polystyrene fibres*, Polymer, Volume **44**, Issue 14, Pages 4029-4034 (2003)

[6.21] V. Beachley and X. Wen, *Effect of electrospinning parameters on the nanofibre diameter and length*, Materials Science and Engineering C. **29**, 663–668 (2009)

[6.22] R. Jalili, M. Morshed, S. A. H. Ravandi, *Fundamental parameters affecting electrospinning of PAN nanofibres as uniaxially aligned fibres*, Journal of applied polymer science, Vol.**101**, pp.4350-4357 (2006)

[6.23] B. K. Gu, M. K. Shin, K. W. Sohn, S. I. Kim, S. J. Kim, S. K. Kim, H. Lee and J. S. Park, *Direct fabrication of twisted nanofibres by electrospinning*, Applied physics letters, Vol. **90**, pp. 263902 (2007)

[6.24] M. V. Kakade, S. Givens, K. Gardner, K. H. Lee, D.B.Chase, J. F. Rabolt, *Electric field induced orientation of polymer chains in macroscopically aligned electrospun polymer nanofibres*, American chemical society, Vol.**129**, pp. 2777-2782 (2007)

[6.25] J. Rafique, J. Yu, J.Yu, G. Fang, K. W. Wong, Z. Zheng, H. C. Ong, W. M. Lau, *Electrospinning highly aligned long polymer nanofibres on large scale by using a tip collector*, *Applied physics letters*, Vol.**91**, pp. 063126 (2007)

[6.26] D. Li, Y. L. Wang, Y.N. Xia, *Electrospinning of polymeric and ceramic nanofibres as uniaxially aligned arrays*. *Nano letters*, Vol.**3**, pp.1167-1171 (2003)

[6.27] E. P. S. Tan, S.Y. Ng, C. T. Lim. *Tensile testing of a single ultrafine polymeric fibre*, Biomaterials, Vol.**26**, pp.1453-1456 (2005)

[6.28] B. M. Mina, G. Leea, S. H. Kim, *Electrospinning of silk fibroin nanofibres and its effect on the adhesion and spreading of normal human keratinocytes and fibroblasts in vitro*, Biomaterials, Vol.**25**, pp. 1289-1297 (2004)

[6.29] M. S. Khil, D. I. Cha, H. Y. Kim, I. S. Kim, N. Bhattarai, *Electrospun nanofibrous polyurethane membrane as wound dressing*, Appl Biomater, Vol.**67B**, pp. 675-679 (2003)

[6.30] R. Dersch, T. Liu, A. K. Schaper, A. Greiner, J. H. Wendorff, *Electrospun nanofibres: internal structure and intrinsic orientation*, Journal of Polymer Science: Part A: Polymer Chemistry. **41** (4):545-553 (2003)

[6.31] R. Dersch, T. Liu, A. K. Schaper, A. Greiner, J. H. Wendorff, *Electrospun nanofibres: internal structure and intrinsic orientation*, Journal of polymer science: part A: polymer chemistry, Vol.**41**, pp.545-553 (2004)

[6.32] C.Y. Xu, R. Inai, M. Kotaki et. al, *Aligned biodegradable nanofibrous structure: a potential scaffold for blood vessel engineering*, Biomaterials, Vol.**25**, pp.877-886 (2004)

[6.33] J. M. Deitzel, J. D. Kleinmeyer, J. K. Hirvonen et. al, *Controlled deposition of electrospun poly(ethylene oxide) fibres*, Polymer, Vol. **42**, pp.8163-8173 (2001)

[6.34] D. H. Sun, C. Chang, S. Li, L.Lin, *Near-Field Electrospinning*, Nano letters, Vol.**6**, pp. 839-842 (2006)

[6.35] M.S. Khil, S. R. Bhattarai, H. Y. Kim, S. Z. Kim, K. H. Lee, *Novel fabricated matrix via electrospinning for tissue engineering*, J Biomed Mater Res Part B: Appl Biomater, Vol.**72B**, pp.117-124 (2005)

[6.36] E. Smit, U. Buttner, R. D. Sanderson, *Continuous yarns from electrospun fibres*, Polymer, Vol. **46**, pp.2419-2423 (2005)

[6.37] W. E. Teo, R. Gopal. R. Ramaseshan, K. Fujihara and S. Ramakrishna, *A dynamic liquid support system for continuous electrospun yarn fabrication*. Polymer, Vol. **48**, pp.3400-3405 (2005)

[6.38] M. B. Bazbouz, G. K. Stylios, *Alignment and optimization of Nylon 6 nanofibres by electrospinning*, Journal of applied polymer Science, **107**, 3023-3032 (2008)

[6.39] L. M. Guerrini, M. C. Branciforti, T. Canova, R. E. S. Bretas, *Electrospinning and characterization of polyamide 66 nanofibres with different molecular weights*, Mat. Res. vol**.12** no.2 SA. Carlos (2009)

[6.40] K. H. Lee, H. Y. Kim,Y. M. La, D. R. Lee, N. H. Sung, *Influence of a mixing solvent with tetrahydrofuran and N, N-dimethylformamide on electrospun poly(vinyl chloride) nonwoven mats,* J Polym Sci Part B: Polym Phys; **40:**2259–68 (2002)

[6.41] D. H. Reneker, W. Kataphinan, A. Theron, E. Zussman, A. L. Yarin, *Nanofibre garlands of polycaprolactone by electrospinning*. Polymer, **43**:6785–94 (2002)

[6.42] Y. T. Jia, J.Gong, X. H. Gu, H. Y. Kim, J. Dong and X. Y. Shen, *Fabrication and characterization of poly (vinyl alcohol)/chitosan blend nanofibres produced by electrospinning method*, Carbohydrate Polymers, **67**, 403–409 (2007)

[6.43] N. Charernsriwilaiwata, P. Opanasopita, T. Rojanarataa, T. Ngawhirunpata, P. Supapholb, *Preparation and characterization of chitosan-hydroxybenzotriazole /polyvinyl alcohol blend nanofibres by the electrospinning technique,* Carbohydrate Polymers **81** , 675–680 (2010)

[6.44] X. Zong, K. Kim, D. Fang, S. Ran, B. S. Hsiao and B. Chu, *Structure and process relationship of electrospun bioabsorbable nanofibre membranes,* Polymer **43** (16):4403–4412 (2002)

[6.45] Y. J. Li, D. Y. Y and X. Y. Zhu, *Crystal forms of Nylon 1012 crystallized from melt and after solution casting*, Eur Polym J, **37**:1849–53 (2001)

[6.46] J. S. Stephens, D. B. Chase, J. F. Rabolt, *Effect of electrospinning process on polymer crystallization chain conformation in Nylon-6 and Nylon-12*, Macromolecules. **37** (3):877-881 (2004)

[6.47] M. Dhanalakshmi, J. P. Jog, *Preparation and characterization of electrospun fibres of Nylon 11*, eXPRESS Polymer Letters Vol.**2**, No.8, 540–545 (2008)

[6.48] X. L. Xie, Y. M. Wing, X. P. Zhou, *Dispersion and alignment of carbon nanotubes in polymer matrix: a review*, Materials Science and Engineering, **49**, 89-112 (2005)

[6.49] R. Andrews, M.C. Wiesenberger, *Carbon nanotube polymer composites*, Current Opinion in Solid State and Materials Science, **8**, 31-37 (2004)

[6.50] L. Yeo and J. R. Friend, *Electrospinning carbon nanotube polymer composite nanofibres,* Journal of Experimental Nanoscience, Vol**. 1**, No. 2177–209 (2006)

[6.51] W. Salalha, Y. Dror, R. L. Khalfin, Y. Cohen, A. L. Yarin and E. Zussman, *Single-walled carbon nanotubes embedded in oriented polymeric nanofibres by electrospinning*, Langmuir, **20** (22): p. 9852-9855 (2004)

[6.52] M.B. Bazbouz, G. K. Stylios, *Novel mechanism for spinning continuous twisted composite nanofibre yarns*, European Polymer Journal, **44**, 1-12 (2008)

Chapter 7: The effect of experimental parameters on the morphology of electrospun PEO nanofibres and analyses their thermal properties

7.1 Introduction

Various applications of nanofibres in medicine and surgery are known so far and have been mentioned elsewhere. The type of fibres required for such purposes are obtained from polymers that are biocompatible and biodegradable. One such polymer is polyethylene oxide (PEO). PEO is often used as an ideal model for electrospinning [1] which carries the additional advantages of good processibility and low cost. PEO is also used in combination with other polymers in order to enhance their processibility and biocompatibility. Polyethylene oxide (PEO) is a commercially available polymer represented by the chemical formula $C_{2nH4n}+2O_{n+1}$. PEO is non-toxic and is used in a variety of medical products such as laxatives and skin creams. The environmental stability of PEO and its ability to easily dissolve in a number of solvents such as water and Ethanol were the reasons that encouraged our choice of the polymer for electrospinning fibres. In the present work the effect of variation of the governing parameters on the electrospinning of PEO solutions is established. The parameters investigated include: solution volumetric flow rate, the applied voltage, flow rate and the nozzle to ground distance. The present study is an attempt to optimise the electrospinning process and identify the process parameters governing it.

7.2 Experimental method and material

A different weight of PEO (Mw~ 300,000 g/mol) was added to 10 ml of water and Ethanol/ water (HPLC grade) at room temperature. The mixture was magnetically stirred for 2 hours to make a homogeneous solution. Aqueous solutions having concentration in the range of 10% to 14 % (by weight) were prepared. Solution properties including conductivity, surface tension, and viscosity were determined. Using the custom made set up fibres were electrospun from the solution at a voltage of 12 kV, 15 kV and 18 kV. The nozzle to collector distance was varied between 8, 11 and 14 cm to focus the spinning jet on the collector. The electric potential, hydrostatic pressure, and the distance between the capillary tip and the collection screen were adjusted so that a stable jet was obtained. By varying the distance between the capillary tip and the

collection screen, either dry or wet fibres were collected on the screen. Fibres were electrospun and collected on aluminium plate in the form of a non-woven mat.

7.2.1 Measurement and characterisation

PEO with water and water/Ethanol (60/40) both solution viscosities were measured with an AR-1000 rheometer, TA Instruments Inc (UK). Surface tension was measured by Model 'OS' Balance/Tensiometer (UK) and to measure the solution electrical conductivy four points were used**.** The electrospun fibres were analyzed under an SEM, model Hitachi S-530 scanning electron microscope (UK). Atomic force microscopy (Model 5400, AFM, UK) was used to characterize the morphology of the electrospun fibres specially their diameter range and their structures. To measure the differential scanning calorimetry**:** Metler DSC 30 (USA) was used. For X-ray diffraction X'Pert-MPD Philips diffractometer (UK) used and to measure the diameters of the electrospun PEO nano fibres, an image analyzer (Image J, US) was used.

7.2.2 Result and discussion

7.2.2.1 Effect of solution properties on fibre morphology

The concentration of PEO with water and water/Ethanol (60/40) was varied from 10 wt.% to 14 wt.% in order to study its effect on the fibre morphology.

Table 7.1, Physical properties of the polymer solution and relation with the fibre diameter.

PEOwith water and Water/Ethanol) conc. (wt.%)	Viscosity(Pa.s)	Surface Tension (mN/m)	Electric conductivity (S/cm)	Fibre diameter(nm)
10	0.577/0.785	60.7/63.2	0.00150/0.00172	250-500/250-650
12	1.156/1.356	61.5/64.3	0.00138/0.00160	250-600/300-750
14	1.876/2.011	63.5/67.4	0.001356/0.00152	300-650/350-850

The results show that changing the solvent by adding Ethanol modifies the solution behaviour because of two effects. First, the increase in the solvent viscosity increases the disentanglement time of the transient entanglements so that the onset of extension thickening occurs at lower strain rates in the presence of Ethanol. Second, Ethanol solutions are poorer solvents than water for PEO. At low viscosities small fibres with beads occur, and with increasing viscosity fibres become thicker while the beads get fewer and merge into the thickening fibres, leading finally to smooth fibre morphology can be shown in figure 7.1. Changing the polymer concentration could alter the solution viscosity, as shown in table 7. 1. A series of samples with different PEO concentrations were electrospun, resulting in various fibre morphology, as shown in figure 7.1. At 10 wt.%, PEO with water solution spindle-like beads were seen and the average fibre diameter between beads was 317 nm. With increasing concentration, 12 wt.% to 14 wt.%, the morphology was changed from beaded fibre to uniform fibre structure and the fibre diameter was also increased from 386 to 452 nm gradually. Above the concentration of 14 wt.%, the polymer solution did not form fibres but formed big droplets falling on the collection target regardless of the electrospinning voltage. A critical concentration of polymer solution needed to be exceeded in electrospinning as extensive chain entanglements are necessary to produce electrospun fibres. The surface tension of the PEO solution depends on both the polymer and solvent. Added Ethanol could increase the surface tension and also increases the viscosity of the PEO/water solution (table 7.1). Fong et. al reported that beaded fibres of PEO were changed gradually from bead-fibres to ultrafine-fibres by addition of Ethanol and Ethanol is a solvent of PEO and its addition increased the solution viscosity is increased with increasing of the Ethanol [2]. Our results are consistent with their study. It showed that lower surface tension and higher evaporation rate of the solvent due to the addition of Ethanol weakened the opportunities of bead formation. In our work, Ethanol addition increase surface tension of aqueous PEO solutions, accompanied with an increase in viscosity and a decrease in electrical conductivity (table7.1).

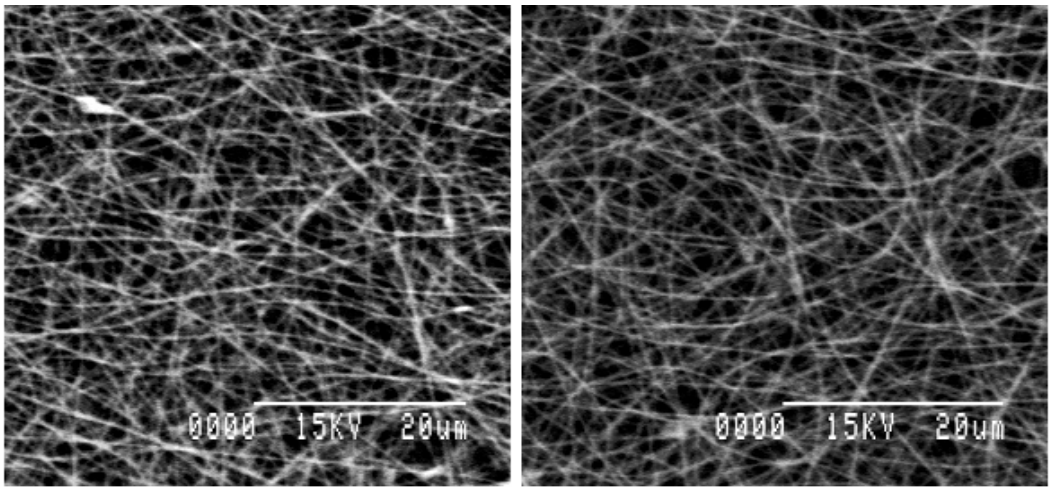

i) ii)

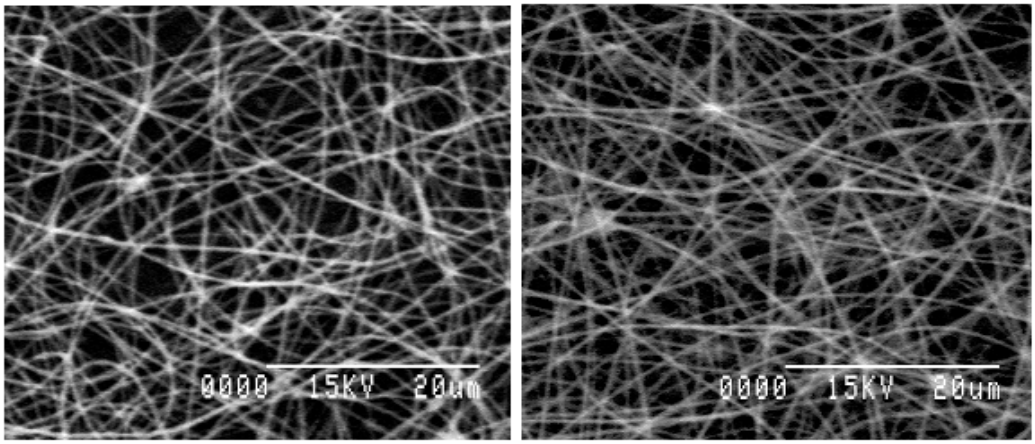

iii) iv)

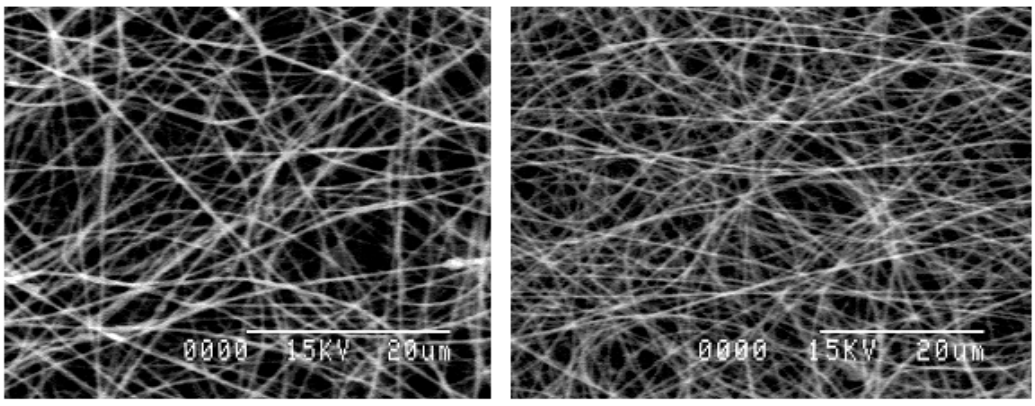

v) vi)

Figure 7.1, SEM figure for PEO with water (i,ii,iii) and water/Ethanol solution (iv,v,vi) where solution were 10 wt.%, 12 wt.% and 14 wt.% and constant applied voltage and collection distance 15 kV and 11 cm respectively.

Table 7.2, Fibre diameter of different polymer solution (PEO/water and PEO/water+Ethanol) where electric field (15 kV) and collection distance (11 cm) constant.

Solution concentration (wt.%)	10		12		14	
Fibre diameter (nm)	264	279	274	342	330	375
	280	335	292	345	335	378
	282	372	294	385	384	450
	285	384	335	397	395	500
	288	390	338	467	465	502
	296	395	372	529	501	559
	298	416	375	545	501	625
	374	474	474	568	526	628
	385	566	542	591	542	637
	418	624	566	720	544	790
Average fibre diameter (nm)	317	423	386	489	452	544
STDEV (nm)	54	104	105	123	84	130

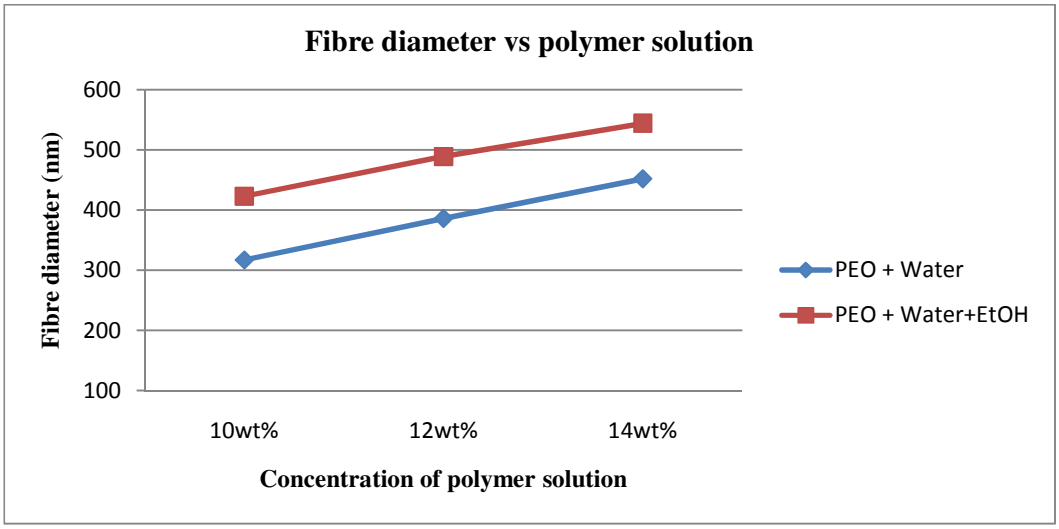

Figure 7.2, Relationship between the average fibre diameter and polymer solution where electric field (15 kV) and collection distance (11 cm) constant.

The viscosity was high enough for stable liquid jet formation and then produced without beaded fibres. Beaded fibres were changed to smooth fibres when Ethanol/water ratio was 40/60. At 10 wt.% PEO with water/Ethanol solution, beads are seen but less then with a PEO with water solution only. The average diameter of the fibre of this solution was observed to be 423 nm (figure 7.2) When the solution concentration increased from 12 wt.% to 14 wt.% the fibre diameter also increased from 489 nm to 544 nm (table 7.2 and figure 7.2). These results suggest that the lower solution concentration facilitated to obtain thinner fibres. Maintaining other processing parameters, fibre diameter increased with increasing solution concentration. This was clearly shown in figure 7.2 where the average diameter of the as-spun PEO fibres was plotted as a function of the solution concentration.

7.2.2.2 Effect of applied voltage on fibre morphology

In electrospinning experiments, the electric current associated with the process, is measured with an Ammeter. In effect, the droplets or fibres bridge the gap between the charged needle and the electrically grounded target. The voltage applied during the electrospinning process plays an important role in determining the shape and diameter of the fibres. The voltage determines the average strength of the electric field together with the distance between the nozzle and the collector. In this experiment 14 wt.% solution of polyethylene oxide in water and water/Ethanol was used. Non woven mats of fibres were electrospun at spinning voltages of 12, 15 and 18 kV. The collector was maintained at a distance of 11 cm from the nozzle throughout the experiment. Three samples were prepared for each particular voltage. These samples were observed in the SEM (figure7.3). The average fibre diameter was evaluated by randomly selecting to 10 different portions of the fibrous mat and averaging the diameter over the number of selected portions. The data collected is shown in table 7.3. The average diameter is reduced from 523 to 471 nm (figure 7.4) as the voltage is increased from 12 to 15 kV when the polymer solutions were PEO with water and PEO with water/Ethanol. In this case the fibre diameter is reduced from 530 nm to 476 nm, and gradually attained a 372 and 379 nm value at 18 kV on both solutions (figure 7.4). Keeping the nozzle to collector constant, an increase in the applied voltage increases the intensity of the electric field across the solution and the collector that further accelerates the whipping motion of the jet resulting in the thinning of the fibres.

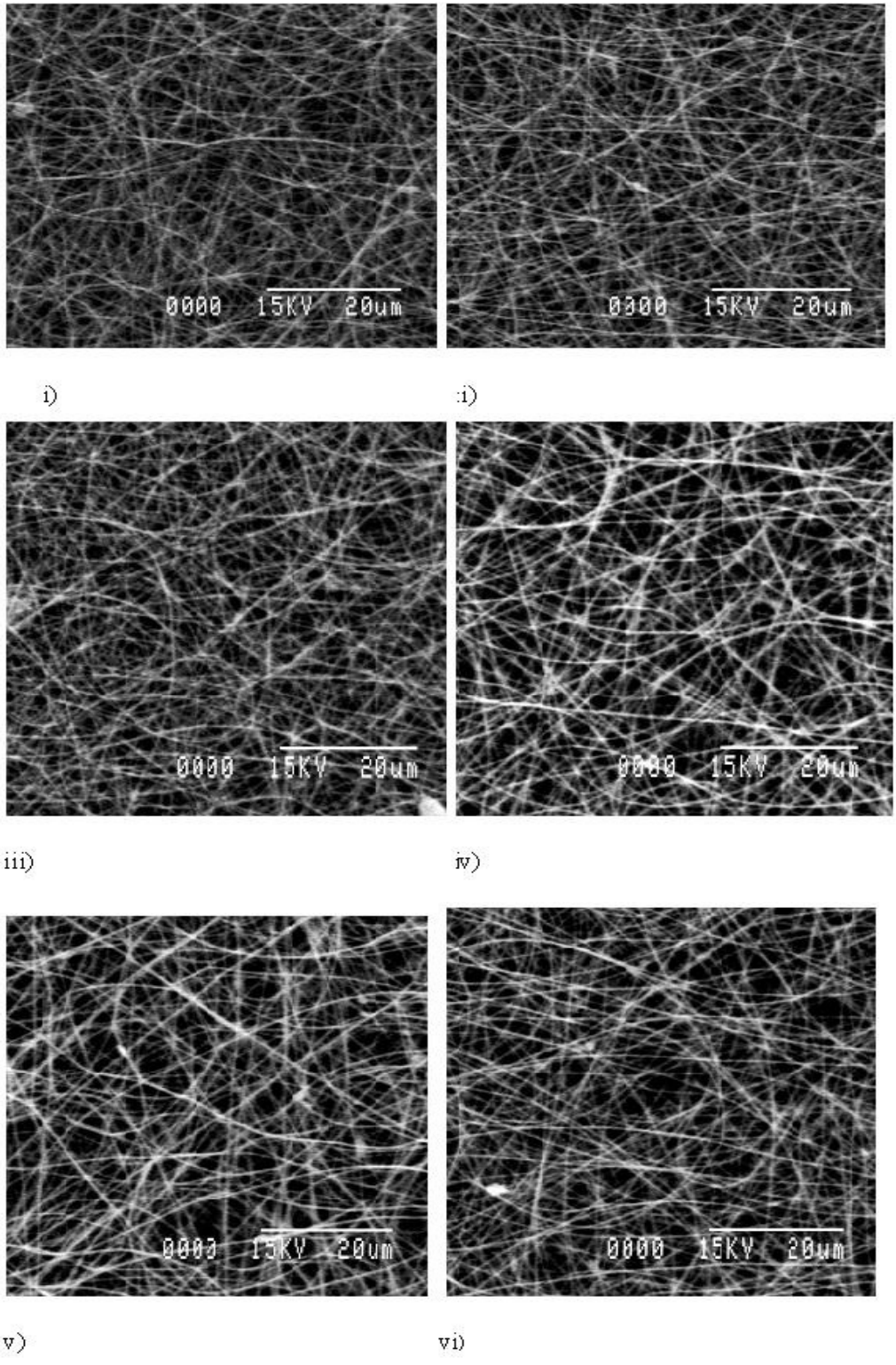

Figure 7.3, SEM figure for PEO with water (i,ii,iii) and water/Ethanol solution (iv,v,vi) where applied voltage were 12 kV, 15 kV and 18 kV and constant polymer solution and collection distance 14 wt.% and 11 cm respectively.

Table 7.3, PEO with water and water/Ethanol solution where applied voltage were 12 kV, 15 kV and 18 kV and constant polymer solution and collection distance 14 wt.% and 11 cm respectively.

Applied voltage (15 kV)	12		15		18	
Fibre diameter (nm)	373	378	370	345	275	275
	383	455	375	348	295	278
	448	456	390	373	351	298
	450	458	392	448	372	350
	497	470	445	478	375	351
	512	475	446	493	376	393
	527	550	448	512	395	440
	621	635	524	548	396	448
	623	637	629	555	430	448
	795	791	695	656	451	512
Average fibre diameter (nm)	523	530	471	476	372	379
STDEV (nm)	128	123	112	100	54	82

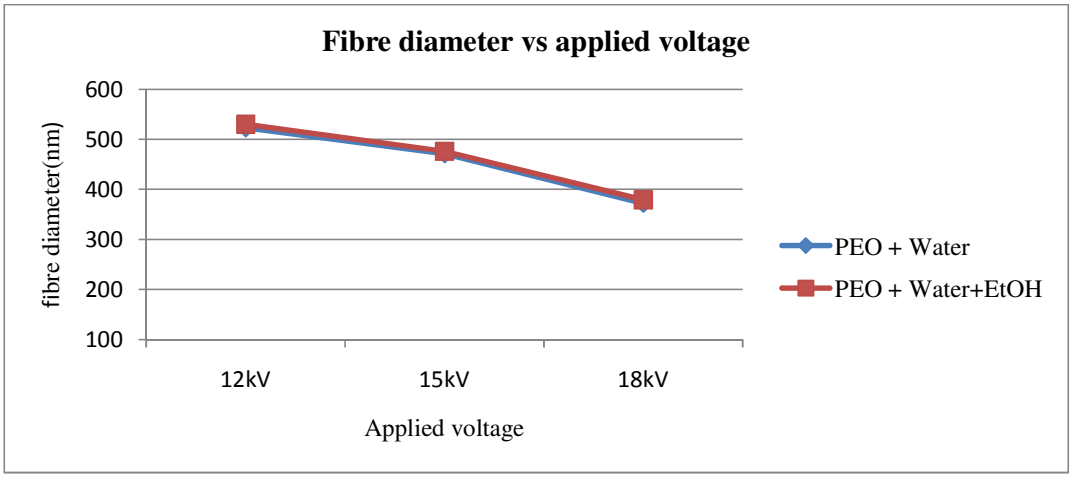

Figure 7.4, The relationship between the average fibre diameter and the applied voltage with concentration of 14 wt.% and spinning distance 11 cm constant.

7.2.2.3 Effect of collector distance on fibre morphology

To assess the effect of collection distance on fibre morphology, the gap between the highly charged needle and the grounded target was 8 cm, 11 cm and 14 cm, keeping all other parameters constant.

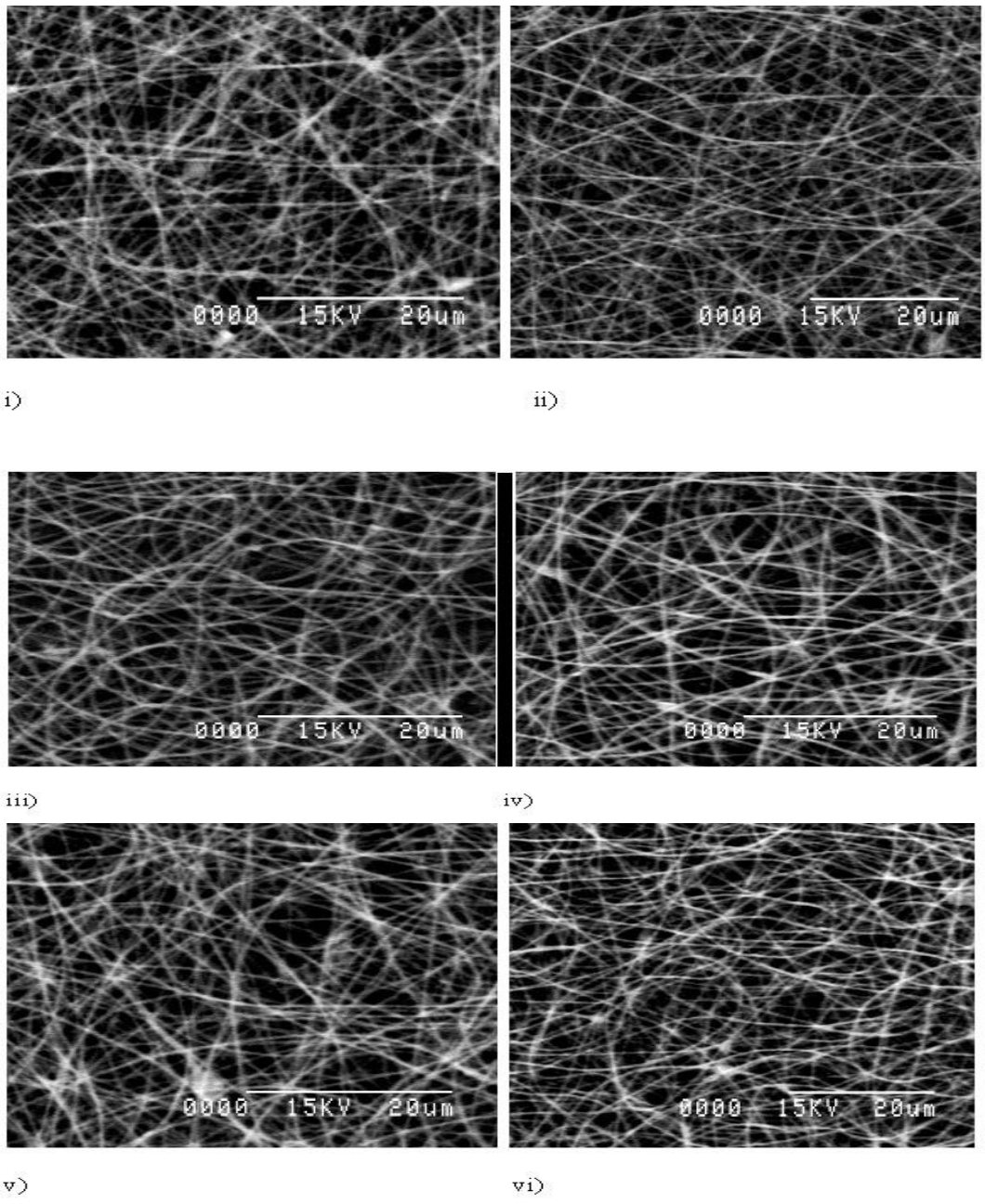

Figure 7.5, SEM images of PEO with water and water/Ethanol solution at 14 wt.%, with different collection distance i) 8cm , ii) 11cm , iii) 14 cm , iv) 8 cm, v) 11cm, vi) 14 cm and applied voltage 15 kV constant.

It was found that, although the fibre size does not change significantly, homogeneously distributed elongated beads start to form along the PEO fibres after reducing the working distance to only 8 cm. The morphology of the PEO with water and water/Ethanol fibres is also influenced by changing the working distance.

Table 7.4, PEO with water and water/Ethanol at constant solution 14 wt.%, and applied voltage 15 kV different collection distance (8cm , 11cm and 14 cm).

Collection distance (8 cm)	8		11		14	
Fibre diameter (nm)	279	359	279	295	264	278
	372	375	294	296	265	301
	384	395	335	337	294	348
	465	450	335	338	295	356
	466	451	384	374	296	370
	474	515	385	385	298	375
	526	600	395	418	337	393
	558	625	416	420	418	395
	566	637	416	467	467	396
	658	638	416	468	529	512
Average fibre diameter (nm)	475	504	365	380	346	372
STDEV (nm)	110	113	51	64	92	63

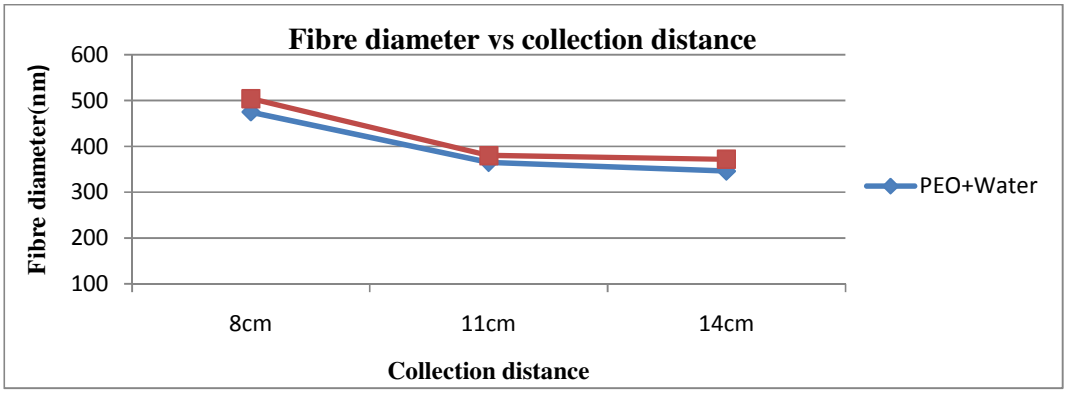

Figure7.6, The relationship between the average fibre diameter and collection distance where solution concentration (14 wt.%) and applied voltage (15 kV) constant.

Fibres were electrospun from a 14 wt.% PEO solution in water and water/Ethanol. The nozzle to collector distance was adjusted at 8, 11 and 14 cm keeping a constant voltage of 18 kV. Three samples were prepared and were dried overnight. The variation in diameter of the fibres with distance is shown in table 7.4 and figure 7.6. The diameter decreases rapidly 475 nm and 365 nm as distance is increased from 8 cm to 11 cm and slowly decreases to 346 nm as distance is increased to 14 cm in PEO with water. When PEO with water/Ethanol was used it provided higher fibre diameter at distances of 8 cm 504 nm, 11 cm 380 nm and 14 cm 372 nm and decreased the fibre diameter when the collection distance increase further as it can be shown at table 7.4 and figure 7.6. It is understood that fibres with smaller diameters are obtained by allowing the jet to work at longer distance in the electric field. This also allows more time for the evaporation of solvent from the fibres that can result in decreasing fibre diameter. If the electric field (15 kV) remained constant, and the distance was increased, fibre diameter was slightly decreased. Longer distance enables greater stretching of the solution jet. Although fibre diameters can be expected to decrease, in the presence of a stronger electric field due to increased stretching, these studies showed no evidence for such a trend. An increase in electrical force can produce contradictory effects since it can increase both whipping instability and mass flow. Figure 7.6 shows how the average fibre diameter drops when the collection distance increases. When the nozzle to collection distance is 8 cm PEO with water and water/Ethanol solutions there are some bead formation (figure.7.5), but as the collection distance increase the beads disappear to produce uniform fibre.

7.2.2.4 Effect of flow rate on fibre morphology

The rate at which the polymer was being ejected from the tip of the syringe was controlled with the help of a syringe pump. A certain minimum value of the solution volume suspended at the end of the needle should be maintained in order to form an equilibrium Taylor cone. Therefore, different morphologies of electrospun nanofibres can be obtained with the change in feeding rates at a given voltage. Figure 7.7 shows the effect of the feeding rate on the morphology of the electrospun nanofibres from the 14 wt.% water and water/Ethanol solution at different feeding rates and constant voltage of 15 kV. At feeding rate of 0.30 ml/h, the feed exceeded the delivery rate of solution with applied electric forces; therefore some of polymer solution is shot as tiny drops on to the collector and on the electrospun nanofibres mat. Too high rate also causes dripping of solution and might thus also cause occurrence of beaded fibres. Higher flow rate would naturally directly increase productivity at least in cases when dripping would

not occur. At lower feeding rate of 0.25 ml/h, a droplet of solution remains suspended at the end of the syringe needle and the electrospinning jet originates from a cone at the bottom of the droplet. The nanofibres produced under this condition have a uniform morphology and no bead defect was present at lower feeding rate of 0.20 ml/h, the solution was removed from the needle tip by the electric forces, faster than the feeding rate of the solution onto the needle tip. This shift in the mass balance resulted in sustained but unstable jet and nanofibres with beads were formed (figure 7.7).

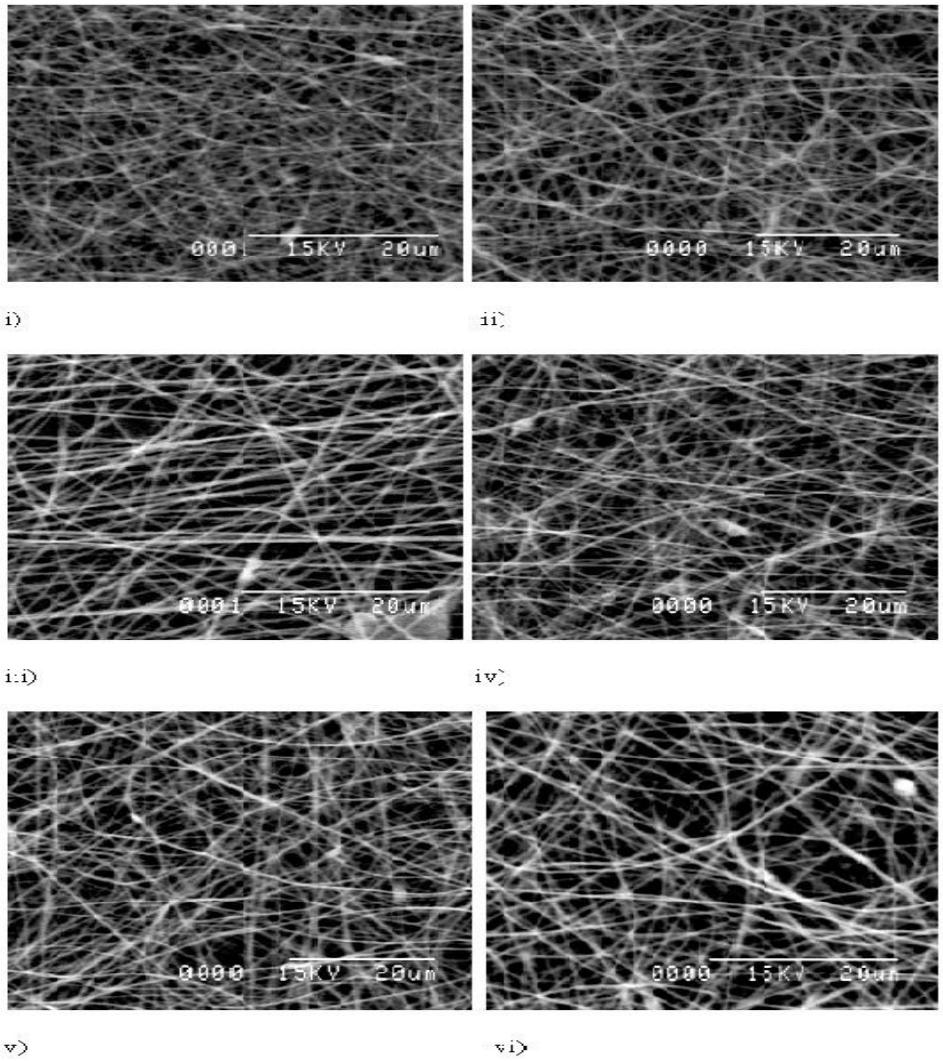

Figure 7.7, SEM images for effect of flow rate of PEO with water and water/Ethanol solution (14 wt.%) on fibre morphology (voltage=15 kV, tip to collector distance 11 cm). Different flow rate i) 0.20 ml/hr, ii) 0.25 ml/hr, iii) 0.30 ml/hr, iv) 0.20 ml/hr, v) 0.25 ml/hr, vi) 0.30 ml/hr.

Too low feeding rate may cause blockages of nozzles, when pendant droplet disappears from the tip which may dry up and thus be sealed by solidified polymer residue. It was also revealed by Baumgarten [3].

Table 7.5, PEO with water and water/Ethanol solution where solution (14 wt.%), applied voltage(15 kV) and collection distance (11cm).

Flow rate (ml/hr)	0.20 ml/hr		0.25 ml/hr		0.30 ml/hr	
Fibre diameter (nm)	285	279	279	356	264	282
	293	372	380	374	295	339
	334	375	385	375	396	349
	356	376	394	377	398	462
	362	395	395	379	418	468
	393	398	415	442	437	479
	395	451	416	452	464	506
	414	452	418	524	467	548
	434	455	435	539	496	571
	435	510	436	603	529	630
Average fibre diameter (nm)	370	406	395	442	416	463
STDEV (nm)	54	64	45	86	84	111

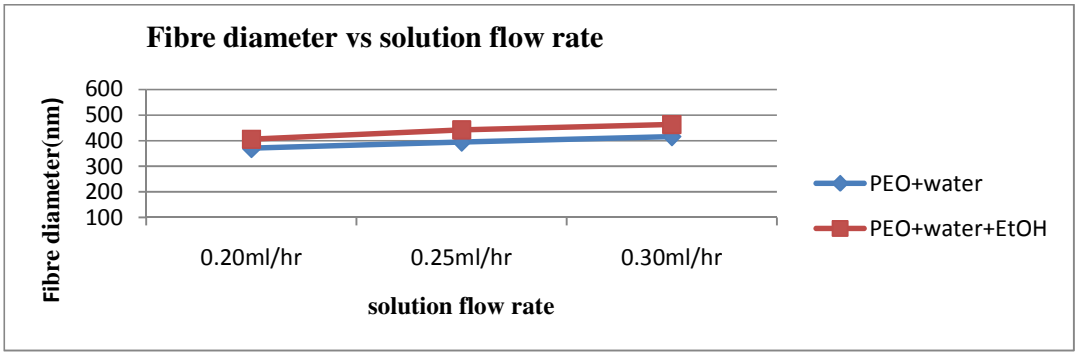

Figure 7.8, Relationship between the average fibre diameter and solution flow rate (0.20 ml/hr, 0.25 ml/hr and 0.30 ml/hr) when the polymer solution (14 wt.%) and electric voltage (15 kV) and collection distance (11 cm) constant.

If we see figure 7.7 then we can see that lower solution flow rate gives fibres with beads. When the solution flow rate increases the uniform beads free fibre diameter also increases. The optimum solution flow rate is 0.20 ml/hr, fibre diameter 370 nm and 406 nm for PEO with water and PEO with water/Ethanol solution was produced respectively. Increases of the solution flow rate to 0.25 ml/hr and 0.30 ml/hr, also increases the fibre diameter from 395 nm to 416 nm and 442 nm to 463 nm for the solution of PEO with water and PEO with water/Ethanol, respectively as shown in the table 7.5 and figure 7.8. So it was found that as the flow rate increased, the fibre thickness and bead density also increased. Lower flow rate reducing fibre diameter and higher flow rates gives higher diameter fibres. Increasing the flow rate has usually been found to increase the fibre and fibre diameter distribution. The control of flow rate can be expected to narrow fibre size distribution, because when flow rate is equivalent to the rate at which the jet carries the solution away, the shape of the solution surface on the tip of the nozzle remains stabile unlike in the case of dripping explained above. This result is the agreement result published by Magelski et. al [3], Hsu et. al [4] ,Cui et. al [5], Ramakrishna. et. al [6].

7. 3 Morphological analysis

Processing parameters must be optimized when electrospun PEO with water and PEO with water/Ethanol nano fibre to get their desired morphology. Submicron PEO fibre mats were prepared by electrospinning of aqueous PEO solutions and aqueous with Ethanol PEO solution. With increasing the concentration of PEO solution, the morphology was changed from beaded fibre to uniform fibre structure and the fibre diameter were also increased. There was a slightly decrease in average fibre diameter with increasing applied electric voltage. Tip to target distance has also significant effects on fibre morphology; however the morphology was slightly changed by the flow rate.

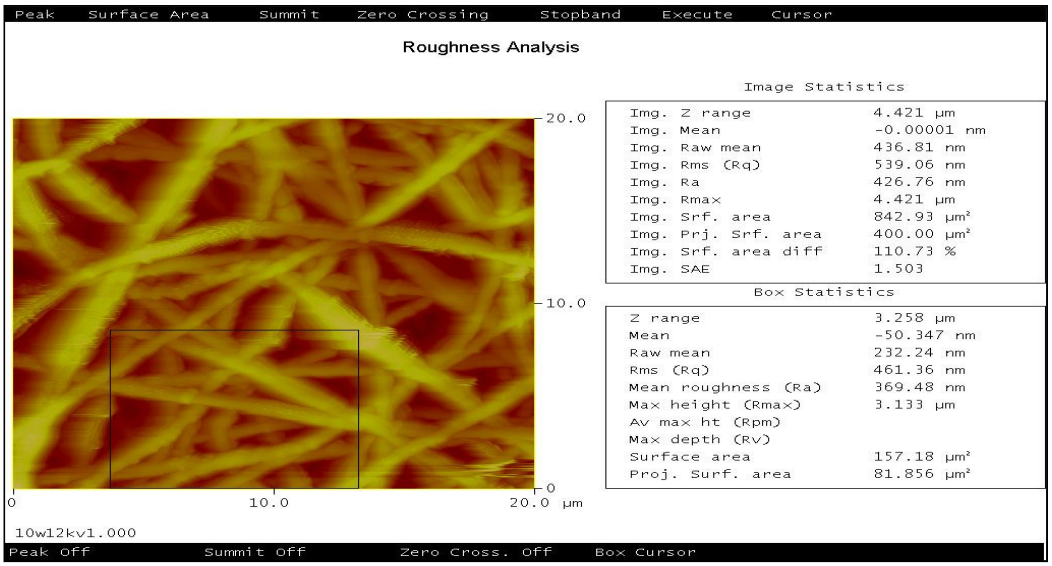
Peak Surface Area Summit Zero Crossing Stopband Execute Cursor
Roughness Analysis
Image Statistics
Img. Z range 4.421 µm
Img. Mean -0.00001 nm
Img. Raw mean 436.81 nm
Img. Rms (Rq) 539.06 nm
Img. Ra 426.76 nm
Img. Rmax 4.421 µm
Img. Srf. area 842.93 µm²
Img. Prj. Srf. area 400.00 µm²
Img. Srf. area diff 110.73 %
Img. SAE 1.503
Box Statistics
Z range 3.258 µm
Mean -50.347 nm
Raw mean 232.24 nm
Rms (Rq) 461.36 nm
Mean roughness (Ra) 369.48 nm
Max height (Rmax) 3.133 µm
Av max ht (Rpm)
Max depth (Rv)
Surface area 157.18 µm²
Proj. Surf. area 81.856 µm²
20.0
10.0
0
0
10.0
20.0 µm
10w12kv1.000
Peak Off Summit Off Zero Cross. Off Box Cursor

i)

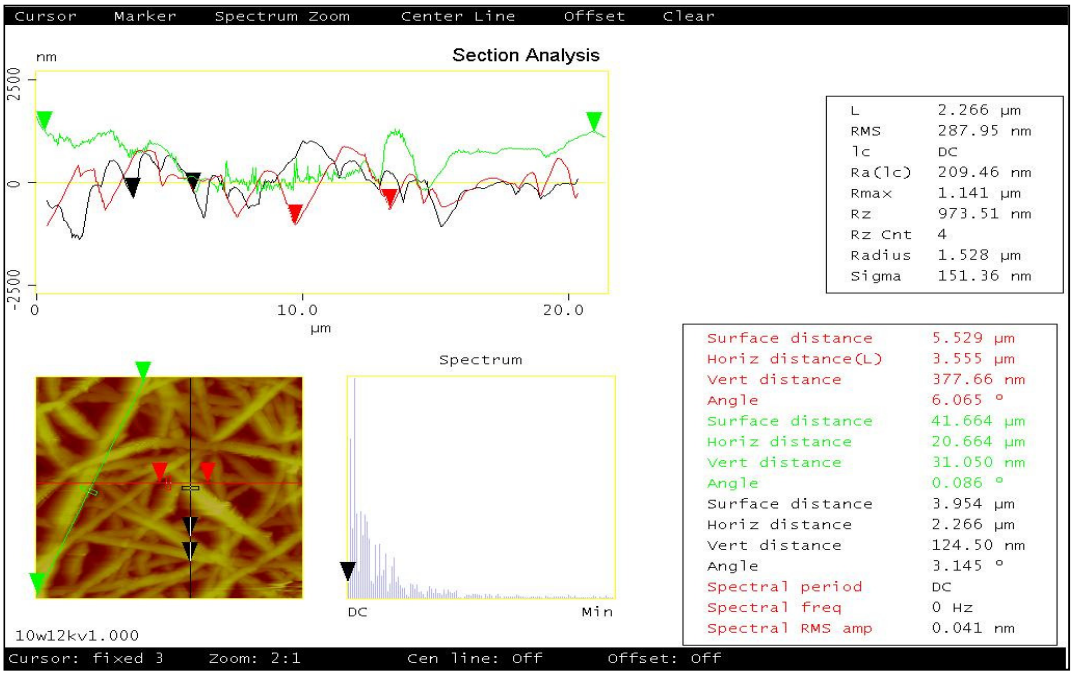
Cursor Marker Spectrum Zoom Center Line Offset Clear
Section Analysis
nm
2500
0
-2500
0
10.0
20.0
µm
L 2.266 µm
RMS 287.95 nm
lc DC
Ra(lc) 209.46 nm
Rmax 1.141 µm
Rz 973.51 nm
Rz Cnt 4
Radius 1.528 µm
Sigma 151.36 nm
Spectrum
DC
Min
Surface distance 5.529 µm
Horiz distance(L) 3.555 µm
Vert distance 377.66 nm
Angle 6.065 °
Surface distance 41.664 µm
Horiz distance 20.664 µm
Vert distance 31.050 nm
Angle 0.086 °
Surface distance 3.954 µm
Horiz distance 2.266 µm
Vert distance 124.50 nm
Angle 3.145 °
Spectral period DC
Spectral freq 0 Hz
Spectral RMS amp 0.041 nm
10w12kv1.000
Cursor: fixed 3 Zoom: 2:1 Cen line: Off Offset: Off

ii)

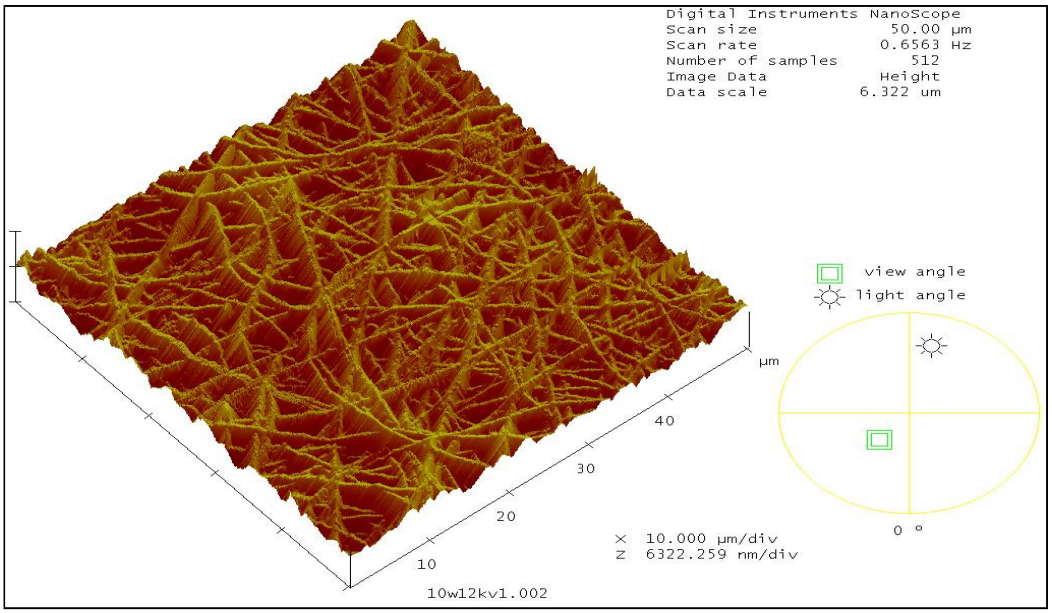
Digital Instruments NanoScope
Scan size 50.00 µm
Scan rate 0.6563 Hz
Number of samples 512
Image Data Height
Data scale 6.322 um
view angle
light angle
µm
40
30
20
10
0 °
X 10.000 µm/div
Z 6322.259 nm/div
10w12kv1.002

iii)

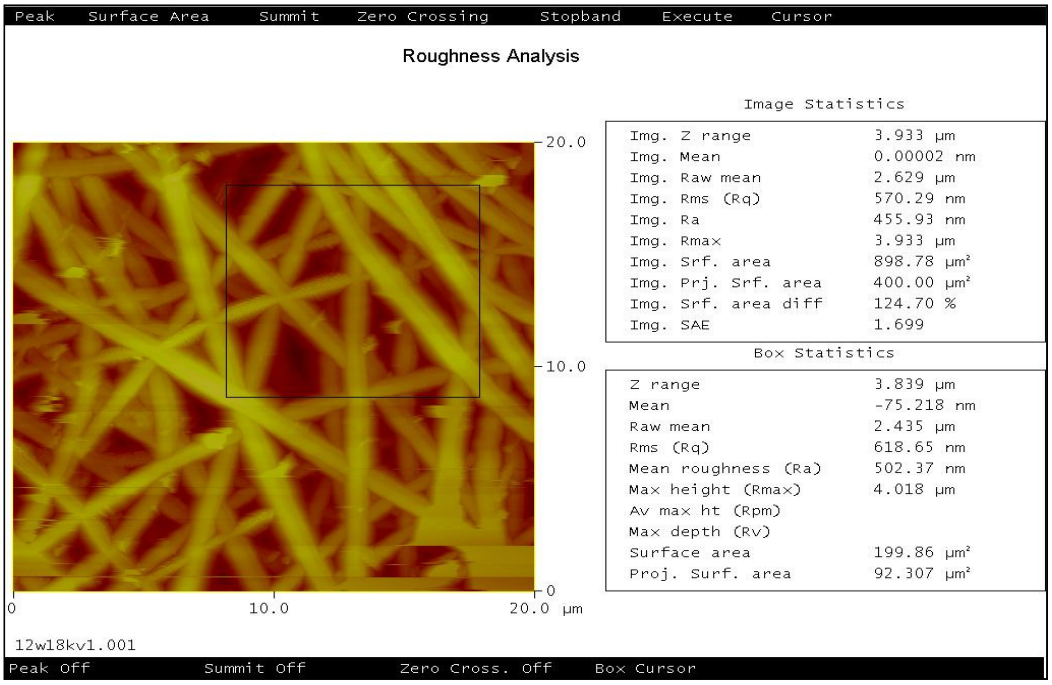
Peak Surface Area Summit Zero Crossing Stopband Execute Cursor
Roughness Analysis
Image Statistics
Img. Z range 3.933 µm
Img. Mean 0.00002 nm
Img. Raw mean 2.629 µm
Img. Rms (Rq) 570.29 nm
Img. Ra 455.93 nm
Img. Rmax 3.933 µm
Img. Srf. area 898.78 µm²
Img. Prj. Srf. area 400.00 µm²
Img. Srf. area diff 124.70 %
Img. SAE 1.699
Box Statistics
Z range 3.839 µm
Mean -75.218 nm
Raw mean 2.435 µm
Rms (Rq) 618.65 nm
Mean roughness (Ra) 502.37 nm
Max height (Rmax) 4.018 µm
Av max ht (Rpm)
Max depth (Rv)
Surface area 199.86 µm²
Proj. Surf. area 92.307 µm²
20.0
10.0
0
0
10.0
20.0 µm
12w18kv1.001
Peak Off Summit Off Zero Cross. Off Box Cursor

iv)

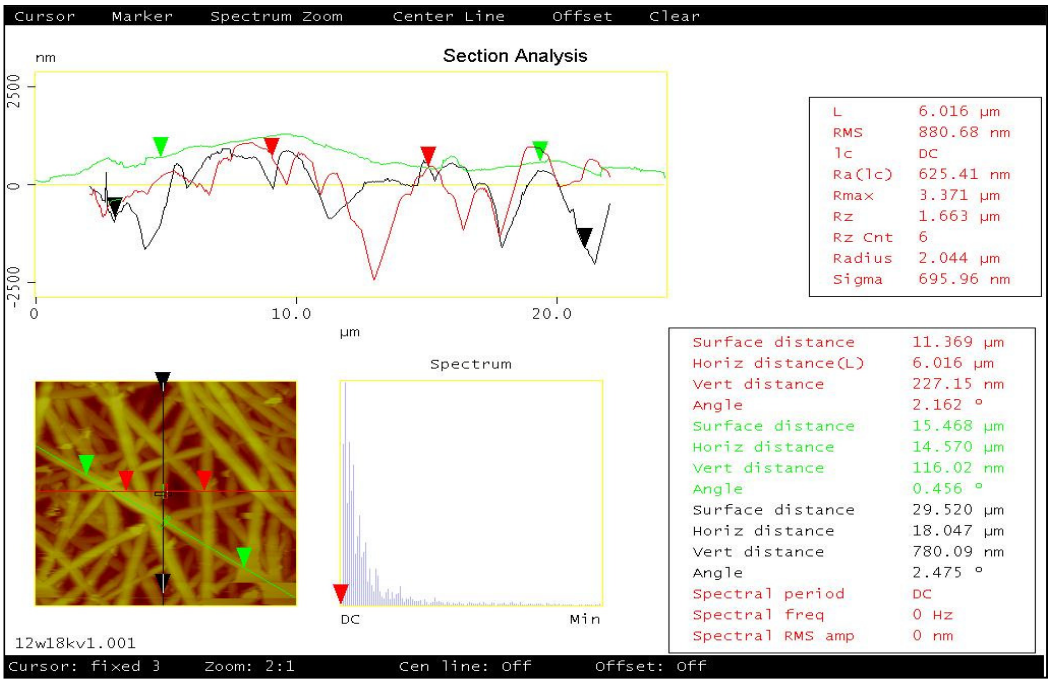

v)

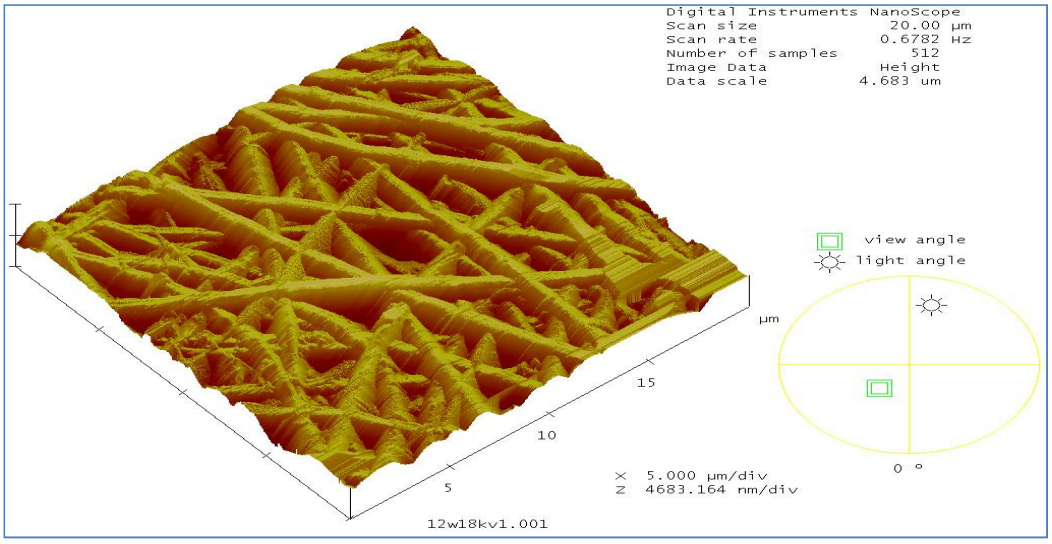

vi)

Figure 7.9, AFM images for PEO/Water and PEO /water/Ethanol nanofibre the polymer solution of 14 wt.%, applied voltage 15 kV and collection distance 11cm, i & iv) roughness analysis, ii &v) section analysis, iii & vi) 3D, where the fibre diameter varies from 400 nm to 700 nm.

The above images (figure 7.9] show that PEO/Water and PEO /water/Ethanol nanofibres. It reveals that the fibre have a smooth surface with a fairly uniform diameter of about 400-700 nm without any noticeable beads on a string. The analyzed AFM images figure 7.9 where the polymer solutions are 14 wt.% and the electric voltage 15 kV and nozzle to collection distance 11 cm uniform fibres are produced.

7.4 Thermal behavior of electrospun PEO nanofibres

Few reports have been focusing on the effect of electrospinning process on the thermodynamic behaviors of obtained fibres [8]. The crystalline properties of the electrospun fibres may also be of primary importance when considering the materials for commercial applications. DSC curves of PEO powder and electrospun fibres were obtained using a Metler DSC 30 (USA) by heating from 30º to 300 °C in N_2 at a heating rate of 10 K/min. Generally PEO begins to degrade when being heated near its melting point. The degradation reaction of PEO is so exothermic that it tends to obscure its melting endothermic in ordinary DSC traces. Zeng et. al [9] noticed that the electrospun PLLA fibres quenched below 0ºC resulted in amorphous fibre structure. After drying the electrospun nanofibres at room temperature, they found that melting point transitions appeared at two peaks by DSC. It was explained that during electrospinning of this polymer molecule had no time to crystallize and hence it could only have an amorphous super molecular structure. Z.M. Huang et. al noted that polymer crystallization does occur during electrospinning when the polymer is in a molten form [8]. Since the super molecular structure changed during the electrospinning the transition points of the polymers also changed. One of them was lower than the normal melting point due to defects existing in crystallization while drying. Below the table described the Transition midpoint ($Tm_)$ for PEO powder and Polymer solution for PEO with water and PEO with water/Ethanol.

Table: 7.6, Diffrential Scanning Calorimetry chart for PEO powder and PEO/water PEO/water+Ethanol polymer nanofibres.

Concentration of polymer (PEO)	Transition midpoint (T_m)
Powder PEO	66.6 C
10% (water)	62.0
12% (water)	61.5
14% (water)	59.5
10% (water+Ethanol)	63.4
12% (water+Ethanol)	63.0
14% (water+Ethanol)	62.0

The PEO powder had a melting temperature, $T_{m,}$ (66.6 C) that were much higher than produced nano fibres (table 7.6). Preliminary experimentation using DSC on PEO powder and solvent (water, water/Ethanol) incorporated electrospun fibre reveals that the crystallinity of PEO is significantly impaired by the introduction of water and Ethanol on its structure. It is a possibility that due to the entanglement of certain solvent species (such as water) with PEO the usual network of intermolecular bond is either deformed or ruptured resulting an weaker interaction and thus lower melting points of the electrospun fibres (table 7.6). The lower heat of fusion and melting mean that the PEO fibre mat contains smaller, less perfect crystals than those in the neat PEO powder. These results are in qualitative agreement with the results presented by J.M Deitzel et al [10], Buchko [11] and Larrondo [12–13] in which relatively low crystallinity was observed for polymer fibres electrospun from the melt state.

For a further verification of these results, XRD was carried out on these PEO powder and electrospun fibres. In order to examine whether the structure of PEO is changed in the electrospinning process, XRD of both the raw material of PEO and the electrospun PEO were measured. The most common technique used to determine the degree of crystallinity is X-ray diffraction (XRD) analysis, figure 7.10

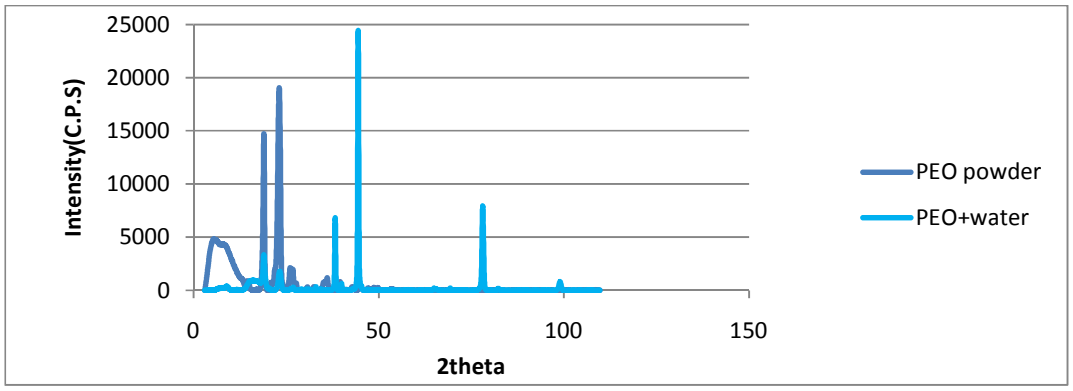

a)

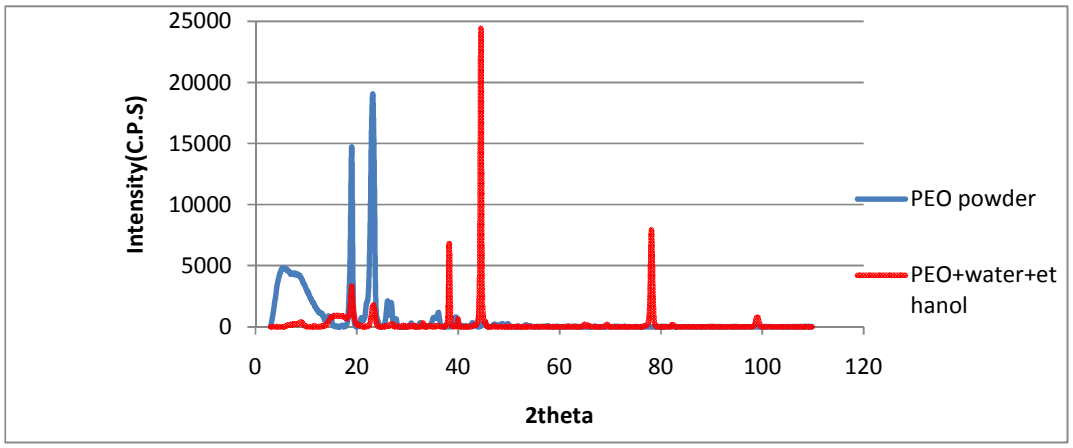

b)

Figure 7.10, XRD patterns from, a) PEO powder (dashed line) and PEO nanofibres (mix with water), b) PEO powder and PEO nanofibres (mix with Ethanol) electrospun both from 14 wt.% solution (solid line).

a & b showed the X-ray diffraction pattern of the crystallize PEO with water and PEO with water/Ethanol nano fibre samples. This figure 7.10 shows that there were slightly changes between the PEO with water and PEO with water/Ethanol.

7.5 Conclusion

Submicron PEO fibre mats were prepared by electrospinning of aqueous PEO and aqueous PEO with Ethanol solutions. With increasing the concentration of PEO solution, the morphology was changed from beaded fibre to uniform fibre structure and the fibre diameter was also increased, with increasing applied electric voltage the fibre diameter decrease and produced finer diameter nanofibres. Tip–target distance had little significant effects on fibre morphology; however the morphology was also changed by

the flow rate. The analyzed results shown that polymer solution concentration of 14 wt.%, an applied voltage 15 kV, volume feed rate 0.20 ml/hr and a spinning collection distance 11 cm produced uniform fibres. DSC and XRD analyses proved that PEO powder are more crystal then the produced nanofibre.

7.6 References

[7.1] S. A. Theron, E. Zussman, A. L. Yarin, *Experimental investigation of the governing parameters in the electrospinning of polymer solutions*, Polymer, **45** (6), 2017–2030 (2004)

[7.2] H. Fong, I. Chun, D. H. Reneker, *Beaded nanofibres formed during electrospinning*, Polymer, **40**, 4585-4592 (1999)

[7.3] P. K. Baumgarten, *Electrostatic spinning of acrylic microfibres,* Journal of colloid and interface Science, **36**, 71 (1971)

[7.4] S. Megelski, J. S. Stephens, D. B.Chase, J. F. Rabolt, *Micro- and nanostructured surface morphology on electrospun polymer fibre,* Macromolecules; **35**:8456–66 (2002)

[7.5] C. M. Hsu, S. Shivkumar, *Nano-sized beads and porous fibre constructs of poly (e-caprolactone) produced by electrospinning*, J Mater Sci; **39** (9):3003–13 (2004)

[7.6] W. Cui, X. Li, S. Zhou and J. Weng, *Investigation on process parameters of electrospinning system through orthogonal experimental design*, J Appl Polym Sci; **103** (5):3105–12 (2007)

[7.7] S. H. Tan, R. Inai, M. Kotaki and S. Ramakrishna, *Systematic parameter study for ultra-fine fibre fabrication via electrospinning process*, Polymer; **46** (16):6128–34 (2005)

[7.8] Z. M. Huang, Y. Z. Zhang, M. Kotaki, S. Ramakrishna, *A review on polymer nanofibres by electrospinning and their applications in nanocomposites*, Compos. Sci. Technol., Vol. **63** No.15, pp.2223-53 (2003)

[7.9] J. Zeng, X. Chen, X. Xu, Q. Liang, X. Bian and L. Yang et al, *Ultrafine fibres electrospun from biodegradable polymer,* J Appl Polym Sci, **89**:1085–92(2003)

[7.10] J. M. Deitzel, J. Kleinmeyer, D. Harris, N. C. B. Tan, *The effect of processing variables on the morphology of electrospun nanofibres and textiles*, Polymer, **42**, 261-272 (2001)

[7.11] C. J. Buchko, L. C. Chen, Y. Shen and D. C. Martin, Processing and microstructural characterization of porous biocompatible protein polymer thin films. *Polymer*; **40**: 7397–7407 (1999)

[7.12] L. Larrondo, S. J. Manley, Journal of Polymer Science, Polymer Physics Edition; **19**:909–20 (1981)

[7.13] L. Larrondo, S. J. Manley, Journal of Polymer Science, Polymer Physics Edition; **19**:921–32 (1981)

Chapter 8: Process optimization of PVA Ferro gel nano fibre blends by the electro spinning process

8.1 Introduction.

PVA (poly vinyl alcohol) is a semi-crystalline, hydrophilic polymer with good chemical and thermal stability, highly biocompatible, non-toxic and high water permeability [1-2]. The electrospinning of PVA solution and its potential applications in the preparation of ultrafine separation filters, biodegradable mats, etc have been reported by many researchers [3-4]. A number of grades of PVA are commercially available, which can be divided into two types: a fully hydrolyzed and partially hydrolyzed, PVA depending on the amount of acetate groups left in the backbone [5]. PVA solutions can form physical gels from various types of solvents and these properties led the use of PVA in a wide range of applications in medical, cosmetic, food, packaging industries and pharmaceuticals [6]. In recent years, much attention has been focused on biomedical applications of PVA hydro gels including contact lenses, artificial organs and drug delivery systems [7]. This is an important step towards R &D in controlled release of biomedical by means of manipulating the pore activities of the PVA by the $FeCl_3$ through magnetic fields. In this present research work, we show structural results on electrospun PVA and $FeCl_3$ blends. The solution flow rate, the effect of electric field and tip-target distance on the morphology of electrospun fibres were evaluated and analyzed. We also report on a novel and easy synthetic route for the fabrication of novel polymer Ferro- gel composite material.

8.2 Experimental

8.2.1 Materials

Poly (vinyl alcohol), 99-100% hydrolyzed approx 86000 g/mol M_w purchased from Across organics, UK and $FeCl_3$ purchased from Sigma Aldrich UK.

8.2.2 Preparation of the solution (PVA/$FeCl_3$)

PVA solutions (polymer concentrations ranging from 6 to 10% (g/ml)) were prepared by mixing the appropriate amount of polymer and water (milli-Q grade) at 100 °C under conditions of vigorous stirring until the polymer was completely dissolved. Solutions

were stored at 80° C overnight and were then cooled to room temperature. PVA Ferro gels (polymer concentration 6% g/ml to10%g/ml and Ferro fluid concentrations ranging from 6 to 10% g/ml) were prepared by mixing the appropriate amount of $FeCl_3$ with aqueous PVA solutions. Homogenization was achieved at 90° C under conditions of vigorous stirring. Samples were stored overnight at 80 °C and were then cooled to room temperature for 1 hour, before being subjected to the electrospinning process.

8.3 Characterization

The samples produced for random nano fibres were collected on aluminium stubs. The morphology of the electrospun PVA/$FeCl_3$ fibres was observed with a SEM, Model Hitachi S-530, UK. The presence of the Ferro gels of the PVA/$FeCl_3$ nanocomposites, collected on carbon-coated copper grids were observed with a JE0L JEM 2010 Transmission Electron Microscope (TEM) operated at 200 kV.

8.4. Results and Discussion

8.4.1 The effect of polymer concentration on fibre morphology

The diameter and morphology of electrospun nanofibres was dependent upon; the solution concentration, the applied electric field strength, the tip to collector distance etc [8-10]. Among these parameters, the concentration or the corresponding viscosity of the electrospun solution was one of the most effective variables to control the fibre morphology and diameter of the PVA Ferro gels, which is in agreement with the work of others [11]. Solution concentration and viscosity are two closely correlated factors, increasing of solution concentration always result in increase of solution viscosity, and decrease of solution concentration always results in decrease of solution viscosity. A series of samples with different PVA/$FeCl_3$ concentrations were electrospun, resulting in various fibre morphologies, as shown in figure 8.1, At 6 wt.% polymer solution the average fibre diameters was 735 nm and beads were observed. Increasing the polymer concentration the morphology was changed from beaded fibre to uniform fibre structure and the fibre diameter was also increased from 789 to 987 nm (figure 8.2 and table 8.1).

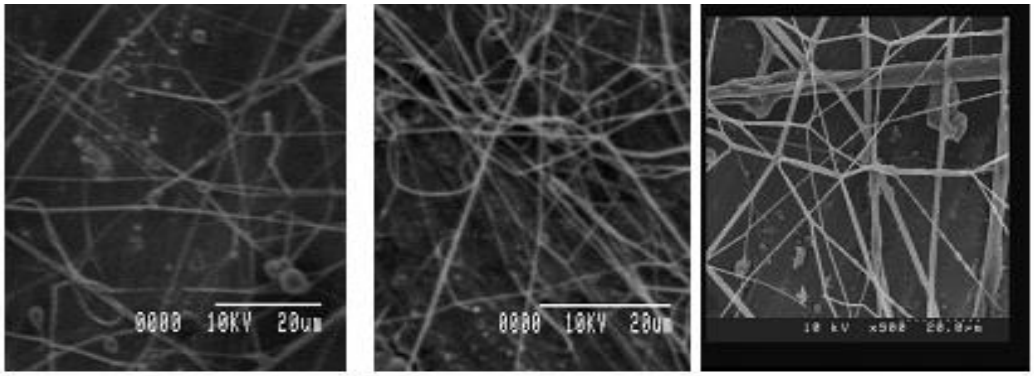

Figure 8.1, SEM micrographs of electrospun fibres from PVA/$FeCl_3$ solution with different solution concentration, voltage 15 kV, tip to target distance 11 cm, flow rate 0.25 ml/hr. PVA/$FeCl_3$ concentration at a) 6 wt.%, b) 8 wt.%, c) 10 wt.%

Table 8.1, Fibre diameter in different polymer concentration (6 wt.%, 8 wt.% and 10 wt.%) at constant electric fields (15 kV) and a constant spinning distance of 11 cm.

Solution concentration (wt.%)	6	8	10
Fibre diameter (nm)	303	345	488
	519	534	732
	629	641	782
	648	653	791
	735	836	970
	812	841	1070
	825	868	1140
	881	974	1244
	982	1087	1273
	1014	1115	1384
Average fibre diameter (nm)	735	789	987
STDEV (nm)	218	246	285

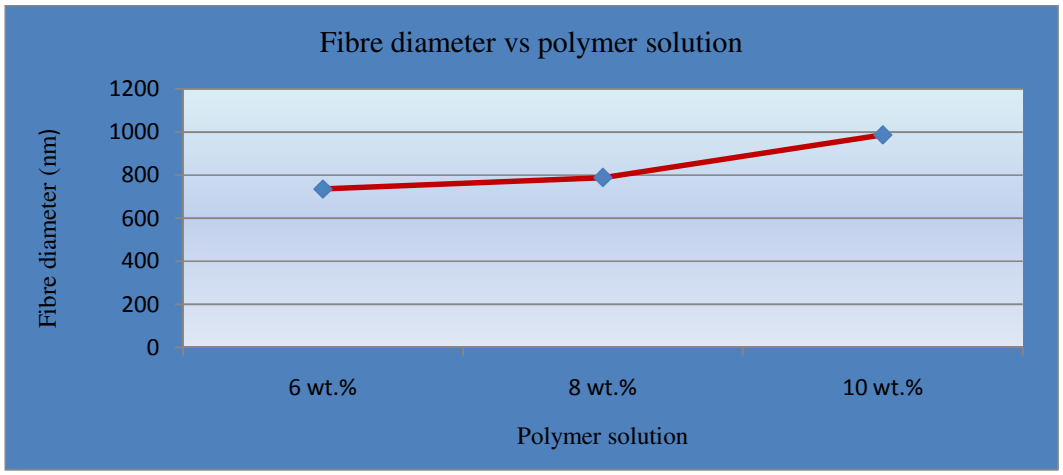

Figure 8.2, The above graph describes the relationships between average fibre diameter and the polymer concentration where applied voltage (15 kV), tip to target distance (11 cm) and flow rate (0.25 ml/hr) constant.

In electrospinning, the coiled macromolecules of the solution are transformed by the elongation flow of the jet into oriented entangled networks that persist with fibre solidification. Below this concentration (less than 6 wt.%) chain entanglements are insufficient to stabilize the jet driven by the surface tension and caused the solution to form beads or beaded fibres. When the polymer solution increases at higher concentrations, viscoelastic forces which resist rapid changes in fibre shape result in uniform fibre formation. But if the solution concentration is too high, it would be impossible to electrospin because of their high viscosity. The changing of the fibre morphology can probably be attributed to a competition between surface tension and viscosity. It has been found that viscosity and surface tension are the most important factors that affect the morphology of the resultant fibres. Uniform fibres obtain higher concentration and lower concentration give fibres with beads. If the concentration decreases the bigger beads are obtains and some spot might be formed.

8.4.2 The effect of applied voltage on fibre morphology

The voltage applied between the capillary and the metal target can be used to control the amount of fibre being formed. The number of droplets or fibres reaching the target is a function of the current flowing across the circuit. Hence the amount of fibre spun can be easily controlled by varying the voltage. At a lower voltage, typical value a droplet of solution remains suspended at the end of the syringe needle, and the fibre jet originates from the cone at the bottom of the droplet. The size of the droplet formed at the end of the capillary is large because the voltage is not high enough to transfer all the solution

to the target. The nano fibres produced under this condition will typically have cylindrical morphology with few bead defects. The bead like structures are undesirable of the electrospinning process caused due to instability of the jet of the polymer solution. A series of experiments were carried out by varying the applied voltage from 12 to 18 kV and tip to target distance at 11 cm. A considerable amount of thin fibres with diameters below 850 nm were found when the applied voltage was above 12 kV. The average diameter of the fibre calculated 892 nm. At lower voltage narrow distribution of fibres were observed. At higher voltages of 15 kV to 18 kV, more fibres were obtained. Increasing the applied voltage will increases the electrostatic repulsive force on the fluid jet which favours the thinner fibre formation. The average fibres calculate 791 nm to 696 nm. The solution will be removed from the capillary tip more quickly as jet is ejected from Taylor cone and thus making larger diameter fibres. As figure 8.3, 8.4 and table 8.2 shows the relationships between the fibre diameter and electric field with a constant concentration were 8 wt.% and the collection distances of 11 cm. This figure shows that voltage played a part to produce uniform and its fibre diameter. It was observed that the diameter of the electrospun fibres was not dramatically changed with varied applied voltage. As the electric field strength increase, the electrostically driven instability increases in magnitude and causes the jet to undergo higher amounts of whipping and plastic stretching that resulted in a decrease of the fibre diameter.

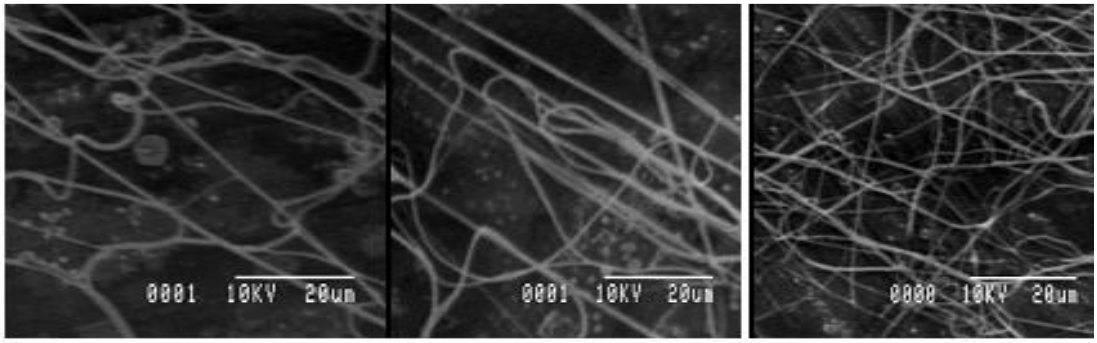

Figure 8.3, PVA/$FeCl_3$ solution of 8 wt.%, collecting distance 11 cm and flow rate 0.25 ml/hr constant and different voltage a) 12 kV, b) 15 kV, c) 18 kV,.

It can be seen in figure 8.3, that exceedingly uniform fibres obtain lower voltage and the average diameter was 800 nm to 900 nm. Higher voltage provides more fibres but not uniformity like variation of the diameter of ultra fine fibre and its asymmetry distribution. The diameter of ultra fibres was reduced by increasing the voltage.

Table 8.2, Fibre diameter in different applied electric voltage (12 kV, 15 kV and 18 kV) at the constant polymer solution (8 wt.%) and collection distance (11 cm).

Applied voltage (kV)	12	15	18
Fibre diameter (nm)	506	453	422
	629	522	500
	633	635	532
	682	650	597
	801	683	620
	830	733	685
	859	820	757
	1089	874	786
	1345	1182	943
	1550	1360	1116
Average fibre diameter (nm)	892	791	696
STDEV (nm)	337	285	212

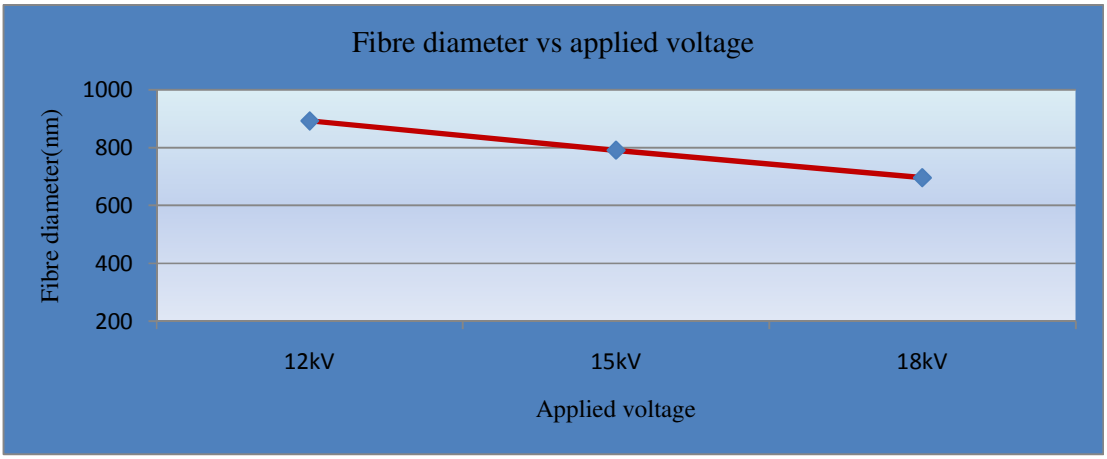

Figure 8.4, The above graph describes the relationship between average fibre diameter and applied electric voltage where polymer solution (8 wt.%), collection distance (11 cm) and flow rate (0.25 ml/hr) constant.

And above the graphs (figure, 8.4) we can say that in general, increasing the applied voltage to a certain level would change the shape of the pendant drop from which the jet

originated so that a stable shape could not be achieved. Finally we can say that voltage affect has also got significant role to control the fibre morphology.

8.4.3 The effect of tip to collector distance on fibre morphology

Tip to target distance actually make no significant effect on the electrospun fibre morphology of fully hydrolyzed PVA and this phenomenon is not yet fully understood and is currently being researched. In order to investigate the effect of the distance between the needle and the collector on the properties of resulting ultra fine fibres, the following spinning condition were fixed. The voltage was fixed at 18 kV and the concentration is 8 wt% and distance at 8 cm, 11 cm, and 14 cm. This result (figure 8.5) indicated that with varying size and thickness can be successfully produced. When the solution jets were elongated and solidified quickly they flowed out of the spinneret tip because of the high conductivity of fully hydrolyzed PVA and $FeCl_3$ used. At low separation distance between the capillary-end and the target, wet fibres were collected, primarily due to the presence of significant amount of residual solvent in the fibres. As the collection distance is increased, the time for the solvent to evaporate increased and as a result, dry solid fibres are collected at the target. With increasing the distance between the capillary-end and the target, the jet underwent a larger amount of electrically driven bending or whipping instability. Consequently, the amount of stretching or elongation of the jet increased resulting in the fibre diameter to decrease. It is the similar result obtained by Jalil et. al [12]. We can see the table 8.3 and figure 8.6 then we easily identify with the effect of the tip to collector distance.

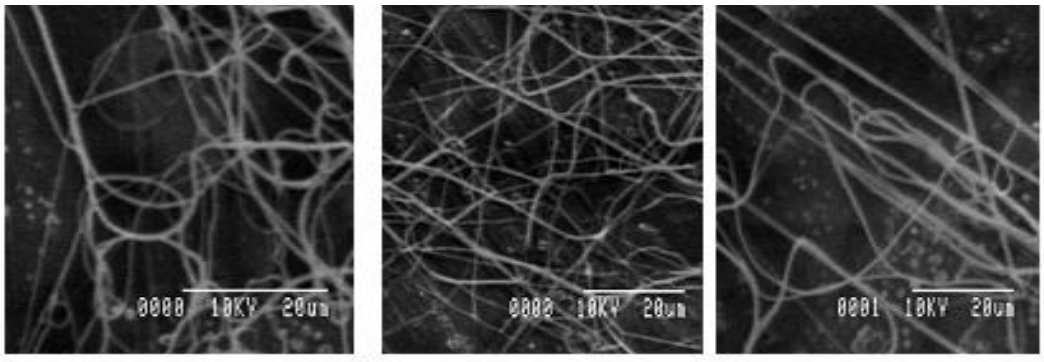

Figure 8.5, PVA/$FeCl_3$ solution of 8 wt.% and collecting distance 8, 11 and 14 cm, voltage 18 kV and flow rate 0.25 ml/hr. a) 8 wt.%, 18 kV, 8 cm and flow rate 0.25 ml/hr, b) 8.wt%, 18 kV, 11cm and flow rate 0.25 ml/hr , c) 8 wt.%, 18 kV, 14 cm and flow rate 0.25 ml/hr.

Table 8.3, Fibre diameter in different collection distance (8 cm, 11 cm, 14 cm) when the polymer solution (8 wt.%) and electric field constant (18 kV).

Collection distance (cm)	8	11	14
Fibre diameter (nm)	481	451	400
	633	551	425
	687	615	456
	755	629	506
	761	670	537
	849	791	537
	943	900	670
	1038	922	779
	1076	952	811
	1230	1105	911
Average fibre diameter (nm)	845	759	603
STDEV (nm)	227	208	178

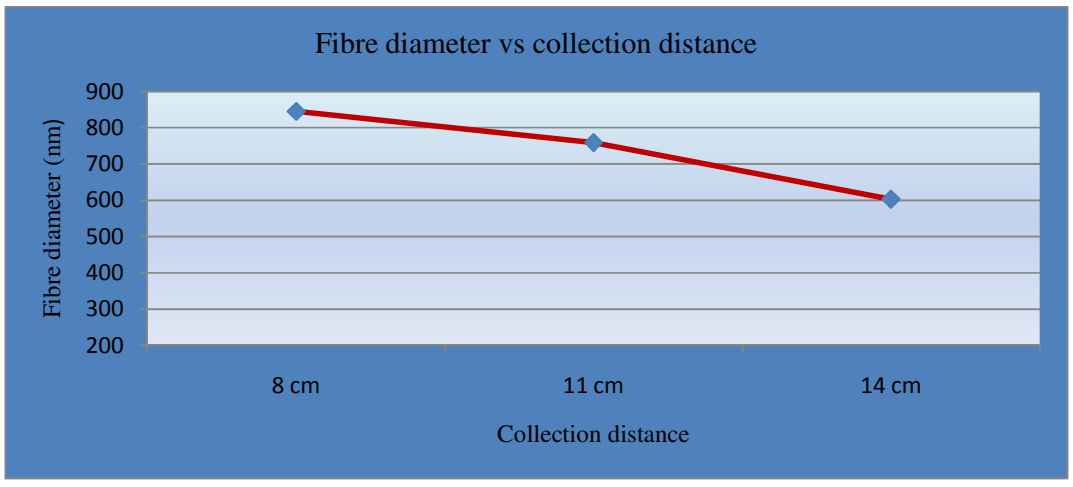

Figure 8.6, Above graph describe the relationships between average fibre diameter and collecting distance, where solution (8 wt.%), applied voltage (18 kV) and flow rate (0.25 ml/hr) constant.

If we see table 8.3 and figure 8.6 then we can see that when the fibre collection distance 8 cm then collected fibre diameter 480 nm to 1230 nm and average fibre diameter 845 nm. Increase the collection distance from 8 cm to 11 cm and 14 cm respectively the fibre diameter also decrease from 452 nm to 1076 nm and 425 nm to 815 nm. The average diameters also lower than shorter distance (8 cm 845 nm), 11 and 14 cm are 759 nm to 603 nm. Finally we understand that the fibres with smaller diameters are obtained by allowing the jet to cover more distance in the electric field. This also allows more time for the evaporation of solvent from the fibres that can result in a decrease in the diameter. In this study, the tip-to-collector distance of 8 cm produced uniform electrospun fibres.

8.4.4 The flow rate effect on fibre morpholgy

The effect of flow rate on the morphological appearance of the fibres obtained can be explained based on the relationships among the three major forces (i.e. the Coulombic, the viscoelastic, and the surface tension forces) influencing the fibre diameters and bead formation. For a given applied potential, the electrostatic force, which carries a charged jet from the spinneret to the target, may increase slightly when compared with the increase in the feed rate as a result of an increase in the PVA/$FeCl_3$ solution flow rate. The excess amount of the material caused by an increase in the PVA/$FeCl_3$ flow rate results in the formation of a droplet at the tip of the spinneret. When the size of the droplet is too big to suspend at the tip of the spinneret, it either drops from the tip or is carried along with a charged jet to the target. This ultimately resulted in an increase in the bead area and the diameters of the obtained fibres with increasing PVA/$FeCl_3$ flow rate, which can be observed qualitatively in figure 8.7.

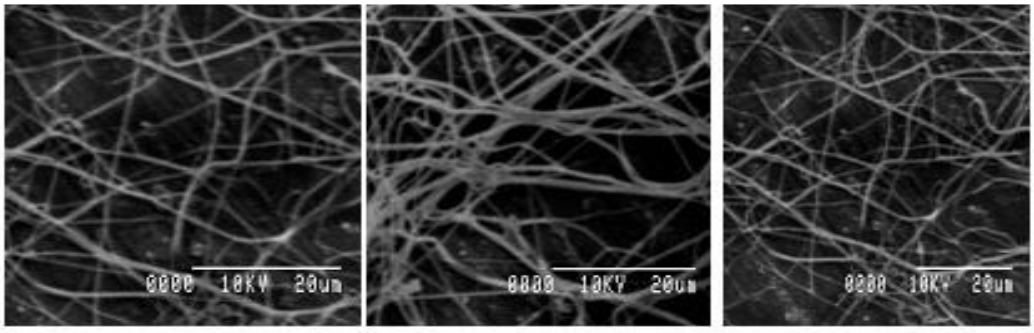

Figure 8.7, PVA/$FeCl_3$ solution of 8 wt.% and collecting distance 11, Voltage 15 kV, flow rate, a) 0.20 ml/hr, b) 0.25 ml/hr and c) 0.30 ml/hr.

Table 8.4, Fibre diameter in different solution flow rate(0.20 ml/hr, 0.25 ml/hr and 0.30 ml/hr) when the polymer solution (8 wt.%) and electric voltage (15 kV) and collection distance (11 cm) constant.

Flow rate (ml/hr)	0.20	0.25	0.30
Fibre diameter (nm)	420	501	506
	469	588	603
	470	595	649
	547	624	659
	548	671	680
	594	727	749
	595	750	759
	601	752	804
	685	789	878
	715	985	1054
Average fibre diameter (nm)	564	698	734
STDEV (nm)	94	135	154

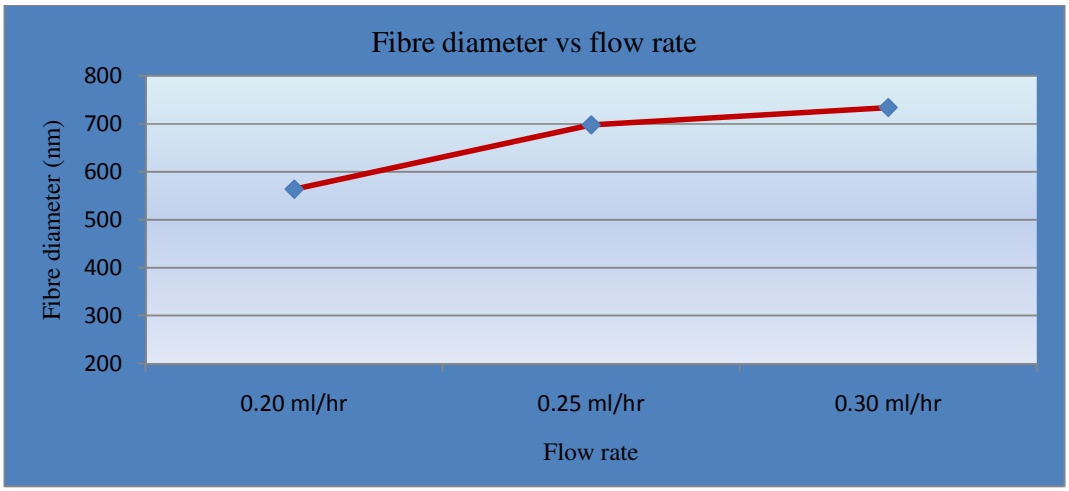

Figure 8.8, Above graph describe the relationships between average fibre diameter and flow rate where polymer solution (8 wt.%), applied voltage (15 kV) and collection distance (11 cm) constant.

Flow rate does not make any change in solution properties such as viscosity, surface tension and conductivity. As flow rate increases, the feeding amount per unit time increases. From the volume conservation, fibre diameter should increase. When the flow rate was 0.20 ml/hr the figure 8.7 (a) and figure 8.8, that time the average fibre diameter observed 564 nm. When the flow rate from 0.20 ml/hr to 0.25 ml/hr and 0.30 ml/hr is increases the fibre diameter (figure 8.8 and table 8.4) is also increased by 698 nm and 734 nm respectively. This is the similar result obtain by Fridrikh et. al [13]. When the flow rate was 0.20 ml/hr there some beads observed (figure 8.7), When the flow rate increased beads also disappeared. Other than bending instability, there can be a fluctuation of charge along the jet during the electrospinning. If the charge density decreases at a specific spot instantaneously, surface tension surpasses the electrostatic repulsive force. As flow rate increases, current between metal needle and collector increases. Then, the possibility to have instability decreases due to the increased current. If flow rate increases, more charge is necessary to initiate the bead. Therefore, it becomes more difficult to form beads as flow rate increases. Higher flow rate produce large diameter fibre and lower flow rate produce smaller diameter fibre.

8.5 TEM observation of the produced PVA/$FeCl_3$ composite fibres

TEM images of the PVA/$FeCl_3$ electrospun fibres are shown in (figure 8.9). After electrospinning Ferro gel particles were distributed in a matrix formed by PVA. This confirms the presence and distribution of Ferro particles in the electrospun nanocomposites.

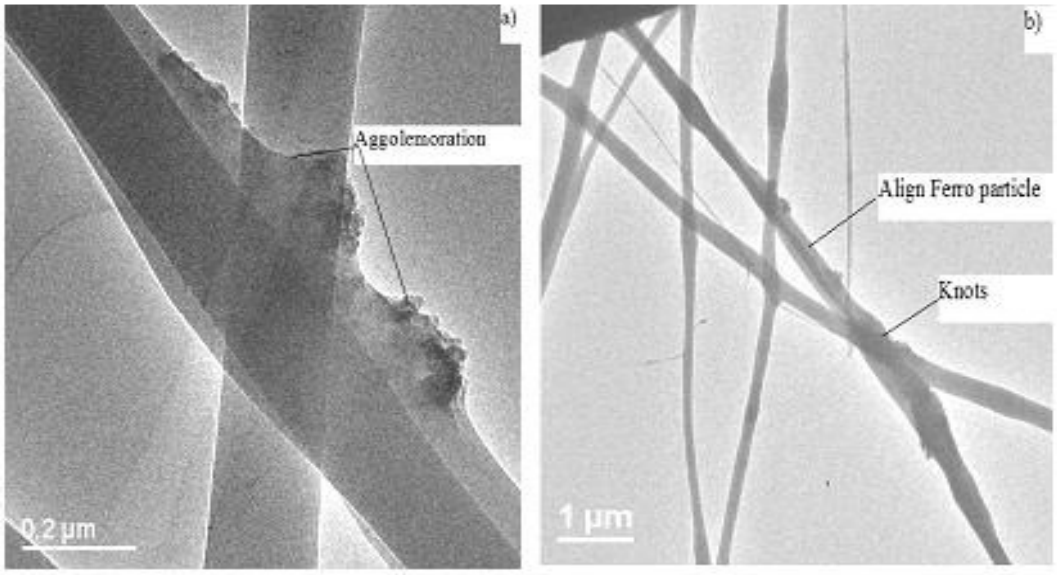

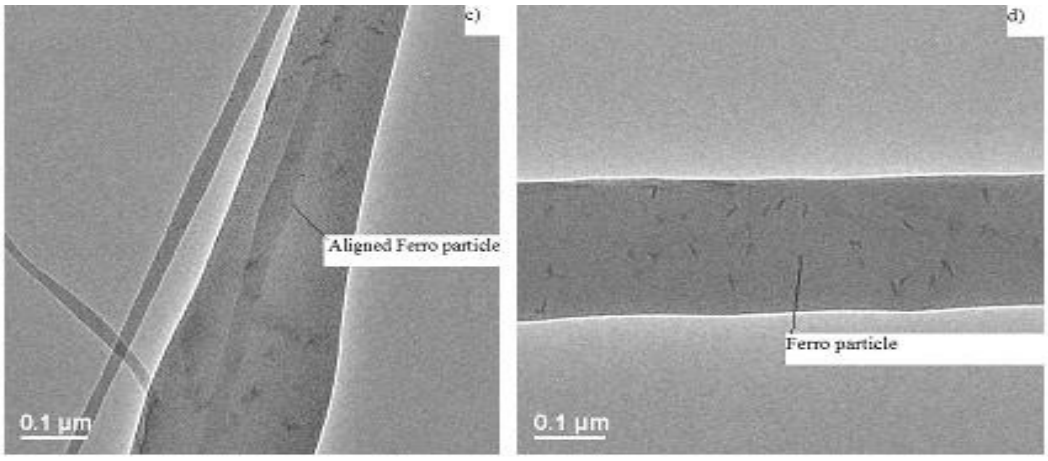

Figure 8.9, Transmission Electron Microscopy images of PVA/$FeCl_3$ composite nanofibres, a) 6 wt.%, b) 8 wt.%, c) 8 wt.% and d) 10 wt.% .

As shown in the figures, localized particle agglomerations were also observed. The agglomerated particles were more often found from the fibres fabricated using lower concentration of Ferro gel solution. Overall fibres were found to possess Ferro particles in and on the fibres. The figure, 8.9 (a, b, c and d) TEM images of PVA/$FeCl_3$ nanofibre containing Ferro particles, showed that Ferro particles appeared as little dark spots inside of the nanofibres.6 wt.% concentration produced aggolomerated fibre, when concentration increase from 6 wt.% to 8 wt.% and 10 wt.% that time the fibre diameter also increase and beads free uniform fibre produced. The figure 8.9, (b) and (c) where we can see the Ferro gel distributed properly and uniform fibre produced. Figure 8.9 (d) also showed the Ferro particle clearly where uniform fibre produced. The solution concentration 8 wt.% PVA/$FeCl_3$ produced uniform nanofibres.

8.6 Magnetic nano fibres

In the above certain condition we got a blended fibre where the fibre contained magnetic power. The electrospun blended nanofibres have unique magnetic properties, with much enhanced coercivities relative to bulk materials. The outstanding features of this approach to get one-dimensional magnetic nanostructure are its simplicity, effectiveness, and ease of assembly. Therefore, electrospun magnetic nanofibres can potentially be used in fabrication of high-density magnetic recording, magnetic sensors, flexible magnets, and spintronic devices. It can be seen figure, 8.10

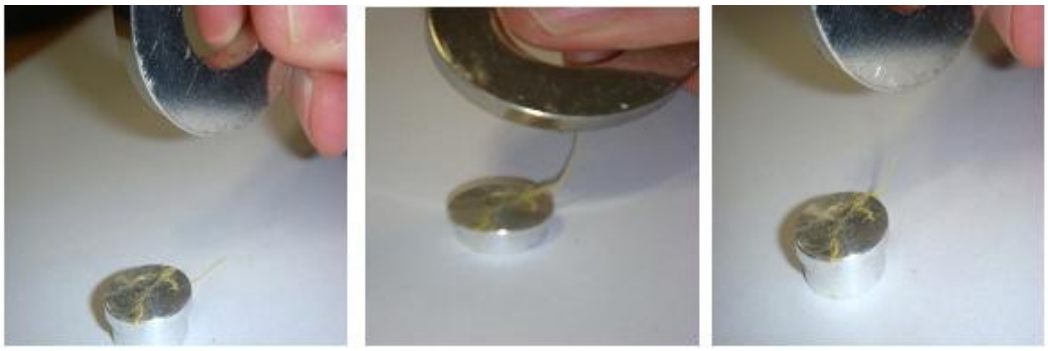

a) b) c)

Figure 8.10, PVA/$FeCl_3$ Blend nano fibres with magnet, it shows the magnetic power of the blended fibre. a) Blended fibre with magnet, b & c) Magnet attracts the fibre.

8.7 Conclusion:

Electrospinning was used to fabricate nano fibres of PVA/$FeCl_3$ blends. The effect of processing parameters such as, the solution concentration, the voltage, the tip-target distance and flow rate on fibre and its morphology has been examined and magnetic nanofibre produced. The electrospinning of PVA/$FeCl_3$ solution was processed and nanofibres with diameter ranging from 600 nm to 1100 nm were obtained depending on the electrospinning conditions. The effects of the concentration, spinning voltage and collection distance between the tips to target, flow rate on the morphological appearance and average diameter of the PVA/$FeCl_3$ fibre was also established investigated. It was concluded that the solution concentration significantly affected the morphology and diameter of the PVA/$FeCl_3$ nano fibres. Lower concentration tended to facilitate the formation of fibres with beads. As the solution concentration, the morphology was changed from beaded fibres to smooth and uniform nano fibre and with increasing nanofibre diameter. The spinning voltage also had an important influence on nanofibre diameter, while the collection distance had a lesser effect on the nanofibre diameter. Flow rate also influence to produce uniform nanofibre. Higher flow rate provides large diameter nanofibre and lower flow rate proves small diameter nanofibre. Nonwoven mats of electrospun fibre extremely flexible and have high surface area to volume ratio due to its fine nanofibre diameter. Success in the development of composite nanofibres by the co-electrospinning has created a new pathway to connect nanoscale effect to macro structure performance. Finer fibres with high uniformity and the application of lower voltage produced magnetic nanofibres that can potentially be used in fabrication

of high-density magnetic recording, magnetic sensors, flexible magnets, and spintronic devices.

8.8 References

[8.1] J. Sheng, Y. Han, L. Wu, X. Yuan, C. Zhang, *Study on morphology of electrospun poly (vinyl alcohol) mats, European polymer journal*, **41**, 423-432 (2005)

[8.2] A. Koski, K. Yim and S. Shivkumar, *Effect of molecular weight on fibrous PVA produced by electrospinning*, Materials letters **58**:493-497 (2004).

[8.3] L.Yao, T. W. Haas, A. G. Elie, G. L. Bowlin, D. G. Simpson and G. E. Wnek, Chem.Mater.**15**, 1860 (2003)

[8.4] A. Koski, K. Yim and S. Shivkumar, *Effect of Molecular Weight on Fibrous PVA Produced by Electrospinning*, Mater.Lett. **58**, 493 (2004)

[8.5] C. J. Zhang,Y. Sheng,Y. Han, L. Wu, X. Yuan, *Study on morphology of electrospun poly (vinyl alcohol) mats*, European polymer journal **41**: 423-432(2005)

[8.6] A. Koski, K. Yim and S. Shivkumar, *Effect of molecular weight on fibrous PVA produced by electrospinning*, Materials letters **58**:493-497 (2004)

[8.7] W. K . Sona. J. H.Youkb, T. S. Leec and W. H. Park, Matter. Letts. **59,** 1571 (2005)

[8.8] H. Fong, I. Chun, D. H. Reneker, *Nanometre diameter fibres of polymer produced by electrospinning*, Nanotechnology **7**, pp. 216–223 (1996)

[8.9] Z. M. Huang, Y. Z. Zhang , S. Ramakrishna and C. T. Lim, *Electrospinning and mechanical characterization of gelatin nanofibres*, Polymer Volume **45**, Issue 15, , Pages 5361-5368 (2004)

[8.10] M. Bognitzki, W. Czado, T. Frees, A. Schsper, M. Hellwig, M. Steinhart, A. Greiner and J. H. Wendorff, *Nanostructured fibres via electrospinning,* Advance materials, **13** (1),70-72 (2001)

[8.11] X. Zong, K. Kim, D. Fang, S. Ran, B. S. Hsiao and B. Chu, *Structure and process relationship of electrospun bioabsorbable nanofibre membranes*, Polymer, Vol. **43**, Issue 16 (2002)

[8.12] R. Jalili, S. A. Hosseini, M. Morshed, *The effects of operating parameters on the morphology of electrospun polyacrilonitrile nanofibres,* Iran Polym J; **14**:1074–81 (2005)

[8.13] S.V. Fridrikh, J.H. Yu, M.P. Brenner, G.C. Rutledge, *Controlling the fibre diameter during electrospinning*, Physical Review Letters **90 ,**144502 (2003)

Chapter 9: Effects of electrospinning process parameters on nanofibres obtained from PEO/Wood pulp blends

9.1 Introduction

Cellulose is a naturally occurring polymer of particular interest due to its abundant availability and biodegradability. These properties make cellulose fibres useful in a wide range of areas, such as filtration, biomedical applications, and protective clothing, paper industry [1] wood that has been ground to a pulp; used in making cellulose products (as rayon or paper). Cellulose, the world's most abundant biomass as well as a biodegradable and renewable polymer, is a major component in wood and other plant substances [2].

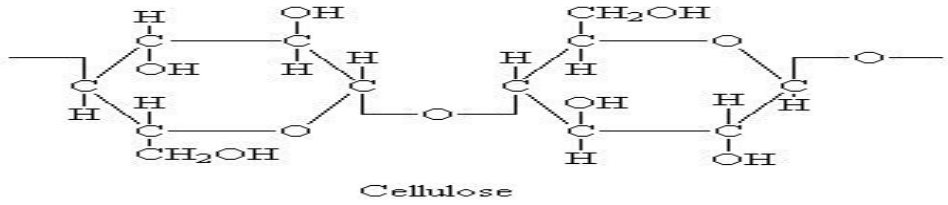

Molecular structure of cellulose [2].

Natural cellulose fibres are hydrophilic. This renders them highly susceptible to loss of mechanical properties upon moisture absorption, which is a critical shortcoming for paper and board applications that require a high degree of dimensional stability and low hygroexpansivity [3]. In addition, the highly polar nature of cellulose makes it poorly compatible with common non-polar polymers used in the production of textiles and composites. Furthermore, commercially-produced pulp fibres are seldom straight and continuous, and contain many deformations along their length which manifest themselves in the form of dislocations, crimps and kinks in the fibre cell wall. Pulp is essentially cellulose in fibrous form. Pulping processes such as the Kraft process remove most of the lignin and hemicelluloses from raw wood, leaving behind cellulose as the main component in the pulp. Wood Pulp has been widely used as the raw material for papermaking. Depending on the process that transforms natural woods into fibrous mass. Regenerated cellulose fibres have been used for various industrial applications, including textiles and precursors for carbon fibres. Lyocell and rayon are two examples of commercially available regenerated cellulose fibres [4]. The electrospun cellulose

fibre from Kraft pulp differentiates itself from conventional regenerated cellulose fibres in that the electrospun fibre diameter can be significantly reduced to below a micrometer. The interest to regenerate cellulose on the nano-scale can be justified by the strength evidence observed in cellulose nanofibrils [3-4]. Electrospinning is capable of producing cellulose fibres smaller than 1000 nm in diameter with continuous length. While cellulose nanofibrils have a high tensile strength of 10 GPa, it is challenging to produce a functioning macrostructure from nanofibrils because of their discrete length (500 nm) [5]. Doshi and Reneker [6] explained that compared to micro-fibres, there is an order of magnitude increase in specific surface area in nanofibres, allowing an efficient load transfer in composite applications. It has been shown that the macro- and micro-structure of polymeric fibres can be re-constructed to produce defect-free fibres using the electrospinning process, by manipulating the process parameters and the polymer solution chemistry. This study was to investigate generation of cellulose based bicomponent fibres by electrospinning of binary mix of PEO and wood pulp. The flexible chain structure and ease of crystallization of PEO are expected to facilitate its separation from the more rigid and bulky wood pulp (cellulose) molecules. The aim of this chapter is to assess the feasibility of producing regenerated nanofibres directly from wood pulp using the electrospinning process and analyse their processing parameter effect during electrospinning process and also process optimization. This study will also do the thermal analysis of PEO, wood pulp and produced blend fibres.

9.2 Experimental

9.2.1 Materials

Polyethylene Oxide (PEO) with an average molecular weight of 300,000 purchased from Fisher scientific, UK was chosen to prepare for the solutions. PEO fibres were electrospun using 10 wt.% to 14 wt.% (w/w) concentrations of PEO in de-ionized water. Wood pulp (Kraft) was purchased from Domtar group, Canada. All solutions were stored at room temperature and all electro-spinning experiments were done at room temperature and atmospheric air.

9.2.2 Preparation of PEO/wood pulp Solutions

The polymer concentration (%) was determined by the percentage of Wood pulp (g) or total mass (g) of wood pulp and PEO in the solvent (ml). PEO solutions were prepared by dissolving the powdered materials in HPLC grade water/Ethanol at room

temperature under a magnetic stir for 24 hour. Wood pulp also dissolved in HPLC grade water/Ethanol under stirring for 24 hour. After cooling to room temperature, a given amount of the PEO solution was mixed with the Wood pulp solution in a certain PEO/Wood pulp mass ratio and then, the mixture was continuously stirred further 12 hour, where the PEO and wood pulp ratio (95/5).

9.2.3 Characterization

9.2.3.1 Morphology

A Scanning Electron Microscope (Hitachi S-530, UK) was used to characterize the morphology of the electrospun nanofibres. The samples were sputter coated with carbon and examined at an accelerating voltage of 10 kV. To measure the diameters of the electrospun PEO/wood pulp nano fibres, an image analyzer, Image J, US used.

9.2.3.2. TEM

The internal structure of materials can be determined or viewed through Transmission Electron Microscopy (TEM). TEM images of the PEO/wood pulp samples were taken on a JEOL.JEM 2010, UK. At an acceleration voltage of 200 kV under low vacuum.

9.2.3.3 Differential Scanning Calorimetry (DSC)

The Differential Scanning Calorimetry (DSC) analyses were carried out using a Metler DSC 30 (USA) differential scanning calorimeter machines. Test samples were heated from 40º to 300º C at a heating rate of 10º C/min. The nitrogen gas flow rate was set as 40 ml/min.

9.2.3.4 X-ray diffraction

X'Pert-MPD Philips diffractometer was used for the analysis. The samples were first ground into powder form (using mortar and pestle) and then put in water suspension to be evenly distributed on a zero background plate. After the samples were air-dried, they were analyzed using XRD. The scanning range was 5˚ to 90˚ at a scanning rate of 0.02˚/sec

9.2.3.5 FTIR

The molecular interactions of the blend electrospun fibres were assayed on a Fourier-transform infrared (FT-IR) spectrometer (Perkin Elmer, UK). The test sample was dissolved laid on a KBr disk.

9.3 Result and discussion

The concentration of PEO/ wood pulp solution for fibre formation was fixed with 10 to 14 % (w/v). Positive voltage applied to polymer solution controlled between 12 to 18 kV with stepwise increase. The flow rates were 0.20 ml/hr to 0.30 ml/hr and tip to collector distance is varies at 8 cm to 14 cm. All electrospinning were carried out at the room temperature. The collector was a grounded circular copper plate covered with a piece of aluminium foil.

9.3.1 Solution concentration effects on fibre morphology

The polymer concentration determines the spinnability of a solution, namely whether a fibre forms or not [7]. Liu et. al, reported that a different specific range of viscosity was appropriate for the formation of uniform nanofibres composed of cellulose [8]. The polymer concentration influences both the viscosity and the surface tension of the solution, both of which are very important parameters in the electrospinning process. If the solution is too dilute then the polymer fibre will break up into droplets before reaching the collector due to the effects of surface tension. However, if the solution is too concentrated then fibres cannot be formed due to the high viscosity, which makes it difficult to control the solution flow rate through the capillary. Thus, an optimum range of polymer concentrations exists in which fibres can be electrospun when all other parameters are held constant. Increasing overall polymer concentrations in solution generally improved fibre formation.

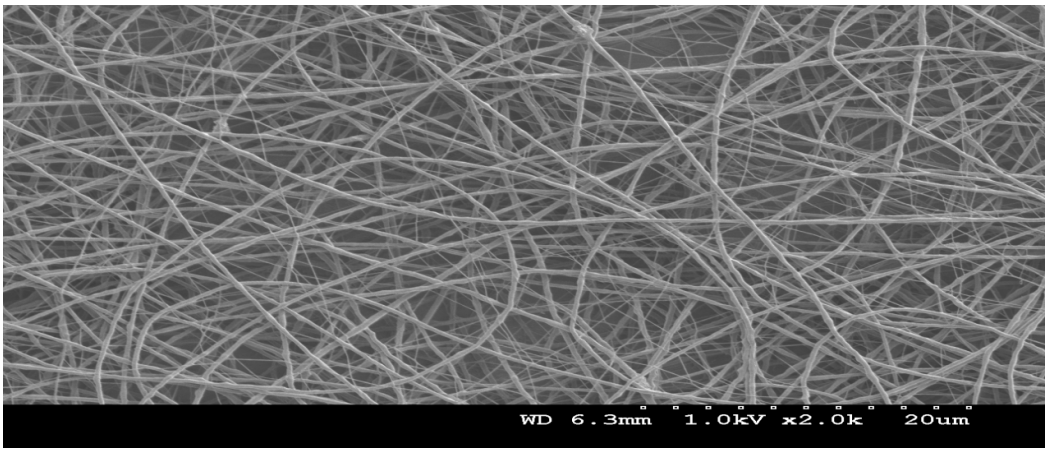

a)

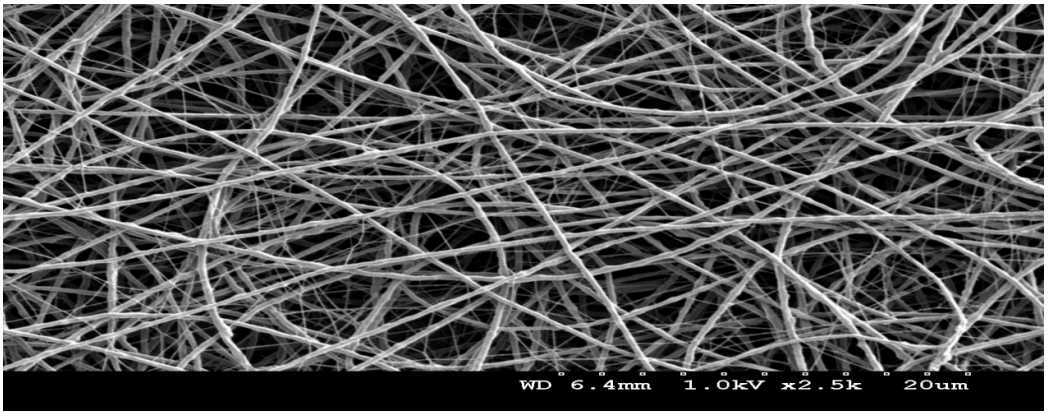

b)

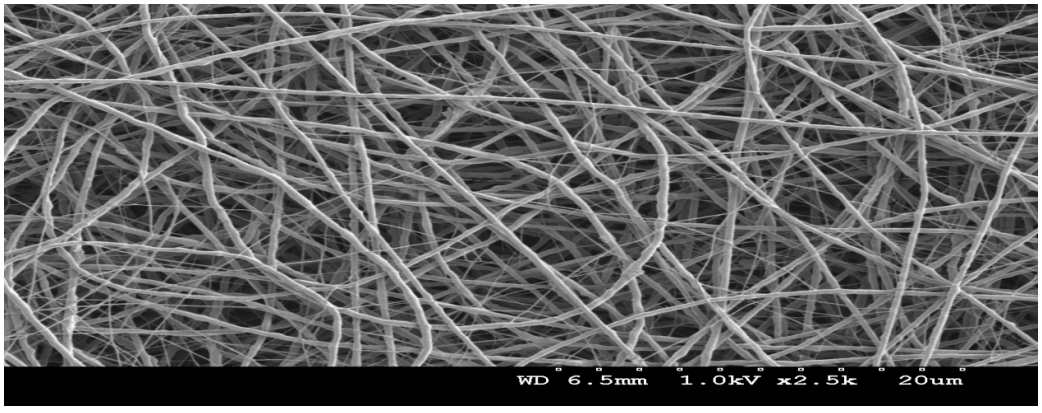

c)

Figure 9.1, SEM figure for PEO/Wood pulp where the polymer solution was a) 10 wt.%, b) 12 wt.% and c) 14 wt.% and the applied voltage and collection distance were 15 kV and 11 cm and flow rate (0.25 ml/hr) constant respectively.

Table 9.1, Fibre diameter in different polymer concentration (10 wt.%, 12 wt.% and 14 wt.%) at constant electric fields (15 kV) and a constant spinning distance of 11 cm.

Solution concentration (wt.%)	10	12	14
Fibre diameter (nm)	269	268	390
	272	333	399
	279	338	422
	284	337	474
	329	411	490
	335	420	497
	354	437	525
	374	453	566
	384	472	578
	421	485	597
Average fibre diameter (nm)	330	395	494
STDEV (nm)	53	72	74

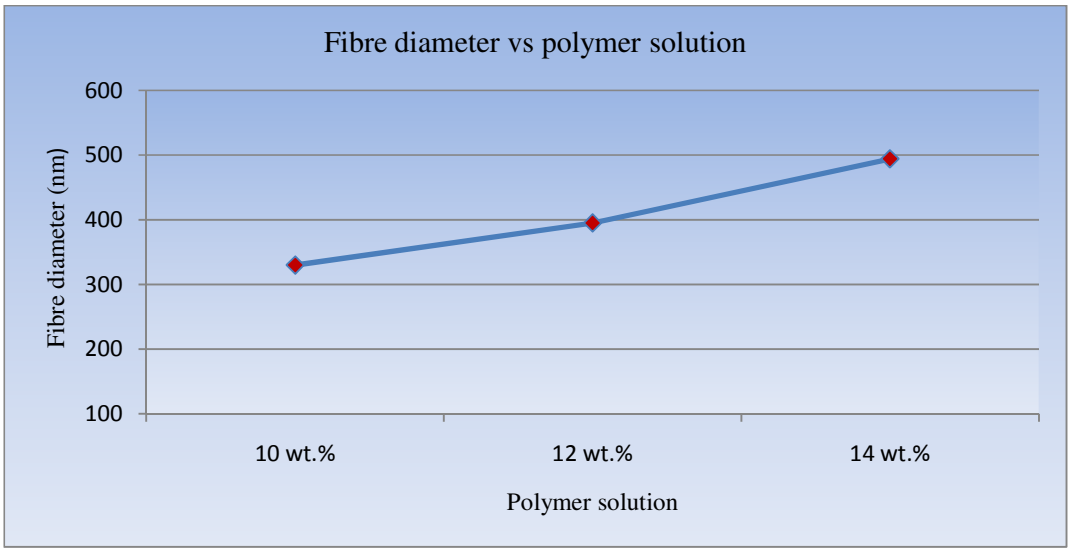

Figure 9.2, The relationships between the average fibre diameters vs. polymer solution where the applied voltage (15 kV), collection distance (11 cm), flow rate (0.25 ml/hr).

A lower concentration solution forms droplets due to the influence of surface tension, while higher concentrations inhibit fibre formation due to higher viscosity. SEM of electrospun PEO/wood pulp fibres prepared from 10 wt.% to 14 wt.% various ratios of PEO/wood pulp are shown in figure, 9.1. The fibres diameters were increased continuously when the polymer solution also increase as shown in figure 9.1(c). The continuous fibres can be seen from figure 9.1(b and c) and also the fibres were found bonded at their contact sites. This caused by incomplete evaporation of solvents (distilled water/Ethanol). At 10 wt.% electrospun polymer solution produced some small amount of bead fibre [figure 9.1(a)]. At low viscosities (*i.e.* low concentrations), the beads are typically spherical as shown in figure 9.1(a), while spindle-like beads are observed at high viscosities (or concentrations), as shown in figure. 9.1 (c). When the polymer solution was more than 12 wt.%, like 14 wt.% the formation of such droplets occurred that due to the capillary breakup of the polymer jet by surface tension and also improper viscosity of this ratio solution to be spun. Unless completely breakup of the polymer jet in order to happen the capillary instability, the beaded fibres occur. As a result of, the polymer jets between the droplets formed electrospun fibres and together with the contraction of the radius of the jets that was driven by surface tension, this lead to the remaining solution to form beads. An increase in polymer solution concentration leads to an increase in solution viscosity, resulting in lower solution spin ability and a smaller extent of fibre elongation during the electrospinning process, and thus larger fibre diameters shown in figure 9.1(c). When the polymer solutions were 10 wt.% that time produced average electrospun fibre diameter was 330 nm. Increase the polymer solution from 12 wt.% to 14 wt.%, the produced average electrospun nano fibre diameter also increases from 395 nm to 494 nm, as seen table 9.1 and figure 9.2. In addition, with increasing concentration, the initial amount of solvent in a small segment of a charged jet decreased, rendering the charged jet able to "dry" much more easily, which cumbered the elongation and thinning of fibres . It is also concluded that lower solution (10 wt.%), finer fibres (average diameter 330 nm) with beads occur and at higher solution (12 wt.%) smoother and thicker fibres (average diameter 494 nm) with a lower proportion of beads are formed. Bead morphology has also been associated with capillary instability. The hypothesis is that at lower concentrations, the chains are insufficiently entangled to provide the high extensional viscosity and strain-hardening behaviour required to resist capillary breakup of the thread line; leading to bead or bead-on-string morphology. At higher solution concentrations, the higher viscosity stabilizes

the fibre, and reduces bead formation. All the above results showed that higher polymer concentrations led to more uniform, but larger fibres.

9.3.2 Applied voltage effect on fibre morphology

A series of experiments was performed with 10 wt.% solution in PEO/wood pulp with water/Ethanol solvent under applied voltage was varied from 12 to 18 kV and the tip-to target distance was fixed at 11 cm. The results are shown in figure, 9.3.

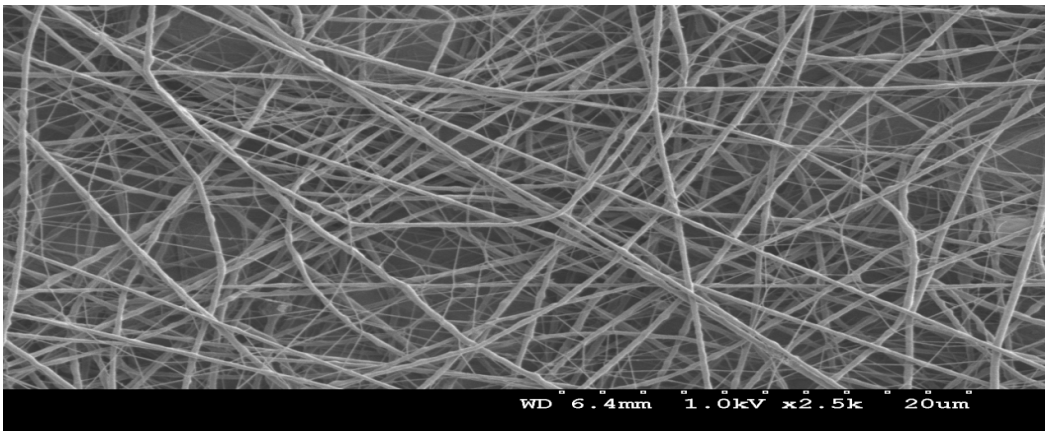

(a)

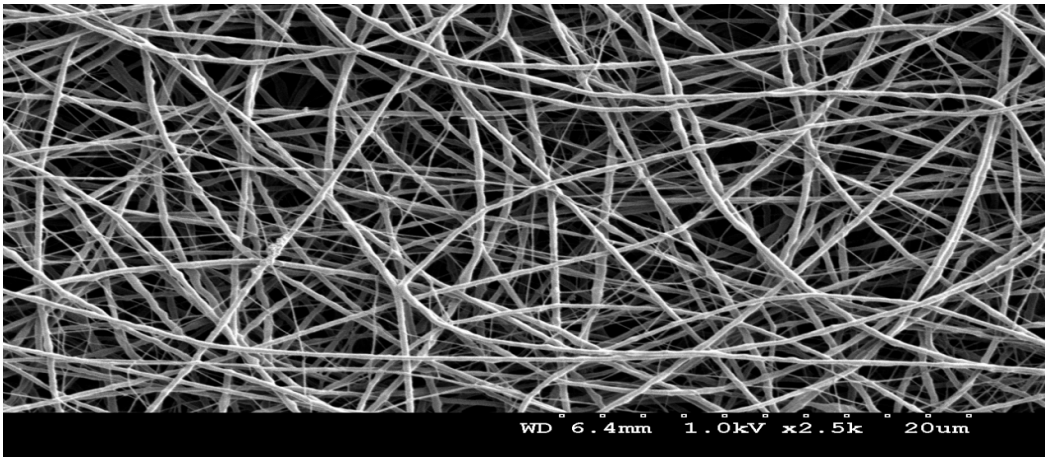

(b)

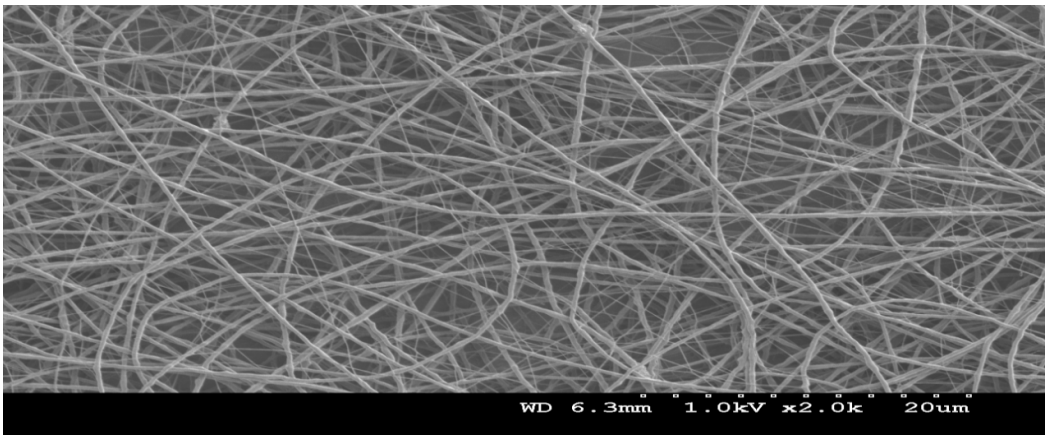

(c)

Figure 9.3 Effect of electric voltage on PEO/wood pulp fibre morphology (Constant solution concentration=10 wt.%, flow rate = 0.25 ml/hr and collection distance 11 cm). Different voltage: (a) 12 kV (b) 15 kV (c) 18 kV.

Table 9.2, Fibre diameter in different applied electric voltage (12 kV, 15 kV and 18 kV) at the constant polymer solution (10 wt.%) and collection distance (11 cm).

Applied voltage (15 kV)	12	15	18
Fibre diameter (nm)	268	216	210
	335	262	245
	339	272	255
	340	306	277
	370	315	292
	372	330	313
	373	332	334
	411	371	339
	521	375	347
	565	382	352
Average fibre diameter (nm)	389	316	296
STDEV (nm)	90	54	49

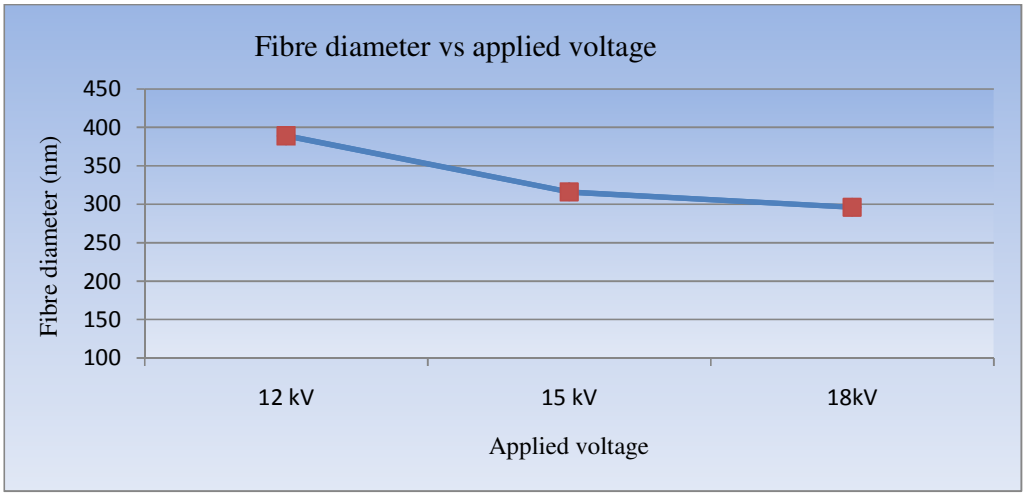

Figure 9.4, The relationships between the average fibre diameter vs. applied voltage where the polymer solution (10 wt.%,) collection distance (11 cm) and flow rate (0.25 ml/hr) constant.

There was a slight decrease in fibre diameter upon increasing the applied voltage. Also, as the voltage increased, the shape of fibre became more regular electrospun mat. Increasing the applied voltage will increase electrostatic repulsion force for fluid jet, which favours thinner fibre formation. But there was not observed a remarkable difference in the morphology. Figure 9.4 shows the effect of the applied voltage on 10 wt.% PEO/wood pulp solution, where constant collector distances 11cm. With an increasing applied voltage, the diameter of electrospun fibres gradually decreased, and the shape of fibre was become regular. The structure of electrospun fibre became the full developed fibre from bead free at 18 kV while mixed shapes observed in the range of 12 to 15 kV of applied voltage. As the applied voltage increased to 12, 15, and 18 kV, the average diameter of fibres decreased from 389, 316 and 296 nm respectively shown in table 9.2 and figure 9.4. The decrease of fibre diameter when applied voltage was increased from 12 to 18 kV could be attributed to the increase of elongation force imposed on the solution jet by increasing voltage. As voltage was increased from 12 to 18 kV, the increase of elongation force could reduce the fibre diameter. However, the higher voltage also accelerated the rate of ejected solution jet to fly from spinneret tip to collection plate and shortened the time for the ejected solution jet to fly from spinneret to collection plate. The short fly time of ejected solution jet to reach the collection plate decreased solvent evaporation from ejected solution jet and also deceased the time for the ejected solution jet being strained under an electric field. The compromise of increasing elongation force and reducing time for solvent evaporation and the time for

solution jet being strained under electric field caused no significant change of fibre diameter as applied voltage was increased from 12 to 18 kV. This result showed that the voltage got a little effect on the electrospinnability of PEO/wood pulp solution.

9.3.3 Tip to collection process effect on fibre morphology

The structure and morphology of electrospun fibres is easily affected by the nozzle to collector distance because of their dependence on the deposition time, evaporation rate, and whipping or instability interval. The distance between the tip of the needle and the grounded plate were chosen 8 to 14 cm to examine the effect on the morphology of electrospun nanofibres. The polymer concentration, applied voltage and feed rate were kept constant at 10 wt%, 15 kV and 0.25 ml/hr. The average fibre diameter 249 nm was observed smaller at 14 cm of collector distance (figure 9.6 and table 9.3). At distance 11 cm the average fibre diameter observed 266 nm and at 8 cm, the solvent was not completely evaporated when fibres were collected on the grounded plate and the average fibre diameter observed 288 nm (figure 9.6 and table 9.3). If the tip-to-collector distance is too large, the electrospinning is not facilitated well due to low electric field formed between the tip and collector.

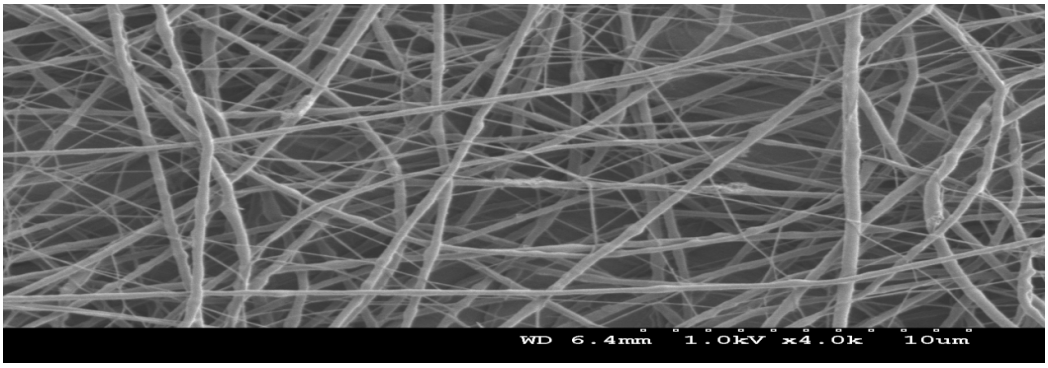

(a)

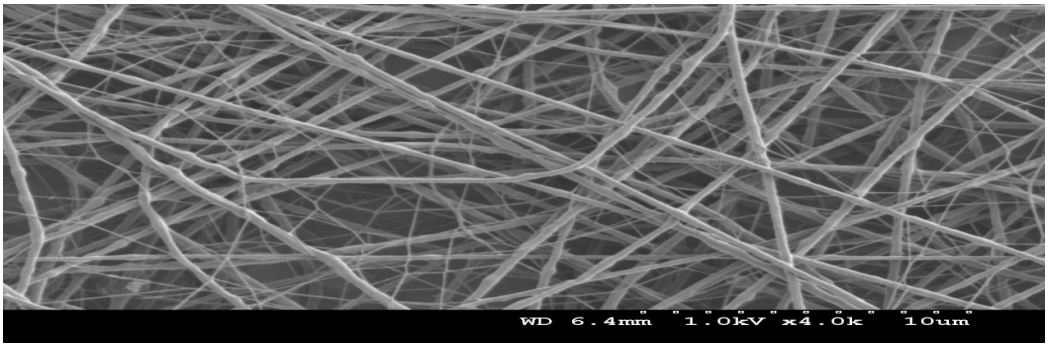

(b)

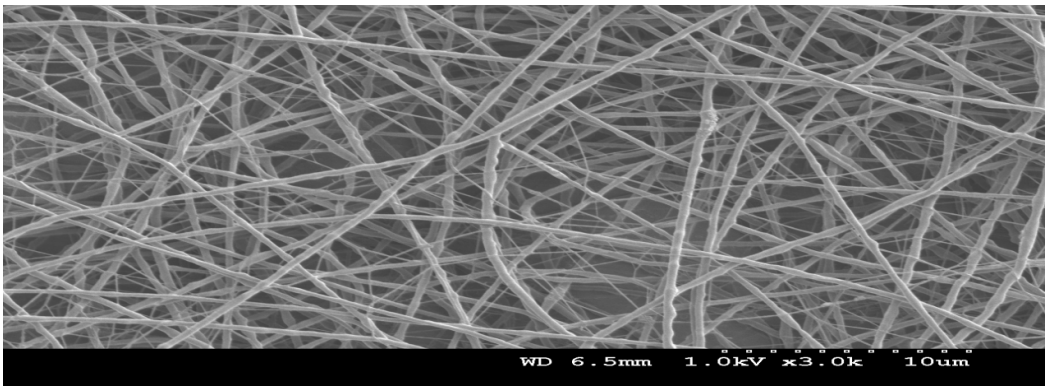

(c)

Figure 9.5, SEM images of PEO/wood pulp nanofibres as a function of polymer solution 10 wt.%, spinning distance at (a) 8 cm and (b) 11 cm and (c) 14 cm (solution 10 wt.%, voltage = 15 kV, feed rate = 0.25 ml/hr).

Table 9.3, Fibre diameter in different collection distance (8 cm, 11 cm, 14 cm) when the polymer solution (10 wt.%) and electric field constant (15 kV).

Collection distance (cm)	8	11	14
Fibre diameter (nm)	225	236	218
	239	239	223
	255	246	225
	259	256	235
	282	257	247
	290	266	250
	297	267	255
	302	277	276
	310	292	280
	339	321	285
Average fibre diameter (nm)	280	266	249
STDEV (nm)	35	26	25

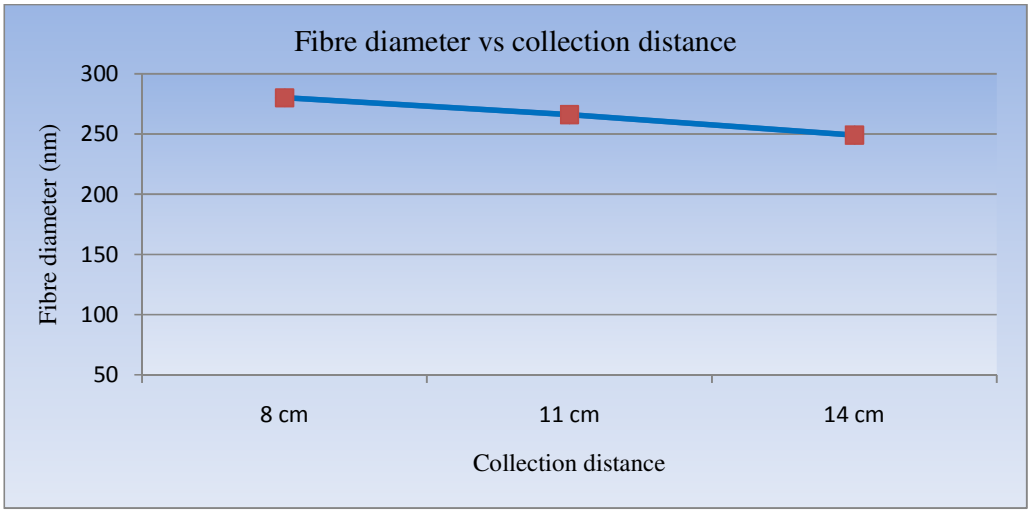

Figure 9.6, The relationships between the fibre diameter vs. collection distance where the polymer solution, applied voltage and flow rate constant.

There are optimum distance between the tip and collector which favours the evaporation of solvent from the nanofibres. The wider gap allowed more time for the fluid jet to stretch fully and solvent to evaporate completely. After increase the collection distance more the collected fibre are dried and stretched fully and the fibre diameter is reduced. Shorter distance (8 cm) give fibre with beads shown at figure, 9.5(a) and longer distance (14 cm) gives uniform fibre shown at figure, 9.5 (b and c). That's why, small distances must be avoided since there is no sufficient time for solvent evaporation and the nanofibre structures will remain wet.

9.3.4 Flow rate effect on fibre morphology

Feed rate was not found to have a significant effect on maximum fibre length, diameter or uniformity over all parameter variations. Once the feed rate is sufficient for forming fibres, higher feed rate only provides more polymer solution than needed, since it was observed that the amount of excess polymer solution formed at the needle tip increased with increasing feed rate. The morphological structure can be changed by changing the solution flow rate as shown in figure, 9.7. When use the flow rate of 0.25 ml/hr, uniform fibre structure was observed. But increasing flow rates, the average fibre diameter was increased and was higher than those fibres spun at lower flow rate, as seen in table 9.4 and figure 9.8. At the flow rate of 0.30 ml/hr, a considerable amount of thick fibres with diameters above 1 µm were found. When the flow rate exceeded a critical value, the delivery rate of the solution jet to the capillary tip exceeded the rate at which the solution was removed from the tip by the electric forces. This shift in the mass-balance

resulted in sustained but unstable jet and fibres with broad distribution in the fibre diameter were formed. As shown in figure 9.7, when the flow rate solution increased from 0.20 to 0.25 ml/hr, the morphology and the diameter distribution of the electrospun PEO/wood pulp fibres did not show obvious changes. The diameters of the electrospun PEO/wood pulp fibres were mostly in the range of 200 to 300 nm. The average diameters of the electrospun fibres measured from SEM micrographs were 278 nm (figure 9.7-a), 295 nm (figure 9.7-b), and 595 nm (figure 9.7- c) when the flow rates were 0.20 ml/hr, 0.25 ml/hr and 0.30 ml/hr, respectively. It shows that the flow rate did not remarkably influence the morphology of the electrospun PEO/wood pulp fibres either.

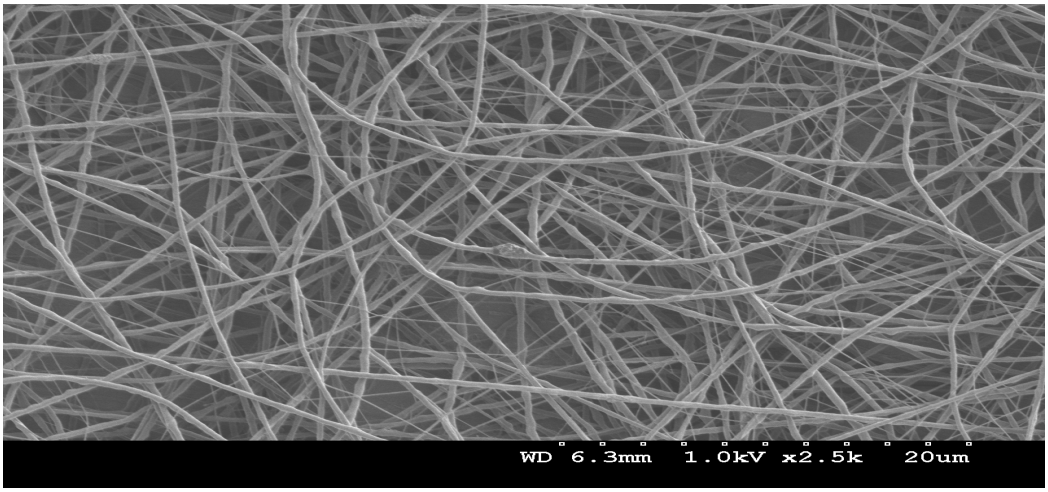

a)

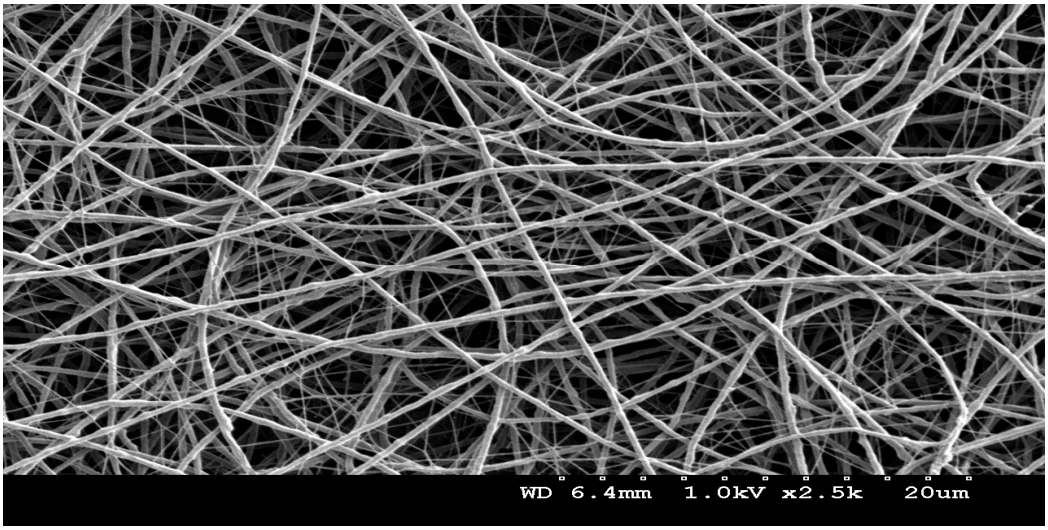

(b)

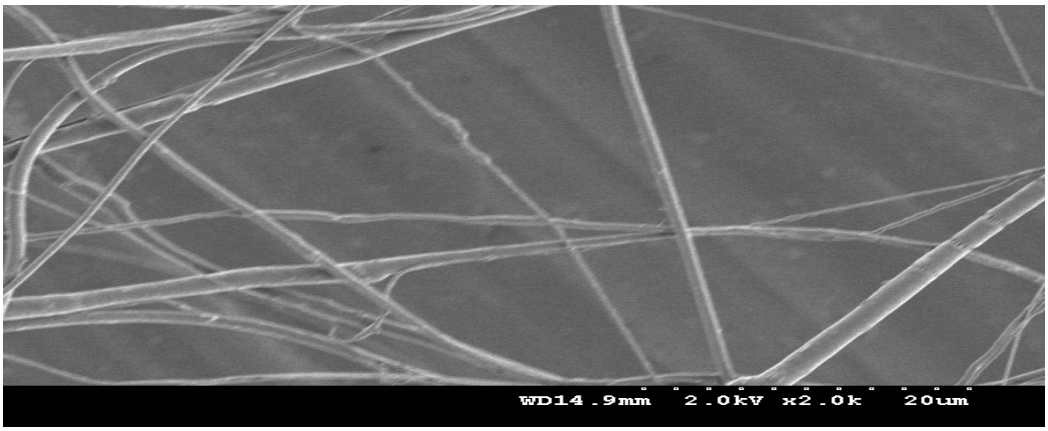

(c)

Figure: 9.7, Effect of flow rate of 10 wt.% PEO/wood pulp solution on fibre morphology (voltage = 15 kV, collection distance 11 cm). Flow rate: (a) 0.20 ml/hr; (b) 0.25 ml/hr; (c) 0.30 ml/hr.

Table 9.4, Fibre diameter in different solution flow rate (0.20 ml/hr, 0.25 ml/hr and 0.30 ml/hr) when the polymer solution (10 wt.%) and electric voltage (15 kV) and collection distance (11 cm) constant.

Collection distance (cm)	0.20	0.25	0.30
Fibre diameter (nm)	222	230	310
	234	236	353
	240	246	404
	248	259	438
	283	284	438
	285	294	500
	290	305	747
	314	334	790
	333	354	882
	335	410	1085
Average fibre diameter (nm)	278	295	595
STDEV (nm)	41	58	262

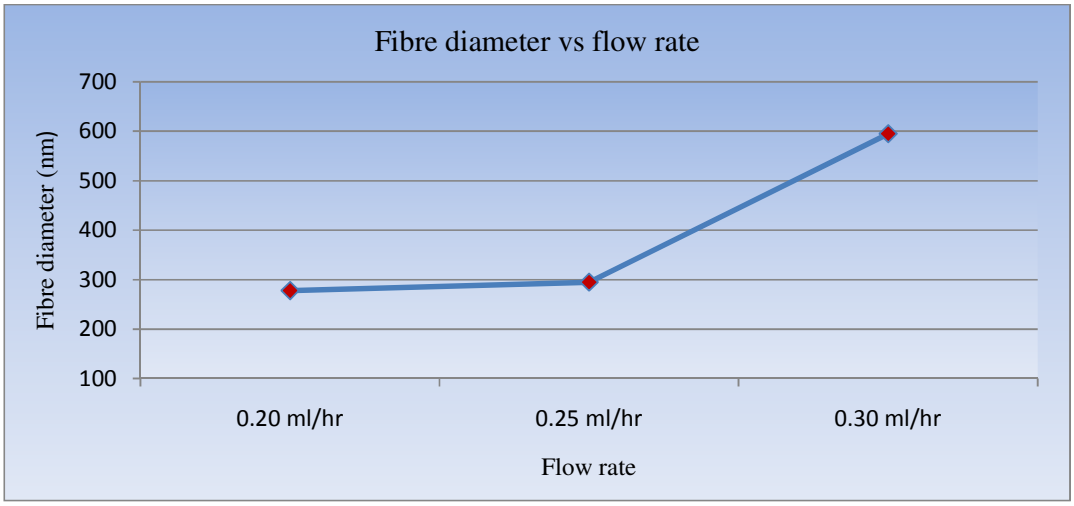

Figure 9.8, The relationships between the fibre diameter vs. flow rate where the polymer solution, applied voltage and collection distance were constant.

Below 0.20 ml/hr no fibres are produced. Flow rates higher than 0.20 ml/hr caused the solution to begin to drip from the needle tip, which caused a globular sample deposition with larger diameter fibres. Above 0.30 ml/hr PEO/wood pulp fibrous deposition does not occur.

9.3.5 TEM analyses of PEO/Wood pulp blend fibre

SEM images of PEO/wood pulp fibres can be seen at 10 wt.% and 12 wt.% producing uniform nanofibres. When increase the solution 14 wt.% that time fibre beads produce. SEM figure 9.9 shows the fibre morphology but we can not see the wood powder inside the nanofibres. TEM shows the wood powder inside the nanofibres is shown in figure 9.10,

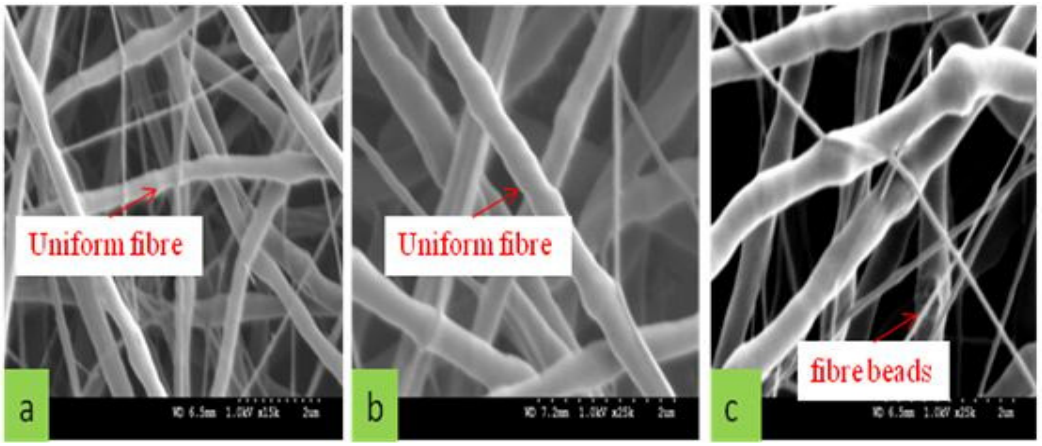

Figure 9.9, SEM images of PEO/Wood pulp blend fibre where the solution concentration was a) 10 wt.%, b) 12 wt.% and c) 14 wt.%.

TEM images of PEO/Wood pulp nanofibres are shown in figure 9.10, it shows TEM micrograph, for the composite fibres containing 5 wt.% of Wood pulp formed by electrospinning. The bright and dark regions correspond to wood pulp, respectively, which confirms the embedment wood pulp into PEO fibres with high degree of dispersion and uniformity. If we see the figure 9.10 (a and b), then we can observe that 10 wt.% solution concentration gives uniform fibre. Figure 9.10(a) presents image of an individual composite fibre, indicating that a flat and homogeneous PEO layer is seamlessly adhered onto the Wood pulp fibre. In figure 9.10 (c and d) 12 wt.% concentration was used showing uniform fibre and also showing the Wood pulp clearly. When the solution concentration is increased beads are formed with lots of knot and aggolomerations , seen at figure 9.10 (e and f). This is due to PEO/Wood pulp not mixing properly or could be polymer impurities.

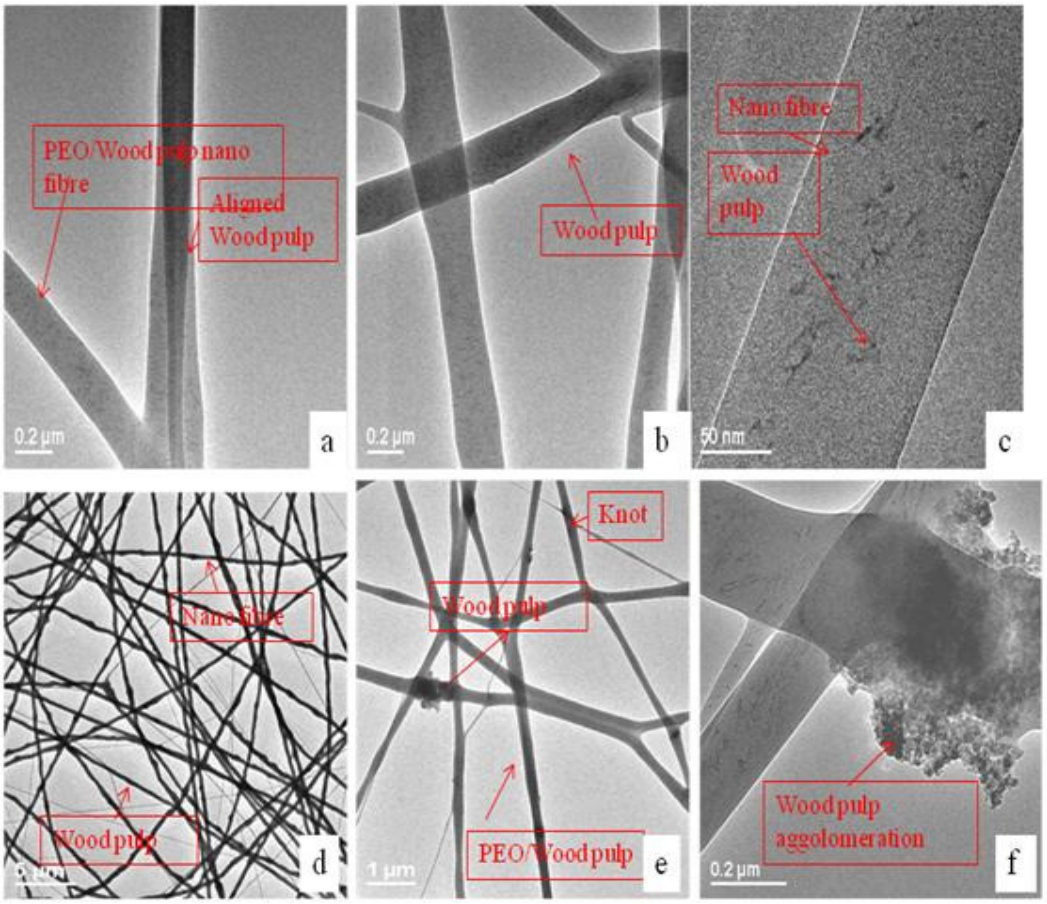

Figure 9.10, TEM images of PEO/Wood pulp blend fibres where the solution was 10 wt.% (a and b), 12 wt.% (c and d) and 14 wt.% (e and f), applied voltage 15 kV and collection distance 11 cm, feed rate 0.25 ml/hr.

9.4 Thermal properties of The PEO/Wood pulp fibre

9.4.1 Differential Scanning Calorimetry (DSC) analysis

Wood pulp based electrospun fibres and wood pulp were analyzed by DSC to examine changes in the phase transitions, including melting, crystallization and exothermic decomposition, due to electrospinning process. The heat flow profiles of PEO and electrospun blend fibres appear very similar to each other in figure 9.11, with the crystallization temperature of both samples appearing at approximately 67º C indicating that there is no significant change in the phase transition temperatures. Thus the impact of solvent to dissolve cellulose to produce homogenous thick solution to produce electrospun nanofibre by electrospinning. Particularly in this case is not prominent.

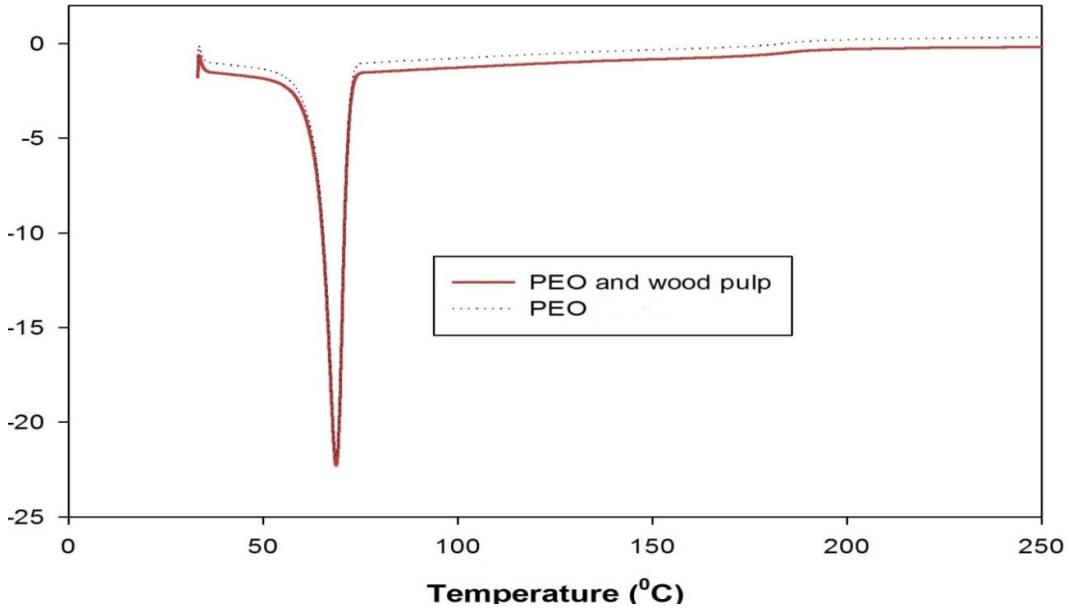

Figure 9.11, DSC curves of PEO powder and PEO/wood pulp nanofibres.

The DSC thermographs (figure 9.11) also revealed the thermal behaviour of PEO powder and PEO/wood pulp composite fibres. The melting point of PEO was measured at 67˚C (figure 9.11) and almost similar melting phenomenon was observed in PEO/wood pulp composite fibres, with the crystallization temperature of both samples appearing at approximately 67˚ C.

9.4.2 X-Ray diffraction

In order to examine whether the structure of PEO/wood pulp is changed in the electrospinning process, XRD of both the raw material of PEO, Wood pulp and the electrospun PEO/Wood pulp were measured. This results are shown figure 9.12.

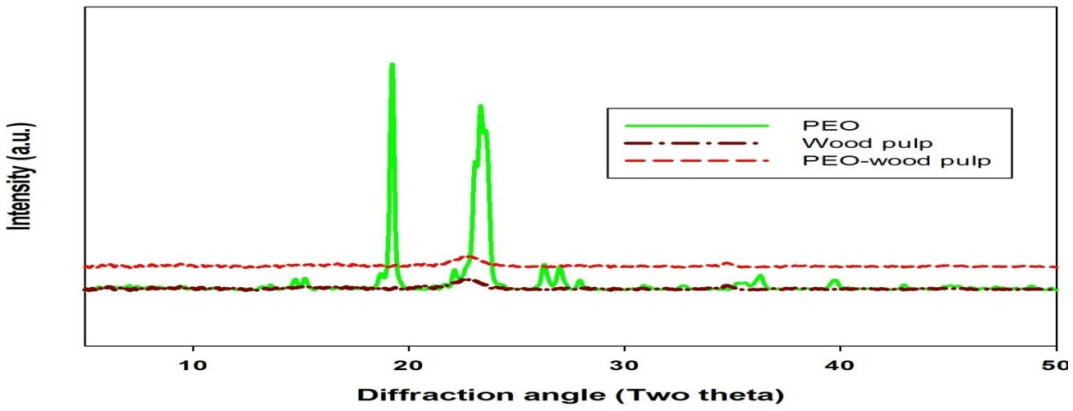

Figure 9.12, XRD patterns of PEO/wood pulp nanofibres for as PEO, prepared composite fibres and wood pulp.

The results illustrated that the crystallinity of PEO/wood pulp fibres was not largely influenced by the content of wood pulp in the PEO/wood pulp fibres. PEO is a semi-crystalline polymer with diffraction peaks at 2θ = 19˚ and 23˚. The wood pulp is also semi- crystalline with diffraction peaks at 22˚C. The composite fibre show different diffraction peaks 21.4˚. The XRD pattern of electrospun fibres shows broader peaks compared to PEO, indicating that there is less crystalline region in the electrospun fibres but more crystalline region than wood pulp. Electrospun fibres appear to have a less crystalline structure of PEO with a shift in the peaks at 21.4˚. The presence of both crystalline and semi-crystalline structure also observed by Zugenmaier [8]. The DSC data also supported his work.

9.4.3 Fourier Transforms Infra Redspectroscopys (FTIR)

In all cases infrared spectra were recorded as KBr discs with a Perkin Elmer (UK) Fourier Transform spectrophotometer from 4000 to 400 cm^{-1} using 32 scans in ATR mode to investigate the nature of the fibre and electrospun mat. The FTIR spectra for pure wood pulp as well as wood pulp and PEO were analysed to study the functional groups and also corresponding changes appeared in composite electrospun nano fibre mats. These are shown in figure 9.13.

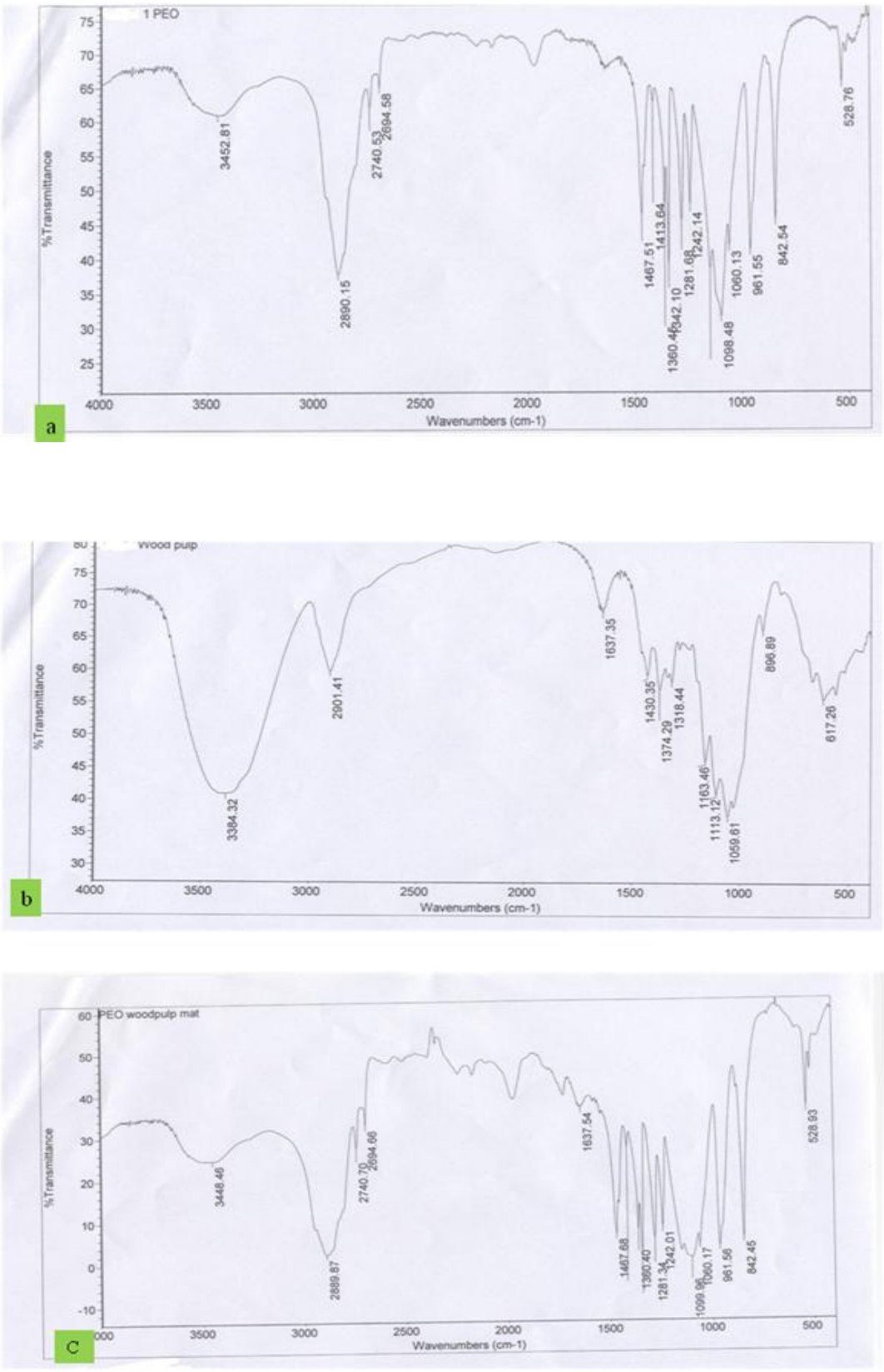

Figure 9.13, The FT-IR spectra of a) PEO powder, b) Wood pulp and c) PEO/Wood pulp.

The significant FTIR spectra for pure PEO, pure wood pulp and the electrospun mats of PEO and wood pulp were studied (within the wavelength range from 4000 to 400 cm^{-1}). In the pure PEO spectrum, an absorption peak due to free –OH group centered at 3453 cm^{-1} appears with a large broad band. In pure wood pulp this peak appears at 3384 cm^{-1}, while in the composite electrospun mat produced from PEO and wood pulp this peak appears at 3448 cm^{-1}, which shows approximately 5 cm^{-1} downward displacement from the actual position of the similar peak of pure PEO and about 64 cm^{-1} upward displacement from the actual position for the similar peak due to free –OH functional group of pure wood pulp. This observation clearly indicates that a significant adhesion force is very active between the two components (PEO and wood pulp) of the composite electrospun mat. Another important observation is, the composite electrospun mat shows a large, broad band due to CH_2 stretching near 2890 cm^{-1} which is in the similar position compared to the similar peak of pure PEO which implies that the composite electrospun mat retains the nature of PEO significantly at least in this case and proving more dominant character of PEO compared to the impact of wood pulp on the mat. Besides this, the band is split into two at 2921 cm^{-1} and 2879 cm^{-1} corresponding to asymmetric CH_2 stretching ($n(CH_2)a$) and symmetric CH_2 stretching ($n(CH_2)s$), respectively. In addition, an identical weak peak (in terms of sharpness and position) near 1638 cm^{-1} is observed in both pure wood pulp and composite electrospun mat and this peak is more identical to wood pulp which corresponds to the bending vibrational mode of hydrated water molecules and also weakly bonded water molecules. This observation somehow related the behaviour of the electrospun mat due to wood pulp though not a very strong argument. Another, significant observation is the spectral bands of the composite electrospun mat comparatively more intense compare to the spectral bands of pure wood pulp, particularly in the spectral range 1500 - 450 cm^{-1}. Two clear CH_2 vibrational modes appear in the composite electrospun mat at 1468 cm^{-1} which, correspond to asymmetric CH_2 bending ($d(CH_2)a$) and near 1381 cm^{-1} which, corresponds to symmetric CH_2 wagging and some C-C stretching ($w(CH_2)s + n(C-C)$). Another, important peak near 1060 cm^{-1} was observed in both pure PEO and electrospun mats (with a very tiny shift from the position as in the case of pure PEO) which indicate C-O-C stretch. These observations clearly demonstrate the impact of both PEO and wood pulp on the spectral nature of the composite electrospun mat.

9.5 Conclusion

Composite fibres of PEO/wood pulp with diameters of hundreds of nanofibres to 1 μm were prepared by electrospinning. The diameters of the composite nanofibres increased with an increase in the concentration of the base PEO/wood pulp solution. The applied electrical potential has significant impact to the size and the surface morphology of the nanofibre. The nanofibre diameter and the bead formation were decreased with increasing collection distance. Flow rate also played significant role to produce uniform nanofibres. Polymer solution concentration of 10 wt.% with applied electric voltage of 15 kV and spinning collection distance of 11 cm, flow rate of 0.25 ml/hr produced uniform nanofibre. TEM, DSC, XRD and FT-IR results showed that the morphology and crystalline phase of composite PEO/wood pulp fibres were not affected by the content of wood pulp.

9.6 References

[9.1] D. R. Salem, *Structure formation in polymeric fibre,* Munich: Hanser Gardner Publications, Inc. p. 296–328 (2001)

[9.2] J. A. Cuculo, N. Aminuddin, M.W. Frey, *Solvent spun cellulose fibres, Chapter in structure formation in polymeric fibre,* Hanser Gardner publications: Munich, P.296-325 (2001)

[9.3] W. Hamad, *On the development and applications of cellulosic nanofibrillar and nanocrystalline materials*, The Canadian Journal of Chemical Engineering, Vol. **84** (2006)

[9.4] J. Brandrup, E. H. Immergut, E. A. Grulke, Eric A. Grulke , D. Bloch , Polymer Handbook, 4th Edition, John Wiley & Sons (1999)

[9.5] M.W. Frey, *Electrospinning cellulose and cellulose derivatives*, Polymer reviews, **48**:378–391, (2008)

[9.6] J. Doshi and D. H. Reneker, *Electrospinning process and applications of electrospun fibres*, J. Electrostatics, **35**, 151-160 (1995)

[9.7] T. J. Sill, H. A. Recum, *Electrospinning: applications in drug delivery and tissue engineering,* Biomaterials, **29**; 1989-2006 (2008)

[9.8] P. Zugenmaier, *Crystalline cellulose and derivatives: characterization and structures*, Publisher: Springer Berlin Heidelberg, ISBN: 3642093191, Germany (2009)

Chapter 10: Potential end uses of produced electrospun nanofibre

10.1 Introduction

Nanofibres can be produced from a wide range of polymers. Electrospinning processes are the easiest way to produce nano fibres. It is currently a well established technique in university laboratories and industry that can fabricate continues fibres with diameter down to a few nanometres. These nanofibres possess one of the highest surface areas to mass ratios among all cohesive porous materials due to their small diameters and mats made from nanofibres are a highly porous [1-2]. A porous structure made out of nanofibres is a dynamic system where the pore size and shape can change, unlike conventional rigid porous structures. Nanofibres can also be linked to form a rigid structure if required. Perhaps the most versatile process for producing nanofibres with relatively high productivity is electrospinning [3]. Moreover, electrospinning can be applied to synthetic and natural polymers, metals, polymer alloys, ceramic, magnetic and polymers functionalised by the addition of drugs, nanoparticles and active agents. The unique characteristics of nanofibres and the functionalities from the polymer themselves make nanofibres as a required candidate for many advanced applications [3-10].

The aim of this chapter is to consider the various end uses of the produced electrospun nanofibres and modifications of the electrospinning design for obtaining nanofibre architectures.

10.2 Industrial application

Nylon 6 is commercially important and one of the well-known members of the polyamides. Nylon 6 is a biodegradable, biocompatible and synthetic polymeric material having good mechanical properties. Nylon 6 is often used to produce fibres with the diameter in the order of 30 μm by conventional melt spinning [11]. On the other hand, the fibres with much more smaller diameters are preferred for many industrial applications. For example, the Nylon 6 fibre-reinforced composites will have good transparent property if the fibre diameter is lower than that of light wavelength. So the new spinning methods with the advantages in producing smaller fibre should be developed to fulfil the industrial requirements, and electrospinning technique is proved to be a powerful method.

Nylon 6 nonwovens, for its toughness, resilience and easy processability are extensively used in various applications including automobile parts, garment interlinings, wipes battery separators, synthetic suede and protective garments. Nylon 6 fibres manufactured into nano nonwovens can further expand its application in specialty materials. Electrospun nanofibre mats have a large specific surface area and an irregular pore structure. The high surface area of the web can provide reactive sites for chemicals, making it a good candidate for chemical protective materials. Nylon 6 nano to micro-pores of nano web provides good moisture and vapor transport properties, which can be applied in breathable sportswear fabrics. Small fibres with large volume of microscopic pores also provide many potential applications including insulating fabric, biomaterials, and high value-added textile fabrics [4, 12-17]. The limitations of Nylon 6 are high moisture pickup, with resulting changes in dimensional and mechanical properties; high mold shrinkage; and notch sensitivity, unless suitably blended for toughness. Among Nylon plastics, Nylon 6.6 is the most widely used because of its overall balance of properties [18]. Zussman et. al applied the technology to structural applications [19-20] Many structural applications depend on the orientation of nanofibres. For example, highly oriented and well-aligned nanofibres are required in fibre based reinforcement applications while randomly distributed nanofibres are required in applications like development of ultra lightweight wing structures for micro air vehicles. Nylon 6.6 nanofibres can easily use protective clothing or can be use as coating with other polymers [21].

10.3 Medical application

The electrospun techniques provide non-wovens of the order of few nanometers with large surface area, ease of functionalisation for various purposes and superior mechanical properties. The possibility of large scale production combined with the simplicity of the process makes this technique very attractive for many different applications. Biomedical field is one of the important application areas among others utilising the electrospun fibres in filtration and protective materials, electrical and optical applications, sensors, nanofibre reinforced composites, etc. Electrospinning can be modified in different ways for combining materials properties with different morphological structures for these applications. Water-soluble polymers like PEO, PVA, Poly(acrylic acid) (PAA), Polyacrylamide, Polyelectrolytes, Polyvinylpyrrolidone (PVP) and Hydroxypropylcellulose (HPC) offer a variety of advantages for electrospinning. The solubility properties of water can be adjusted by the pH,

temperature, or the addition of surfactants or other solvents (for example, alcohols). Electrospun fibres of water-soluble polymers decompose rapidly on contact with water. While this property may be of interest for biomedical applications, additional stabilization of these fibres by cross-linking is necessary for other technical applications (for example, filters and textiles). Despite the variety of synthesis possibilities, only a rather small number of water-soluble polymers have been electrospun from water or solvent mixtures containing water, PEO and PVA can be use as a different molecular weight and both polymers are versatile for electrospinning because they are both soluble in many solvents including water [23-34]. Because of good biocompatibility PEO fibres are very much interesting for biomedical applications [35]. Compared to PEO, PVA offers an even larger scope of variations because its degree of hydrolysis and hence, its water solubility can be adjusted. The hydroxy groups in PVA can be used for chemical reactions either before or after electrospinning. The crystallinity and, hence the water resistance of electrospun fibres of PVA can be distinctly increased by treatment with solvents [36]. Many biopolymers, modified biopolymers, and blends of biopolymers with synthetic polymers have been processed into nanofibres by electrospinning. Very specific conditions are often necessary, such as the use of special solvents or the processing of the materials as blends (for example, with PEO or PVA). For tissue engineering application electrospun collagen with hexafluoroisopropyl alcohol [37-39] or as a blend with PEO [40-41], PCL [42] or PLA-*co*-PCL [43]. Electrospun fibres of inorganic systems are often obtained through the use of polymer composites with inorganic components or of sol-gel systems [22]. Blend fibres are generally fabricated by electrospinning ternary solutions of two polymers and a solvent.

A large number of polymer/metal oxide (or metal sulfide) composite fibres have been produced by electrospinning in combination with sol-gel processes. PVA mix with $FeCl_3$ produced electrospun fibre can be use as a magnetic fibre [44]. Cellulose fibre mixing with different polymer makes the produced electrospun fibre ready for different application. Cellulose is a naturally occurring polymer of particular interest due to its abundant availability and biodegradability. These properties make cellulose fibres useful in a wide range of areas, such as filtration, biomedical applications. Wood pulp with PEO polymer mixing together and produced fibre suitable for paper industries or can be use as a bio composites or tissue paper [45].

10.4 Conclusion

The advantages of electrospinning are the production of very thin fibres with large surface area, ease of functionalisation for various purposes, superior mechanical properties and ease of process. These advantages provide a wide range of opportunities for their use in many different industrial applications, biomedical applications, from tissue engineering, drug release, implants, biotransformation to wound healing. This renewed interest can be attributed to electrospinning's relative ease of use, adaptability, and the ability to fabricate fibres with diameters on the nanometer size scale. While much has been learned about the electrospinning process over its long history, researchers are still gaining new insights and developing new ways of utilizing this technique for industrial, tissue engineering wound dressing and drug delivery applications. Although trialling the produced nanofibres for end use application is outside this study , an overview of potential usages bringing the work of others show the way work forward.

10.5 References

[10.1] J. Fang, H. T. Niu, T.Lin and X.G Wang, *Application of electrospun nanofibres*, Chinese Science Bulletin, **53,** 2265-2286 (2008)

[10.2] C. Burger, B. S. Hsiao, B. Chu, *Nanofibrous materials and their applications*, Annual Review Materials Research, **36**, 333-368 (2006)

[10.3] S. Ramakrishna, K. Fujihara, W. Teo, T.Yong, Z.Ma and R. Ramaseshan, *Electrospun nanofibres :solving globel issues*, Materials today,Vol. **9**, No 3,40-50 (2006)

[10.4] A. Greiner, J. H. Wendorff, *Electrospinning: a fascinating methods for the preparation of ultrathin fibres*, Angewandte Chemic International Edition, **46**, 5670-5703 (2007)

[10.5] Z. M. Huang, Y. Z. Zhang, M. Kotaki, S. Ramakrishna, *A review on polymer nanofibres by electrospinning and their applications in nano composites*,Composites Science and Technology, **63**, 2223-2253 (2003)

[10.6] C. P. Barnes, S. A. Sell, E. D. Boland, D. G. Simpson, G. L. Bowlin, *Nanofibre technology:designing the next generation of tissue engineering scaffolds*,Advanced Drug Delivery Reviews, **59**,1413-1433 (2007)

[10.7] J. Lannutti, D. Reneker, T. Ma, D. Tomasko and D. Farson, *Electrospinning for tissue engineering scaffolds*, Material Science and Engineering, C, **27**, 504-509 (2007)

[10.8] H. Liu, Y.L. Hsieh, *Ultrafine fibrous cellulose membranes from electrospinning of cellulose acetate.*J. Polym. Sci. Part B; Polym. Phys., **40**, 2119–2129(2002)

[10.9] I. S. Chronakis, *Novel nanocomposites and nanoceramics on polymer nanofibres using electrospinning process a review*, Journal of material processing Technology, **167**, 283-293 (2005)

[10.10] W. Sigmund, J. Yuh, H. Park, V. Maneeratana, G. Pyrgiotakis, A. Daga, J. Taylor, J. C. Nino, *Processing and structure relationshops in electrospinning of ceramic fibre systems*, Journal of American Ceramic Society, **89**, 395-407 (2006)

[10.11] H. R. Pant, M. P. Bajgai, C. Yi, R. Nirmala, K. T. Nam, W. B. H. Y. Kim, *Effect of successive electrospinning and the strength of hydrogen bond on the morphology of electrospun Nylon-6 nanofibres*, Colloids and Surfaces A: Physicochem. Eng. Aspects, **370**, 87–9 (2010)

[10.12] J. M. Deitzel, W. Kosik, S. H. McKnight, N. C. B. Tan, J. M. Desimone and S. Crette, *Electrospinning of polymer nanofibres with specific surface chemistry*. Polymer, **43** (3):1025–9 (2002)

[10.13] H. Dai, J. Gong, H. Kim and D. Lee, *A novel method for preparing ultra-fine alumina-borate oxide fibres via an electrospinning technique*. Nanotechnology ;**13**:674–7 (2002)

[10.14] D.H. Reneker, A.L. Yarin, H. Fong, S. Koombhongse, *Bending instability of electrically charged liquid jets of polymer solutions in electrospinning*. J Appl Phys; **87:**4531–47 (2000)

[10.15] G.T. Kim, Y.C.Ahn, J. K. Lee, *Characteristics of Nylon 6 nanofilter for removing ultra fine particles*. Korean J Chem Eng; **25** (2):368–72 (2008)

[10.16] Y. J. Ryu, H.Y. Kim, K. H. Lee, H. C. Park and D. R. Lee, *Transport properties of electrospun Nylon 6 nonwoven mats*, Eur Polym J; **39** (9):1883–9 (2003).

[10.17] N. Fedorava, B. Pourdeyhimi, *High strength nylon micro-and nanofibre based nonwovens via spunbonding*, J Appl Polym Sci; **104** (5):3434–42 (2007)

[10.18] L. Lingaiah, K.N. Shivakumar, R. Sadler, *Electrospinning of Nylon-66 polymer nanofabrics*, American Institute of Aeronautics and Astronautics (2008)

[10.19] E. Zussman, X. Chen,W. Ding, L. Calabri, D. A. Dikin, J. P. Quintana, R. S. Ruoff, *Mechanical and structural characterization of electrospun PAN-derived carbon nanofibres*, Carbon, Vol. **43**, pp. 2175-2185 (2005).
[10.20] E. Zussman, A. L.Yarin, D. Weihs, *A micro-aerodynamic decelerator based on permeable surfaces of nanofibre mats*, Experiments in Fluids, Vol. **33**, pp. 315-320 (2002)
[10.21] M. M. Chowdhury and G. K. Stylios, *Effect of processing parameters on Nylon 6.6 nanofibres and their morphology,* Green Chemistry and Engineering International Conference on Process Intensification and Nanotechnology,Albany, USA, p 161-172 (2008)
[10.22] A. Greiner, J. H. Wendorff, *Electrospinning: A Fascinating Method for the Preparation of Ultrathin Fibres,* Volume **46**, Issue 30, Pages 5670 – 5703 (2007)
[10.23] J. Doshi, G. Srinivasan, D.H. Reneker, *High modulus polymers: a novel electrospinning process*, Polym. News*,* **20***:p.*206-207 (1995)
[10.24] H. Fong, I. Chun, D. H. Reneker, *Beaded nanofibres formed during electrospinning,* Polymer, **40** (16), pp. 4585-4592 (1999)
[10.25] J. M. Deitzel, J. Kleinmeyer, D. Harris, N. C. B. Tan, *The effect of processing variables on the morphology of electrospun nanofibres and textiles*, Polymer, **42**, 261–272 (2001)

[10.26] Y. M. Shin, M. M. Hohman, M. P. Brenner, G. C. Rutledge, *Experimental characterization of electrospinning: The electrically forced jet and instabilities*, Polymer, **42** (25), pp. 9955-9967 (2001)
[10.27] S. A. Theron, E. Zussman, A. L. Yarin, Polymer, **45**, 2017-2030 (2004)
[10.28] W. K. Son, J. H. Youk, T. Seung Lee, W. H. Park, *The effects of solution properties and polyelectrolyte on electrospinning of ultrafine poly(ethylene oxide) fibres*, Polymer , **45**, 2959-2966 (2004)

[10.29] R. Kessick, J. Fenn, G. Tepper, *The use of AC potentials in electrospraying and electrospinning processes*, Polymer, **45**, 2981-2984 (2004)

[10.30] P. Tsai, H. L. Schreuder-Gibson, Adv. Filtr. Sep. Technol., **16**, 340-3539 (2003)
[10.31] V. K. Daga, M. E. Helgeson, E. Matthew, N. J. Wagner, J. Polym. Sci. Part B, **44**, 1608-1617 (2006)
[10.32] N. Tomczak, N. F. van Hulst, G. J. Vancso, Macromolecules , **38**, 7863-7866 (2005)

[10.33] M. L. Bellan, J. Kameoka, H. G. Craighead, Nanotechnology, **16**, 1095-1099 (2005)

[10.34] M. Chowdhury and George. K. Stylios, *Ultramide Nylon 6 and PEO nano fibres electrospun from solutions in an organic acid: and water solution Optimization of processing parameters and compare those parameters*, The Nanotechnology Conference and Trade show, Santa Clara, USA, May 20-24 (2007)

[10.35] N. B. Graham, *Poly (ethylene oxide) and related Hydrogels and Hydrogels in medicine and pharmacy*, Vol. II (Ed.: N. A. Peppas), CRC, Boca Raton, pp. 96-97 (1986)

[10.36] *C. Zhang, X. Yuan, L. Wu, Y. Han,* and *J. Sheng*, *Study on morphology of electrospun poly (vinyl alcohol) mats*, Eur. Polym.J., **41**, 423-432 (2005)

[10.37] J. A. Matthews, D. G. Simpson, G. E. Wnek and G. L. Bowlin, *Electrospinning of Collagen Nanofibres*, Biomacromolecules, **3** *(2):* 232-238 (2002)

[10.38] K. S. Rho, L. Jeong, G. Lee, B. M. Seo, Y. J. Park, S. D. Hong, S. Roh, J. J. Cho, W. H. Park and B. M. Min, *Electrospinning of collagen nanofibres: Effects on the behaviour of normal human keratinocytes and early-stage wound healing*, Biomaterials, **27**, 1452-1461 (2006)

[10.39] B. M. Min, S. W. Lee, J. N. Lim, Y.You, T. S. Lee, P. H. Kang and W. H. Park, *Chitin and chitosan nanofibres: electrospinning of chitin and deacetylation of chitin nanofibres,* Polymer, **45**, 7137-7142 (2004).

[10.40] L. Buttafoco, N. G. Kolkman, P. Engbers-Buitjenhuijs, A. A. Poot, P. J. Dijkstra, I. Vermes, J. Feijen, *Electrospinning of collagen and elastin for tissue engineering applications,* Biomaterials, **27**, 724-734 (2006)

[10.41] L. *Huang, K. Nagapudi, R.P. Apkarian, E.L.Chaikof, Engineered collagen-PEO nanofibres and fabrics*, J. Biomater. Sci.: Polym. Ed., **12,** 979-993 (2001)

[10.42] J. Venugopal, L. L. Ma, T. Yong, S. Ramakrishna, Cell Biol. Int. **29**, 861-867 (2005)

[10.43] W. He, T. Yong, W. E. Teo, Z. Ma, S. Ramakrishna, *Fabrication and endothelialization of collagen-blended biodegradable polymer nanofibres: potential vascular graft for blood vessel tissue engineering,* Tissue Eng., **11**, 1574-1588 (2005)

[10.44] T. Wan, M.Chowdhury and G. Stylios, *The formation and morphology of PVA Ferrogel nanofibre by the electrospinning process*, Materials Science Forum Vol. **650** pp 361-366, Switzerland (2010)

[10.45] M. Chowdhury and G. Stylios, *Morphological study of Woodpulp/PEO blend nano fibres*, 6th International conference on Modification, Degradation and Stabilization of Polymers ,Athens,Greece,CD Rom, 5 – 9 September (2010)

Chapter 11: Conclusion and future work

11.1 Conclusion

This study has investigated the effect of processing parameters on the following polymers**;** Nylon 6, Nylon 6.6, PEO, PVA and Wood pulp. These polymers are important for a number of industrial and biomedical applications but in literature they have not yet fully been investigated. All selected polymers have successfully been converted into nano fibres and their process optimization established for good quality, uniform nano fibres.

Nanofibres produced under this study exhibited a variety of coils, loops and bends which might be resulted primarily from the bending instability of the jet. It is also possible that the beads might form end of the Taylor's cone splitting into many mini-jets and each mini-jet disintegrating into small droplets. The fibres were formed when the jet at the end of the Taylor's cone underwent elongational flow and then broke up into several stable mini-jets that accelerated toward the collector. During transition of the mini-jet to the collector, each mini jet might further split into smaller jets with almost equal diameter. Splaying determined the size of the final fibre obtained on the collector.

In this context the Nylon 6 and Nylon 6.6 polymer solutions successfully spun with the addition of formic acid and PEO using water and water/Ethanol. On the other hand PVA was mixed with Ferric Chloride and Wood pulp was mixed with PEO and water/Ethanol as polymer solutions and has successfully produced nanofibres. The impact of different processing parameters on electrospun nanofibres were studied using extensive microscopic studies such as, SEM, AFM and TEM.

Nylon 6, Nylon 6.6, PEO, PVA/$FeCl_3$, PEO/Wood pulp optimum parameters are as follows: Solution concentrations, applied electric field, tip to collector distance and solution flow rate.

i) **Nylon 6***:* The diameter of the electrospun Nylon 6 fibre is affected by processing parameters. Electrospun Nylon 6 nanofibres with a smaller diameter, 553 nm produced with a lower polymer solution concentration, 15 wt.% but nonuniform/beaded fibres were found if these polymer solutions were either too high (above 25 wt.%) or too low

(less than 20 wt.%). The applied voltage (above 12 kV) reflects on the force to pull a solution out from the spinneret, so higher applied voltage (18 kV) affected the charge density and thus electrical force, which influence the elongation of the jet during electrospinning. Uniform Nylon 6 nanofibres were produced under polymer solution concentration of 20 wt.% and applied voltage of 15 kV, volume feed rate 0.20 ml/hr and a spinning distance of 8 cm.

ii) **Nylon 6.6**: The increasing viscosity, expectedly, increased the diameters (150 nm to 1300nm) of Nylon 6.6 nano fibres. Nylon 6.6 smallest nanofibres were observed with the higher range strength of the electric field. Flow rate also changed Nylon 6.6 nanofibre diameter as higher flow rate gave larger diameter nanofibre and lower flow rate gave smaller diameter nanofibre. The optimum condition of 25 wt.% solution concentration, applied voltage at 15 kV, collection distance at 8 cm and flow rate at 0.20 ml/hr produced uniform Nylon 6.6 nanofibres. Aligned nanofibres were produced from Nylon 6.6 based polymer solution. This was possible by using a purpose built set up using two grounded copper collector disks to produce a gap space to allow the nanofibre alignment within this space. With this set up and using the similar mechanism a bundle of aligned nylon 6.6 nanofibre was obtained and the morphology of the aligned nanofibres was investigated. The optimum distance between collector and disks for spinning aligned nanofibres with acceptable density was 4-5 cm producing uniform aligned fibre. DSC and X-ray analysed with the Nylon 6.6 granules and the Nylon 6.6 nano mat which clearly described that there is no major different with them and Nylon nanofibres crystallinity increased due to the electrospinning enhances the polymer crystallization by chain orientation within the fibre. Nanocomposite fibres were produced by mixing of MWCNT with Nylon 6.6 with good dispersion and its morphological study showed the inclusion of the nanotubes along the axis of Nylon 6.6. It can be use as reinforcement in cars and aeroplane.

iii) **PEO**: Submicron PEO fibre mats were prepared by electrospinning of aqueous PEO and aqueous PEO with Ethanol solutions. The addition of Ethanol to an aqueous PEO solution decreased the volume charge density when all the other parameters were kept constant. This showed that the main advantage of Ethanol in the mixture used in the electrospinning process was not related to the volume charge density, but rather to a higher evaporation rate, which facilitated nanofibre solidification. With increasing the concentration of PEO solution from 10 wt.% to 14 wt.%, the morphology changed from beaded fibre to uniform fibre structure and the fibre diameter was also increased, with

increasing applied electric voltage the fibre diameter decrease and produced finer, 372 nm and 379 nm diameter nanofibres. Tip to target distance had little significant effects on fibre morphology; however the morphology changed by the flow rate. Optimum conditions of polymer solution concentration of 14 wt.%, an applied voltage of 15 kV, volume feed rate 0.20 ml/hr and a spinning collection distance 11 cm produced uniform nanofibres. DSC and XRD analyses proved that PEO powder is more crystal then the produced nanofibre. It is envisaged that the solvent used in the formulation of dispersion of PEO causes certain sort of deformation by altering the natural molecular arrangement or the orientation of the polymer chain which is proved from the observed DSC and XRD result.

iv) **PVA/$FeCl_3$** : The solution concentration significantly affected the morphology and diameter of the PVA/$FeCl_3$ nano fibres. Lower concentration (6 wt.%) tended to facilitate the formation of fibres with beads. As the solution concentration increase to 8 wt.% and 10 wt.%, the morphology was changed from beaded fibres to smooth and uniform nano fibre and with increasing nanofibre diameter. The spinning voltage also had an important influence on nanofibre diameter, while the collection distance had a lesser effect on the nanofibre diameter. Flow rate also influences the production of uniform nanofibre. Higher flow rate (0.30 ml/hr) provides large diameter nanofibre (average diameter 734 nm) and lower flow rate (0.20 ml/hr) proves small diameter nanofibre (average diameter 564 nm).

v) **PEO/Wood pulp**: Increasing the solution concentration increased the produced PEO/Wood pulp nanofibre diameter. The applied electrical potential has significant impact to the size and the surface morphology of the PEO/Wood pulp nanofibre. The PEO/Wood nanofibre diameter and the bead formation were decreased by increasing the collection distance. The flow rate also played significant effect to producing uniform PEO/Wood pulp nanofibres. Optimum conditions with solution concentration of 10 wt.% with applied electric voltage of 15 kV and spinning collection distance of 11 cm and flow rate 0.25 ml/hr produced uniform nanofibres. TEM, DSC, XRD and FT-IR investigation concluded that the morphology and crystalline phase of composite PEO/Wood pulp nanofibres were not affected by the content of wood pulp.

Electrospinning has emerged to be a simple, elegant, and scalable technique to fabricate polymeric nanofibres over other nanofibres fabrication techniques. It is an important and promising technology for producing different nanofibres, further continuous

research is needed to address many issues, including, enhancement of mechanical properties, manufacturing of continuous nanofibre yarns, nonwoven mats as well as venturing towards woven fabrics incorporating functional coatings.

11.2 Future work

Further research can be carried out as continuation of this thesis in the following areas:

1. Characterisation of the nanofibres using mechanical drawing techniques.

3. Production and characterisation of carbon nanotube based composite nanofibres.

3. Quantification of the alignment and dispersion of SWCNT

4. Evaluation of the mechanical properties of a nano mat and investigation align mat.

5. Evaluation of the mechanical properties of the impregnated composite nanofibrils

6. Production of continuous nano-yarn.

7. Production of large and continuous nano mats.

8. Nano spraying.

9. Fabric functional coating.

Appendices

Appendix A

Polymer solution for electrospun process which used by different researcher:

No	Polymer	Polymer classification	Solvent	Application	Ref *
1	Polyethylene oxide (PEO)	Synthetic polymer	water	Biomedical applications	1
2	Polyvinyl alcohol (PVA)	Synthetic polymer	water	Chemical applications	2
3	Polyvinyl phenol (PVP)	Synthetic polymer	water	Antimicrobial agents	3
4	Polylactic acid (PLA)	Biodegradable polymer	Dimethylformamide, DMF	Medical applications	4
5	Polycaprolactone (PCL)	Biodegradable polymer	Chloroform: MEthanol (3: 1)	Tissue engineering	5
6	Polyacrylonitrile (PAN)	Organosoluble synthetic polymer	Dimethylformamide, DMF	Protective textiles	6
7	Polycarbonate (PC)	Organosoluble synthetic polymer	Dimethylformamide, DMF	Filtration	7
8	Polystyrene (PS)	Organosoluble synthetic polymer	Dimethylformamide, DMF	Filtration	8
9	Polybenzimidzole (PBI)	Organosoluble synthetic polymer	Dimethylaccetamide, DAA	Protective clothing	9
10	Polyethylene Terephtalate(PET)	Organosoluble synthetic polymer	Dichloromethane	Composites	10
11	Polyurethanes (PU)	Organosoluble synthetic	Dimethylformamide, DMF	Protective clothing	11

12	Polyvinylchloride (PVC)	Organosoluble synthetic polymer	Dimethylformamide: tetrahydrofuran	Protective clothing	12
13	Polyvinylidene fluoride(PVDF)	Organosoluble synthetic polymer	Dimethylformamide: Dimethylaccetamide	Flat ribbons	13
14	Aliphatic PA (Nylon 6)	Organosoluble synthetic polymer	Formic acid	Filtration	14
15	Nylon6.6	Organosoluble synthetic polymer	Formic acid	Protective textiles	15
16	Collagen	Biopolymer	Hexafluoroisopropyl alcohol	Tissue engineering	16
17	Regenerated silk (Bombyx mori)	Biopolymer	Hexafluoracetone	Wound dressing	17
18	Chitosan	Biopolymer	Formic acid or acetic acid	Wound dressing	18
19	Cellulose	Biopolymer	NMO/water	Membranes	19
20	Cellulose acetate, CA	Biopolymer	acetic acid	Membranes	20

References:

[1] V.K. Daga, M.E. Helgeson, E. Matthew, N.J. Wagner, *Electrospinning of neat and laponite-filled aqueous poly(ethylene oxide) solutions*, Journal of Polymer Science part B: Polymer Physics, **44**, 1608-1617 (2006)

[2] S.L. Shenoy, W.D. Bates, G. Wnek, *Correlation between electrospinnability and physical gelatin*, Polymer, **46**, 8990-9004 (2005)

[3] Q. Yang, Z. Li, Y. Hong, Y. Zhao, S. Qiu, C. Wang, Y. Wei, *Influence of solvents on the formation of ultrathin uniform poly(vinyl pyrrolidone) nanofibres with electrospinning*, Journal of Polymer Science part B: Polymer Physics, **42**, 3721-3726 (2004)

[4] S.H. Tan, R. Inai, M. Kotaki, S. Ramakrishna, *Systematic parameter study for ultra-fine fibre fabrication via electrospinning process*, Polymer, **46**, 6128-6134 (2005)

[5] Z.M. Huang, C.L. He, A. Yang, Y. Zhang, X.J. Han, J. Yin, Q. Wu, *Encapsulating drugs in biodegradable ultrafine fibres through co-axial electrospinning*, Journal of Biomedical Materials Research part A, **77**, 169-179 (2006)

[6] J. McCann, M. Marquez, Y. Xia, *Highly porous fibres by electrospinning into a cryogenic liquid*, Journal of the American Chemical Society, **128**, 1436-1437 (2006)

[7] R.V.N. Krishnappa, K. Desai, C. Sung, *Morphological study of electrospun polycarbonates as a function of the solvent and processing voltage*, Journal of Materials Science, **38**, 2357-2365 (2003)

[8] S.C. Baker, N. Atkin, P.A. Gunning, N. Granville, K. Wilson, D. Wilson, J. Southgate, *characterization of electrospun polystyrene scaffolds for three-dimensional in vitro biological studies*, Biomaterials, **27**, 3136-3146 (2006)

[9] H.L. Schreuder-Gibson, P. Gibson, K. Senecal, M. Sennett, J. Walker, W. Yeomans, D. Ziegler, P.P. Tsai, *Protective textile materials based on electrospun nanofibres*, Journal of Advanced Materials, **34**, 44-55 (2002)

[10] K.H. Hong, T.J. Kang, *Hydraulic permeabilities of PET and nylon 6 electrospun fibre webs*, Journal of Applied Polymer Science, **100**, 167-177 (2006)

[11] S. Kidoaki, I.K. Kwon, T. Matsuda, *Structural features and mechanical properties of in situ-bonded meshes of segmented polyurethane electrospun from mixed solvents*, Journal of Biomedical Materials Research part B, **76**, 219-229 (2006)

[12] R. Ramaseshan, S. Sundarrajan, Y. Liu, R.S. Barhate, N.L. Lala, S. Ramakrishna, *Functionalized polymer nanofibre membranes for protection from chemical warfare stimulants*, Nanotechnology, **17**, 2947-2953 (2006)

[13] S. Koombhongse, W. Liu, D.H. Reneker, *Flat ribbons and other shapes by electrospinning*, Journal of Polymer Science part B: Polymer Physics, **39**, 2598-2606 (2001)

[14] M. Chowdhury and G. Stylios, *Investigation of nano fibre production by the electrospinning process*, The 3rd International Congress of Nanotechnology 2006, Sanfrancisco,USA, October 30-November 2(2006)

[15] M.Chowdhury,G.K.Stylios, *Effect of processing parameters on nylon 6.6 nanofibres and their morphology,* Green Chemistry and Engineering International Conference on Process Intensification and Nanotechnology, Albany, USA, p 161-172, (2008)

[16] K.S. Rho, L. Jeong, G. Lee, B.M. Seo, Y.J. Park, S.D. Hong, S. Roh, J.J. Cho, W.H. Park, B.M. Min, *Electrospinning of collagen nanofibres: effects on the behavior of normal human keratinocytes and early-stage wound healing*, Biomaterials, **27**, 1452-1461 (2006)

[17] J. Ayutsede, M. Gandhi, S. Sukigara, M. Micklus, H.E. Chen, F. Ko, *Regeneration of bombyx mori silk by electrospinning part 3: characterization of electrospun nonwoven mat*, Polymer, **46**, 1625-1634 (2005).

[18] K. Ohkawa, D. Cha, H. Kim, A. Nishida, H. Yamamoto, *Electrospinning of Chitosan*, Macromolecular Rapid Communication, **25**, 1600-1605 (2004)

[19] C.W. Kim, M.W. Frey, M. Marquez, Y.L. Joo, *Preparation of submicron-scale electrospun cellulose fibres via direct dissolution*, Journal of Polymer Science part B: Polymer Physics, **43**, 1673-1683 (2005)

[20] H. Liu, Y.L. Hsieh, *Ultrafine fibrous cellulose membranes from electrospinning of cellulose acetate*, Journal of Polymer Science part B: Polymer Physics, **40**, 2119-2129 (2002)

Appendix B

List of publication

Journal publication

1. **M. M. Chowdhury** and G. Stylios, Investigating nano fibre production by the electrospinning process, International Journal of Clothing Science and Technology, UK Vol 18, Number 6 (2006)

2. **M. Chowdhury** and G.K.Stylios, Investigation of nano fibre production by electrospinning process & process optimization, Vol 1.Issue 6, Spinning textiles, India, (2007)

3. **M. Chowdhury** and G.K.Stylios, Review of the early attempt to date on electrospinning, Bangladesh textile journal, Vol. 6, Issue8, ISSN 1998-2712 (2009)

4. Taoyu Wan, **Mohammad Chowdhury** and George.K.Stylios, The Formation and morphology of PVA Ferrogel nanofibre by the electrospinning process, The Journal of Materials Science Forum,Vol. 650 pp 361-366 (2010)

5. **Mohammad Chowdhury** and George.K.Stylios, Analyses the effect of experimental parameters on the morphology of electrospun Polyethylene oxide nanofibres and their thermal properties, **Accepted**, The Journal of Textile Institute, UK (2010)

6. **Mohammad Chowdhury** and George.K.Stylios, Process optimization and alignment of PVA/ $FeCl_3$ nano composite fibres by electro spinning, **Accepted,** The Journal of Material Science, UK (2010)

Conference proceeding

1. **M. Chowdhury** and G.K.Stylios, Nano fibre and its medical application, Research in support of Medicine, Health and Safety PG research Conference, Edinburgh,UK, CD Rom, 15th June (2006)

2. **M. M. Chowdhury** and George. K. Stylios, Investigation of nano fibre production by the electrospinning process, The 3rd International Congress of Nanotechnology 2006, Sanfrancisco,USA, CD Rom ,October 30-November 2 (2006)

3. **M. M. Chowdhury** and George.K.Stylios, Processing parameter effects and morphology of electrospun nano fibre, The 3rd Nanotechnology Transfer Executive Summit in Europe, December 3-4, (2007)

4. **M. Chowdhury** and George.K.Stylios, Ultramide nylon 6 and PEO nano fibres electrospun from solutions in an organic acid: and water solution Optimization of processing parameters and compare those parameters, The Nanotechnology Conference and Trade show, Santa Clara, USA, May 20-24 (2007)

5. **M. M. Chowdhury** and George.K.Stylios, Effects of processing parameters and their morphology during electrospinning, Cascadia Nanotech Symposium, CD Rom, March 4-5th Vancouver, Canada (2008)

6. **M. Chowdhury** and Geroge.K.Stylios, Processing parameter effects and morphology of the electrospun nano fibre, 2nd International Conference on Advanced Nano Materials, Aveiro, Portugal, CD Rom, June 22nd-25th (2008)

7. **M. M. Chowdhury** and George.K.Stylios, Effect of processing parameters on nylon 6.6 nano-fibres and their morphology, Green Chemistry and Engineering International Conference on Process Intensification and Nanotechnology, Albany, New York State, USA, BHR Group - ISBN 978 1 85598 101 0 , 15th – 18th September (2008)

8. T. Wan, **M. Chowdhury** and G.Stylios, The formation of electrostatic spinning Ferro magnetic gel nano fibre. China Materials Conference, October 14 -17, Suzhou, China (2009)

9. **Mohammad Chowdhury**, Taoyo Wan and George.K.Stylios, The Formation and morphology of PVA Ferrogel nanofibre by the electrospinning Process, 4th International Technical textile congress, Istanbul, Turkey, CD Rom, 16-18 May (2010)

10. **M. Chowdhury** and G.Stylios, Morphological study of Woodpulp/PEO blend nano fibres, 6th International conference on Modification, Degradation and Stabilization of Polymers ,Athens, Greece, CD Rom, 5 – 9 September (2010)